INDEPENDENT-PARTICLE POTENTIAL-ENERGY SURFACES
FOR CHEMICAL REACTIONS

Thesis by

Robert Charles Ladner

In Partial Fulfillment of the Requirements

For the Degree of

Doctor of Philosophy

California Institute of Technology

Pasadena, California

1972

(Submitted November 30, 1971)

ACKNOWLEDGEMENTS

During my stay at Caltech, many people have helped me. Chief among them has been Bill Goddard who has been of great aid and without whom this work would not have been done. He has been a continual source of excellent advice, encouragement, and inspiration. Bill has also been a real friend. The theoretical chemistry group at Caltech has also been of great help, particularly Don Truhlar, Tom Dunning, Al Wagner, and Dave Huestis.

I would like to extend special thanks to the staff of the Booth Computing Center for aid in carrying out the computations reported here. Above all, I would like to thank E. Kent Gordon, Kiku Matsumoto, Lesley Benson, and the entire staff of operators.

Of those people who have helped me while at Caltech, I would certainly like to thank those who have helped me enjoy some of the more sensuous pleasures of life. These include George A. Petersson, Harold Wayland, James Brown, Dennis Matson, Bay Vintners, Imports, Jurgensen's Grocery Company, and Trader Joe's.

I would like to thank Adria Larson for her excellent and good-natured help in the preparation of the text, tables, and figures.

I would like to thank the National Science Foundation for a five-year graduate fellowship, the Caltech Chemistry Department for financial assistance, and all the donors who have supported Caltech.

Finally, I want to thank several people who helped me come to Caltech. First of all my parents who gave me life, nurtured and sustained me through my early years and taught me a deep respect

for knowledge. Then a small number of excellent teachers whom I encountered in the Houston Public Schools, especially Ralph Teter, Jack McCullough, Kate Timme, and Samuel Abrams. And, last but not least, members of the Rice University Faculty, especially J. E. Kilpatrick, Ronald Magid, Phil Brooks, and Ted Lewis.

INTRODUCTION

My graduate work at Caltech has centered on the problem of calculating and understanding potential energy surfaces (PES) for chemical reactions. In this I have tried to use independent-particle wavefunctions because they have proven so useful in understanding chemical systems in the past. The most widely known and used independent-particle wavefunction (IPWF) is the Hartree-Fock (HF) wavefunction, which has been very useful in the study of the properties and geometries of bound molecules. It is well known, however, that HF does not describe bond-breaking very well, and so I looked into other IPWF that might be useful.

At the time I began this work, Bill Goddard had developed a new method or set of methods collectively called GI.[1] Since these methods removed the double occupancy restriction (which seemed to be the main cause of HF's bad description of bond-breaking) but retained the independent-particle picture, I undertook a study of the reaction

$$CH_4 + H \rightarrow CH_3\cdot + H_2 \qquad (1)$$

using the GF method. It quickly became apparent that this project was a bit too ambitious, since I could not afford to vary all of the nuclear coordinates. By holding the three nonreacting protons in a triangle and forcing some other restrictions on nuclear motion, however, I was able to map part of the surface.

As I prepared for my candidacy exam, I was looking for propositions and Bill Goddard suggested I look into the problem of Li hyperfine coupling. The G1 approach gave a good energy but a poor value for the Fermi contact term, while GF gave a much poorer energy but a very

good value for the contact term. The problem was to find a new IPWF that would give the good G1 energy and the good GF contact term. This led to the development of the SOGI method, which did just what was required (at least for Li).

The energy improvement of SOGI over G1 for Li, however, was tiny. My new method would be of little worth if it could only give very small energy corrections for atoms and improve spin-density values. In fact, when SOGI was applied to larger atoms, the spin densities were not so good. I was curious to see if there were cases in which optimizing the spin-coupling would cause a significant improvement in the energy. The transition state of H_3 proved to be just such a case. It was then that I realized that the GF calculations on (1) were probably meaningless or nearly so, since the spin-coupling will always change in the course of a reaction and this was not possible in GF. The development of the SOGI method and its application to a few systems, including two reactive ones, is discussed in Chapter I, which was published in the Journal of Chemical Physics, 51, 1073 (1969).

These calculations on H_3 and H_4 led me to believe that the SOGI method was just the independent-particle method I had wanted for treatment of chemical reactions, and I began a more thorough investigation of linear H_3 and linear LiH_2. The study of H_3 was to establish how accurately one could obtain a PES with SOGI, since very accurate CI calculations on H_3 were available for comparison.[3,4] The calculations on LiH_2 were undertaken to investigate the effect of restricting the spin-coupling and to see how and how well SOGI would describe a reaction that had an asymmetric transition state[5] and that was highly exothermic.

The results of these calculations are given in Chapter II, which should be published shortly.[6] A shorter, less detailed discussion of these calculations and of the conclusions drawn has also been published in the Journal of the American Chemical Society[7] but is not included here.

Bill Goddard has taken the orbital picture of these reactions as well as the calculation of Woody Wilson[8] on H_4 and has produced a very exciting interpretation[9,10] that allows him to make predictions about whole classes of reactions. These predictions are based on SOGI calculations on H_3, H_4, LiH_2, and some calculations by George Levin on allyl ions and radical and butadiene.[11] What is needed to extend the theory are studies of molecules with nonbonded pairs and of excited states.

The third section of this thesis is a study of the excited states of H_3 that could arise from H_2 $^1\Sigma_g^+$ + H(n = 2) or H_2 $^3\Sigma_u^+$ + H(1s). In that section I examine the results of SOGI and G1 calculations on those excited states and explain the nature of the states in terms of orbitals and spin-coupling. I believe that those studies give significant insight into the processes involved in reactions of excited states.

REFERENCES

1. W. A. Goddard, Phys. Rev. 157, 73, 81 (1967); idem, J. Chem. Phys. 48, 450, 5337 (1967).

3. I. Shavitt, R. M. Stevens, F. L. Minn, and M. Karplus, J. Chem. Phys. 48, 2700 (1968).

4. B. Liu reported by A. D. McLean in Proceedings of the Conference on Potential Energy Surfaces in Chemistry, University of California, Santa Cruz, August 10-13, 1970, W. A. Lester, Jr., Ed. (IBM Research Laboratory, San Jose, California, 1971), Publication No. RA 18, January 14, 1971 (No. 14748), p. 102.

5. In discussing PES's of reactions, we use the term "transition state" to mean the region of the PES near the saddle point. We do not think of a distinct state of the system as in the Transition State Theory of H. Eyring in S. Glasstone, K. J. Laidler, and H. Eyring, The Theory of Rate Processes (McGraw-Hill Book Co., New York, 1941).

6. R. C. Ladner and W. A. Goddard III, "The Orbital Description of the H_2 + D $\rightleftharpoons$ H + HD and LiH + H $\rightleftharpoons$ Li + H_2 Exchange Reactions," to be submitted for publication in J. Chem. Phys.

7. W. A. Goddard III and R. C. Ladner, "A Generalized Orbital Description of the Reactions of Small Molecules," accepted for publication in J. Amer. Chem. Soc.

8. C. W. Wilson, Jr., and W. A. Goddard III, "Ab Initio Calculations on the H_2 + D_2 = 2HD Four-Center Exchange Reactions. II. Orbitals, Contragradience Energy, and the Reaction Surface," accepted for

publication in J. Chem. Phys.

9.   W. A. Goddard III, J. Amer. Chem. Soc. $\underset{\sim}{92}$, 7520 (1970).

10.   W. A. Goddard III, "Selection Rules for Chemical Reactions Using the Orbital Phase Continuity Principle," accepted for publication in J. Amer. Chem. Soc.

11.   G. Levin, Candidacy Report, California Institute of Technology, 1971.

ABSTRACT

A new independent-particle method, the spin-coupling optimized GI (SOGI) method is described. This method removes many of the restrictions of the Hartree-Fock (HF), valence bond (VB), and GI methods. This method is applied to the two reactive systems of linear H_3 and linear LiH_2. The results of the H_3 calculations are carefully compared with CI results. The shapes of the potential energy surfaces (PES's) are explained in terms of the SOGI orbitals. Finally, the SOGI method is applied to the excited states of H_3, both linear and nonlinear.

TABLE OF CONTENTS

I. Improved Quantum Theory of Many-Electron Systems.

V. The Spin-Coupling Optimized GI Method

Improved Quantum Theory of Many-Electron Systems. V. The Spin-Coupling Optimized GI Method*

Robert C. Ladner† and William A. Goddard III‡

Arthur Amos Noyes Laboratory of Chemical Physics,§ California Institute of Technology, Pasadena, California 91109

(Received 6 February 1969)

The previously developed GI methods have an arbitrary aspect since they are based on a particular representation of the symmetric group. Here we remove this arbitrariness by optimizing the representation, that is, optimizing the spin-coupling scheme simultaneously with the optimization of the orbitals. The resulting wavefunctions, called the spin-coupling optimized GI or SOGI wavefunctions, have all of the general properties of GI wavefunctions including the independent particle interpretation and are found as the solutions to a set of coupled differential equations which differ from the GI equations only in that the equations are constructed from a different representation of the symmetric group. We have applied this method to the ground state and some excited states of Li, to the ground states of Be$^+$ and B^{++} and to the ground state of LiH. In each of these cases, we found that the SOGI wavefunction was only slightly different from the G1 wavefunction and led to very similar energies and other spatial properties. For the spin density at the nucleus, however, SOGI led to much better results. In order to illustrate the effects of spatial symmetry on the SOGI orbitals, we examined the lowest $^1B_{1g}$, $^3A_{2g}$, and ^3E_u states of square H$_4$ and the $^2\Sigma_u{}^+$ state of linear symmetrical H$_3$. We find that in three of these cases optimization of the spin representation is crucial to providing an adequate description of the state. To investigate how the SOGI method would describe chemical reactions, the SOGI wavefunctions were computed for several other nuclear configurations of the H$_3$ system along the reaction path. These calculations showed that the spin coupling changed significantly during the reaction H$_2$+H$\rightleftharpoons$H+H$_2$ and that the variation of the SOGI orbitals provides a clear description of the changes in bonding which occur during this reaction.

I. INTRODUCTION

In Paper I[1] of this series, we considered a set of operators $G_i{}^\mu$ having the property that $G_i{}^\mu\Phi\chi$ is an eigenfunction of $\hat{S}^2$ and satisfies Pauli's principle for arbitrary functions Φ of the spatial coordinates of the N electrons and χ of the spin coordinates. For a given value of S and M_s, we can generally find several, say f^μ, linearly independent spin functions or ways of coupling the individual electron spins. The superscript μ of $G_i{}^\mu$ is determined by the total spin S and the subscript i indicates which of the f^μ coupling schemes is used. The spin functions used in Papers I[1] and II[2] are constructed with Wigner projection operators[3] based on Young's orthogonal irreducible representation[4] of S_N; the construction of this representation is considerably facilitated through the use of Young tableaux.[1,4] The quantity μ corresponds to a Young shape of one or two columns and i corresponds to a particular standard tableau. We will call the spin functions based on Young's orthogonal representation standard spin functions.

We showed in Paper I that, although the f^μ different operators $G_i{}^\mu$ are linearly independent, the exact wavefunction can be written in the form $G_i{}^\mu\Phi\chi$ using any

one $G_i{}^\mu$ operator and a suitable *product* of spin functions in χ if the spatial function Φ is sufficiently general,

$$\Psi^{\text{exact}}=G_i{}^\mu\Phi^{i,\text{exact}}\chi. \tag{1}$$

(The $\Phi^{i,\text{exact}}$ will be different for different values of i.)

In Paper II,[2] we considered a function of the form

$$\Psi_{\text{GI}}=G_i{}^\mu\Phi^{i,\text{product}}\chi, \tag{2}$$

where $\Phi^{i,\text{product}}$ is restricted to be a product of one-electron spatial orbitals and required that these spatial orbitals be the *best possible* ones. The result was a coupled set of integro-differential equations,

$$\hat{H}_k{}^{\mu i}\phi_k=\epsilon_k\phi_k \qquad k=1, 2, \cdots, N \tag{3}$$

for the best orbitals. (The integro-differential-permutational operator $\hat{H}_k{}^{\mu i}$ depends on μ, i, and all the orbitals ϕ_j, except ϕ_k.) Since the orbitals $\{\phi_k\}$ optimize the energy for the wavefunction Ψ_{GI}, they are referred to as the GI orbitals, and the equations (3) for these orbitals are called the GI equations.

Even though the exact wavefunctions can be written in the form of (1) for *any* i, the constraint implied by a product Φ may be more restrictive for some i's than for others; that is, our approximate wavefunction Ψ_{GI} depends on which of the spin-coupling schemes (denoted by i) we have selected. The standard spin functions are used in the GI method because Young's orthogonal representation of S_N is easier to construct than other equivalent representations. This imposes an arbitrary restriction on the wavefunction because there is nothing physically special about the standard spin functions and because we can construct a new $G_i{}^\mu$-like operator, $G_i{}^{\mu L}$, which yields a wavefunction in which the spin part is a general linear combination of

[1] W. A. Goddard III, Phys. Rev. 157, 73 (1967), hereafter referred to as Paper I.
[2] W. A. Goddard III, Phys. Rev. 157, 81 (1967), hereafter referred to as Paper II.
[3] E. P. Wigner, *Group Theory* (Academic Press Inc., New York, 1959), p. 118.
[4] D. E. Rutherford, *Substitutional Analysis* (Edinburgh University Press, Edinburgh, Scotland, 1948).

orthogonal transformation to the representative matrices, $\mathbf{U}^\mu(\tau)$, to obtain

$$\mathbf{U}^{\mu L}(\tau) = \mathbf{L}\mathbf{U}^\mu(\tau)\mathbf{L}^{-1}, \tag{12}$$

where $\mathbf{L}$ is a general orthogonal matrix. We can define new orthogonal units with these transformed matrices

$$O_{ri}{}^{\mu L} = (f^\mu/N!)\sum_{\tau \in S_N} U_{ri(\tau)}{}^{\mu L}\hat{\tau}$$
$$= \sum_{kl} L_{rk}L_{il}O_{kl}{}^\mu, \tag{13a}$$

$$\omega_{ri}{}^{\bar\mu L} = \zeta_{\lambda ri}(f^\mu/N!)\sum_{\sigma \in S_N}\zeta_\sigma U_{ri(\sigma)}{}^{\mu L}\hat\sigma$$
$$= \zeta_{\lambda ri}\sum_{kl}\zeta_{\lambda kl}L_{rk}L_{il}\omega_{ki}{}^{\bar\mu}. \tag{13b}$$

Now we define a new $G_i{}^\mu$-like operator $G_i{}^{\mu L}$ as

$$G_i{}^{\mu L} \equiv \sum_r \zeta_{\lambda ri}O_{ri}{}^{\mu L}\omega_{ri}{}^{\bar\mu L}. \tag{14}$$

Since $\mathbf{L}$ is a completely general rotation, the initial orientation of our spin function (specified by i) is of no consequence, but for the sake of definiteness we will fix i to be 1. Since i is always 1, we will normally omit it and write $G_i{}^{\mu L}$ as $G^{\mu L}$. In discussing a particular system, we will fix μ and omit it thereafter writing G^L for $G^{\mu L}$.

Since the transformed orthogonal units satisfy Eqs. (9) and (10), the arguments of Sec. I of Paper I apply directly to show that $G^{\mu L}\Phi\chi$ is an eigenfunction of S^2 and satisfies Pauli's principle. Similarly from the arguments of Sec. II of Paper I we have that

$$E = \langle G^{\mu L}\Phi\chi \mid H \mid G^{\mu L}\Phi\chi\rangle / \langle G^{\mu L}\Phi\chi \mid G^{\mu L}\Phi\chi\rangle$$
$$= \langle\Phi \mid H \mid O_{11}{}^{\mu L}\Phi\rangle\langle\chi \mid \omega_{ff}{}^{\bar\mu L}\chi\rangle / (\langle\Phi \mid O_{11}{}^{\mu L}\Phi\rangle\langle\chi \mid \omega_{ff}{}^{\bar\mu L}\chi\rangle)$$
$$= \langle\Phi \mid H \mid O_{11}{}^{\mu L}\Phi\rangle / \langle\Phi \mid O_{11}{}^{\mu L}\Phi\rangle. \tag{15}$$

At this point we will restrict Φ to be a product of one-electron spatial orbitals and require that the energy be stationary not only against first-order variations in each orbital but also against first-order variations in $\mathbf{L}$. That is, we require that the spatial orbitals and the spin coupling scheme be optimal simultaneously.

The energy expression can be rewritten as

$$E = \sum_{ij} L_{1i}L_{1j}\langle\Phi \mid H \mid O_{ij}{}^\mu\Phi\rangle / \sum_{kl} L_{1k}L_{1l}\langle\Phi \mid O_{kl}{}^\mu\Phi\rangle. \tag{16}$$

We must minimize the energy subject to the constraints that $\sum_k L_{1k}{}^2 = 1$ and that $\langle\phi_m \mid \phi_m\rangle = 1$ for all m. Therefore we introduce Lagrange multipliers and minimize the expression

$$I = \left(\sum_{ij} L_{1i}L_{1j}\langle\Phi \mid H \mid O_{ij}{}^\mu\Phi\rangle / \sum_{mn} L_{1m}L_{1n}\langle\Phi \mid O_{mn}{}^\mu\Phi\rangle\right) - \sum_k \epsilon_k\langle\phi_k \mid \phi_k\rangle - \lambda\sum_n L_{1n}{}^2. \tag{17a}$$

This leads to a set of $N + f^\mu$ coupled equations for the best Φ and L. The N equations for the best Φ are integro-differential equations and we will call them the spatial SOGI equations. They can be written so that the only permutational operator which appears is the transformed orthogonal unit $O_{11}{}^{\mu L}$. The f^μ equations for the best $\mathbf{L}$ are nonlinear algebraic equations which involve Φ only in the integrals $\langle\Phi \mid H \mid O_{ij}{}^\mu\Phi\rangle$ and $\langle\Phi \mid O_{ij}{}^\mu\Phi\rangle$ and these occur as coefficients; we will refer to these equations as the spin SOGI equations, since $\mathbf{L}$ determines the spin coupling scheme.

When making variations in Φ, we can take the sums over i and j of Eq. (17a) back into the integral to give

$$I = (\langle\Phi \mid H \mid O_{11}{}^{\mu L}\Phi\rangle / \langle\Phi \mid O_{11}{}^{\mu L}\Phi\rangle) + \sum_k \epsilon_k\langle\phi_k \mid \phi_k\rangle + \lambda\sum_n L_{1n}{}^2. \tag{17b}$$

From this expression we obtain the following set of equations, using exactly the arguments of Sec. I of Paper II:

$$H^L(k)\phi_k = \epsilon_{kk}\phi_k \qquad k = 1, 2, \cdots, N, \tag{18}$$

where

$$H^L(k)\phi_k = \left\{ D_k{}^k\hat{h}\phi_k + \sum_{j,v\neq k}\langle v \mid k\rangle D_{jk}{}^k v\hat{h}\phi_j + \sum_{s,u\neq k}\langle s \mid \hat{h} \mid k\rangle D_{uk}{}^{ks}\phi_u + \sum_{uvst\neq k}\langle s \mid \hat{h} \mid t\rangle\langle v \mid k\rangle D_{tku}{}^{svk}\phi_u \right.$$

$$+ \sum_{j,t\neq k}\left[\left(\int\phi_j\hat{g}\phi_t\right)D_{kt}{}^{kj}\phi_k + \left(\int\phi_j\hat{g}\phi_k\right)D_{tk}{}^{kj}\phi_t\right] + \sum_{jstv\neq k}\left(\int\phi_j\hat{g}\phi_t\right)\langle v \mid k\rangle D_{tsk}{}^{jkv}\phi_s$$

$$\left. + \sum_{jstu\neq k}\langle st \mid \hat{g} \mid kj\rangle D_{kju}{}^{stk}\phi_u + \tfrac{1}{2}\sum_{ijstuv\neq k}{}'\langle st \mid \hat{g} \mid ij\rangle\langle v \mid k\rangle D_{ijku}{}^{stvk}\phi_u - E\sum_{u,v\neq k}\langle v \mid k\rangle D_{ku}{}^{vk}\phi_u \right\}. \tag{19}$$

Here we have redefined $D_j{}^i$ to be the coefficient of $\phi_i{}^*(i)\phi_j(i)$ in $\int\Phi^*O_{11}{}^{\mu L}\Phi(dx_i{}')$, $D_{jl}{}^{ik}$ to be the coefficient of $\phi_i{}^*(i)\phi_k{}^*(k)\phi_j(i)\phi_l(k)$ in $\int\Phi^*O_{11}{}^{\mu L}\Phi(dx_{ik}{}'')$, etc. This redefinition of the D matrices is the only difference between the spatial SOGI equations and the GI equations.

If we define $\mathfrak{IC}_{ij} \equiv \langle\Phi \mid H \mid O_{ij}{}^\mu\Phi\rangle$ and $\mathfrak{N}_{ij} \equiv \langle\Phi \mid O_{ij}{}^\mu\Phi\rangle$, the spin SOGI equations are

$$\left[\sum_i L_{1i}(\mathfrak{IC}_{ip} + \mathfrak{IC}_{pi})\right]\left(\sum_{kl} L_{1k}L_{1l}\mathfrak{N}_{kl}\right) - \left(\sum_{ij} L_{1i}L_{1j}\mathfrak{IC}_{ij}\right)\left[\sum_k L_{1k}(\mathfrak{N}_{pk} + \mathfrak{N}_{kp})\right] - 2\lambda L_p\left(\sum_{ij} L_{1i}L_{1j}\mathfrak{N}_{ij}\right)^2 = 0 \qquad p = 1, \cdots f^\mu. \tag{20}$$
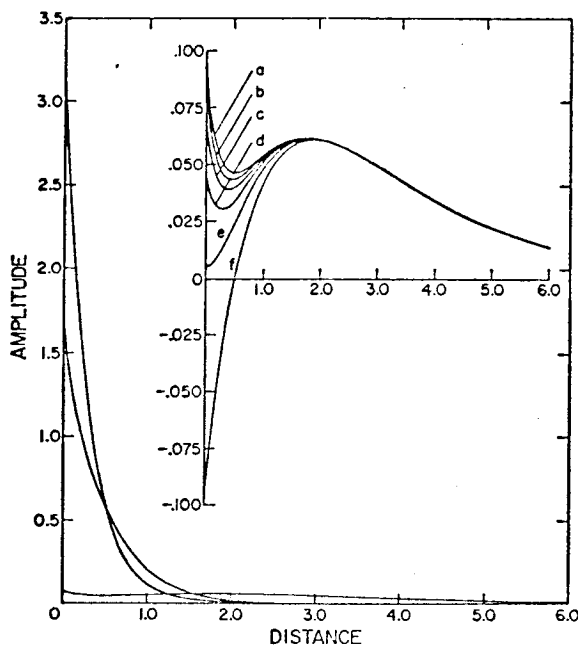
FIG. 1. Orbitals for the $2\,^2S$ state of Li. The large drawing is of the SOGI orbitals ($\Xi=0.434°$); the core orbitals remain essentially unchanged when Ξ is within $10°$ of 0. The insert shows the valence orbital for various values of Ξ; a: $\Xi=0$, b: $\Xi=0.434°$, c: $\Xi=1.0°$, d: $\Xi=2.0°$, e: $\Xi=4.0°$, f: $\Xi=10°$. Distance is in atomic units.

the standard spin functions. The exact wavefunctions can again be written as

$$\Psi^{\text{exact}}=G_i^{\mu L}\Phi^{i,L,\text{exact}}\chi. \tag{4}$$

We now consider approximate wavefunctions of the form

$$\Psi_{\text{GIL}}=G_i^{\mu L}\Phi^{i,L,\text{product}}\chi \tag{5}$$

and select i, L, and $\Phi^{i,L,\text{product}}$ such that the energy is the lowest possible, which leads to a new set of coupled integro-differential equations analogous to (3),

$$\hat{H}_k^{\mu iL}\phi_k=\epsilon_k\phi_k \qquad k=1,\cdots N \tag{6}$$

for the best orbitals. Since this approach is a generalization of the GI method, which eliminates the arbitrariness in choice of spin function and yet retains the independent particle interpretation, we will refer to it as the spin-coupling optimized GI or SOGI method. We will show that the SOGI wavefunction, referred to in (5) as Ψ_{GIL}, is the best possible wavefunction which can be interpreted in terms of N spatial orbitals as if an electron were moving in each orbital in the self-consistent field due to the electrons in the $N-1$ other orbitals. In addition, we will show that the SOGI wavefunction has all the general properties of GI wavefunctions; e.g., the virial, Hellmann–Feynman, Brillouin, and Koopmans theorems still apply[5] (for a fixed spin function). We also show that the SOGI method can be considered as the synthesis of the valence bond and Hartree–Fock methods.

---

[*] W. A. Goddard III, J. Chem. Phys. 48, 5337 (1968).

In Sec. II we derive the general equations for determining the SOGI orbitals and consider some aspects of spatial symmetry restrictions. In order to demonstrate various aspects of the SOGI method we report in Sec. III the results of SOGI calculations on some three- and four-electron atoms and molecules.

II. THE SPIN-COUPLING OPTIMIZED GI METHOD

A. The SOGI Equations

The G_i^μ operators were defined in Paper I by the equation

$$G_i^\mu=\sum_r \zeta_{\lambda_{ri}}O_{ri}^\mu\omega_{\bar{r}i}^{\bar\mu}, \tag{7}$$

where O_{ri}^μ and $\omega_{\bar{r}i}^{\bar\mu}$ are orthogonal Wigner projection operators[3] based on Young's orthogonal representation of S_N, and $\zeta_{\lambda_{ri}}$ is the parity of the permutation λ_{ri} which changes the ith standard Young tableau S_i^μ into the rth standard Young tableau S_r^μ. For a spin-independent Hamiltonian H the energy is given by Eq. (15) of Paper I

$$E=\langle G_i^\mu\Phi\chi\mid H\mid G_i^\mu\Phi\chi\rangle/\langle G_i^\mu\Phi\chi\mid G_i^\mu\Phi\chi\rangle$$
$$=\langle\Phi\mid H\mid O_{ii}^\mu\Phi\rangle/\langle\Phi\mid O_{ii}^\mu\Phi\rangle \tag{8}$$

which results from the fact that the orthogonal units obey the following equations[1,3,4]:

$$O_{ij}^\alpha O_{kl}^\beta=\delta_{\alpha\beta}\delta_{jk}O_{il}^\alpha, \tag{9a}$$

$$\omega_{\bar{i}j}^{\bar\alpha}\omega_{\bar{m}\bar{n}}^{\bar\mu}=\delta_{\alpha\mu}\delta_{jm}\omega_{\bar{i}\bar{n}}^{\bar\mu} \tag{9b}$$

and

$$\langle O_{ij}^\mu\Phi_1\mid\Phi_2\rangle=\langle\Phi_1\mid O_{ji}^\mu\Phi_2\rangle, \tag{10a}$$

$$\langle\omega_{\bar{m}\bar{n}}^{\bar\alpha}\chi_1\mid\chi_2\rangle=\langle\chi_1\mid\omega_{\bar{n}\bar{m}}^{\bar\alpha}\chi_2\rangle. \tag{10b}$$

The orthogonal units are defined by[1,3,4]

$$O_{ri}^\mu=(f^\mu/N!)\sum_{\tau\in S_N}U_{ri(\tau)}^\mu\hat\tau, \tag{11a}$$

$$\omega_{\bar{r}i}^{\bar\mu}=\zeta_{\lambda_{ri}}(f^\mu/N!)\sum_{\sigma\in S_N}\zeta_\sigma U_{ri(\sigma)}^\mu\hat\sigma, \tag{11b}$$

where the $U^\mu(\tau)$ are orthogonal matrices which yield the μth irreducible representation of S_N. Picking a set of representative matrices is equivalent to picking a set of orthogonal (not necessarily normalized) basis vectors in the f^μ-dimensional space of spin functions. A convenient way of constructing the U^μ's is described in Paper I and involves the use of Young tableaux. The arbitrariness in the GI method results from choosing our one spin function to be one of the arbitrarily chosen basis vectors in the f^μ-dimensional space of spin functions. This arbitrariness can be removed by allowing for a general rotation of the coordinate axes in our space of spin functions. We will require that this rotation give the best single spin function possible. We now derive the necessary equations for finding this optimum spin function.

The rotation is most easily obtained by applying an

orthogonal transformation to the representative matrices, $\mathbf{U}^\mu(\tau)$, to obtain

$$\mathbf{U}^{\mu L}(\tau) = \mathbf{L}\mathbf{U}^\mu(\tau)\mathbf{L}^{-1}, \qquad (12)$$

where $\mathbf{L}$ is a general orthogonal matrix. We can define new orthogonal units with these transformed matrices

$$O_{ri}{}^{\mu L} = (f^\mu/N!) \sum_{\tau \in S_N} U_{ri(\tau)}{}^{\mu L} \hat{\tau}$$

$$= \sum_{kl} L_{rl} L_{il} O_{kl}{}^\mu, \qquad (13a)$$

$$\omega_{\bar{r}i}{}^{\bar{\mu}L} = \zeta_{\lambda_{ri}}(f^\mu/N!) \sum_{\sigma \in S_N} \zeta_\sigma U_{ri(\sigma)}{}^{\mu L} \hat{\sigma}$$

$$= \zeta_{\lambda ri} \sum_{kl} \zeta_{\lambda kl} L_{rl} L_{il} \omega_{\bar{k}l}{}^{\bar{\mu}}. \qquad (13b)$$

Now we define a new $G_i{}^\mu$-like operator $G_i{}^{\mu L}$ as

$$G_i{}^{\mu L} = \sum_r \zeta_{\lambda ri} O_{ri}{}^{\mu L} \omega_{\bar{r}i}{}^{\bar{\mu}L}. \qquad (14)$$

Since $\mathbf{L}$ is a completely general rotation, the initial orientation of our spin function (specified by i) is of no consequence, but for the sake of definiteness we will fix i to be 1. Since i is always 1, we will normally omit it and write $G_i{}^{\mu L}$ as $G^{\mu L}$. In discussing a particular system, we will fix μ and omit it thereafter writing G^L for $G^{\mu L}$.

Since the transformed orthogonal units satisfy Eqs. (9) and (10), the arguments of Sec. I of Paper I apply directly to show that $G^{\mu L}\Phi\chi$ is an eigenfunction of S^2 and satisfies Pauli's principle. Similarly from the arguments of Sec. II of Paper I we have that

$$E = \langle G^{\mu L}\Phi\chi \mid H \mid G^{\mu L}\Phi\chi \rangle / \langle G^{\mu L}\Phi\chi \mid G^{\mu L}\Phi\chi \rangle$$

$$= \langle \Phi \mid H \mid O_{11}{}^{\mu L}\Phi \rangle \langle \chi \mid \omega_{\bar{1}\bar{1}}{}^{\bar{\mu}L}\chi \rangle / (\langle \Phi \mid O_{11}{}^{\mu L}\Phi \rangle \langle \chi \mid \omega_{\bar{1}\bar{1}}{}^{\bar{\mu}L}\chi \rangle)$$

$$= \langle \Phi \mid H \mid O_{11}{}^{\mu L}\Phi \rangle / \langle \Phi \mid O_{11}{}^{\mu L}\Phi \rangle. \qquad (15)$$

At this point we will restrict Φ to be a product of one-electron spatial orbitals and require that the energy be stationary not only against first-order variations in each orbital but also against first-order variations in $\mathbf{L}$. That is, we require that the spatial orbitals and the spin coupling scheme be optimal simultaneously.

The energy expression can be rewritten as

$$E = \sum_{ij} L_{1i} L_{1j} \langle \Phi \mid H \mid O_{ij}{}^\mu \Phi \rangle / \sum_{kl} L_{1k} L_{1l} \langle \Phi \mid O_{kl}{}^\mu \Phi \rangle. \qquad (16)$$

We must minimize the energy subject to the constraints that $\sum_k L_{1k}{}^2 = 1$ and that $\langle \phi_m \mid \phi_m \rangle = 1$ for all m. Therefore we introduce Lagrange multipliers and minimize the expression

$$I = \left(\sum_{ij} L_{1i} L_{1j} \langle \Phi \mid H \mid O_{ij}{}^\mu \Phi \rangle / \sum_{mn} L_{1m} L_{1n} \langle \Phi \mid O_{mn}{}^\mu \Phi \rangle \right) - \sum_k \epsilon_k \langle \phi_k \mid \phi_k \rangle - \lambda \sum_n L_{1n}{}^2. \qquad (17a)$$

This leads to a set of $N + f^\mu$ coupled equations for the best Φ and $\mathbf{L}$. The N equations for the best Φ are integro-differential equations and we will call them the spatial SOGI equations. They can be written so that the only permutational operator which appears is the transformed orthogonal unit $O_{11}{}^{\mu L}$. The f^μ equations for the best $\mathbf{L}$ are nonlinear algebraic equations which involve Φ only in the integrals $\langle \Phi \mid H \mid O_{ij}{}^\mu\Phi \rangle$ and $\langle \Phi \mid O_{ij}{}^\mu\Phi \rangle$ and these occur as coefficients; we will refer to these equations as the spin SOGI equations, since $\mathbf{L}$ determines the spin coupling scheme.

When making variations in Φ, we can take the sums over i and j of Eq. (17a) back into the integral to give

$$I = (\langle \Phi \mid H \mid O_{11}{}^{\mu L}\Phi \rangle / \langle \Phi \mid O_{11}{}^{\mu L}\Phi \rangle) + \sum_k \epsilon_k \langle \phi_k \mid \phi_k \rangle + \lambda \sum_n L_{1n}{}^2. \qquad (17b)$$

From this expression we obtain the following set of equations, using exactly the arguments of Sec. I of Paper II:

$$H^L(k)\phi_k = \epsilon_k \phi_k \qquad k = 1, 2, \cdots, N, \qquad (18)$$

where

$$H^L(k)\phi_k = \left\{ D_k{}^k \hat{h}\phi_k + \sum_{j,i \neq k} \langle i \mid k \rangle D_{jk}{}^k \hat{h}\phi_j + \sum_{s,i \neq k} \langle s \mid \hat{h} \mid k \rangle D_{ks}{}^k \phi_i + \sum_{u,s,i \neq k} \langle s \mid \hat{h} \mid t \rangle \langle i \mid k \rangle D_{sit}{}^{sk}\phi_u \right.$$

$$+ \sum_{j,i \neq k} \left[\left(\int \phi_j{}^*\hat{g}\phi_i \right) D_{ik}{}^k\phi_i + \left(\int \phi_j{}^*\hat{g}\phi_i \right) D_{ik}{}^k\phi_i \right] + \sum_{j,i \neq k} \left(\int \phi_j{}^*\hat{g}\phi_i \right) \langle i \mid k \rangle D_{ik}{}^{jk}\phi_i$$

$$+ \sum_{j,i \neq k} \langle si \mid \hat{g} \mid kj \rangle D_{kj i}{}^{sij}\phi_i + \frac{1}{2} \sum_{ij,s \neq k}{}' \langle si \mid \hat{g} \mid ij \rangle \langle i \mid k \rangle D_{sij}{}^{sijk}\phi_i - E \sum_{i,v \neq k} \langle i \mid k \rangle D_{iv}{}^k\phi_i \right\}. \qquad (19)$$

Here we have redefined $D_j{}^i$ to be the coefficient of $\phi_i{}^*(i)\phi_j(i)$ in $\int \Phi^* O_{11}{}^{\mu L}\Phi(dx')$, $D_{jl}{}^{ik}$ to be the coefficient of $\phi_i{}^*(i)\phi_k{}^*(k)\phi_j(i)\phi_l(k)$ in $\int \Phi^* O_{11}{}^{\mu L}\Phi(dx'')$, etc. This redefinition of the D matrices is the only difference between the spatial SOGI equations and the GI equations.

If we define $\mathcal{H}_{ij} = \langle \Phi \mid H \mid O_{ij}\Phi \rangle$ and $\mathcal{S}_{ij} = \langle \Phi \mid O_{ij}\Phi \rangle$, the spin SOGI equations are

$$\left[\sum_i L_{1i}(\delta\mathcal{H}_{ip} + \delta\mathcal{H}_{pi}) \right] \left(\sum_{kl} L_{1k} L_{1l} \mathcal{S}_{kl} \right) - \left(\sum_{ij} L_{1i} L_{1j} \mathcal{H}_{ij} \right) \left[\sum_k L_{1k}(\mathcal{S}_{kp} + \mathcal{S}_{pk}) \right] - 2\lambda_s \left(\sum_{ij} L_{1i} L_{1j} \mathcal{S}_{ij} \right)^2 = 0 \qquad p = 1, \cdots, f. \qquad (20)$$
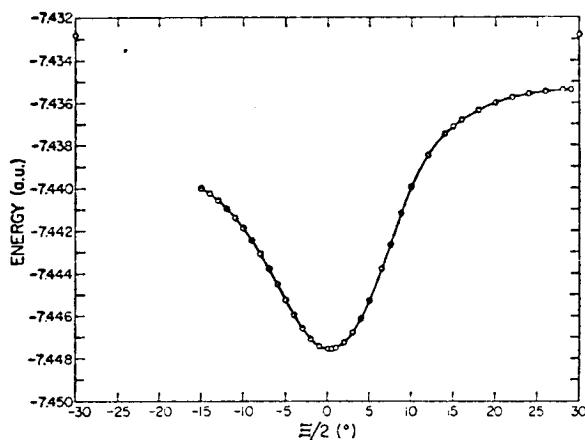
FIG. 2. Energy as a function on representation parameter, Ξ, for the 2^2S state of Li.

These equations are simple nonlinear algebraic equations. Since they involve $\mathfrak{IC}_{ij}$ and $\mathfrak{N}_{ij}$ for all i and j, and since the evaluation of all of these quantities frequently requires a great deal of effort, it will often be expedient to find the optimum L by actually calculating the energy for various values of the parameters of L until a minimum is found.

B. The Independent Particle Interpretation and Other Properties of SOGI Wavefunctions

Each $H^L(k)$ operator in (18) is equivalent to the Hamiltonian of an electron moving in the (nonlocal) field due to electrons in the $N-1$ other orbitals. Since ϕ_k is an eigenfunction of this operator, we can interpret each ϕ_k as the eigenstate of an electron moving in the field due to $N-1$ other electrons. That is, the SOGI orbitals can be given an independent particle interpretation (IPI) just as the GI orbitals were.[2]

In the independent particle interpretation we interpret each spatial orbital of the N-electron wavefunction as the eigenstate of an electron moving in the average (self-consistent) potential due to electrons in the other $N-1$ orbitals. The criteria we use for such an independent particle interpretation are the following: (i) There must be no more than N different spatial orbitals since there are only N electrons. (ii) Each spatial orbital must be an eigenfunction of an operator equivalent to the Hamiltonian for an electron moving in the field due to the nuclei and in some average field due to electrons in the other $N-1$ orbitals. (iii) This average field in (ii) can be nonlocal but it must be obtained directly from applying the variational principle to the energy. As discussed elsewhere[2] the Hartree-Fock, UHF, and GI wavefunctions satisfy these criteria and can be given an independent particle interpretation (IPI). However configuration-interaction (CI) and

multiconfiguration SCF[6] (MC-SCF) wavefunctions do not satisfy (ii) and usually not (i) and cannot be given the IPI. In addition extended Hartree-Fock methods which use spatial projection operators[7] do not necessarily satisfy (i) [e.g., for H_2 such a wavefunction[7] might involve two σ orbitals, four π orbitals (two π_x and two π_y), four δ orbitals, etc.] and thus cannot be given the above IPI. In the valence bond (VB) wavefunction,[8] (i) is satisfied but the orbitals are not functionally optimized so that (ii) and (iii) are not satisfied and the VB wavefunction cannot be given the IPI. However we have shown[9] that the G1 wavefunction corresponds to a generalization of the VB wavefunction in which all orthogonality and double occupation constraints are removed and the orbitals are functionally optimized, and thus the G1 method is the direct generalization of the VB method which does lead to the IPI.

The criteria in (i)–(iii) are sufficient to require that the many-electron wavefunction be expressible as a product of N spatial orbitals and a suitable spin function with this perhaps operated on with an operator which does not change the form of the orbitals (if they were changed the space spanned by the orbitals would in general enlarge to dimensions larger than N). Thus the operator may involve permutations but not spatial projection operators. If all the orbitals in Φ are allowed to be different the operator must take care of both the spin symmetry and Pauli principle. The most general operator which does this and nothing more is
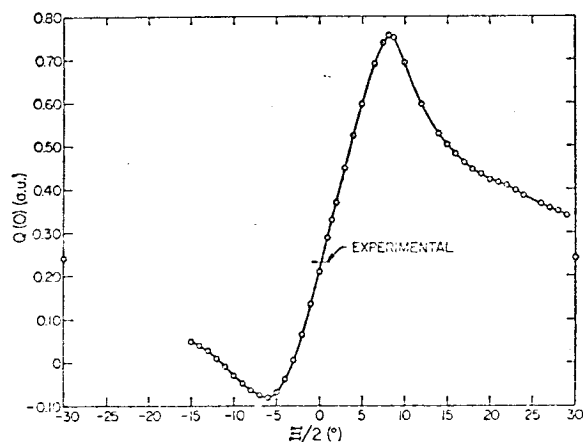
$$\sum_i c_i G_i^\mu,$$

FIG. 3. Spin density at the nucleus, $Q(0)$, as a function of representation parameter Ξ for the 2^2S state of Li.

[6] G. Das and A. C. Wahl, J. Chem. Phys. 44, 87 (1966); A. C. Wahl, P. J. Bertoncini, G. Das, and T. L. Gilbert, Intern. J. Quant. Chem. 1S, 123 (1967).
[7] E. R. Davidson and L. L. Jones, J. Chem. Phys. 37, 2966 (1962); C. F. Bunge, Phys. Rev. 154, 70 (1967).
[8] H. Eyring, J. Walter, and G. E. Kimball, Quantum Chemistry (John Wiley & Sons, Inc., New York, 1944), p. 218.
[9] W. A. Goddard III, Phys. Rev. 169, 120 (1968).

where the c_i are arbitrary. But from Appendix C of Paper I we have[10]

$$G_i^\mu \Phi \chi = f^\mu \mathcal{Q}[\Phi(\omega_{ii}^\mu \chi)], \qquad (21a)$$

and thus we have

$$\sum_i G_i^\mu \Phi \chi = f^\mu \mathcal{Q}[\Phi(\sum_i c_i \omega_{ii}^\mu \chi)]. \qquad (21b)$$

But $\sum_i c_i \omega_{ii}^\mu \chi$ is just some arbitrary vector in the f^μ-dimensional spin space and hence can be written as

$$\sum_i c_i \omega_{ii}^\mu \chi = \omega_{11}^{L\mu} \chi$$

in terms of the L-transformed representation. Thus

$$\sum_i c_i G_i^\mu \Phi \chi = f^\mu \mathcal{Q}[\Phi(\sum_i c_i \omega_{ii}^\mu \chi)]$$

$$= G^{\mu L} \Phi \chi, \qquad (21c)$$

and the SOGI wavefunction is the optimum wavefunction yielding the above described independent particle interpretation.

In the early years of the application of quantum mechanics, two popular types of wavefunctions were the MO and valence-bond (VB) or Heitler–London wavefunctions where the MO wavefunction was just a special case of HF using a minimum set of basis functions. Since these methods led to somewhat different wavefunctions, questions concerning which was best arose. This was partly settled by Van Vleck and Sherman[11] who showed that starting with either function inclusion of sufficient other configurations would eventually lead to the same final wavefunction. For example, for H_2 with a minimum basis set, the VB and HF wavefunctions are both special cases of the Weinbaum[12]
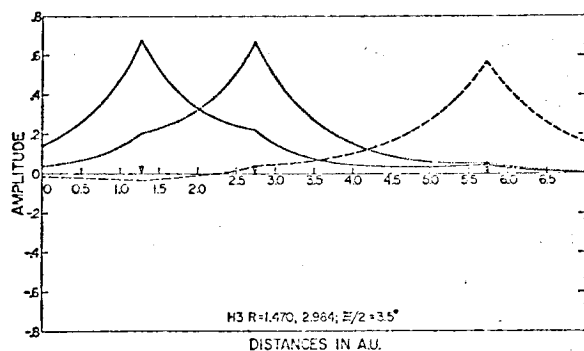

FIG. 4. SOGI orbitals for H_3: $R_{AB} = 1.470$, $R_{BC} = 2.984$; $\Xi/2 = 3.5°$. —— orbital 1, ··· orbital 2, --- orbital 3.

[10] $\mathcal{Q}$ is the antisymmetrizer,

$$\mathcal{Q} = (1/N!) \sum_\tau \zeta_\tau \tau,$$

where τ operates on both spatial and spin coordinates and ζ_τ is the parity of τ.

[11] J. H. Van Vleck and A. Sherman, Rev. Mod. Phys. 7, 167 (1935).
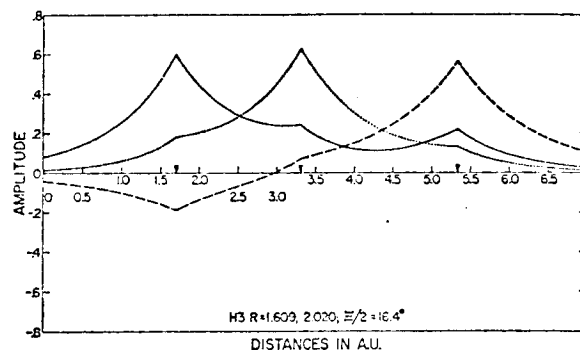[12] S. Weinbaum, J. Chem. Phys. 1, 593 (1933); C. A. Coulson and I. Fischer, Phil. Mag. 40, 386 (1949).

FIG. 5. SOGI orbitals for H_3: $R_{AB} = 1.609$, $R_{BC} = 2.020$; $\Xi/2 = 16.4°$. —— orbital 1, ··· orbital 2, --- orbital 3.

wavefunction. However the Weinbaum wavefunction for H_2 is equivalent to the SOGI wavefunction for a minimum basis set (also equivalent to G1 and GF).[2] In fact for any number of electrons the VB (or Heitler–London) and HF methods and their natural generalizations the G1 and GF methods are special cases of the SOGI method. Hence we can consider the SOGI wavefunction as the generalization and synthesis of the HF and VB or Heitler–London methods which in addition still yields an interpretation in terms of independent particle states.

In addition to the IPI all other general properties of GI wavefunctions (e.g., the Hellmann–Feynman, Brillouin, virial, and Koopmans theorems[5]) hold also for the SOGI wavefunction (for fixed L) as can be seen in Ref. 5.

Wavefunctions of the form

$$\mathcal{Q}[\Phi(\sum_i c_i \Theta_i)], \qquad (21d)$$

where Θ_i are the orthogonal spin coupling functions and Φ is a product of orbitals that have been dealt with by several other workers. Lunell[13] has solved for the wavefunction of the ground state Li using a form like (21d) where he optimized both the C_i and one of the orbitals of Φ and Kaldor[14] has solved for both the $2\,^2S$ and $2\,^2P$ states of Li using a wavefunction of the form (21d) with optimized orbitals. By (21b) and (21c) Kaldor's wavefunction can be considered as a SOGI wavefunction and Lunell's is a special case in which the orbitals were not all solved for self-consistency. In addition Musher[15a] has taken published G1 and GF calculations for Li and calculated the coefficients C_i in (21d) without reoptimizing the orbitals, and Taylor and Harris[15b] have optimized the coefficients C_i in (21d) for several systems without functionally optimizing the orbitals.

[13] S. Lunell, Phys. Rev. 173, 85 (1968).
[14] U. Kaldor (private communication).
[15] (a) J. Musher (to be published); (b) H. S. Taylor, J. Chem. Phys. 39, 3382 (1963); H. S. Taylor and F. Harris, ibid. 1012 (1963).
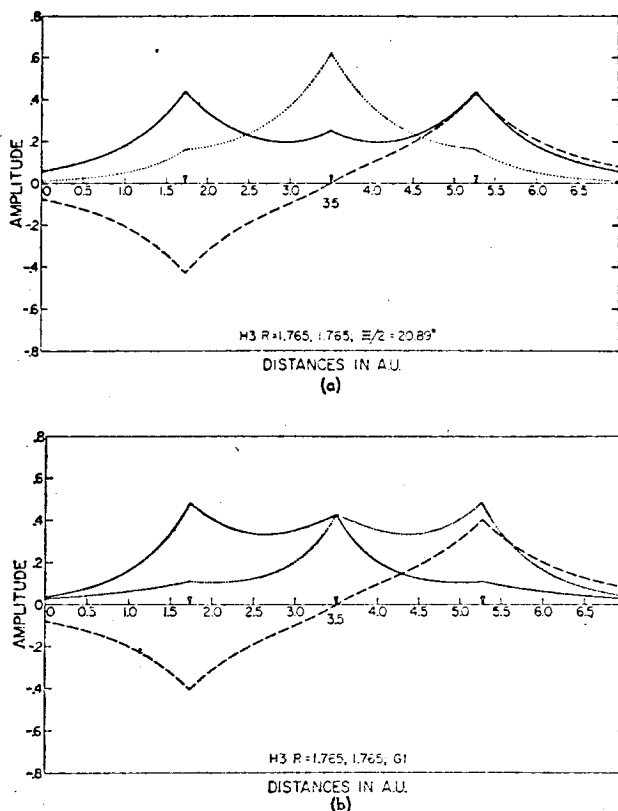
FIG. 6. (a) SOGI orbitals for the saddle point of H_3: $R_{AB} = R_{BC} = 1.765$, $\Xi/2 = 20.89°$. —— orbital 1, $\cdots$ orbital 2, $---$ orbital 3. (b) Optimum left–right correlated (G1) orbitals for the saddle point of H_3: $R_{AB} = R_{BC} = 1.765$, —— orbital 1, $\cdots$ orbital 2, $---$ orbital 3.

C. Spatial Symmetry

Although the SOGI wavefunction has the correct spin and permutational symmetry, we must also ensure that our SOGI many-electron wavefunction transforms as a basis function for some irreducible representation of the group $\mathcal{G}$ of spatial transformations which leave the nuclei unchanged. Just as for GI,[2,5] in some cases the SOGI orbitals are symmetry functions[16] for $\mathcal{G}$ and in some cases they have lower symmetry. In addition, if the SOGI orbitals are *not* symmetry functions for $\mathcal{G}$, there may be some constraints on L in order that the many-electron wavefunctions have the correct symmetry.

We will consider only spatially nondegenerate states for which $\hat{R}\Psi_{\text{SOGI}} = \pm\Psi_{\text{SOGI}}$ where $\hat{R}$ is some symmetry operation. Since $\hat{R}$ is symmetric in the electron coordinates, it commutes with $\mathcal{G}$ and $O_{11}{}^{\mu L}$ and we have that

$$\hat{R}\Psi_{\text{SOGI}} = \mathcal{G}[(O_{11}{}^{\mu L}(\hat{R}\Phi))\chi]. \tag{22}$$

Let $\hat{R}$ be a generator of $\mathcal{G}$ for which $\hat{R}\Psi_{\text{SOGI}} = +\Psi_{\text{SOGI}}$, then

$$\mathcal{G}[(O_{11}{}^{\mu L}(\hat{R}\Phi))\chi] = \mathcal{G}[(O_{11}{}^{\mu L}\Phi)\chi]. \tag{23}$$

---

[16] By a symmetry function for $\mathcal{G}$ we mean a basis function for an irreducible representation of $\mathcal{G}$.

This equation can usually be satisfied if Φ is composed of symmetry functions, but this is not a necessary condition. Suppose that Φ is constructed from orbitals which are symmetry functions of the subgroup $\mathcal{G}'$ which is obtained by deleting the generator $\hat{R}$ from $\mathcal{G}$. Further suppose that Φ is such that the effect of $\hat{R}$ is merely to interchange the orbitals among themselves; that is, $\hat{R}\Phi = \pm\hat{\tau}_R\Phi$ where τ_R is some permutation. Now if $O_{11}{}^{\mu L}\tau_R = \pm O_{11}{}^{\mu L}$, Eq. (23) is satisfied despite the fact that the orbitals of Φ are symmetry functions only of the subgroup $\mathcal{G}'$. If $\hat{R}$ is such that $\hat{R}\Psi = -\Psi$, we have the same results if $\hat{R}\Phi = \pm\tau_R\Phi$ and $O_{11}{}^{\mu L}\tau_R = \mp O_{11}{}^{\mu L}$.

To see what condition this imposes on L, we expand τ_R in terms of the transformed orthogonal units (letting L^α be the f^α-dimensional unit matrix if $\alpha \neq \gamma$, and $L^\mu = L$)

$$\tau_R = \sum_{ij\alpha} O_{ij}{}^{\alpha L^\alpha} U_{ij}{}^{\alpha L^\alpha}(\tau_R), \tag{24}$$

then

$$O_{11}{}^{\mu L}\tau_R = O_{11}{}^{\mu L}\sum_{ij\alpha} U_{ij}{}^{\alpha L^\alpha}(\tau_R)O_{ij}{}^{\alpha L^\alpha}$$

$$= \sum_j O_{1j}{}^{\mu L}U_{1j}{}^{\mu L}(\tau_R). \tag{25}$$

Since the $O_{ij}{}^{\mu L}$ are linearly independent, we have that $O_{ii}{}^{\mu L}\hat{\tau}_R = \pm O_{11}{}^{\mu L}$ only if $U_{1j}{}^{\mu L}(\tau_R) = \delta_{ij}$, which imposes one constraint on L. Under some circumstances this condition cannot be satisfied, in which case the SOGI orbitals must be symmetry functions. In many cases, however, the condition on L can be satisfied and the use of nonsymmetry orbitals is possible. Some examples will be considered in the discussion of the H_3 and H_4 calculations below.

Consider a molecular system such as linear, equidistant H_3 which is stretched or compressed symmetrically. For large spacing, it is energetically favorable for orbitals to localize about the various nuclei, and we expect the SOGI wavefunction to have a spin part (L) which allows this localization and a spatial part composed of permutationally related nonsymmetry functions (an orbital on each H). For small internuclear distances, delocalization of the orbitals is energetically favorable, and we expect the SOGI wavefunction to have a spatial part composed of symmetry functions and a completely general spin part. This means that, for systems which are pulled apart symmetrically, there will be a discontinuity in the slope of the energy vs distances curve where we switch from localized to delocalized bonding. Although this discontinuity of slope is not a real effect, it is interesting to see how the ideas of localized and delocalized independent particle states arise naturally and how a choice can be made for each system on purely energetic grounds. In polyatomic systems, the physically interesting processes usually do not involve symmetrical dissociations so that the discontinuity of slope is of little physical or chemical consequence. However, such
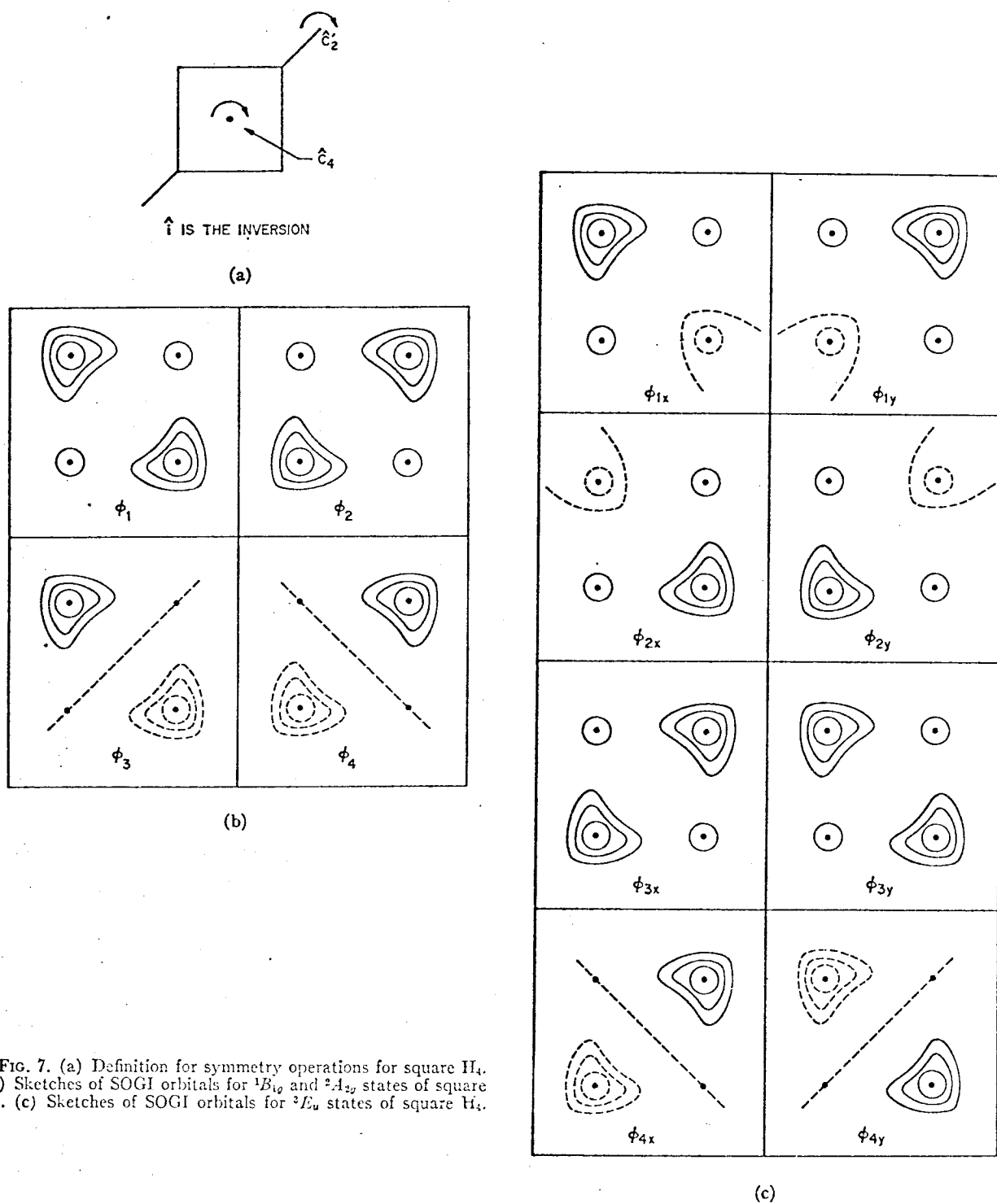
FIG. 7. (a) Definition for symmetry operations for square H_4. (b) Sketches of SOGI orbitals for $^1B_{1g}$ and $^2A_{2g}$ states of square H_4. (c) Sketches of SOGI orbitals for ^2E_u states of square H_4.

R. C. LADNER AND W. A. GODDARD III

TABLE I. SOGI and G1 wavefunctions for the ground state of Li ($\Xi/2 = 0.217° \pm 0.001°$).

Function	ζ	ϕ_1SOGI	ϕ_1G1	ϕ_2SOGI	ϕ_2G1	ϕ_3SOGI	ϕ_3G1
1s	3.0	1.14368	1.14370	0.60987	0.60984	0.02804	0.03189
4s	5.33	−0.10348	−0.10348	0.12715	0.12709	−0.00228	−0.00208
3s	5.40	−0.07808	−0.07810	0.07854	0.07853	0.00060	0.00069
3s	3.00	0.00542	0.00550	0.27260	0.27246	0.02045	0.02124
3s	1.347	0.01569	0.01549	−0.00398	−0.00362	0.28602	0.28571
3s	0.841	−0.00255	−0.00292	−0.00004	0.00063	0.63560	0.63501
4s	0.732	0.03458	0.03446	−0.01551	−0.01531	0.06863	0.06854
3s	0.62	−0.03799	−0.03793	0.01738	0.01731	0.05573	0.05576
ϵ (orbital energy)		−2.84409	−2.8427	−2.46128	−2.4588	−0.19616	−0.19615

transitions are of theoretical interest and have been suggested by Mott[17] to be relevant in the discussion of conduction and other properties of such solids as NiO. Since the SOGI wavefunctions dissociate correctly and can naturally lead directly to either localized or delocalized orbitals without requiring additional Wannier-like localizations as in the HF method, it would seem that the SOGI wavefunctions would form a suitable foundation on which to discuss ideas such as the Mott transition.

III. RESULTS AND DISCUSSIONS

Since the spatial SOGI equations are of exactly the same form as the G1 equations, we solve them in the same way. We expand the unknown orbitals in terms of a finite basis set

$$\phi_i = \sum_\mu \chi_\mu C_{\mu i} \qquad (26)$$

and solve for the coefficients iteratively. (The equations could also be solved numerically.) Existing three- and four-electron G1 programs were adapted to do SOGI calculations by changing only the sections which calculate the D matrices.

A. Three-Electron Doublet States

First we will consider some three-electron doublet states. In this case there are two linearly independent spin states, $f^\mu = 2$. The standard representation is given in Paper I (Appendix A) and the general transformations L to new spin functions is given by

$$L(\Xi) = \begin{pmatrix} \cos(\Xi/2) & \sin(\Xi/2) \\ -\sin(\Xi/2) & \cos(\Xi/2) \end{pmatrix}. \qquad (27)$$

Thus in addition to optimizing the three orbitals ϕ_a, ϕ_b, and ϕ_c, we must optimize the single parameter Ξ, which

just corresponds to a rotation angle in the two-dimensional space of spin functions. From (21) we have that

$$G^{\mu L}\Phi\chi = f^\mu \alpha (\Phi \omega_{ff}{}^{\mu L}\chi) \qquad (28)$$

or expanding ω

$$G^{\mu L}\phi_a\phi_b\phi_c\alpha\beta\alpha = \tfrac{2}{3}\alpha\{\phi_a\phi_b\phi_c[\alpha\beta\alpha(1+\tfrac{1}{2}\cos\Xi+\tfrac{1}{2}\sqrt{3}\sin\Xi)$$
$$+\alpha\alpha\beta(-\tfrac{1}{2}+\tfrac{1}{2}\cos\Xi-\tfrac{1}{2}\sqrt{3}\sin\Xi)+\beta\alpha\alpha(-\tfrac{1}{2}-\cos\Xi)]\}. \qquad (29)$$

In (27) we have that $L(\Xi+360°) = -L(\Xi)$; however in (29) we see that Ξ, $\Xi+120°$, and $\Xi+240°$ lead to equivalent wavefunctions if we interchange the orbitals appropriately. Thus we need consider only a 120° range of Ξ, which we will usually take as −60° to +60°. If $\Xi=0$ we have

$$G^{\mu L}\phi_a\phi_b\phi_c\alpha\beta\alpha = G_1{}^\mu\phi_a\phi_b\phi_c\alpha\beta\alpha \qquad (30a)$$

and by optimizing the orbitals we get the G1 wavefunction. If $\Xi=60°$,

$$G^{\mu L}\phi_a\phi_b\phi_c\alpha\beta\alpha = -G_f{}^\mu\phi_a\phi_c\phi_b\alpha\alpha\beta, \qquad (30b)$$

and by optimizing the orbitals we get the GF wavefunction [note that in (30b) the roles of the second and third orbitals are interchanged]. If $\Xi=-60°$ we obtain

$$G^{\mu L}\phi_a\phi_b\phi_c\alpha\beta\alpha = \tfrac{1}{2}G_f{}^\mu\phi_c\phi_b\phi_a\alpha\alpha\beta \qquad (30c)$$

and by optimizing the orbitals we again get the GF wavefunction (here the roles of the first and third orbitals have been interchanged). Thus by varying Ξ we can go continuously from G1 to GF. We will find below that in most cases the optimum angle Ξ is near zero and the G1 wavefunction is nearly as good as the SOGI wavefunction. However, for H₃ near the transition states the optimum angle Ξ is significantly different from zero.

---

[17] N. F. Mott, Proc. Phys. Soc. (London) A62, 416 (1949).

QUANTUM THEORY OF MANY-ELECTRON SYSTEMS. V

TABLE II. Properties for three-electron atoms (entries for GF, HF, UHF, CI, and experimental are taken directly from Ref. 19).

	G1	SOGI	GF	HF	CI	Exptl
			A. Energies			
2^2S Li	−7.44756038	−7.44756516	−7.432813	−7.432725	−7.4779	−7.47807
3^2S Li	−7.32517867	−7.32517894	−7.310216	−7.310210	···	−7.35410
2^2P Li	−7.38011191	−7.38011631	−7.365091	−7.365069	−7.40838	−7.41016
3^2P Li	−7.30819798	−7.30819844	−7.293189	−7.293186	···	−7.33715
2^2S Be$^+$	−14.29162398	−14.29163664	−14.27762	···	···	···
2^2S B^{++}	−23.38990151	−23.38991969	−23.37632	···	···	···

	G1	SOGI	GF	HF	UHF	
			B. Density at the nucleus, $\langle \sum_i \delta(r_i) \rangle$			
2^2S Li	13.8646	13.8646	13.8159	13.8160	13.8159	
3^2S Li	13.7594	13.7594	13.7067	13.7080	13.7067	
2^2P Li	13.7052	13.7052	13.6534	13.6534	13.6535	
3^2P Li	13.7179	13.7180	13.6661	13.6660	13.6661	
2^2S Be$^+$	35.1392	35.1392	35.111	···	···	
2^2S B^{++}	71.4976	71.4975	71.493	···	····	

	G1	SOGI	GF	HF	UHF	CI	Exptl
			C. Spin density at the nucleus, $Q(0) = 2\langle \sum_i \delta(r_i)\hat{s}_z(\sigma_i) \rangle$				
2^2S Li	0.20957	0.22654±0.0001	0.2406	0.1667	0.2248	0.2249	0.2313
3^2S Li	0.04873	0.0529	0.05622	0.03864	0.05253	···	···
2^2P Li	0.0	−0.0172	−0.02304	0.0	−0.01747	−0.02222	
3^2P Li	0.0	−0.00547±0.0001	−0.007318	0.0	−0.005531	···	···
2^2S Be$^+$	0.94671	0.9938±0.0015	1.008	···	···	···	···
2^2S B^{++}	2.4303	2.516±0.001	2.521	···	···	···	···

	G1	SOGI	GF	HF	UHF	CI	
			D. Orbital dipole constant, $\langle \sum_i [l_z(r_i)/r_i^3] \rangle$				
2^2P Li	0.058693	0.058725	0.05861	0.05848	0.05852	a	
3^2P Li	0.0176467	0.017649	0.01760	0.01759	0.01760	···	

	G1	SOGI	GF	HF	
			E. Second moment of r, $\langle \sum_i r_i^2 \rangle$		
2^2S Li	18.6642	18.6626	18.6090	18.6376	
3^2S Li	119.571	119.569	119.447	119.480	
2^2P Li	28.690	28.685	28.692	28.716	
3^2P Li	172.203	172.198	172.511	172.536	
2^2S Be$^+$	6.559	6.559	6.545 ·	···	
2^2S B^{++}	3.4135	3.4135	3.4094	···	

[a] $(1/r^3)_{orb} = 0.05974$, $(1/r^3)_{dip} = 0.05923$.

R. C. LADNER AND W. A. GODDARD III

TABLE III. Optimum values of Ξ for three-electron atoms.

		Optimum Ξ (deg)
Li	2^2S	0.434 ± 0.002
Li	3^2S	0.098 ± 0.001
Li	2^2P	-0.396 ± 0.001
Li	3^2P	-0.118 ± 0.002
Be$^+$	2^2S	0.626 ± 0.004
B^{++}	2^2S	0.680 ± 0.008

1. Three-Electron Atoms and Ions

Calculations were carried out on the ground states ($2\,^2S$) of Li, Be$^+$, and B^{++} and on the $3\,^2S$, $2\,^2P$, and $3\,^2P$ excited states of Li.

Both G1[9] and GF[13] calculations for the ground states ($2\,^2S$) of Li, Be$^+$, and B^{++} have been reported elsewhere. GF calculations for the excited states of Li[19] have also been reported. Here we use similar but slightly larger basis sets of 7 to 9 Slater orbitals, chosen so that the cusp condition is satisfied exactly.[20] For a given nuclear charge, the core orbitals of all states can be described well by four or five functions. Once the orbital exponents of these functions have been optimized for one state, they can be transferred to other states and only the exponents of functions used in describing the valence orbital need to be reoptimized. The orbital exponents of the s functions were optimized for G1, and, since the G1 and SOGI orbitals were very similar, the exponents were not reoptimized for the optimum value of L. We found that the p functions used in GF calculations were also appropriate for SOGI calculations.

Calculations and Discussion: The most prominent result of these calculations is that the spatial properties of these systems are described in essentially the same way by both the G1 and SOGI wavefunctions. In Table I and Fig. 1[21] we compare the G1 and SOGI orbitals for the $2\,^2S$ state of Li. For all states considered the optimum Ξ was within $1°$ of zero (which corresponds to G1) as shown in Table II. As shown in Table III this led to similar values of energy, density at the nucleus, and other measures of the spatial charge distribution, but for the spin density at the nucleus, $Q(0)$, this small difference in spin coupling led to significant changes. The G1 wavefunction led to good values for all these properties except $Q(0)$,[5] and we

see in Table III that the SOGI value of $Q(0)$ is much improved over the G1 value. For the Li $2\,^2S$ state we obtain 0.2265 for SOGI which is 2.1% smaller than the experimental value of 0.2313; for this state the G1 value is 0.2096, the GF value is 0.2406, and the HF value is 0.1667. For the Li $2\,^2P$ state we obtain a $Q(0)$ of -0.0172 as compared to a G1 and HF value of zero, a GF value of -0.0230, and a CI value of -0.0222. In this case the experimental value of -0.0182 is obtained indirectly and may not be reliable.[19,22] Lunell[13] has carried out a calculation on the $2\,^2S$ state Li which is nearly equivalent[23] to SOGI and which yields $Q(0)=0.2264$ and $E=-7.447536$ as compared to the SOGI results of $Q(0)=0.2265$ and $E=-7.447565$.

We see from Table II that the optimum angles Ξ in the $2\,^2S$ and $2\,^2P$ states have nearly the same magnitude but opposite sign and similarly for the $3\,^2S$ and $3\,^2P$ states. In the case of positive Ξ the spin polarization (or core polarization) induced in the core is positive ($2\,^2S$ and $3\,^2S$) and for negative Ξ it is negative ($2\,^2P$ and $3\,^2P$). As we go from the $n=2$ to the $n=3$ states the magnitude of Ξ gets smaller which means that core is more nearly correctly described as a singlet pair. This is reasonable since in the limit of $n=\infty$ we have Li$^+$ and the core is exactly singlet coupled as in G1.

Although only the case of the optimum Ξ is of physical importance, it is of some interest to compare the properties and optimum orbitals for various Ξ and examine how the wavefunctions change as we go from G1 through SOGI to GF. In Fig. 2 we show $Q(0)$ as a function of Ξ. We see that near $\Xi=0$ (i.e., G1), $Q(0)$ varies linearly but rapidly with Ξ. From Fig. 2 we see that except near G1 and GF most wavefunctions lead to quite poor values of $Q(0)$ [e.g., $Q(0)=0.76$ at $\Xi=16°$] even though they have the correct spin and interchange symmetry and satisfy a variational principle on the orbitals. In Fig. 3 we show the variation of energy with Ξ. The minimum is at $\Xi=0.434\pm0.004°$ and was unchanged by an increase in the size of the basis set. The difference in $Q(0)$ for $\Xi=0$ and the optimum Ξ is due primarily to differences in the spin part of the wavefunction. In fact, if we calculate $Q(0)$ with $\Xi=0.434$ but use the G1 orbitals, we obtain $Q(0)=0.2296$ as compared to 0.2265 for the SOGI orbitals. For Ξ in the region $50°$ to $60°$ we experienced some difficulty in convergence because of near linear

[18] W. A. Goddard III, J. Chem. Phys. 48, 1008 (1968).

[19] W. A. Goddard III, Phys. Rev. 176, 106 (1968).

[20] That is we use one 1s Slater orbital with $\zeta=Z$ and all other s orbitals with $n\geq3$, one 2p Slater orbital with $\zeta=Z/2$ and all other p orbitals with $n\geq4$. See C. C. J. Roothaan and P. S. Kelly, Phys. Rev. 131, 1177 (1963).

[21] The expansion coefficients for the orbitals of this and all other systems discussed in the paper are available upon request.

[22] K. C. Brog, T. G. Eck, and H. Wieder, Phys. Rev. 153, 91 (1967); see also Ref. 19.

[23] Lunell[13] states that he has used a general form of spin orbital. His use of only one spatial function for each spin orbital, however, allows his wavefunction to be reduced to the form

$$\mathcal{A}[\phi_a(1)\phi_b(2)\phi_c(3)\omega_{II}{}^{pT}\alpha\beta\alpha], \qquad (31)$$

which is equivalent to the SOGI wavefunction (see Sec. II). Furthermore, Lunell has chosen his core orbitals to be those appropriate for Li$^+$ rather than solving for them self-consistently for Li.

dependence of the orbitals. The point at 60° agrees with independent GF calculations. However, the wavefunctions near $\Xi=60°$ do not connect smoothly with the GF function indicating an instability in the GF function. It is interesting to note that for all four states of Li the UIIF value of $Q(0)$ is quite close to the SOGI value (see Table IIc).

In summary, these calculations indicate that the G1 description of the spatial properties of three-electron atoms is quite good. That is, to a very good approxi-

FIG. 9. The standard Young tableaux for the shape [3, 2].

mation, the two core electrons are singlet paired (as in G1); only for spin-dependent properties is it important to allow for a more general coupling of the electron spins. When this more general coupling is introduced, we obtain a very good value for $Q(0)$ for the $2\,^2S$ state and perhaps the $2\,^2P$ state of Li.

2. The H_3 System

Physically it is clear that, for three-electron atoms, Ξ should be near zero since Ξ should be determined primarily by the core electrons (for a two-electron ion the ground state is a singlet which corresponds to $\Xi=0$, the addition of valence electrons should not change this appreciably since they are much further from the nucleus). In addition, for a system such as HeH at typical molecular distances, we expect Ξ to be primarily determined by the pair of orbitals on the He and hence to be near zero. However, for a system of three hydrogen atoms the optimum pairing should be a function of nuclear configuration and should be significantly different from zero for some configurations. We have carried out SOGI calculations for several points on the reaction path of $H_2+D\rightarrow H+HD$ with the primary objectives being to determine (1) how well the SOGI method will predict potential energy surfaces for chemical reactions, (2) how the SOGI orbitals change as the system moves along the minimum energy reaction path, and (3) how spatial symmetry restrictions enter into our descriptions of a chemical reaction.

Basis Sets and Configurations: We used the following linear nuclear configurations which were on the minimum-energy path reported by Shavitt et al.[24]: point 1, $R_{AB}=1.40$, $R_{BC}=\infty$; point 2, $R_{AB}=1.470$, $R_{BC}=2.984$; point 3, $R_{AB}=1.609$, $R_{BC}=2.020$; point 4, $R_{AB}=R_{BC}=1.765$. For points 2–4 we used a basis set of nine Slater orbitals composed of two $1s$ functions and a $2p\sigma$ on each center. The orbital exponents for points 2[25] and 3[25] were estimated from data given in the paper by Shavitt et al.[24] The orbital exponents for point 4[26] are the same as those used by Shavitt et al.[24] For point 1, we used seven Slater orbitals, three on each of the protons in H_2 $(1s, 2s, 2p\sigma)^2$ and a $1s$ on the lone proton.

FIG. 8. (a) Orbital 1 of the $^3A_{2g}$ state of square H_4. The edge of the figure is 7.0 a.u. long; shortest distance between protons is 2.54 a.u. The lowest contour is 0.01 and the interval between contours is 0.024; the highest contour is 0.322. Based on the Gaussian basis set (see text). (b) Orbital 3 of the $^3A_{2g}$ state of square H_4. Scale as in (a). Lowest contour 0.01, highest contour 0.41, interval 0.01.

[24] I. Shavitt, R. M. Stevens, F. L. Minn, and M. Karplus, J. Chem. Phys. 48, 2700 (1968).

[25] The integrals for this calculation were carried out with the Polke-Pitzer version of the Cambridge Slater integral program.

[26] The integrals for this calculation were carried out with the McLYOSH polyatomic Slater integral program (QCPE #104).

R. C. LADNER AND W. A. GODDARD III

TABLE IV. G1, SOGI, and CI energies for various linear configurations of H_3.

R_{AB}	R_{BC}	E_{G1}	E_{SOGI}	Ξ	E_{CI}[a]
1.4	∞	−1.651526	−1.651526	0°	−1.66959
1.470	2.984	−1.641824	−1.642236	3.5°	−1.663036
1.609	2.020	−1.620887	−1.626282	16.4°	−1.653359
1.765	1.765	−1.599776[b]	−1.623820	20.9°	−1.652073

[a] The CI energy is from Ref. 24 and was calculated with a 15 basis function set.

[b] This calculation was restricted so that orbitals 1 and 2 were symmetry related (see Sec. III.A.2); this is not necessarily the best G1 wavefunction.

Results and Discussion for H_3: Let us first consider the symmetry properties of the orbitals for the saddle point, linear equidistant H_3. The symmetry group is $D_{\infty h}$ and the lowest electronic state has $^2\Sigma_u^+$ symmetry. One way for the many-electron wavefunction Ψ to have the proper symmetry is to construct Φ from two σ_g orbitals and one σ_u orbital. In this case, there are no restrictions on L. Another way for Ψ to have the proper symmetry is to have Φ such that the effect of $\hat{m}$ (the mirror plane perpendicular to the molecular axis) interchange orbitals 1 and 2 while orbital 3 is a σ_u function. From Sec. II.A, we see that the many-electron wavefunction will have $^2\Sigma_u^+$ symmetry if

$$U_{11}^{[2,1]L}((12)) = 1. \qquad (31)$$

Since, for a general Ξ, $U_{11}^{[2,1]L}((12)) = \cos\Xi$, the constraint (31) is satisfied only if $\Xi = 0$. Therefore there are two possible (spatial symmetry allowed) descriptions of saddle point. We can use symmetry orbitals (σ_g and σ_u) and couple the spins in a general way or we can have orbitals 1 and 2 be symmetrically related nonsymmetry functions coupled by the G1 spin function. For the saddle point found by Shavitt et al.[24] ($R_{AB} = R_{BC} = 1.765$ a.u.), we have carried out the calculation both ways and find that the optimum wavefunction using nonsymmetry functions leads to an energy of −1.59978 a.u., whereas the optimum SOGI wavefunction using symmetry functions yields an energy of −1.62382 a.u. Thus at the saddle point the optimum orbitals are symmetry functions.

Figures 4–6 are plots of the SOGI orbitals for nuclear configurations 2–4. The G1, SOGI, and CI energies, the optimum values of Ξ, and the SOGI orbital energies are given in Table IV. The barrier height from the SOGI calculations is ~17 kcal as compared to an experimental value[27] of 9.8 kcal and a value from the CI calculations[24] of 11 kcal. The predicted barrier height might be slightly lower if basis functions and saddle-point configurations appropriate for the SOGI wavefunction were used rather than those from the CI calculations. However, the decrease would probably not be large.

From Figs. 4, 5, and 6 we see that the best inde-

[27] I. Shavitt, J. Chem. Phys. 49, 4048 (1968).

pendent particle description of the reaction is as follows: For large separations between H_2 and H, the orbitals 1 and 2 which are localized on H_A (the H farther from the lone H) and H_B (the H nearer the lone H) form a bond between H_A and H_B and are also weakly bonding to H_C (the lone H). Orbital 3 which is localized on H_C has a node midway between H_A and H_B and is weakly bonding to H_B and antibonding to H_A, with these two effects roughly cancelling. As we move along the minimum-energy path, orbitals 1 and 2 remain approximately equally bonding by strengthening the H_B–H_C bond and weakening the H_A–H_B bond. At the saddle point, these two orbitals are σ_g functions and the H_A–H_B and H_B–H_C bonds are equivalent. In response to these changes in orbitals 1 and 2, the negative lobe of orbital 3 gets larger and larger until at the saddle point it becomes the σ_u orbital. Thus, even at the saddle point, this orbital is roughly nonbonding. As we pass over the saddle point in the exchange reaction the σ_u orbital begins to localize on H_A and the σ_g orbitals begin to localize on H_B and H_C and eventually form $H + H_2$. We see that throughout the reaction there are two strongly bonding orbitals and one nonbonding orbital and that it is not necessary to break a bond during the chemical reaction. Thus the SOGI orbitals yield a clear and reasonable description of the $H + H_2$ reaction.

An alternate independent-particle description of the saddle point is for orbitals 1 and 2 to localize the right and left, but we have shown above that this is possible only if the G1 spin coupling is used. The best (G1) localized orbitals are shown in Fig. 6, but, since the energy of this (G1) wavefunction is so much worse than that of the optimum wavefunction using symmetry orbitals, we see that this is not a very good description of the system for this spacing.

B. Four-Electron Systems

1. The LiH Molecule

The ground state of LiH is a singlet and the spin representation is two dimensional. In this case the representation matrices are just the same as for a three-electron doublet (four elements of S_i map onto each matrix). Thus $\Xi = 0$ corresponds to G1 and $\Xi = 60°$

QUANTUM THEORY OF MANY-ELECTRON SYSTEMS. V

TABLE V. G1, SOGI, and CI energies for square H_4 (length of side = 2.54 a.u.). See Sec. II.A.2 for basis set information.

	G1	SOGI	Ξ	Υ	CI
		A. Minimum basis set			
$^1B_{1g}$	−1.96926	−2.057685	62.4°±0.2°	···	−2.057685
$^3A_{2g}$	−1.983395	−2.036985	70.50°	70.52878°	−2.036985
^3E_u	−1.865595	−1.865595	0.	···	−1.865595
		SOGI	Ξ	Υ	
		B. Ten basis functions			
$^1B_{1g}$		−2.06235	62.5	···	
$^3A_{2g}$		−2.048271	69.2	70.52878°	
^3E_u		−1.87863	0.0		

is GF. Here we would expect for the coupling in the core orbitals on the Li atom to be dominant and hence the optimum angle should be close to zero. In fact this is the case, $\Xi = -0.105 \pm 0.002°$ and the energy decreases by about 3×10^{-7} in going from G1[28] to SOGI.[29] Thus the G1 wavefunction for LiH has nearly the optimum spin coupling.

2. The H_4 System

We expect the greatest departures from G1 to occur in a system such as H_4 for which the spin coupling is determined by the nuclear configuration. In order to illustrate various aspects for the SOGI wavefunctions for such systems we will consider some low-lying singlet and triplet states of square H_4.

Basis sets and configurations: All calculations were for the nuclear configuration with the H's at the corners of a square with a side of length $2.54 a_0$.[30] We considered the lowest two states for this configuration, $^1B_{1g}$ and $^3A_{2g}$, and also a higher-lying ^3E_u state. Two different basis sets were used. The smaller[25] was a minimum basis set of four Slater orbitals, one centered at each proton and with an orbital exponent of $\zeta = 1.05$ (this is approximately optimum for the $^1B_{1g}$ state[31]). A larger basis set based upon four 1s Gaussians and one 2p Gaussian on each center and contracted to one s-like and one p-like orbital on each center was also used.[32] For this basis set the contraction was carried out[33] so that the four Gaussians approximated a Slater 1s orbital with $\zeta = 1.05$.

[28] W. E. Palke and W. A. Goddard III, J. Chem. Phys. 50, 4524 (1969).

[29] The integrals for this calculation were carried out with the Nesbet–Stevens diatomic Slater integral program.

[30] This distance was found to be near the optimum R for the $^1B_{1g}$ state of $D_{4h}H_4$ by minimum basis set CI calculations.[31]

[31] C. W. Wilson, Jr., and W. A. Goddard III, J. Chem. Phys. 51, 716 (1969).

[32] The integrals for this calculation were carried out with the Dunning version of the Murray Geller Gaussian integrals program.

[33] S. Huzinaga, J. Chem. Phys. 42, 1293 (1965).

Four-Electron Triplet States: The SOGI spin variation for the four-electron singlet state was considered above; here we will discuss the spin variation for triplet states. In this case $f^\mu = 3$ and the general transformation L is a function of two parameters Ξ and Υ and is given by

$$L(\Xi, \Upsilon) = \begin{pmatrix} \cos\Xi/2 & \sin\Xi/2 \sin\Upsilon/2 & \sin\Xi/2 \cos\Upsilon/2 \\ -\sin\Xi/2 & \cos\Xi/2 \sin\Upsilon/2 & \cos\Xi/2 \cos\Upsilon/2 \\ 0 & -\cos\Upsilon/2 & \sin\Upsilon/2 \end{pmatrix}. \tag{32}$$

In this case $\Xi = 0$ corresponds to G1; $\Xi = 180°$ and $\Upsilon = 0$ corresponds to GF; and $\Xi = 180°$ and $\Upsilon = 180°$ corresponds to G2.

Spatial Symmetry Restrictions: We will discuss the symmetry properties of the orbitals for all three states first, beginning with the $^3A_{2g}$ and $^1B_{1g}$ states, since they are closely related. It is only necessary to consider the generators of D_{4h} (the symmetry of the nuclear configuration) and, in each case, we will examine the effect of the C_4 element of D_{4h} and determine if the orbitals can be related in such a way that they are symmetry functions only for the subgroup D_{2h}. The orbitals used to construct the $^3A_{2g}$ and $^1B_{1g}$ states have the same symmetry; the different spatial symmetry of the many-electron wavefunctions arises through the difference in the spin coupling. These orbitals are sketched in Fig. 7(b). The product function $\Phi = \phi_1\phi_2\phi_3\phi_4$ has the following properties:

$$\hat{C}_4\Phi = -(12)(34)\Phi, \tag{33a}$$

$$C_2\Phi = (12)(34)\Phi, \tag{33b}$$

$$\hat{i}\Phi = \Phi. \tag{33c}$$

From (32c) we see that the state must be "g." From Sec. II.A, we know that the state will be A_{2g} if

$$U_{11}{}^{\mu L}[(12)(34)] = -1$$

and B_{1g} if

$$U_{11}{}^{\mu L}[(12)(34)] = +1.$$

For a $^1A_{2g}$ state, this gives the condition that

$$U_{11}{}^{[2,1]L}((12\ (34)) = -\cos^2\tfrac{1}{2}\Xi$$

$$+ \tfrac{1}{3}\sin^2\tfrac{1}{2}\Xi\,\sin^2\tfrac{1}{2}\Upsilon - (4\sqrt{2}/3)\sin^2\tfrac{1}{2}\Xi\,\cos\tfrac{1}{2}\Upsilon\,\sin\tfrac{1}{2}\Upsilon$$

$$- \tfrac{1}{3}\sin^2\tfrac{1}{2}\Xi\,\cos^2\tfrac{1}{2}\Upsilon = -1. \quad (34)$$

This condition is satisfied if

$$-\tfrac{1}{3}\sin^2\tfrac{1}{2}\Upsilon + (4\sqrt{2}/3)\cos\tfrac{1}{2}\Upsilon\,\sin\tfrac{1}{2}\Upsilon + \tfrac{1}{3}\cos^2\tfrac{1}{2}\Upsilon = 1, \quad (35a)$$

or

$$(2\sqrt{2}/3)\sin\Upsilon + \tfrac{1}{3}\cos\Upsilon = 1, \quad (35b)$$

or

$$\sin\Upsilon = 2\sqrt{2}/3 \quad \text{and} \quad \cos\Upsilon = \tfrac{1}{3} \quad (35c)$$

or finally

$$\Upsilon = 70.52878\cdots^\circ \quad (35d)$$

(there is no condition on Ξ).

For the $^1B_{1g}$ state, we have the condition that $U_{11}{}^{[2,2]L}((12)(34)) = +1$, but this condition is always satisfied since $(12)(34)$ is an element of the invariant subgroup and is represented by the unit matrix in this representation.

We have not discussed the case of a spatially degenerate state, but an example should make the procedure clear. Consider the orbitals sketched in Fig. 7(c). The following relations are easily seen:

$$\hat{C}_4\Phi_x = \Phi_y, \qquad \hat{C}_4\Phi_y = -(12)\Phi_x,$$

$$\hat{\imath}\Phi_x = -(12)\Phi_x, \qquad \hat{\imath}\Phi_y = -(12)\Phi_y,$$

$$\hat{C}_2'\Phi_x = (12)\Phi_x, \qquad \hat{C}_2\Phi_y = -\Phi_y, \quad (36)$$

where $\Phi_x = \phi_{1x}\phi_{2x}\phi_{3x}\phi_{4x}$ and $\Phi_y = \phi_{1y}\phi_{2y}\phi_{3y}\phi_{4y}$. For the many-electron functions $\Psi_x = G^{\mu L}\Phi_x\chi$ and $\Psi_y = G^{\mu L}\Phi_y\chi$ to form an E_u state, it is necessary that

$$\hat{C}_4\Psi_x = \Psi_y, \qquad \hat{C}_4\Psi_y = -\Psi_x,$$

$$\hat{\imath}\Psi_x = -\Psi_x, \qquad \hat{\imath}\Psi_y = -\Psi_y,$$

$$\hat{C}_2'\Psi_x = \Psi_x, \qquad \hat{C}_2'\Psi_y = -\Psi_y. \quad (37)$$

The relations in (37) are satisfied if $O_{11}{}^{\mu L}(12) = O_{11}{}^{\mu L}$, which implies that $U_{11}{}^{\mu L}((12)) = +1$. For a general Ξ, $U_{11}{}^{[2,1]}((12)) = \cos\Xi$, so that only G1 allows the use of symmetrically related nonsymmetry functions.

In summary we find that: (1) For the $^1B_{1g}$ state the SOGI orbitals need only have D_{2h} symmetry rather than D_{4h}. (2) For the $^3A_{2g}$ state the SOGI orbitals must have D_{4h} symmetry unless the angle Υ is $70.52878\cdots^\circ$. In this case the orbitals need only have D_{2h} symmetry and the restriction on Υ implies a constant relative proportion of G2 and GF coupling with an arbitrary

amount of G1 coupling. (3) For the ^3E_u state the orbitals must have D_{4h} symmetry unless $\Xi = 0$ (i.e., G1). In this latter case the orbitals may have D_{2h} symmetry. In none of these cases are the SOGI orbitals *forced* to have lower than D_{4h} symmetry. Rather we have just catalogued the possible regions where lower symmetry orbitals are *allowed*.

Results and Discussion for H_4: We find from the calculations with both basis sets that the SOGI orbitals for the $^1B_{1g}$ and $^3A_{2g}$ states do *not* have D_{4h} symmetry and have symmetries just as outlined above. In fact we find that the SOGI orbitals for these two states are nearly indistinguishable; the many-electron wavefunctions differ mainly in the spin coupling used. We see from the sketches in Fig. 7, and plots in Fig. 8, that in both $^1B_{1g}$ and $^3A_{2g}$ states there is essentially a bond and antibond along each diagonal. The presence of these antibonding orbitals explains why the energy of H_4 is so very much higher than that of $H_2 + H_2$. It is interesting to note here that the SOGI energy for the minimum basis set is identical with the complete CI energy[31] for the same basis set. Thus while these wavefunctions are equivalent, the SOGI wavefunction through the independent particle interpretation allows a visualization of the wavefunction which might be completely lost in the CI form.

From Table V we see that the addition of p basis functions lowered the energies slightly but did not change the spin representations significantly. The optimum angle for the $^1B_{1g}$ state is $\Xi = 62.5^\circ$ which is very close to the GF value of 60°.

We see that in the lowest singlet state, $^1B_{1g}$, for square H_4 with $R = 2.54a_0$ the orbitals are delocalized over pairs of atoms (along the diagonal). However, for squares of very large R the lowest state must be $^1A_{2g}$ for which each orbital is localized on one atom. In addition for very small R it would seem that the optimum orbitals would have D_{4h} symmetry and be delocalized over all four atoms. Thus if we start at $R = \infty$ and retain square symmetry for all R we pass through regions in which the orbitals are successively delocalized in what approximates a series of Mott transitions.[17] This point will be further developed elsewhere.

C. Considerations for Larger Numbers of Electrons

At this point we will discuss briefly a set of calculations which we have not yet carried out in order to illustrate simplifications in applying SOGI which are expected to be appropriate for larger numbers of electrons.

Consider the reaction

$$\text{LiH} + \text{H} \rightleftharpoons \text{Li} + \text{H}_2. \quad (38)$$
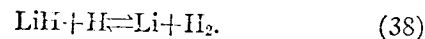
The system is a five-electron doublet and the appropriate representation of S_5 is five dimensional. If we were to allow a completely general coupling of the electron

spins, we would have to simultaneously optimize four parameters controlling the spin coupling as well as the five spatial orbitals; all of this for each nuclear configuration. However, on physical grounds, and on the basis of the calculations on Li and LiH, we expect the core electrons to be very nearly singlet paired for all nuclear geometries. From this we can see that only the mixing of the first and third standard spin basis functions (Fig. 9) is important since all others correspond to breaking the pairing of the Li core. Thus by introducing only one spin-coupling parameter, we can expect to obtain an accurate description of this reaction. This approach becomes increasingly more important as the system becomes larger. For the reaction $CH_4 + H \rightleftharpoons CH_3 + H_2$ or $CH_4 + H \rightleftharpoons CH_3^- + H_2$, there are 132 different spin-coupling states. Hence to allow for a general spin-coupling scheme, we would have to introduce 131 new nonlinear parameters. If we assume, however, that the electrons in the unbroken bonds and in the core of the carbon atom remained paired, we need introduce only one new parameter to allow a general coupling among the electrons in the bonds being broken and formed.

IV. CONCLUSIONS

We have developed a way of eliminating the arbitrariness in the choice of spin function in the GI method. This method has been applied to three-electron atoms and three- and four-electron molecules. For three-electron atoms it was found that the G1 wavefunction is very nearly optimum and that only the spin-depend-

ent properties changed significantly when the spin coupling was optimized. A very good value for the spin density at the nucleus was obtained for the ground state of Li, and for the $2\,^2P$ state the results were much improved over the G1 values. Similarly for LiH the G1 wavefunction had nearly the optimum spin coupling and only a minor improvement occurred in the energy in going to SOGI. For the unstable molecular systems H_3 and H_4, however, we found that optimization of the spin-coupling was necessary in order to properly and consistently describe the system.

Thus these calculations indicate that the SOGI method may allow a proper description of the Fermi contact portion of the hyperfine interaction of atoms and molecules. More importantly however is that the SOGI method may allow a good description of the changes which occur as bonds are formed, broken, and distorted during chemical reactions.

II. The Orbital Description of the $H_2 + D \rightleftharpoons H + HD$
and $LiH + H \rightleftharpoons Li + H_2$ Exchange Reactions

I. INTRODUCTION

A major goal of theoretical chemistry is to explain the mechanisms and rates of chemical reactions. To do this we must determine the electronic energy of the system as a function of the nuclear coordinates; that is, we must obtain the potential energy surface (PES) of the system. However, the determination of potential energy surfaces of chemical accuracy (i.e., to better than 1 kcal/mole) is costly even for such simple reactions as

$$H_2 + D \rightleftharpoons H + HD \tag{1}$$

and

$$LiH + H \rightleftharpoons Li + H_2. \tag{2}$$

It is currently inordinately expensive to investigate the mechanisms for more important reactions (such as

$$H_2CCO - H_2CCO \rightarrow \begin{array}{c} H_2C-C \\ \\ C-CH_2 \end{array}$$
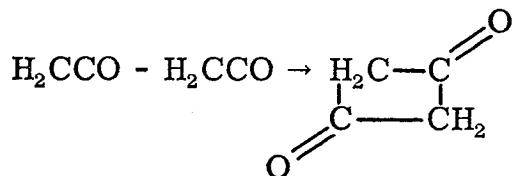
or the addition of fluorinated ethylene to butadiene) at the level of accuracy attainable for reactions (1) and (2). By using more approximate methods, we can calculate the energies of such large systems at a few points on the PES, but even this is frightfully expensive. Thus, in order to progress toward the consideration of the mechanisms of the chemically interesting reactions, we want to develop concepts and principles that will allow us to predict the basic features of the potential energy surfaces, without detailed calculations. An example

of significant progress toward this end has been the work of Hoffmann and Woodward,[1] which allows the qualitative consideration of a vast variety of reactions through use of simple correlation diagrams and requiring little or no calculation beyond elementary considerations of the ordering of energy levels of molecules.

Since a major objective in examining reactions will be to abstract generally useful concepts and principles, we will employ the spin-coupling optimized GI (SOGI) method.[2] This method is a self-consistent generalization of the valence bond method[3] and leads to a simple orbital interpretation of the wavefunction while allowing a proper description of the process of breaking a bond.

In this paper we report SOGI calculations for reactions (1) and (2) for a large number of linear geometries. Reaction (1) is already well characterized experimentally and theoretically so that we can assess the accuracy to be obtained from SOGI wavefunctions. On the other hand, very little work, either experimental or theoretical, has been reported for (2), so that this work may add to both our qualitative and quantitative understanding of this system. We should note here that reactions (1) and (2) represent two quite different kinds of reactions, with (1) being thermoneutral while (2) is quite exothermic (55 kcal/mole) (or endothermic depending upon direction).

First we discuss some details of the theoretical calculations (Sec. II). This is followed by a consideration of potential surfaces for reactions (1) and (2) (Sec. III) and an examination of the orbitals for these reactions (Sec. IV) and is concluded with a general discussion of the results (Sec. V).

II. COMPUTATIONAL METHODS AND DETAILS

A. The Wavefunctions

In the Hartree-Fock method the wavefunction is taken as a Slater determinant

$$A(\Phi\chi), \tag{3}$$

where A is the N-electron antisymmetrizer, χ is a product of one-electron spin functions, and Φ is a product of orbitals (one-electron spatial functions), each of which is variationally optimized. For two electrons, (3) becomes

$$A[\phi_a(1)\phi_b(2)\alpha(1)\beta(2)] = \phi_a\phi_b\alpha\beta - \phi_b\phi_a\beta\alpha, \tag{4}$$

where the total wavefunction (4) is unnormalized and the ordering of the orbitals and spinfunctions is used to indicate electron number. If ϕ_a and ϕ_b are different, then (4) is a mixture of singlet and triplet character. In order to obtain a proper description of the spin symmetry, we must take the orbitals of (4) as doubly occupied

$$\phi_a = \phi_b. \tag{5}$$

But double occupation of the orbitals as in HF often leads to incorrect dissociation (i.e., an improper description of the wavefunction for large internuclear distances) as shown in Fig. 1a for H_2. For the study of reactions we want both the correct spin symmetry and the proper dissociation. To accomplish this, we replace the antisymmetrizer in (3) with the group operator $G^{\mu L}$, which simultaneously

ensures both the proper spin symmetry and the Pauli symmetry.[2a]
Thus the wavefunction is of the form

$$\Psi = G^{\mu L}(\Phi\chi). \tag{6}$$

The superscript μ denotes the total spin of the system and L determines
the particular way in which the individual electronic spins are coupled
to give the total spin. This coupling is given by a matrix, L, relating
the optimum coupling to the standard couplings used in Young's ortho-
gonal representation of $\mathcal{A}_N$ (the symmetric group). The total wave-
function Ψ in (6) can be written in several alternative forms, two of
which are

$$\Psi = (\sum_{i=1}^{f_\mu} C_i G_i^\mu)\Phi\chi \tag{7a}$$

$$= A[(O_{11}^{\mu L}\Phi)\chi], \tag{7b}$$

where f_μ is the number of different couplings that give the total spin
denoted by μ (i.e., the number of canonical valence bond structures),
the C_i's are numerical coefficients, the G_i^μ are the standard group
operators defined in terms of the standard Young tableaux, and $O_{11}^{\mu L}$
is a Wigner projection operator defined in terms of the optimum
coupling, $\underset{\sim}{L}$,

$$O_{11}^{\mu L} = \sum_{\substack{i=1 \\ j=1}}^{f_\mu} L_{1j}L_{1i}O_{ji}^\mu. \tag{8}$$

The energy of the wavefunction in (6) is

$$E = \langle \Psi | \mathcal{H} | \Psi \rangle / \langle \Psi | \Psi \rangle = \langle \Phi | \mathcal{H} | O_{11}^{\mu L} \Phi \rangle / \langle \Phi | O_{11}^{\mu L} \Phi \rangle. \tag{9}$$

The SOGI wavefunction is obtained by optimizing E against first-order variations both in $\underset{\wedge}{L}$ and in the orbitals of Φ.

For two electrons, there is only one singlet coupling and the SOGI wavefunction is identical to the G1 wavefunction with the form

$$G_1^S[\phi_a \phi_b \alpha \beta] = A[O_{11}^S(\phi_a \phi_b)\alpha \beta] = A[(\phi_a \phi_b + \phi_a \phi_b)\alpha \beta]$$

$$= (\phi_a \phi_b + \phi_b \phi_a)(\alpha \beta - \beta \alpha). \tag{10}$$

The optimum orbitals ϕ_a and ϕ_b for the ground state of H_2 are shown in Fig. 2 as a function of internuclear distance, R. As would be expected, the orbitals are essentially hydrogen 1s orbitals at large R but distort (hybridize and delocalize) as R decreases. We will denote this orbital coupling by the figure

$$\boxed{a \quad b} \; . \tag{11}$$

Similarly, there is only one triplet coupling for two electrons and the SOGI or G1 wavefunction is of the form

$$G_1^t[\phi_a \phi_b \alpha \alpha] = A[O_{11}^t(\phi_a \phi_b)\alpha \alpha] = (\phi_a \phi_b - \phi_b \phi_a)\alpha \alpha; \tag{12}$$

this orbital coupling we denote by the figure

$$\boxed{\begin{array}{c} a \\ b \end{array}} \; . \tag{13}$$

For three or more electrons, there is usually more than one coupling scheme that yields a particular total spin. For the three-electron doublet case, there are two spin couplings and two standard group operators,[2b]

$$G_i^d[\phi_a\phi_b\phi_c\alpha\beta\alpha] = A[(O_{ii}^d\phi_a\phi_b\phi_c)\alpha\beta\alpha] = A\{[(\phi_a\phi_b + \phi_b\phi_a)\phi_c]\alpha\beta\alpha\} \quad (14)$$

$$G_f^d[\phi_a\phi_b\phi_c\alpha\beta\alpha] = A[(O_{ff}^d\phi_a\phi_b\phi_c)\alpha\beta\alpha]$$

$$= A[(\phi_a\phi_b\phi_c + \phi_b\phi_a\phi_c - \phi_c\phi_a\phi_b - \phi_b\phi_c\phi_a)\alpha\beta\alpha] \quad (15)$$

$$= A[\{(\phi_a\phi_b + \phi_b\phi_a)\phi_c\}\alpha\beta\alpha] - A[\{(\phi_c\phi_b + \phi_b\phi_c)\phi_a\}\alpha\beta\alpha].$$

The wavefunction (14) is denoted as[4]

$$\boxed{\begin{array}{cc} a & b \end{array}} \\ \boxed{c} \qquad , \qquad (16)$$

which indicates symmetric (singlet) coupling of ϕ_a and ϕ_b followed by antisymmetric coupling of ϕ_c to the $[\phi_a, \phi_b]$ pair to obtain the proper doublet spin symmetry. The wavefunction (15) is denoted as

$$\boxed{\begin{array}{c|c} a & b \end{array}} \\ \boxed{c} \qquad , \qquad (17)$$

which indicates antisymmetric (triplet) coupling of ϕ_a and ϕ_c followed by symmetric coupling of ϕ_b to the $[\phi_a, \phi_c]$ pair to obtain the proper doublet spin symmetry. We see that the spin coupling of (14) is just that of a simple valence bond wavefunction, and from the last line of (15) we see that the GF spin coupling can be expressed as a linear combination of two simple valence bond couplings, or symbolically,

$$\boxed{\begin{array}{|c|c}\hline a & b \\\hline c & \\\hline\end{array}} = \boxed{\begin{array}{|c|c}\hline b & a \\\hline c & \\\hline\end{array}} - \boxed{\begin{array}{|c|c}\hline b & c \\\hline a & \\\hline\end{array}} . \qquad (18)$$

As we have said, these standard couplings can be combined to give a more general coupling and this coupling can be optimized. In some cases, we find that certain standard couplings can be neglected without significantly affecting either the energy or the shape of the orbitals. This not only simplifies the mechanics of calculations but also makes the results more easily interpretable.

The ground state of Li^+ is a singlet with the orbital coupling shown in (11). The lowest triplet state of Li^+ is much higher, so it is not surprising that the optimum coupling for Li is nearly the G1 coupling shown in (14) and (16). For H_3, however, we must use a general spin coupling because all three orbitals have roughly the same energy. In this case the general spin coupling corresponds to using linear combinations of both valence bond structures.

For a four-electron singlet, there are two coupling schemes. The G1 coupling is denoted by

$$\begin{array}{|c c|}\hline a & b \\\hline c & d \\\hline\end{array} \qquad (19)$$

and the GF by

$$\begin{array}{|c|c|}\hline a & b \\\hline c & d \\\hline\end{array} . \qquad (20)$$

For LiH we need consider only the G1 coupling for the same reason as in Li. In Fig. 3 we show the two valence orbitals of LiH as a function of internuclear distance. Here we see that even at $R = 8a_0$ the Li valence orbital has delocalized somewhat onto the H (this amounts to building in ionic characters). As R decreases further, the Li valence orbital hybridizes and delocalizes until at R_e ($3.09a_0$) it is quite modified from the atomic form. On the other hand, the H 1s orbital changes very little in this process. Thus the LiH bond can be considered essentially as a one-electron bond.

For the five-electron doublet, there are five couplings denoted by

$$
\begin{array}{ccccc}
\young(ab,cd,e) & \young(ab,cd,e) & \young(ab,cd,e) & \young(ab,cd,e) & \young(ab,cd,e) \\
G1 & G2 & G3 & G4 & G5 = GF
\end{array}
\tag{21}
$$
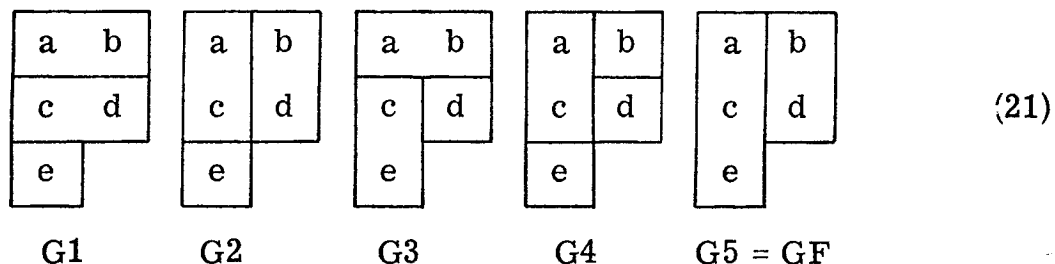
In the case of LiH_2, as with Li and LiH, we need consider only the coupling schemes that singlet couple the Li core functions, i.e., G1 and G3. Note that if we ignore the Li core electrons and treat this as a three-electron system, it is completely analogous to the H_3 system.

Since the SOGI wavefunction is obtained by minimizing the energy with respect to variations both in the orbitals and the transformation $\underset{\sim}{L}$, it has the following properties: (i) each orbital is different (no double occupation) and usually[5] cannot be taken as orthogonal to

any other orbital; there are as many orbitals as electrons; (ii) each orbital is an eigenfunction of an operator equivalent to the Hamiltonian of an electron moving in the field due to the nucleus plus some average field due to electrons in the N - 1 other orbitals; and (iii) the average field in (ii), though nonlocal, is obtained directly by applying the variational principle to the energy. In short, the wavefunction can be given in an independent particle interpretation (IPI).

The IPI of our wavefunction is very important because it is by examining changes in the independent-particle states for various reactions that we would hope to find general concepts and principles for understanding the mechanisms of chemical reactions.

B. Basis Sets

In the calculations reported herein, we have used nuclear-centered Gaussian basis sets. On each hydrogen, we placed six s and two p_z primitive functions[6] that were contracted to three s and one p_z functions as given in Table I. The scale for the s set of functions was taken as 1.10 since this led to good results for both the atom and the H_2 molecule (near R_e), as indicated in Table II. The scale of the p functions and the contraction coefficients for both the s and p functions were optimized for the H_2 molecule at (R = 1.40 a_0), resulting in a contraction still adequate for other H-H distances between 1.4 and ∞. Thirteen s and three p primitive functions were used on the lithium atom, with the orbital exponents for the first ten s functions chosen

from Huzinaga-type fits to the Slater basis functions of a small basis G1 calculation on Li atom. The orbital exponents of the p's and more diffuse s functions were optimized for LiH (R = 3.015). This primitive set was contracted to five s and three p functions, as given in Table I.

The basis sets were chosen in this way so that they would be flexible enough to treat all nuclear geometries equivalently (without additional adjustment). Table II compares the energy of H_2 obtained with our basis with the results of using a large basis[7]; we see that our hydrogen basis set is adequate for all R. Our basis for Li also leads to good results for the Li atom and LiH molecule, as shown in Table II. The only deficiency in the Li basis is the lack of d polarization functions on the Li. We believe that the basis set is adequate for the entire surface. The potential curves, calculated by various methods, for H_2 and LiH are shown in Figure 1.

III. ENERGY SURFACES

A. $H_2 + D \rightleftharpoons H + HD$

The potential surface for linear H_3 has been studied extensively. The most complete calculation was that of Shavitt, Stevens, Minn, and Karplus[8] (hereafter denoted as SSMK) using configuration interaction (CI) and considering a number of linear geometries. More limited CI calculations were reported by Edmiston and Krauss,[9] and Conroy and Bruner[10] reported results obtained with correlated wavefunctions (the energies were extrapolated, leading to approximate energies but no upper bound on the exact energies). Recently, Liu[11] has carried out the most accurate calculations for the saddle point (considering only the symmetric linear configuration). In this section, the emphasis will be upon the comparison of the potential surface as obtained from the best other calculation, the SSMK surface.

In Fig. 4a we show the potential surface of linear H_3. In Fig. 4b the axes for the coordinates R_{ab} and R_{bc} are skewed so as to diagonalize the kinetic energy (thus the classical motion of the nuclei is the same as the motion of a ball on this surface).[12] For comparison, the SSMK surface is shown in Fig. 4c where we see that the shape is qualitatively similar to the SOGI surface. Figure 5a shows an energy profile along the reaction coordinate for SOGI and the SSMK paths I and II, and figure 5b shows the energy profile for SOGI and SSMK II on a line through the saddle point perpendicular to the reaction coordinate.

In Table III we compare the saddle point geometries and barrier height as calculated for H_3 using various methods. Here we see that the barrier height is about half way in between the best Hartree-Fock results and the best CI results. Even so, the remaining errors are much too large for use in computing reaction rates by calculations of the dynamics of the collisions. The saddle-point geometry obtained with SOGI is 1.807 a_0, about 0.03 a_0 larger than from the comparable CI calculations by SSMK, whereas the Hartree-Fock results lead to 1.725 a_0, about 0.035 a_0 less than the comparable CI calculations by Liu.[11]

SSMK have suggested that correlation errors near the H_3 saddle point should be about 50% greater than obtained using the comparable method for H_2. This seems to be a reasonable method of estimation and indeed leads to very similar estimates of the H_3 barrier height for a variety of methods and bases as shown in the last column of Table III. For SOGI the estimate of the barrier is 10.4 kcal/mole, in reasonable agreement with the estimate of 9.8 ± 0.2 kcal/mole obtained by Shavitt[13] from a consideration of the empirical data and the SSMK surface. The consistency of using such a simple approach of estimation suggests that there may be a way to correct approximately for correlation errors at other geometries; however, one cannot just scale the surface since the saddle-point geometry must change. In this regard it is interesting that the SOGI (sp) wavefunction of H_2 leads to a bond length 0.025 a_0 larger than the experimental value, while it leads to an H_3 saddle-point geometry 0.047 a_0 larger than the

best CI result; hence there may well be some way of scaling geometries while correcting for correlation.

The curvatures at the saddle point of H_3 for both the symmetric and antisymmetric stretch are given in Table III along with the curvature for H_2. Here we see that there is good agreement between the CI and SOGI results.

In considering the motion along the reaction path, the vibrationally adiabatic approximation assumes that the quantum number of the transverse vibration is conserved. Since the curvature for the transverse motion is different at the saddle point than at infinity, the effective reaction barrier is not the same as the barrier height obtained directly from the potential surface. Correcting for the symmetric stretch leads to an effective barrier of 14.0 kcal for the zero-vibrational state. However, correcting in addition for the bending zero-point motion at the saddle point (using the bending force constant from SSMK) leads to an effective barrier of 16.8 kcal.

B. LiH + H $\rightleftharpoons$ Li + H$_2$

The potential surface for linear LiH$_2$ as obtained from the SOGI calculations is shown in Fig. 6. Considering LiH and H to be the reactants, the reaction is quite exothermic (55.2 kcal/mole).[14] (The LiH bond has a strength of 50.3 kcal).[14] For such an exothermic reaction, the transition state is expected to have a geometry similar to that of the reactants (the Hammond postulate)[15] if the reaction is concerted. We see in Fig. 6 that this is indeed the case. The bond length calculated for LiH is 3.09 a$_0$[16] while at the saddle point the geometry is $R_{LiH} = 3.20$ a$_0$ and $R_{HH} = 3.10$ a$_0$. The LiH bond length at the saddle point is only slightly longer than for the reactants, while the HH bond length is over twice that of the products ($R_{HH} = 1.425$ a$_0$). The calculated barrier height is 5.1 kcal/mole, about one-tenth of the energy of the bond to be broken.

We see from Fig. 6 that starting at the LiH end and proceeding along the reaction path,[23] the LiH bond length increases slowly as the H comes closer. Thus we would not expect vibrational excitation to be important for overcoming the barrier, translation energy alone should be sufficient.[17]

On the other hand, starting at the H$_2$ end, the H$_2$ bond length changes only very gradually as the Li approaches and does not lead naturally to the saddle-point geometry. In this case it would appear that, if the H$_2$ is in a low vibrational state, very few collisions would lead to a scattering path passing near the saddle point, since the classical turning point for H$_2$ ($\nu = 0$) is ~ 1.75 a$_0$. Thus, even for

total energies well above that required to pass over the barrier, the reaction cross section might well remain low if the H_2 is not vibrationally excited.

To give some idea of how much vibrational energy might be required to drive the reverse of reaction (2), we have calculated the vibrational structure of H_2 using the SOGI potential energy curves shown in Fig. 1.[18] Energy levels as well as average values of R are given for H_2, HD, D_2, ^{7}LiH, and H_3 (symmetric stretch only) in Table IV. If H_2 is initially in the $\nu = 6$ state, the system has ~ 7 kcal/mole more energy than required to go over the barrier. Furthermore, the average value of R for this state is 2.196 a_0 and the classical turning point is ~ 3.0 a_0. It is certainly plausible that the vibrational energy of H_2 could be converted to potential energy to drive the reaction. For $\nu = 6$, however, only a small fraction of initial vibrational phases would lead to reactive collisions. For $\nu = 10$, on the other hand, the system has ~ 31 kcal/mole more than required to go over the barrier and the average value of R is 3.082 with the classical turning point being ~ $4a_0$, which should give a very large cross-section for reaction.

Since we have not considered non-linear cases and could not calculate a bending mode for the saddle point, we have made only the following rough estimate of the stretching vibrational energy. Near the saddle point, the reactive mode is mostly H-H motion so the transverse mode is mostly LiH motion. Therefore, we have taken the energies calculated for $R_{HH} = 3.00$ as the potential for the transverse motion; the force constant for this potential is 0.155 a.u. The

correct reduced mass for the transverse mode could be between 14/9 a.m.u. (pure ^{7}Li vs. H_2 motion) and 8/9 a.m.u. (pure H vs. ^{7}LiH motion), which puts the zero point energy between 2.31 kcal/ mole and 3.05 kcal/mole. The zero point energy for ^{7}LiH is 1.83 kcal/mole. Thus, the zero point energy is higher at the saddle point than in LiH, even neglecting the bending mode, and the effective barrier should be at least 2 kcal higher than the barrier in the potential surface.

IV. THE ORBITAL DESCRIPTION
A. The $H_2 + D \rightleftharpoons H + HD$ Reaction

The GI orbitals of H_2 are given in Fig. 2. From Fig. 7a and Table Va we see that as the hydrogens approach each other the orbitals hybridize and delocalize in such a way as to increase their overlaps from that of atomic orbitals at the same distance.[19] In this case the spatial part of the wavefunction has the form

$$(\phi_a \phi_b + \phi_b \phi_a) \tag{22}$$

and the dominant term in the intermolecular potential has the form[20]

$$\Delta E \sim \frac{S_{ab}^2 \, \tau}{1 + S_{ab}^2} \, . \tag{23}$$

(This discussion holds equally well for the valence orbitals of LiH as can be seen from Fig. 7b and Table Vb.) For three electrons, the best orbital product wavefunction would have the form

$$\phi_a \phi_b \phi_c + \phi_b \phi_c \phi_a + \phi_c \phi_a \phi_b + \phi_a \phi_c \phi_b + \phi_b \phi_a \phi_c + \phi_c \phi_b \phi_a \tag{24}$$

with the SCF orbitals having larger overlaps than the frozen orbitals at the same distance. However, for spin one-half particles there is no spin function that can be combined with (24) to yield the totally antisymmetric wavefunction required for Fermions.

For HeH at large distances, the wavefunction has the form in (8), where ϕ_a and ϕ_b are He atom orbitals and ϕ_c is on the H. The

intermolecular potential is now repulsive and is dominated by terms proportional to S_{ab}^2, S_{bc}^2, and $S_{ac}S_{bc}$. Thus the self-consistent orbitals[21] readjust so as to reduce these intermolecular overlaps (over that for atomic orbitals) as shown in Fig. 8, and Table VI.

For H_2H at large separation between the H_2 and H, the wavefunction is also as in (8) and the orbitals again change as expected from Fig. 8(some differences occur since ϕ_b now has a much larger overlap with ϕ_c than does ϕ_a). The orbitals for several points along the reaction path are shown in Fig. 9, where each column refers to a different orbital and each row corresponds to a different geometry (the bottom row is for the saddle point). Here we see that the two bonding orbitals (ϕ_a and ϕ_b) gradually delocalize onto the D but retain a high overlap at each point. That is, this bonding pair stays highly bonding during the reaction. At the same time, the nonbonding orbital ϕ_c builds in nodes in the region of the bonding pair, resulting in smaller overlaps than would otherwise be expected (see Table VII). Indeed, at the saddle point the two bonding orbitals are gerade and the nonbonding orbital is ungerade, so that the nonbonding orbital is orthogonal to the bonding orbitals.

In order to investigate the importance of the nonbonding orbital being ungerade at the saddle point, we also carried out calculations in which this orbital was forced to be symmetric. As shown in Table VIII, this leads to an energy increase of 6.5 eV. Thus it is very important for the ϕ_c orbital to be ungerade in the transition region.

Another matter that needs to be discussed here is the permutational coupling of the orbitals. From Fig. 9 we see that at the

saddle point the SOGI orbitals can be described approximately as

$$\phi_a = \chi_1 + \chi_3$$

$$\phi_b = \chi_2 \tag{25}$$

$$\phi_c = \chi_1 - \chi_3 \; ,$$

where χ_1, χ_2, and χ_3 are s-like basis functions on the three centers (left to right). For the G1 coupling, substitution of (25) into (8) results in

$$G_{11}^{\mu}[\phi_a \phi_b \phi_c \alpha\beta\alpha] = A[(\chi_1\chi_2 + \chi_3\chi_2 + \chi_2\chi_1 + \chi_2\chi_3)(\chi_1 - \chi_3)\alpha\beta\alpha]$$

$$= A[-\chi_1\chi_2\chi_3 + \chi_3\chi_2\chi_1 + \chi_2\chi_1\chi_1 - \chi_2\chi_1\chi_3 + \chi_2\chi_3\chi_1 - \chi_2\chi_3\chi_3]\alpha\beta\alpha \tag{26}$$

$$= A\{[\chi_3\chi_1\chi_2 + \chi_2\chi_3\chi_1 - 2\chi_1\chi_2\chi_3 + \chi_2\chi_1\chi_1 - \chi_2\chi_3\chi_3]\alpha\beta\alpha\},$$

and thus leads to a fair amount of ionic character in the wavefunction. On the other hand, for GF coupling the wavefunction (9) becomes

$$2A\{[O_{ff}^d(\chi_3\chi_2\chi_1 - \chi_1\chi_2\chi_3)]\alpha\beta\alpha\}$$

$$= 2A\{[\chi_3\chi_2\chi_1 + \chi_2\chi_3\chi_1 - \chi_1\chi_2\chi_3 - \chi_2\chi_1\chi_3]\alpha\beta\alpha\} \tag{27}$$

$$= 2A\{[\chi_3\chi_1\chi_2 + \chi_2\chi_3\chi_1 - 2\chi_1\chi_2\chi_3]\alpha\beta\alpha\},$$

which differs from (26) by lacking ionic terms. Thus we would expect the GF coupling to be important in the transition region, and in fact it is.

B. The LiH + H $\rightleftharpoons$ Li + H$_2$ Reaction

The orbitals for points along the reaction path of LiH + H $\rightleftharpoons$ Li + H$_2$ are given in Fig. 10. Here we see changes just as for H$_2$ + D $\rightleftharpoons$ H + HD. The bonding orbitals of the reactions delocalize over all three centers in the transition region and relocalize to form the bond of the product while retaining large overlaps (Table IX).

Now the saddle point is not symmetric in a group theoretical sense, but it is still symmetric in an energy sense. That is, at the saddle point the bonding pair is equally bonding in both the LiH and HH regions and the remaining orbital is equally antibonding in these regions. Thus topologically the orbitals of LiH$_2$ are quite similar to those of H$_3$.

As can be seen in Table IX, the spin coupling changes in LiH$_2$ are comparable to those of H$_3$ even though the orbitals at the saddle point may not be so well approximated by (25).

V. DISCUSSION

In both reactions (1) and (2) we found that the bonding pair of orbitals remain highly overlapping as we proceed from the reactants, through the saddle point, to the products. Thus, we might view the bond as flipping or shifting from one pair or nuclei to another during the reaction. At the same time the bonding pair is shifting, say, from left to right, we must allow the nonbonding orbital starting on the right to shift to the left. However, in order to not disrupt the bonding pair it is necessary for this nonbonding orbital to remain approximately orthogonal to the bonding pair (this arises essentially from the Pauli Principle). As a result, the nonbonding orbital changes phase during the reaction. Normally one would not expect the phase of an orbital to have any consequence (the energy is invariant under a sign change in any orbital). However, as discussed elsewhere[24] the phase becomes important if the nonbonding orbital is actually bonded to some other atom. Indeed we have found using simple considerations of the continuity and changes in orbital phases during reactions, that one can readily predict selection rules for general classes of reactions.

A more technical application of this research is to indicate how one might pick basis functions and configurations for CI calculations on reactive systems. In the case of linear H_3, for example, we might start with the configurations $1\sigma^2 3\sigma$ and $2\sigma^2 3\sigma$ to sigma correlate the bonding electrons. The configuration $1\sigma 2\sigma 3\sigma$, however, is required to allow changes in spin coupling. Furthermore, we expect that at the saddle point both 1σ and 2σ are $\underline{g}$ functions while 3σ is $\underline{u}$.

Configurations $1\pi^2 2\sigma$ and $1\pi^2 3\sigma$ should be included to allow angular correlation of the bonding pair (where the 1π is selected from a π-split SOGI calculation). In addition to these configurations, it should be sufficient to include only single excitations to the higher orbitals [e.g., $1\sigma^2 n\sigma_u$, $1\sigma 3\sigma n\sigma_g$, $1\sigma 2\sigma n\sigma_u$ (using both spin couplings)].

In conclusion, the SOGI results for H_3 are in good agreement with the more exact results of Shavitt et al.[8] and Liu[11] and give an excellent qualitative understanding of the processes involved. This, together with the very reasonable results for LiH_2 and the work of Wilson[22] on H_4, suggests that SOGI independent particle wavefunctions form a good conceptual basis for theoretical work on reactions. This is not to say that the SOGI method is the best for actually calculating PES's because the accuracy obtained for given cost is not especially good. Independent particle wavefunctions, however, are easy to think about and one can use them to develop concepts for predicting about reactions (without detailed computations). Eventually, it may be possible to predict what features of molecular structure will make reactions easier or more difficult, thereby allowing us to predict which of two competing "allowed" reactions will proceed most readily.

REFERENCES

1. R. B. Woodward and R. Hoffmann, Angew. Chem. $\underset{\sim}{8}$, 781 (1969).

2. (a) W. A. Goddard III, Phys. Rev. $\underset{\sim}{157}$, 81 (1967); (b) R. C. Ladner and W. A. Goddard III, J. Chem. Phys. $\underset{\sim}{51}$, 1073 (1969).

3. W. E. Palke and W. A. Goddard III, J. Chem. Phys. $\underset{\sim}{50}$, 4524 (1969).

4. W. A. Goddard III, Phys. Rev. $\underset{\sim}{169}$, 120 (1968).

5. If a set of orbitals are antisymmetrically coupled in each spin coupling (tableaux) used, then the orbitals may be taken as mutually orthogonal. In the five-electron case, if we used only the G2, G4, and G5 couplings shown in (21), we could take "a" and "c" as orthogonal, but "b" and "d" could be taken as orthogonal only if we exclude the G4 coupling.

6. S. Huzinaga, J. Chem. Phys. $\underset{\sim}{42}$, 1293 (1965).

7. J. D. Bowman, Jr., J. O. Hirschfelder, and A. C. Wahl, J. Chem. Phys. $\underset{\sim}{53}$, 2743 (1970).

8. I. Shavitt, R. M. Stevens, F. L. Minn, and M. Karplus, J. Chem. Phys. $\underset{\sim}{48}$, 2700 (1968).

9. C. Edmiston and M. Krauss, J. Chem. Phys. $\underset{\sim}{45}$, 1833 (1966).

10. H. Conroy and B. Bruner, J. Chem. Phys. $\underset{\sim}{42}$, 4047 (1965); ibid. $\underset{\sim}{47}$, 921 (1967).

11. B. Liu reported by A. D. McLean in Proceedings of the Conference on Potential Energy Surfaces in Chemistry, University of California, Santa Cruz, August 10-13, 1970, W. A. Lester,

Jr., Ed. (IBM Research Laboratory, San Jose, California, 1971), Publication No. RA 18, January 14, 1971 (No. 14748), p. 102.

12. For three particles of mass m_1, m_2, and m_3 in a line, a common set of coordinates is the center of mass, X, and the two internal distances, r_{12} and r_{23}. If we define

$M \equiv m_1 + m_2 + m_3$ and $q_1 = \sqrt{m/m_3}\, r_{12}$ and

$$q_2 = \frac{(m_1 + m_2)}{\sqrt{m_1 + m_2}} \left\{ \frac{m_1 r_{12}}{(m_1 + m_2)} + r_{23} \right\},$$ we obtain a diagonal T

matrix; $2T = M\dot{X}^2 + \dfrac{m_1 m_2 m_3}{M(m_1 + m_2)} \left\{ \dot{q}_1^2 + \dot{q}_2^2 \right\}$.

13. I. Shavitt, J. Chem. Phys. $\underline{49}$, 4048 (1968).

14. See Table II.

15. G. S. Hammond, J. Am. Chem. Soc. $\underline{77}$, 334 (1955).

16. The experimental R_e for LiH is $3.015\ a_0$. G. Herzberg, Molecular Spectra and Molecular Structure. I. Spectra of Diatomic Molecules (D. Van Nostrand Co., Inc., Princeton, New Jersey, 1967).

17. J. C. Polanyi and W. H. Wong, J. Chem. Phys. $\underline{51}$, 1439 (1969).

18. These were calculated with a Numerov numerical integration method with an energy correction formula due to   Cooley, Math. Comp. $\underline{15}$, 363 (1961).

19. The symbol S_{AB}^{SCF} refers to the overlap between the self-consistent G1 orbitals A and B. S_{AB}^{Frozen} refers to the overlap between frozen atomic orbitals that give rise to A and B.

20. C. W. Wilson, Jr., and W. A. Goddard III, Chem. Phys. Letters $\underline{5}$, 45 (1970).

21. The basis set for the HeH calculations consisted of seven s-type and five p-sigma uncontracted Gaussians on He and four s-type contracted Gaussians (from seven s-type primitives) and three p-sigma uncontracted Gaussians on H. The exponents of the He s-functions ranged from 192.4388 to 0.0637066, the He p-sigma exponents ranged from 1.553506 to 0.018133. The H s-type exponents are those given in Table I plus a diffuse function $\zeta = 0.0331667$. The H p-sigma exponents were 2.44001, 0.56748, and 0.18916.

22. C. W. Wilson, Jr., and W. A. Goddard III, J. Chem. Phys. submitted for publication.

23. The reaction path was drawn by eye on a skewed-axis PES (see Fig. 6b). The curve was begun at the saddle point and was continued in both directions so that it crossed perpendicular to each contour line. At the LiH + H end, the direction of the curve as it crossed contour A was well-defined but would have led to shorter Li-H distance than the asymptotic Li-H distance. Therefore, we bent the curve so that it followed the asymptote. In this region the PES is very flat so that the reaction path is not well-defined. A similar procedure was used at the H_2 asymptote.

24. W. A. Goddard III, J. Am. Chem. Soc. 92, 7520 (1970); W. A. Goddard III and R. C. Ladner, ibid. 93, 0000 (1971); W. A. Goddard III, ibid. 94, 0000 (1972).

TABLE I.   Contracted Gaussian basis functions.

A.   Hydrogen basis functions.

	ζ_i	C_i
S	82.4736	0.00234426
S	12.3983	0.01772734
S	2.83924	0.0862417
S	0.814717	0.261700
S	0.271838	1.0
S	0.099482	1.0
P_z	2.44001	0.0060962
P_z	0.567483	0.0215045

B.   Lithium basis functions.

   1.   S functions

ζ_i	C_{i1}	C_{i2}	C_{i3}
7935.625	0.0001198	0.00006451	0.00000334
1176.8352	0.0009532	0.00050357	0.00002678
262.04646	0.00516471	0.00276280	0.00014165
71.913630	0.02279773	0.01123455	0.0061083
22.913010	0.08311079	0.03405256	0.00187656
8.15271	0.25759311	0.05544363	0.00437338
3.14527	0.40275427	0.19518164	0.00301758
1.29178	0.26392108	0.48017325	-0.01239931
0.55079	0.11691635	0.31590126	-0.07573432
0.19366	0.00973744	0.03265028	-0.02091724
0.08511	-0.00099095	-0.00661337	0.43734231

TABLE I. (continued)

Two uncontracted S functions with $\zeta = 0.03540$ and 0.01460 were added to these to give five S functions.

---

    2. P functions.

Three uncontracted 2p Gaussians with $\zeta = 0.744321$, 0.17628, and 0.054507 were used.

TABLE II. H, H_2, Li and LiH with various basis sets and methods.

A. Basis-set and correlation errors vs R for H_2.

R	E (hartrees) (present work)	E (hartrees) G1 - Σ limit[a]	Correlation Energy[a] (hartrees)	Basis Set Error[b]	
				(hartrees)	kcal
1.3	-1.14855715	-1.14913320	0.0232127	0.00057605	0.361
1.4	-1.1516073	-1.15214823	0.0223262	0.00054090	0.339
1.425	-1.15172805				
1.450	-1.15163334				
1.5	-1.15086762	-1.15140136	0.0214523	0.00053374	0.335
1.6	-1.14744936	-1.14799196	0.0205879	0.00054260	0.340
2.0	-1.12031722	-1.12089613	0.0172351	0.00057891	0.363
3.0	-1.04771581	-1.04809155	0.0092203	0.00037574	0.236
4.0	-1.01280364	-1.01308762	0.0032813	0.00028398	0.178
5.0	-1.00255689	-1.00284659	0.0009160	0.00028970	0.182
∞	-0.99971738	-1.00000000	0.0	0.00028262	0.179

B. Li Atom: $2\,^2S$ State.

G1: present basis set = -7.4475332; G1: best basis set[a] = -7.447560;

HF^b = -7.432727; CI^c = -7.4779; Experimental[d] = -7.47807.

C. G1 vs CI and experimental for H_2 and LiH. (All quantities are in hartree atomic units except as noted.)

		R_e	$E(R_e)$	D_e (kcal/mole)	Force Constant
H_2:	Present work SOGI	1.426	-1.151728	95.4	0.3447
	Bowman et al.[a] SOGI	1.430	-1.152319	95.5	0.3762
	SSMK 15BF CI	1.4018	-1.16959	106	0.36
	Experimental[c]	1.4008	-1.17445	109	0.365
LiH:	G1: present work	3.092	-8.0175370	44.0	0.05646
	Hartree-Fock[d]	3.034	-7.987315	34.2	e
	CI^f	e	-8.003513[g]	44.2[h]	e
	Experimental[i]	3.015			

[a] Bowman, Hirshfelder, and Wahl, J. Chem. Phys. 53, 2743 (1970).

[b] Taken as $E_{present work} - E_{G1 - \Sigma limit}$.

[c]

[d] P. E. Cade and W. Huo, J. Chem. Phys. 47, 614 (1967).

[e] From quadratic fit to lowest three energies.

[f] C. Bender and E. Davidson, J. Chem. Phys. 49, 4222 (1968).

[g] The 1s orbital on Li was doubly-occupied for all configurations, which adds a constant correlation error to the energy at all distances.

[h] For dissociation to Li with doubly-occupied 1s orbital.

[i]

TABLE III. Energies of Linear H_3 by Various Methods. All quantities in Hartree atomic units except as noted.

		H_3 Saddle Point		$H_2 + H \infty$		Barrier (Kcal/mole)	Force Constants[a]			
		E(Hartrees)	R(ao)	E(Hartrees)	Re		k(H_2) a.u.	$A_{11}(H_3)$ a.u.	$A_{22}(H_3)$ a.u.	$A_{33}(H_3)$ a.u.
Hartree-Fock	SPD[b]	-1.59484	1.725	-1.63360	1.40					
SOGI	SP	-1.624026	1.807	-1.651587	1.426	17.3	.345	.285	---	-.0609
CI	SP[c]	-1.6521	1.764	-1.66959	1.4018	11.0	.36	.31	.024	-.061
	SPD[b]	-1.6576	1.76	-1.67363	1.40	10.1				
Experimental[d]		-1.6580	---	-1.67445	1.4008	9.8±.2	.365			

a We use the same definitions of force constants as SSMK, Ref. 8.

b Reference 11.

c Reference 8.

d Reference 13.

TABLE IV. Vibrational Energies of H$_2$ and LiH.

(All quantities are in hartree atomic units. Masses used: H = 1.007825 a.m.u., D = 2.014 a.m.u.; ^{7}Li = 7.016 a.m.u., 1 a.m.u. = 1836.109 electron masses.)

ν	H$_2$		HD		D$_2$		H$_3$		^{7}LiH	
	E	$\langle R \rangle$	E	$\langle R \rangle$	E	$\langle R \rangle$	E	$\langle R \rangle$	E	$\langle R \rangle$
0	-1.1240947	1.577	-1.1434707	1.469	-1.1449718	1.451	-1.6197174	3.661	-8.0146146	3.146
1	-1.1070987	1.683	-1.1276489	1.556	-1.1319215	1.532	-1.6112896	3.757	-8.0089630	3.246
2	-1.1422094	1.475	-1.1126705	1.647	-1.1194375	1.605	-1.6031058	3.857	-8.0034935	3.350
3	-1.0912004	1.796	-1.0985192	1.742	-1.1076093	1.681	-1.5951679	3.960	-7.9982107	3.457
4	-1.0763939	1.918	-1.0851875	1.843	-1.0961302	1.760			-7.9931199	3.569
5	-1.0626879	2.050	-1.0726759	1.951	-1.0852972	1.842			-7.9882271	3.686
6	-1.0501052	2.196	-1.0609931	2.068	-1.0750111	1.930			-7.9835391	3.810
7	-1.0386836	2.361	-1.0501559	2.195	-1.0652761	2.023			-7.9790632	3.943
8	-1.0284778	2.553	-1.0401894	2.336	-1.0561002	2.122			-7.9748079	4.085
9	-1.0195630	2.786	-1.0311282	2.498	-1.0474949	2.230			-7.9707826	4.239
10	-1.0120432	3.082	-1.0230179	2.685	-1.0394755	2.348			-7.9669977	4.408

TABLE Va. Total energy (E), G1-orbital overlap $(S_{AB}^{SCF})^a$, Frozen-orbital overlap $(S_{AB}^{Frozen})^a$, orbital energy (ϵ_a), and exchange kinetic energy $(T^{C\ell})^b$ for H_2. Basis set shown in Table I. All quantities are shown in hartree atomic units.

R	E	S_{AB}^{SCF}	S_{AB}^{Frozen}	ϵ_a	T^x
0.85	-1.02609065	0.8740997	0.893646	-0.7945906	-0.147423
1.10	-1.12422358	0.8450657	0.833345	-0.7394547	-0.1551423
1.30	-1.148557149	0.8176371	0.780440	-0.7019394	-0.1579785
1.425	-1.151728047	0.7987028	0.746114	-0.6811800	-0.1586881
1.50	-1.150867619	0.7867051	0.725245	-0.6696316	-0.1588028
1.80	-1.135600054	0.7341451	0.641263	-0.6294672	-0.1572006
2.25	-1.099899183	0.642942	0.519731	-0.5840851	-0.1482257
2.50	-1.080278234	0.5871187	0.457168	-0.5650105	-0.1392930
3.50	-1.025754664	0.3568382	0.255934	-0.5197170	-0.0805010
5.00	-1.002556886	0.1249618	0.091760	-0.5019005	-0.0147973
$\infty = $ 100.0	-0.999717383	0.0	0.0	-0.4998587	0.0

[a] See Ref. 30.

[b] See Ref. 22.

TABLE Vb. Total energy (E), G1-orbital overlap $(S_{AB}^{SCF})^a$, Frozen-orbital overlap $(S_{AB}^{Frozen})^a$, orbital energies (ϵ_a and ϵ_b), and exchange kinetic energy $(T^{C\ell})^b$ for LiH. Basis set shown in Table I. All quantities are shown in hartree atomic units.

R	E_{Total}	S_{AB}^{SCF}	S_{AB}^{Frozen}	ϵ_{2a} (Li)	ϵ_{2b} (H)	T^x
*1.00	-7.3134088	0.700502	0.617533	-0.253127	-0.458434	-0.112124
1.50	-7.7684049	0.757052	0.596969	-0.292393	-0.518427	-0.256979
2.50	-8.0026939	0.771886	0.524027	-0.291428	-0.494470	-0.408040
3.015	-8.0173619	0.749701	0.473388	-0.280741	-0.473536	-0.445582
3.09	-8.01753689	0.744929	0.465556	-0.279020	-0.470812	-0.449712
3.20	-8.0172304	0.737324	0.453924	-0.276419	-0.467040	-0.455160
4.00	-8.0038167	0.665000	0.367154	-0.255564	-0.448944	-0.474281
6.00	-7.9628982	0.390620	0.181290	-0.211816	-0.466262	-0.419405
8.00	-7.9495154	0.141177	0.075406	-0.198231	-0.495029	-0.358214
∞	-7.9473919	0.0	0.0	-0.196150	-0.499859	0.0

[a] See Ref. 30.

[b] See Ref. 22.

TABLE VI. HeH at R = 3.30, Energies and Orbital Overlaps.
(All quantities in hartree atomic units.)

	Frozen Orbitals	G1 - SCF	G1 at R = ∞
E	-3.3689079	-3.3705143	-3.3773274
S_{ab}	0.8790347	0.8787471	0.8790347
S_{ac}	0.0953190	0.0727359	0.0
S_{bc}	0.1915120	0.1629936	0.0

TABLE VIIa. Overlaps and Orbital Energies along the Reaction Path of Linear H_3.[a]

Geometry	$R_{H_aH_b}$	$R_{H_bH_c}$	S_{ab}	S_{ac}	S_{bc}	ϵ_a	ϵ_b	ϵ_c
A	3.00	1.40	0.802125	0.0731475	0.225992	-0.6859627	-0.6866783	-0.4910542
--	2.50	1.40	0.8056272	0.1005474	0.3048296	-0.6910195	-0.691103	-0.4746754
B	2.20	1.50	0.802130	0.1140061	0.3451689.	-0.6822718	-0.6843005	-0.4594546
C	2.00	1.65	0.812575	0.102287	0.303698	-0.6838727	-0.67572606	-0.4453563
D	1.90	1.75	0.832144	0.0612713	0.177302	-0.7058064	-0.67219119	-0.4344739
E	1.80	1.80	0.8451508	0	0	-0.7243746	-0.6769058	-0.4277182

[a] All quantities in hartree atomic units.

TABLE VIIb. Classical Kinetic Energy (T^{Cl})^a, Exchange Kinetic Energy (T^x)^a, Electronic Energy, Total Energy, and Spin-Coupling Coefficients Along the Reaction Path of Linear H_3.^{b}

$R_{H_aH_b}$	$R_{H_bH_c}$	T^{Cl}	T^x	E_{Elect}	E_{Total}	C_{G1}	C_{G_2}
3.00	1.40	1.8285640	-0.130148284	-2.917272134	-1.64238036	0.9985852	-0.0531748
2.50	1.40	1.82757988	-0.11106646	-3.005064191	-1.634368221	0.993555	-0.113350
2.20	1.50	1.783171591	-0.100610396	-3.02039774	-1.629415352	0.9800010	-0.1989928
2.00	1.65	1.740641922	-0.10181383	-3.00579365	-1.625760444	0.9541367	-0.2993713
1.90	1.75	1.730787385	-0.10923037	-2.99605836	-1.6243413995	0.9371062	-0.3490444
1.80	1.80	1.743156320	-0.113136791	-3.012907852	-1.624018965	0.93258915	-0.3609397

^{a} See Ref. 22 for definitions.

^{b} All quantities are shown in hartree atomic units.

TABLE VIII. Comparison of Lowest $\underline{g}$ and $\underline{u}$ States of Linear Symmetric H_3 [a].

	H_3	H_3^+	
$R_1 = R_2 = 1.70\,a_0$			
$1^2\Sigma_u^+$ (ℓru) G1	-1.59790824	$1^1\Sigma_g^+$ (ℓr)	-1.2489326
$1^2\Sigma_u^+$ ($gg'u$) SOGI	-1.62046861	$1^1\Sigma_g^+$ (gg')	-1.2261434
$1^2\Sigma_g^+$ (ℓrg) G1	-1.3783697		
$R_1 = R_2 = 1.55\,a_0$			
$1^2\Sigma_u^+$ (ℓru) G1	-1.5912390	$1^1\Sigma_g^+$ (ℓr)	-1.2527228
$1^2\Sigma_u^+$ ($gg'u$) SOGI	-1.6096592	$1^1\Sigma_g^+$ (gg')	-1.2312538
$1^2\Sigma_g^+$ (ℓrg) G1	-1.3847354		
$1^2\Sigma_g^+$ ($gg'g''$) SOGI	-1.3632507		

[a] All quantities in hartree atomic units.

TABLE IXa. Orbital overlaps and orbital energies for valence orbitals of linear LiH$_2$ near reaction path.[a]

Geometry	R_{LiH_a}	$R_{H_aH_b}$	S_{ab}	S_{ac}	S_{bc}	ϵ_a	ϵ_b	ϵ_c
A	3.10	3.50	0.752928	0.296524	0.2031576	-0.282767	-0.474232	-0.3908928
-	3.10	3.00	0.759770	0.390553	0.281002	-0.2874222	-0.48418113	-0.3369322
B	3.20	3.00	0.7537325	0.3912514	0.284491	-0.2848935	-0.48154318	-0.3356856
C	3.30	2.80	0.7368527	0.4920810	0.2461485	-0.304315	-0.4955782	-0.2761460
D	3.50	2.50	0.5982924	0.0895088	-0.3250922	-0.555103	-0.5589735	-0.1952377
E	4.00	1.57	0.772449	-0.0434524	-0.163949	-0.6990133	-0.6974864	-0.1864244
F	4.80	1.43	0.7972672	-0.036545	-0.123507	-0.7018589	-0.7000622	-0.1911201

[a] All quantities in hartree atomic units.

TABLE IXb. Classical Kinetic Energy $(T^{C\ell})^a$, Exchange Kinetic Energy $(T^X)^a$, Electronic Energy, Total Energy, and Spin-Coupling Coefficients Along the Reaction Path of Linear·LiH$_2$.^{b}

R_{LiH_a}	$R_{H_aH_b}$	$T^{C\ell}$	T^X	E_{Elect}	E_{Total}	C_{G1}	C_{G2}	C_{G3}	C_{G4}	C_{G5}
3.10	3.50	8.9605595	-0.424661	-10.219815012	-8.511813336	0.999268	-0.00313690	-0.0381109	0.0071315	-0.00022488
3.10	3.00	8.959652405	-0.42384213	-10.30185888	-8.508980335	0.9886605	-0.003198656	-0.15012664	-0.00140269	-0.00043933
3.20	3.00	8.948856822	-0.43251516	-10.2639095	-8.50920524	0.9847923	-0.0032658	-0.1736986	0.001400684	-0.003983
3.30	2.80	8.994372827	-0.50800524	-10.2679453	-8.509908254	0.949220	-0.0038798	-0.3145840	0.00128002	-0.0012853
3.50	2.50	8.87776117	-0.45516925	-10.27746876	-8.520325902	0.9790182	-0.1126935	-0.2037243	0.00080839	-0.0042627
4.00	1.57	9.047010245	-0.486952516	-10.51166526	-8.586122943	0.9998202	-0.000513762	-0.0185715	0.00191244	-0.00327007
4.80	1.43	9.104093413	-0.49013213	-10.39941264	-8.593571005	0.9999384	-0.000222529	-0.0103898	0.00216426	-0.00324605

^{a} See Ref. 22 for definitions.

^{b} All quantities are shown in hartree atomic units.
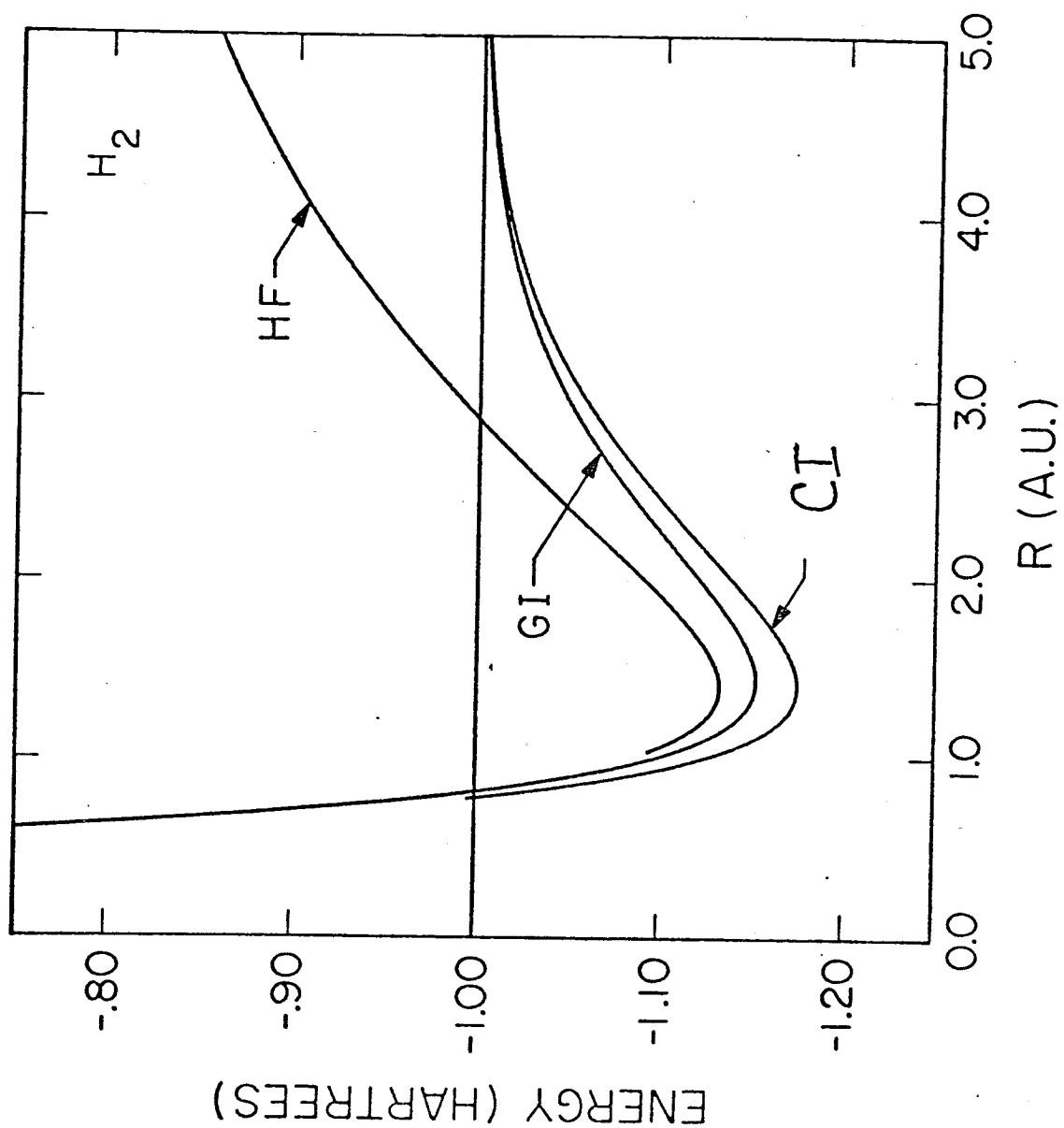
FIG. 1a.   Potential curves of H_2. The zero of energy for each
curve is two neutral hydrogen atoms as calculated with
the same basis set. Hartree-Fock energies from S.
Fraga and B. Ransil [J. Chem. Phys. 35, 1967 (1961)]
and CI energies from W. Kolos and L. Wolniewicz [J.
Chem. Phys. 41, 3663 (1964)].
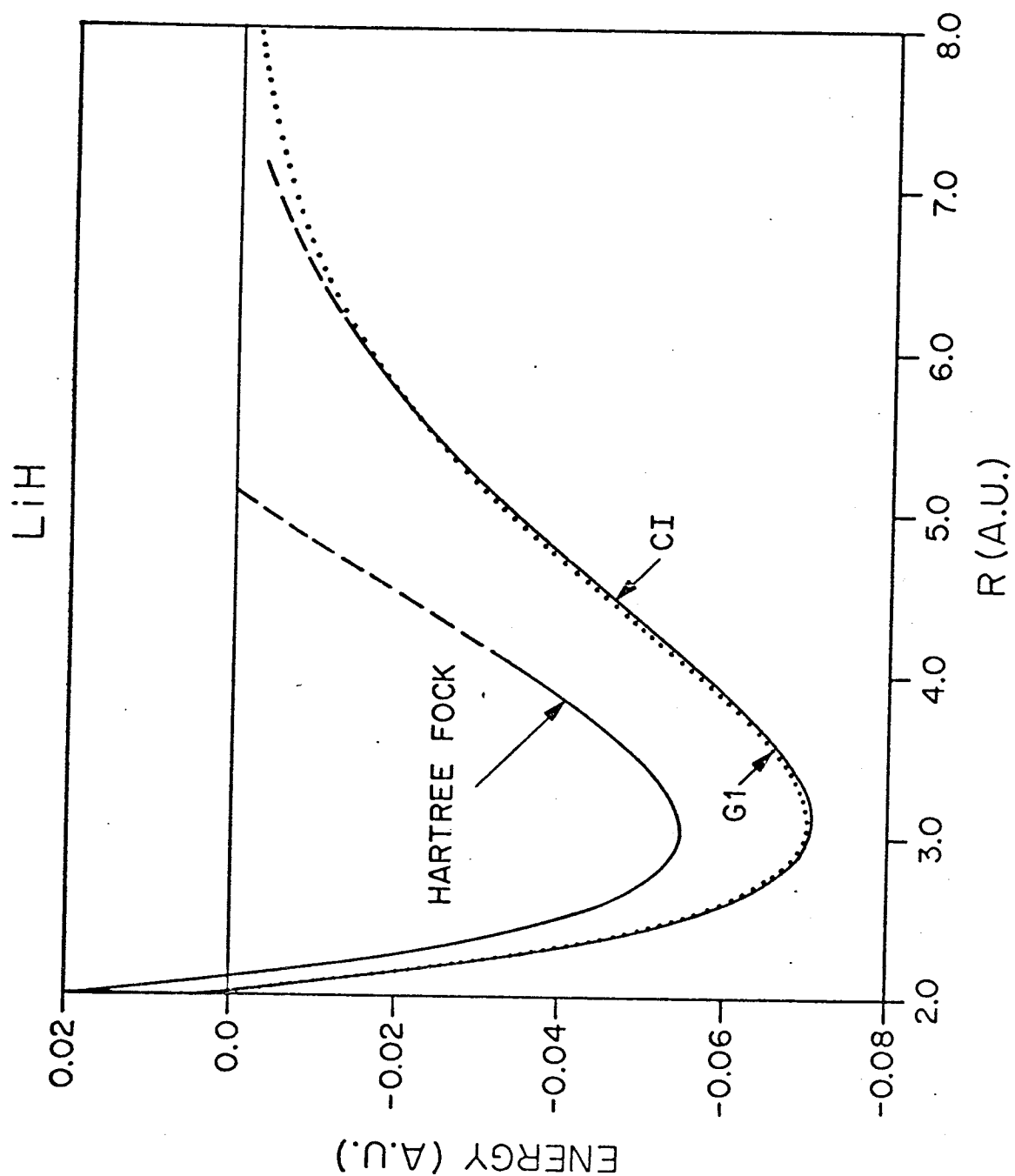
FIG. 1b. Potential curves of LiH. The zero of energy for each curve is the energy for the neutral atoms as calculated by the same method. Hartree-Fock energies from P. E. Cade and W. Huo [J. Chem. Phys. 47, 614 (1967)]; CI energies from C. Bender and E. Davidson [J. Chem. Phys. 49, 4222 (1968)]; G1 energies calculated with basis set of Table I.

FIG. 2. G1 orbitals for H_2 as a function of R. The upper box at

each distance is a contour map of the left-hand orbital (ϕ_a)

and the lower box is a line-plot of the amplitude of each

orbital plotted along the internuclear axis. For all contour

plots in this paper, the interval between contours (Δ) is

0.06 a.u. unless otherwise noted. Atom locations are

marked by crosses (+) on contour plots and by triangles

($\blacktriangle$) on line-plots. Notice that the orbitals are not sym-

metrical about the center of symmetry but go into each

other under inversion.

H₂ SOGI
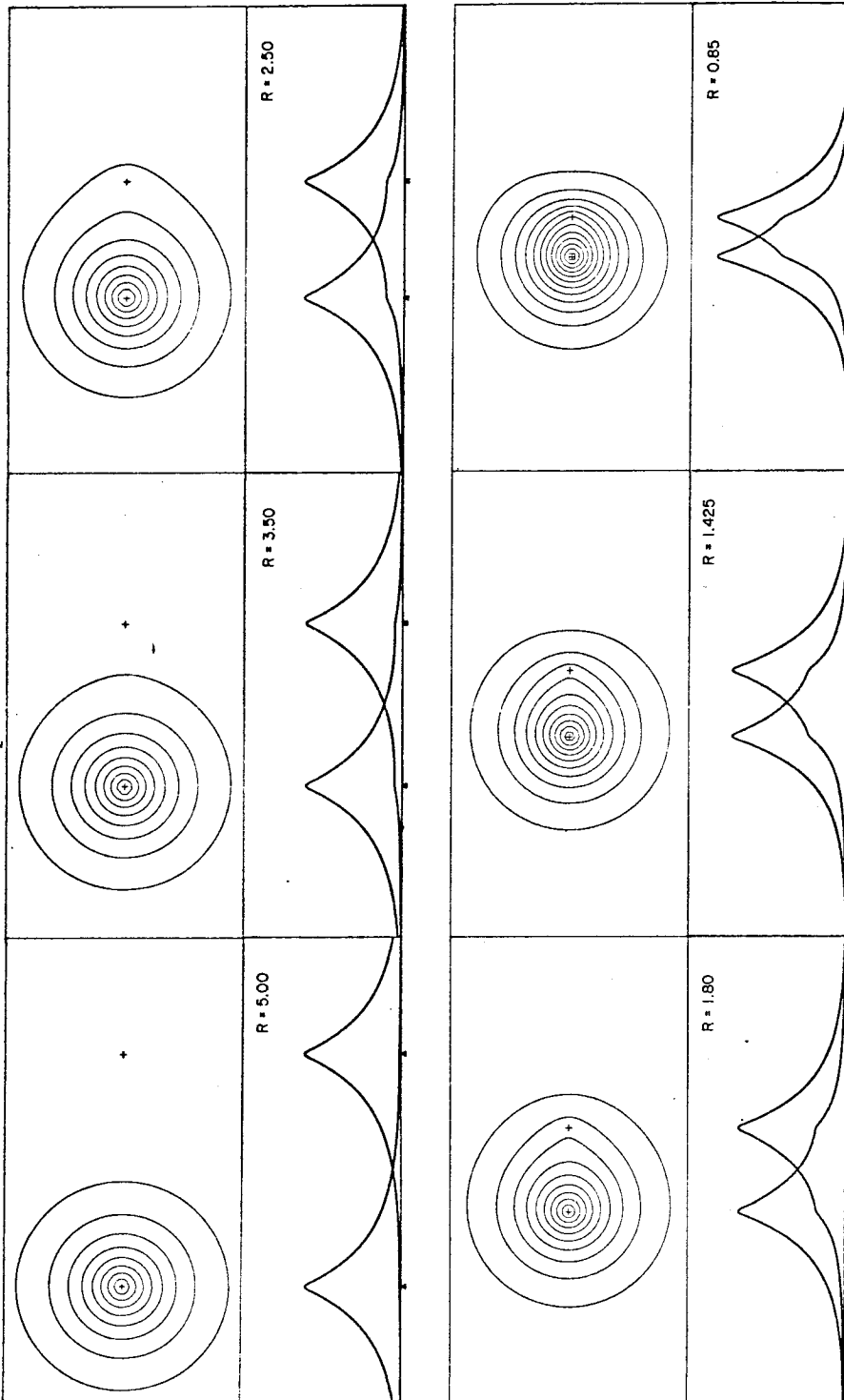
LIH SOGI
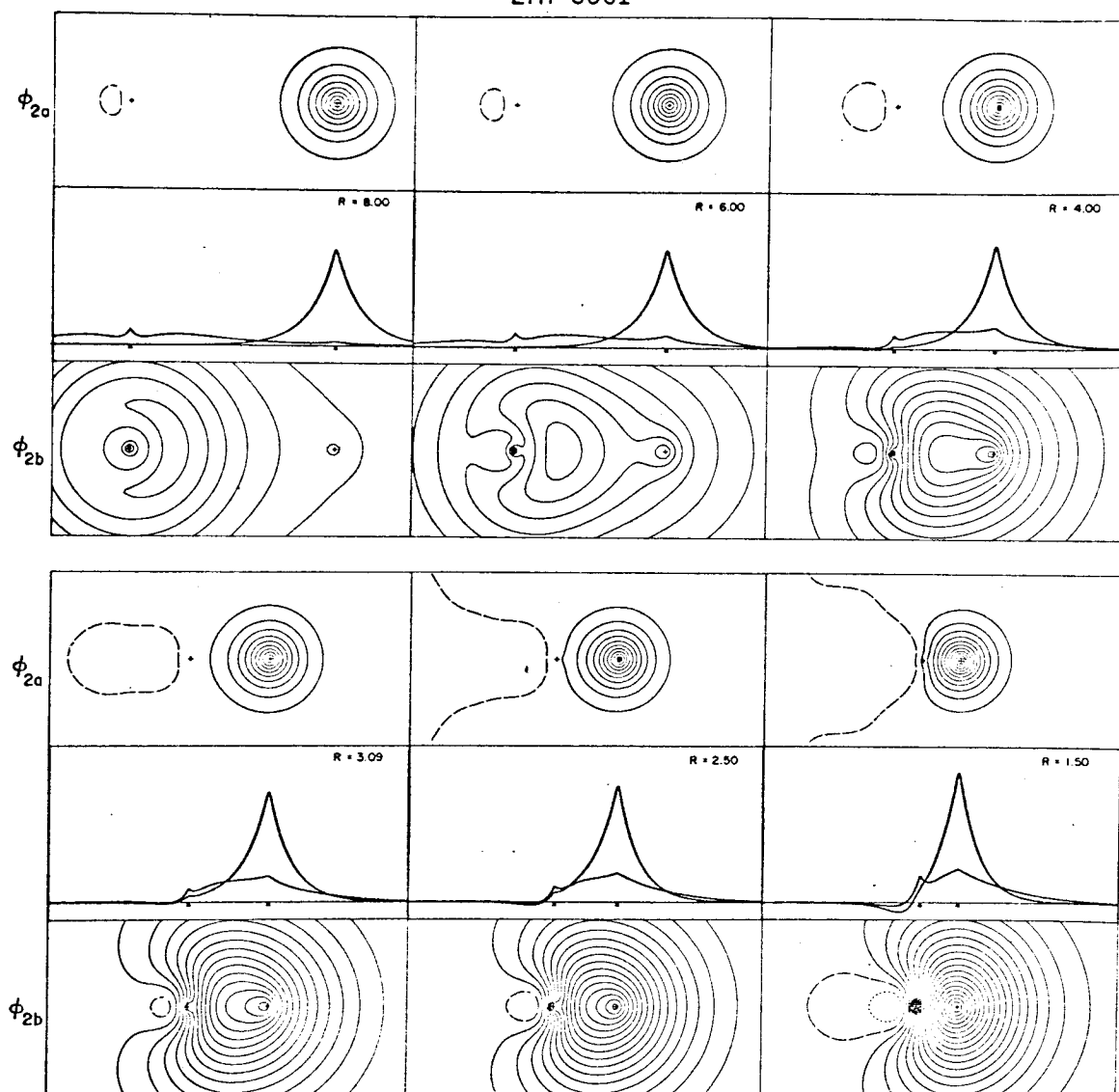
FIG. 3.   G1 valence orbitals for LiH as a function of R. In each
case, the Li is on the left and the H on the right.   The
upper box is the tight, hydrogen-like orbital plotted with
a contour interval of 0.06 a.u.   The center box is a line-
plot of both orbitals (to the same scale) along the molecular
axis.   The lower box is the diffuse, Li 2s-like orbital
plotted with an interval of 0.01 a.u.
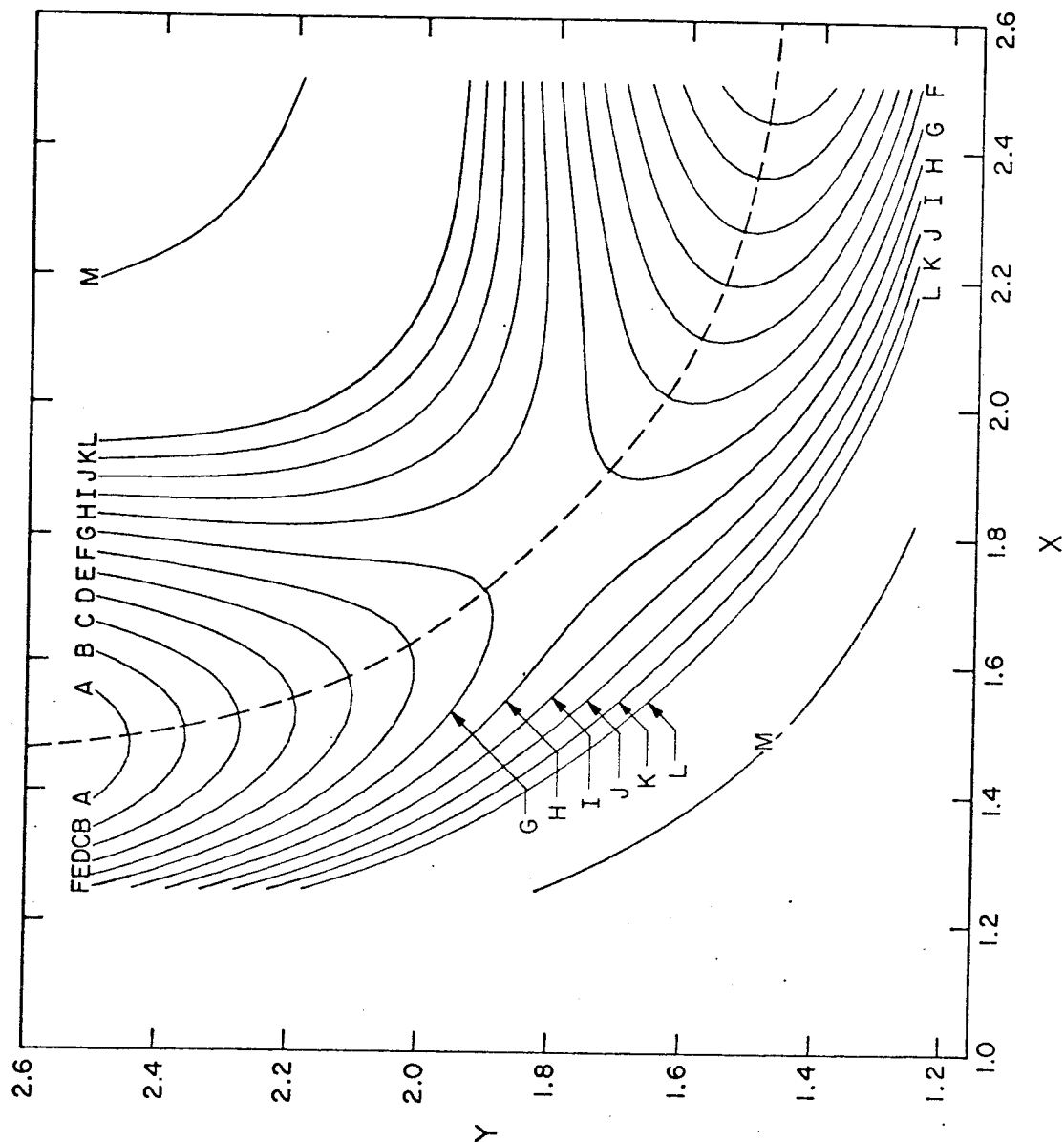
FIG. 4a. SOGI potential-energy surface for linear H_3. $X = R_{H1-H2}$, $Y = R_{H2-H3}$. We have subtracted 0.0281 hartrees from all our total energies so that the energy of the SOGI surface as its saddle point will be the same as the energy of the SSMK surface (Fig. 4c) at its saddle point. The saddle point is taken as 11.35 kcal/mole. Contour A is at 5 kcal/mole and L is at 16 kcal/mole, with the contours in between differing by 1 kcal/mole. M is at 25 kcal/mole.

FIG. 4b.   SOGI potential energy surface for linear H_3. The coordinates that diagonalize T are shown orthogonal. The spacing between contours is 1 kcal/mole; the lowest contour is 11 kcal/mole above H_2 + H, the highest is 25 kcal/mole and the saddle point is 17.3 kcal/mole.
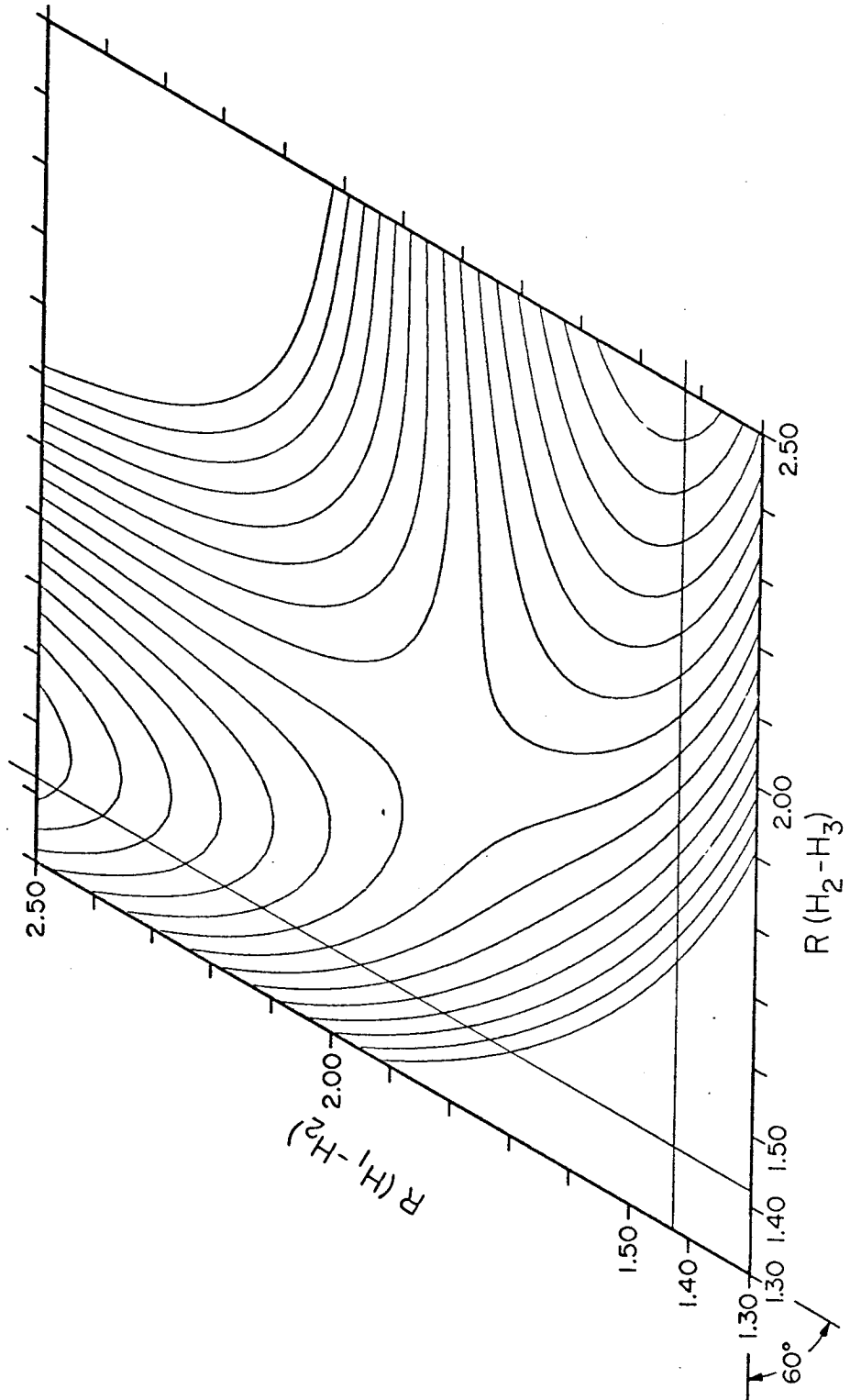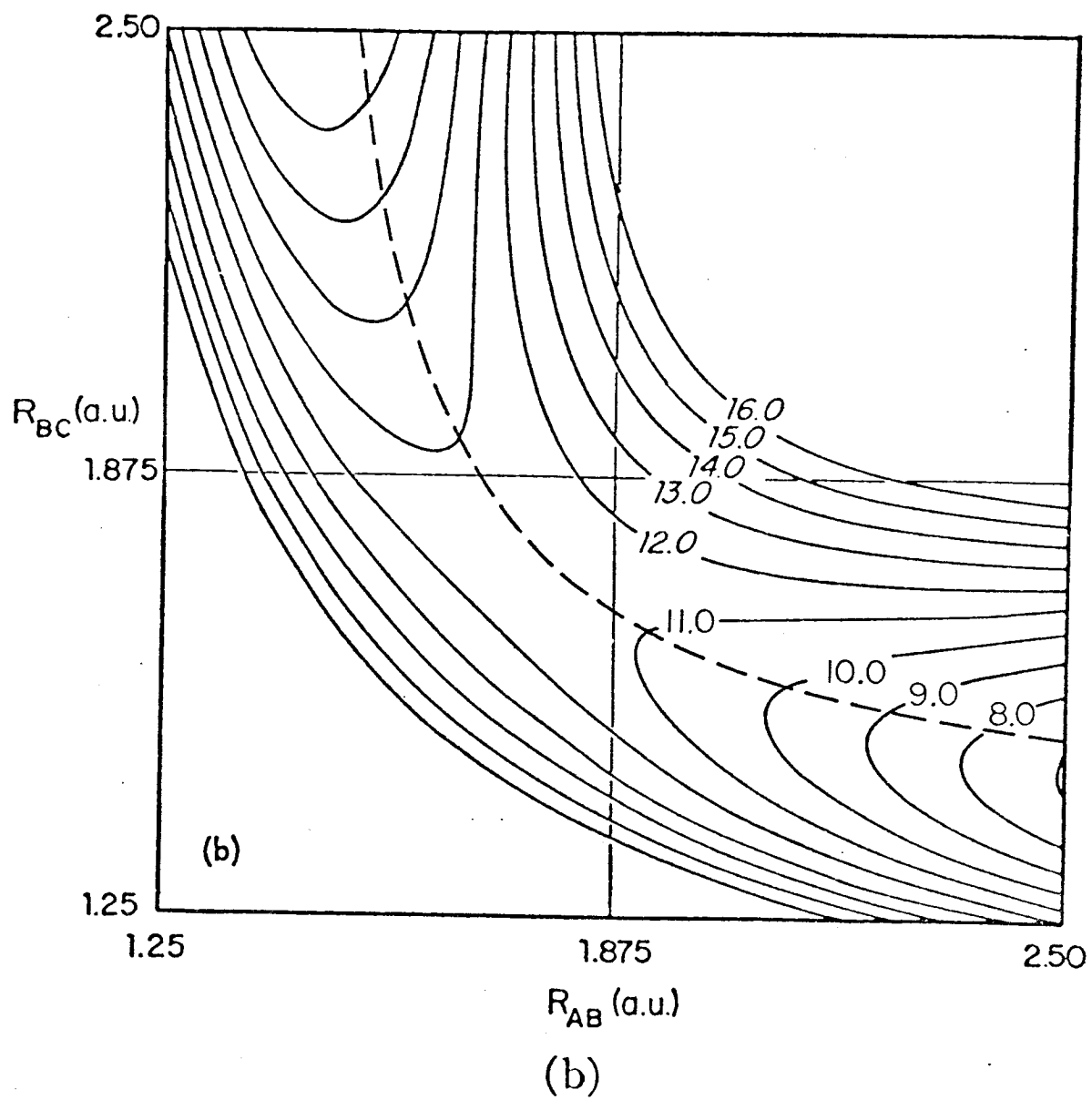
FIG. 4c.   CI potential energy surface for linear H_3 from SSMK (Ref. 8).
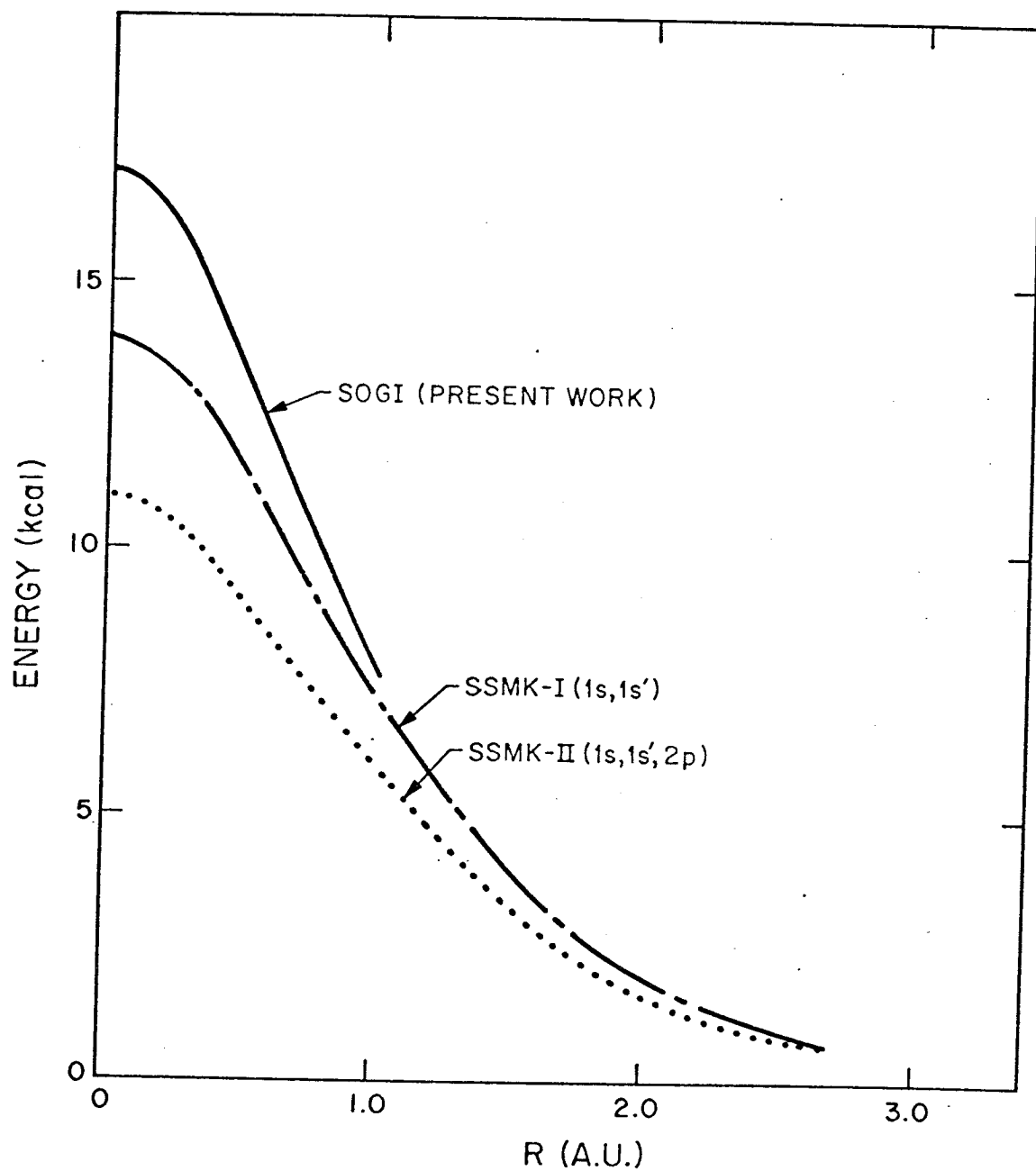
FIG. 5a.   Energy profile along reaction path of linear H_3 for SOGI, SSMK-I, and SSMK-II (Ref. 8).
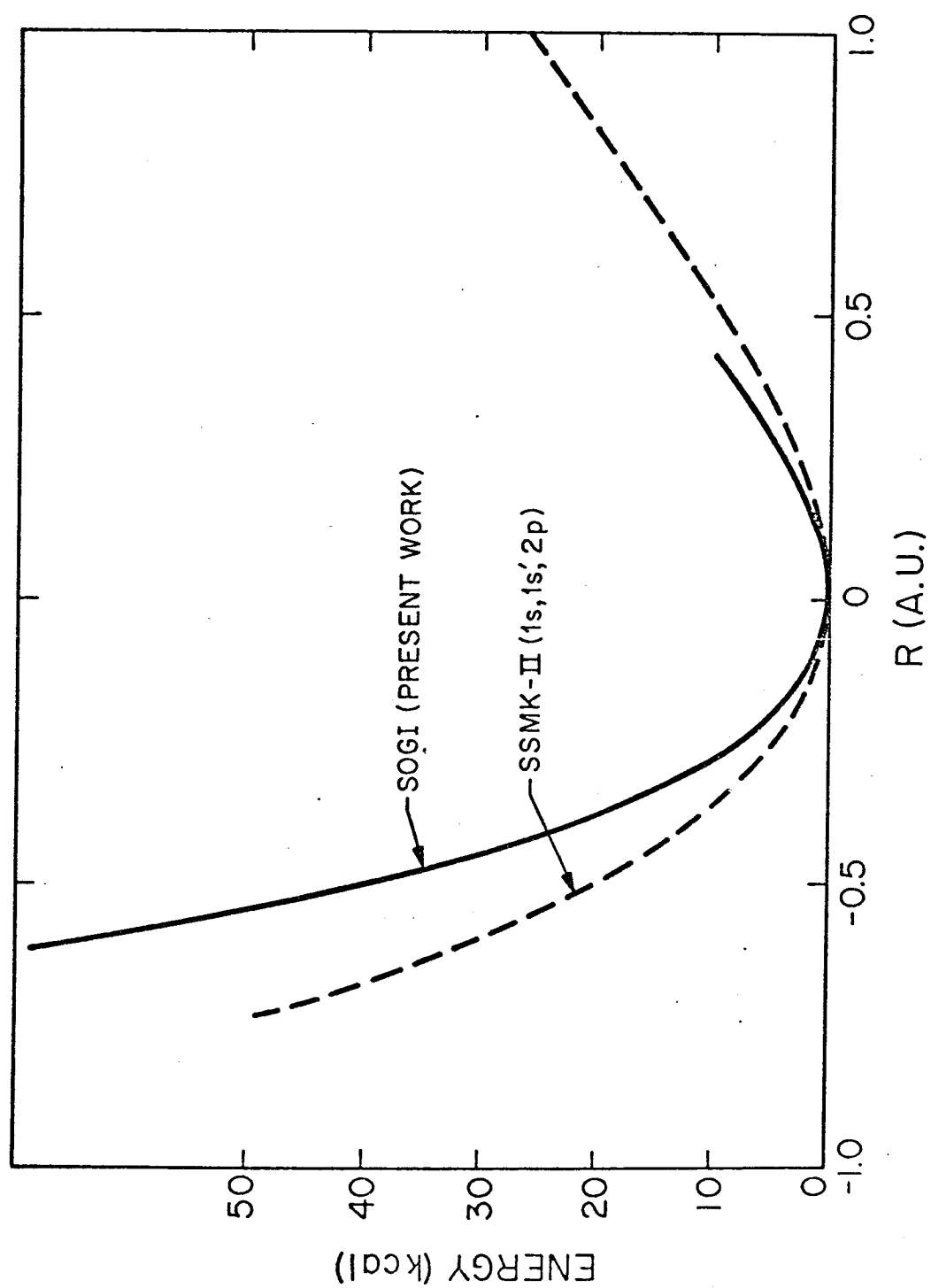
FIG. 5b. Energy profile for linear H_3 perpendicular to the reaction path at the saddle point and SSMK (Ref. 8).
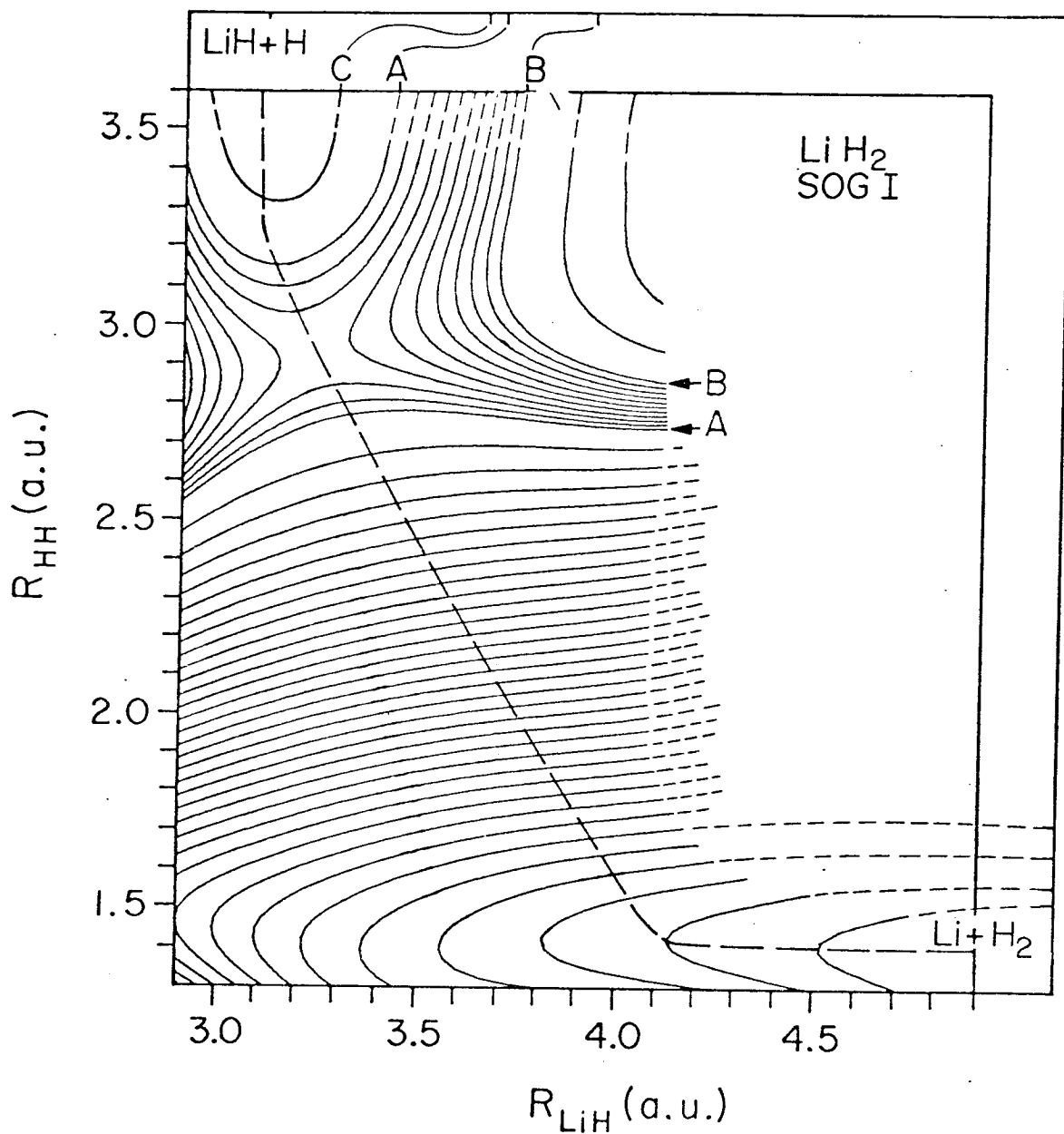
FIG. 6a.   SOGI potential-energy surface for Linear LiHH.   Contour

level C is at -8.51125   hartrees, level A is at -8.510

hartrees, and B is at -8.505 hartrees.   Between A and B,

contours are 0.0005 hartree apart.   Below A, the contours

are 0.0025 hartree apart.   At the upper edge we have

indicated where the contours C, A, and B occur at the LiH +

H limit by tick marks identified by curved lines from the

labels "C", "A", and "B".   The dashed line indicates an

approximate reaction path (see Ref. 23).
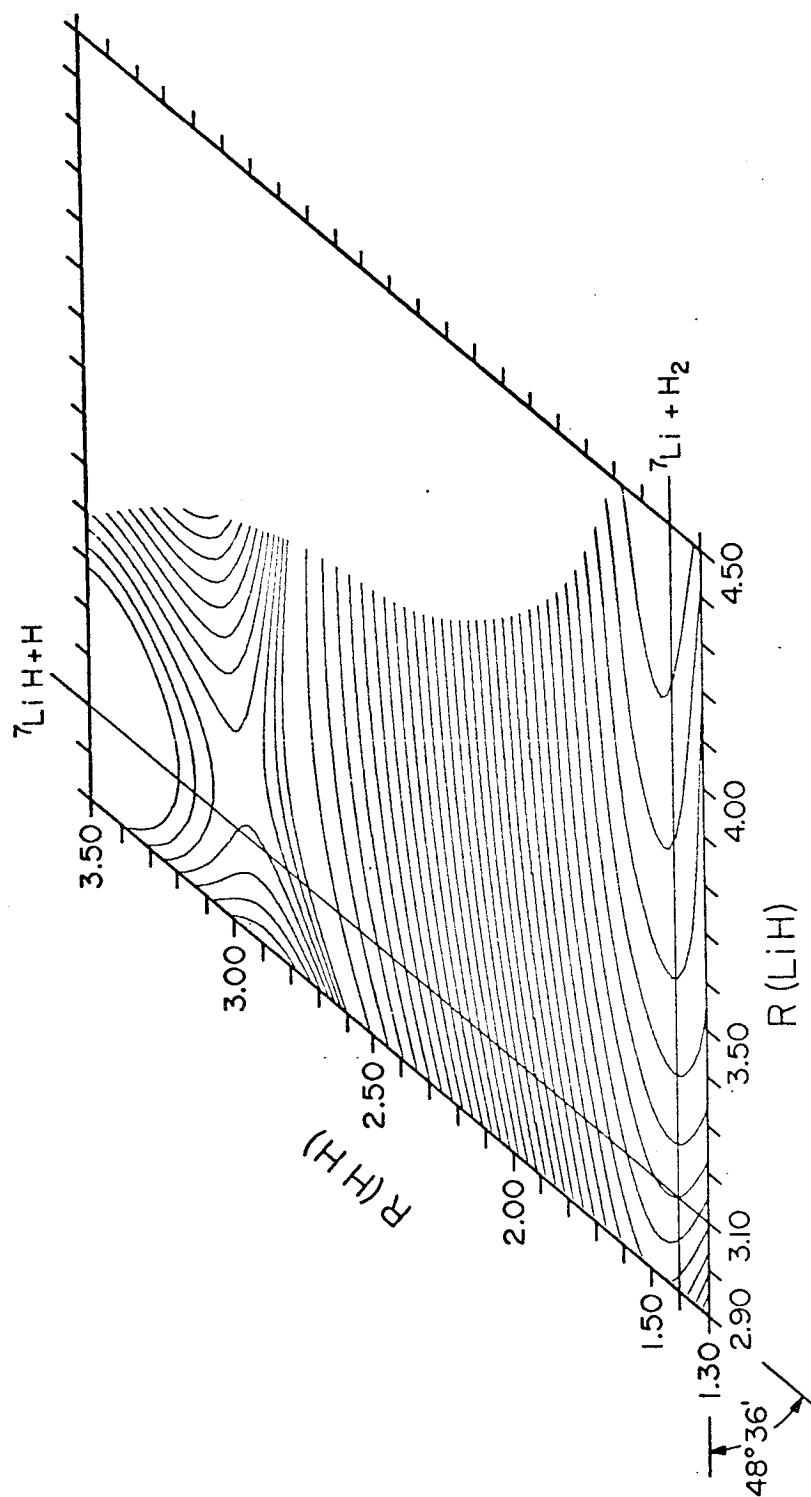
FIG. 6b.   SOGI potential-energy surface for Linear ^{7}Li ^{1}H^{1}H with T

diagonal (see Ref. 12).   The contour levels are the same

as those used in Fig. 6a except level C is omitted.
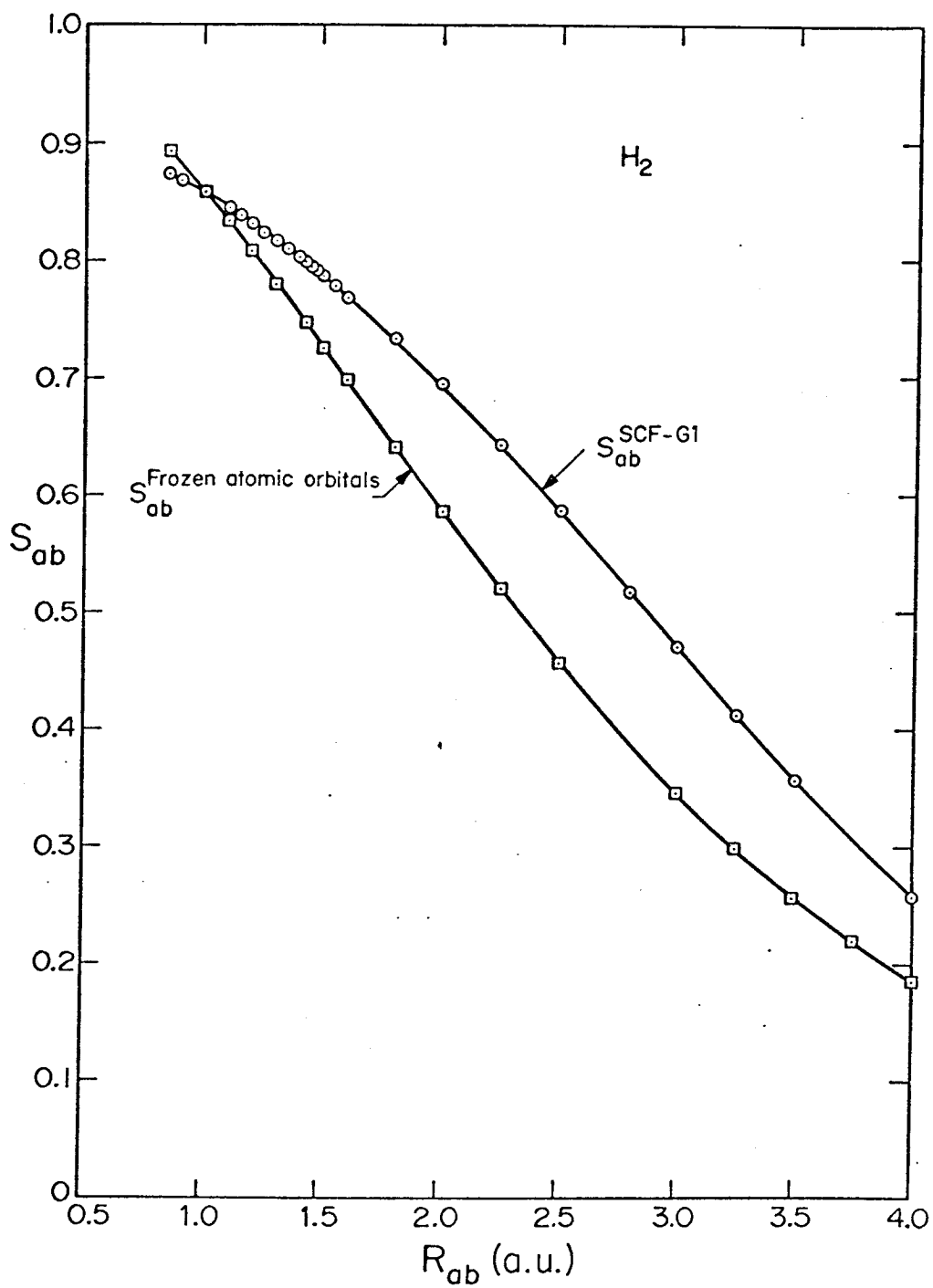
FIG. 7a.   Overlaps of self-consistent G1 orbitals and frozen atomic orbitals for H_2.
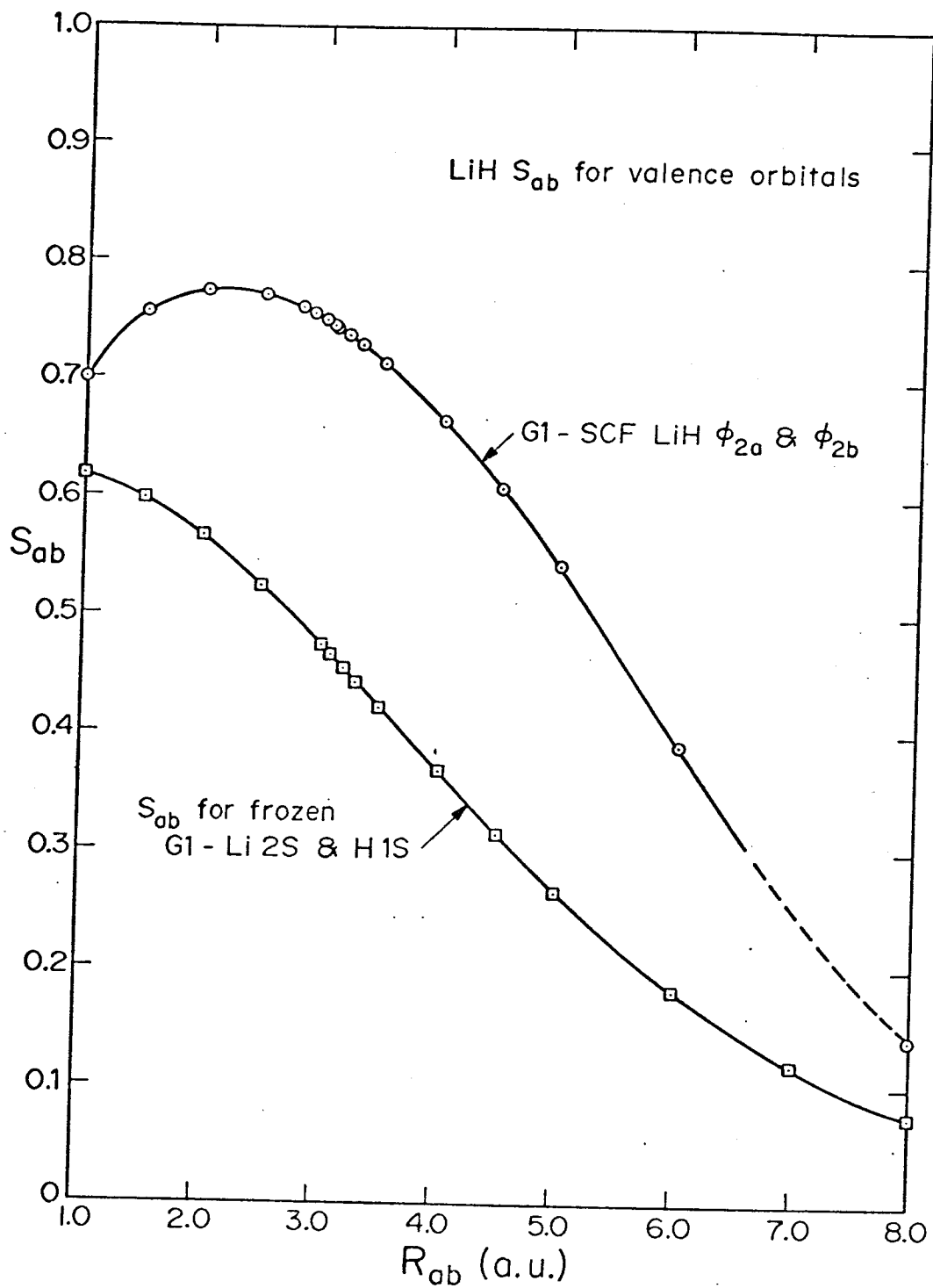
FIG. 7b.   Overlaps of self-consistent G1 orbitals and frozen atomic orbitals for LiH.
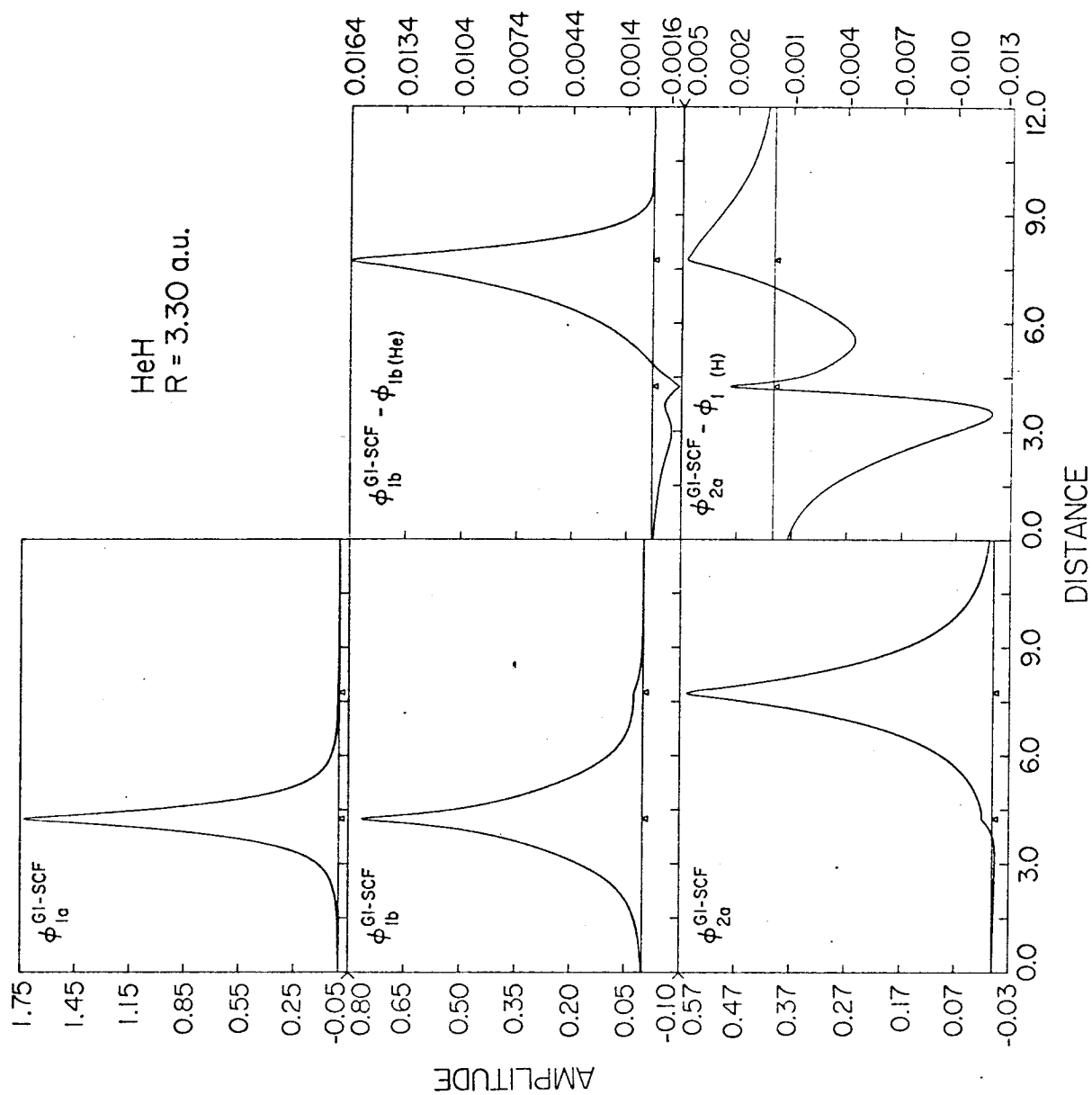
FIG. 8.   G1 orbitals for He-H.   Distances in bohrs and amplitude

in atomic units.
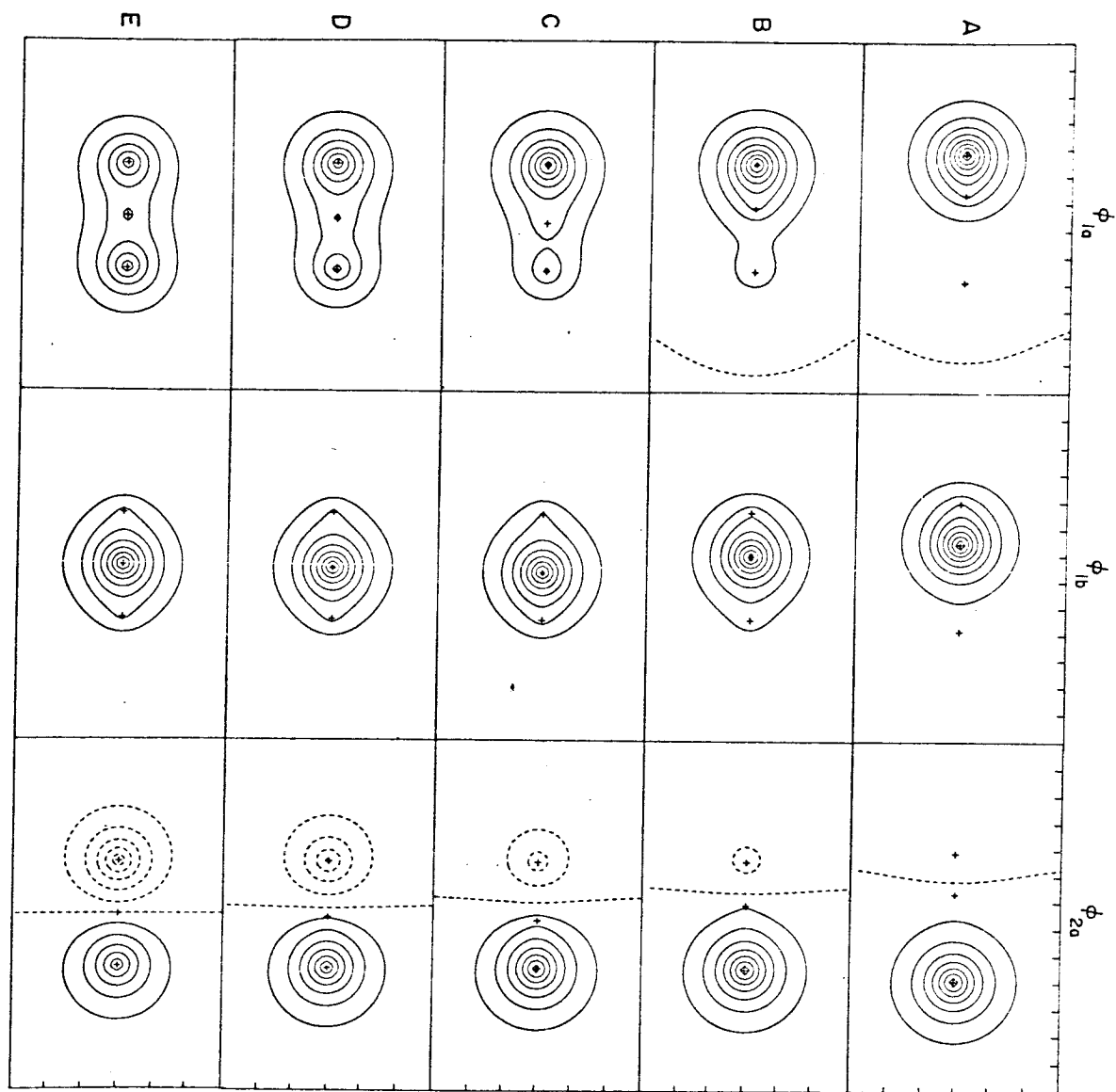
FIG. 9.   SOGI orbitals for linear H_3. Each row refers to a particular geometry, each column to a particular orbital. The letters A through E refer to the "Geometry" column of Table VIIIa. The contour interval is 0.06 a.u. and each plot is 12.0 a_0 by 7.0 a_0. ϕ_{1a} and ϕ_{1b} are the bonding pair and ϕ_{2b} is the nonbonding pair.

FIG. 10a. SOGI valence orbitals near the reaction path for linear

LiH_2. The large rows correspond to different geometries

(denoted by the letters A, B, etc., which refer to Table

IXa) and the columns to different orbitals. Each large row

is composed of a row of contour plots above a row of line

plots of the same orbitals. The columns are all 15 a_0

wide. The contour plots are 10 a_0 high and the contour

interval is 0.06 a.u. except as noted. The line plots all

run from -0.20 a.u. to 0.70 a.u.

ϕ_{1a} ϕ_{1b} ϕ_{2a}
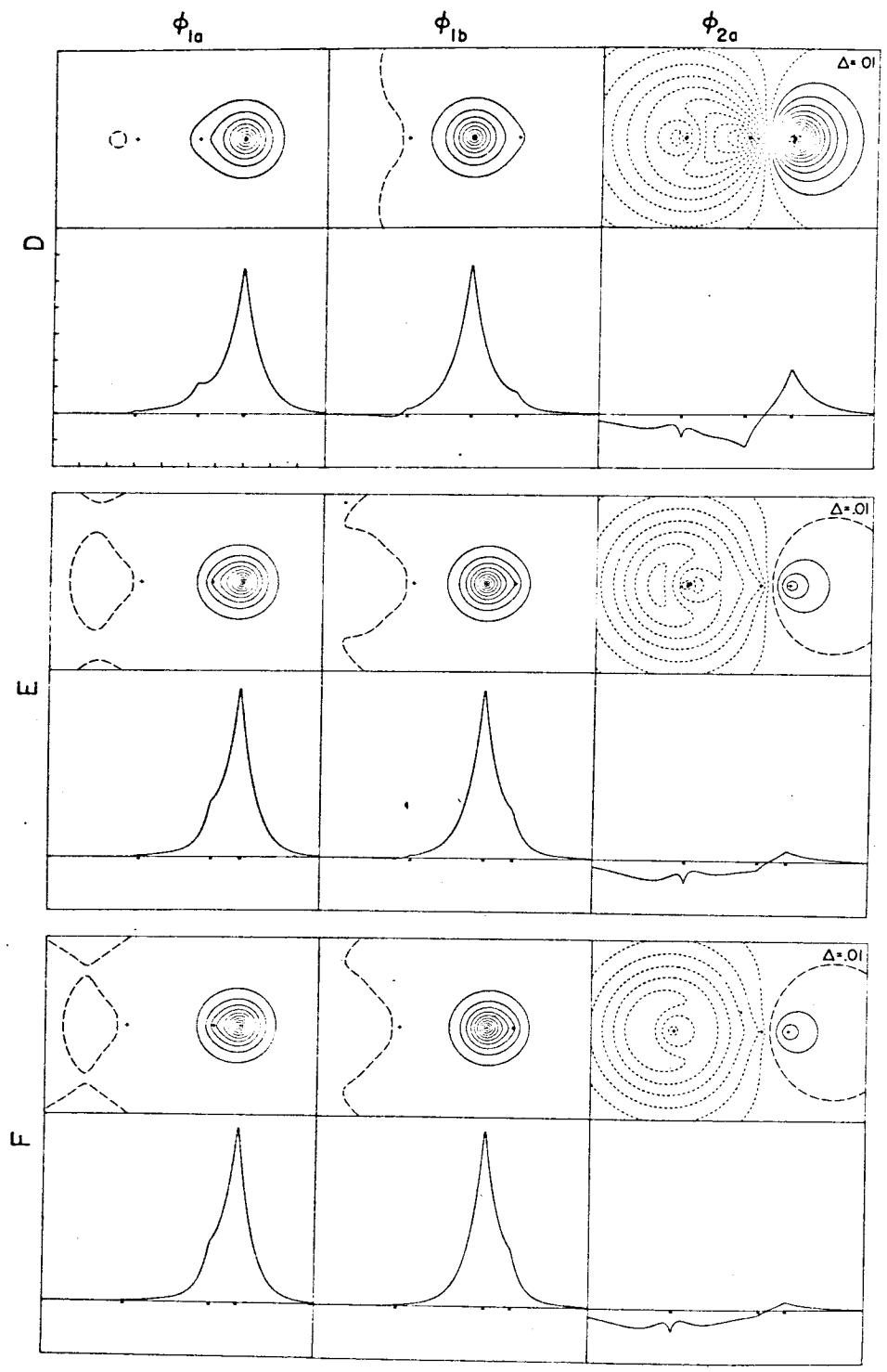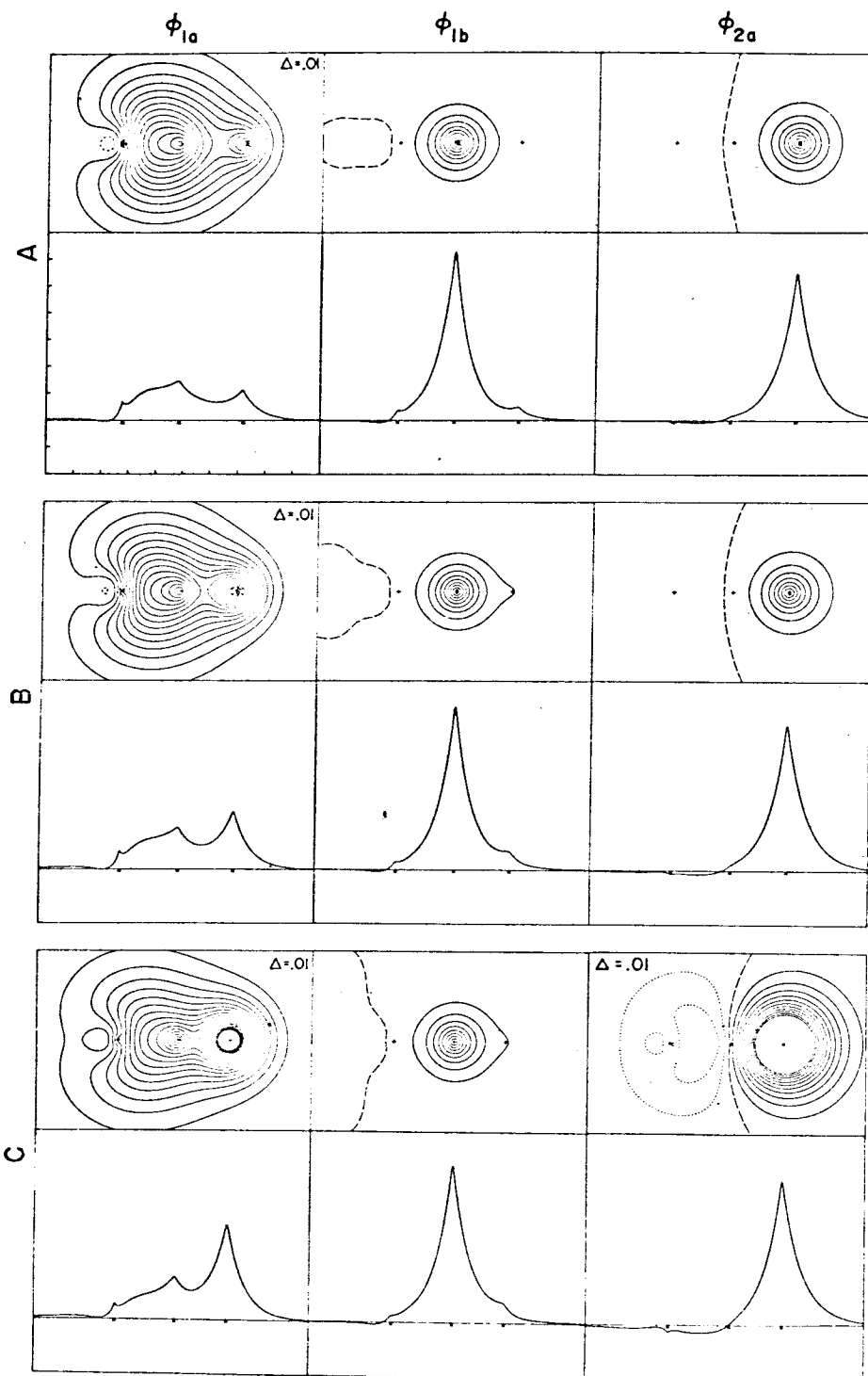
FIG. 10b. SOGI valence orbitals near the reaction path for linear
LiH$_2$. See Fig. 10a.

III. Potential Energy Surfaces for Reactions
Involving Excited Atoms and Molecules.

INTRODUCTION

The SOGI calculations on $H_2 + D$ and $LiH + H$ discussed in Chapter II illustrate how the SOGI method provides an accurate but easily understood description of chemical reactions and therefore provides an excellent basis for making predictions about whole classes of reactions without detailed calculations. Unfortunately, the results of Chapter II are limited to the lowest electronic state for each geometry. In the final chapter of this thesis we discuss the extension of the SOGI method to reactions involving electronically excited atoms and molecules.

Although there have been several studies with a variety of methods of potential-energy surfaces (PES) for ground-state systems, there have been very few accurate, detailed studies of surfaces for excited states. Conroy[1] has calculated PES's for excited states of H_3^{++} and H_3^+ in C_{2v} geometry, but then only for the lowest state of each symmetry. Furthermore, Conroy's wavefunction does not lead to an independent-particle interpretation so that the changes in the wavefunction that cause the PES's to have structure are not easily visualized.

We have carried out SOGI, G1, and CI calculations on several geometries of H_3 and obtained the first four or five states at each geometry. The aim of this study was not to provide detailed excited-state PES's, but rather to discover if the SOGI method gives a good description of excited states for arbitrary geometries and to find out if the SOGI or G1 orbitals for these excited states leads to a meaningful interpretation of these states.

Section I contains the technical details of solving for excited states. Section II contains the energy results of the SOGI and CI

calculations. Section III is a discussion of the orbitals, and the conclusions are reported in Section IV.

I. TECHNIQUES

A. Excited States

Calculation of self-consistent SOGI wavefunctions has been approached in two ways. The first method is the one described in Chapter I, which we call the Hamiltonian method in which one forms and diagonalizes N (the number of electrons) Hamiltonian matrices $(\mathcal{H})$. These Hamiltonians are formed from trial orbitals (ϕ_i); the ith Hamiltonian $(\mathcal{H}_i)$ depends on all the orbitals except ϕ_i and one of the eigenfunctions of $\mathcal{H}_i$ is taken as the new ϕ_i in the iterative procedure. When one is solving for the ground state, one always selects the lowest eigenvector of each Hamiltonian. However, as has been pointed out by Goddard[2] and Melius and Goddard[3], one can obtain excited states by consistently selecting a higher root of one or more Hamiltonians. When this procedure converges to a stationary state, we obtain an upper bound to one of the excited states of the system. Exactly which excited state one obtains is not clear in general since multiple orbital excitation may lead to low-lying excited states, which would not appear unless one suspected their existence and specifically looked for them. Thus, picking the nth solution of some $\mathcal{H}_k$ insures that we obtain an upper bound on the nth state, but we may in reality obtain a good approximation to a higher state. This method has been applied to the excited states of Li,[2] and the results are quite satisfactory, however, one must scrutinize the results carefully.

The method used in this research is based on the Hamiltonian-Supermatrix method described in Appendix I. In this method, one constructs a supermatrix ($\underset{\sim}{B}$) and a vector $\vec{X}$ such that

$$\underset{\sim}{B}\vec{\delta} = \vec{X},\tag{1}$$

where $\vec{\delta}$ is the change in the wavefunction and $\vec{X}$ measures how far the trial function is from a stationary point. We must solve (1) for $\vec{\delta}$, given $\underset{\sim}{B}$ and $\vec{X}$; that is, we must invert $\underset{\sim}{B}$. Unfortunately, $\underset{\sim}{B}$ is singular because it is the matrix of second derivatives of the energy with respect to variations in the wavefunction, and there are variations that do not change the energy (such as renormalizing). Therefore, we resort to the following procedure.

Consider a nonsingular real symmetric matrix $\underset{\sim}{A}$ and the orthogonal matrix $\underset{\sim}{V}$ such that

$$\underset{\sim}{\tilde{V}}\,\underset{\sim}{A}\,\underset{\sim}{V} = \underset{\sim}{a},\tag{2}$$

where $\underset{\sim}{a}$ is the diagonal matrix of eigenvalues of $\underset{\sim}{A}$. Inverting $\underset{\sim}{a}$ is trivial;

$$(\underset{\sim}{a}^{-1})_{ij} = (a_{ij})^{-1}\delta_{ij}\tag{3}$$

(where δ_{ij} is a Kronecker delta). Once we have $\underset{\sim}{a}^{-1}$, $\underset{\sim}{A}^{-1}$ is easy,

$$\underset{\sim}{A}^{-1} = \underset{\sim}{V}\,\underset{\sim}{a}^{-1}\underset{\sim}{\tilde{V}}.\tag{4}$$

When we diagonalize $\underset{\sim}{B}$, however, we find several zero eigenvalues (indicating that the matrix is singular). Our procedure is to set the inverse of these zero eigenvalues to zero; this is called deleting the eigenvalue. The remaining eigenvalues of $\underset{\sim}{B}$ can be either positive or negative. We have given the following interpretation to the eigenvalues and eigenvectors; the eigenvalues are modes of change in the wave-

function and the eigenvalue indicates which way the change will affect the energy. Positive eigenvalues appear for modes that will lower the energy (as seen from the trial function) and negative eigenvalues for ways of raising the energy. When solving for the ground state, there are normally no negative eigenvalues, meaning that every change made will lower the energy. When the nth excited-state[4] SOGI wave-function is used to form $\hat{B}$, we find n negative eigenvalues. Thus, to find the nth excited state of a system (starting from some trial function), we retain n negative eigenvalues of $\hat{B}$.[5] This procedure has some of the same problems as the Hamiltonian method since retaining n negative eigenvalues only insures that we are at least as high as the n excited state. Carl Melius[3] has used this procedure on excited states of LiH and has obtained very satisfactory results. David Huestis[6] has used this same method in his projected-G1 study of the excited states of H_2.

One problem remains and that is picking the spin coupling. When solving for the ground state, the procedure is to do one iteration of adjusting the spatial orbitals and then to find the best spin coupling for the new orbitals. When solving for excited states, this procedure will not work. This is because the orbitals that form the nth excited state for one spin coupling may produce an approximation to the ground state for some other spin coupling. Indeed, the spin-coupling optimization tries to do just this and the iterative procedure breaks down. Therefore, we solve for the nth excited state at each of a series of fixed spin couplings and select the spin coupling that gives the lowest energy for that state.

One method of computing wavefunctions for excited states that does not suffer from so much ambiguity is the CI method. When enough configurations of the right form, constructed from a suitable basis set, are used, one only has to solve for the first n eigenvalues of the CI matrix to obtain (n - 1) excited states plus the ground state. Obtaining accurate energies and wavefunctions for arbitrary excited states with CI is not trivial, since one must select the suitable basis set and pick the right configurations; this process is an area of active research. The close agreement between energies and main configurations of SOGI and CI excited states, for the cases we have considered, indicates that the SOGI results are essentially correct.

B. Basis Sets for SOGI and G1

SOGI and G1 calculations were carried out for six linear and three nonlinear geometries shown in Table I. For the linear geometries, only sigma/functions were used since pi and higher functions would not enter into the wavefunction. Similarly, for the nonlinear cases, only functions symmetric with respect to the molecular plane were included. Three geometries (called A, B, and C in Table I) of $D_{\infty h}$ symmetry were chosen near the minimum found by Conroy[1] in the linear symmetric H_3^+ potential curve. For these, as well as two asymmetric geometries called D and E, we chose a basis of three contracted S-type Gaussians and two contracted p-type Gaussians on each center; this basis is shown in Table IIa. The basis was chosen to give good values of the 1S and 2S energy of hydrogen at infinity. The basis was supposed to give a similarly good value for the 2p state, but a clerical error

spoiled this. This error should not affect our results too much. For the nonlinear cases and the remaining linear cases, a similar set of S-type functions were used, but only a single contracted p-function in each direction was used. This p-function would give a good value for the energy of the 2p state of H as shown in Table IIb.

C. Basis Sets for CI

The SOGI orbitals were used to reorganize the atomic basis set for CI calculations. For any geometry of H_3 where all the atoms are reasonably close together, the excited state wavefunctions can be approximated by[8]

$$\mathcal{A}\,[q_1\,\phi_a^2\,\phi_{Cn} + q_2\phi_b^2\,\phi_{Cn} + q_3(\phi_a\phi_b\phi_{Cn})], \tag{5}$$

where the ϕ's are orthogonal, ϕ_a and ϕ_b are the first two natural orbitals for H_3^+, ϕ_{Cn} is an orbital appropriate for the nth state, $(\phi_a\phi_b\phi_{Cn})$ stands for both the doublet open-shell functions that we can make from these three orbitals, and q_1, q_2, and q_3 are numerical coefficients. [The two parts of $(\phi_a\phi_b\phi_{Cn})$ really have separate coefficients.] Therefore we chose the first two orbitals of the ground state of H_3 as ϕ_a and ϕ_b; the orbitals ϕ_{Cn} were taken as the third orbital of the nth SOGI state. Additional functions (χ_i) were introduced until there were as many orbitals as atomic basis functions. These orbitals were then orthogonalized and normalized by a Gram-Schmidt procedure beginning with ϕ_a. The integrals over atomic basis functions were then transformed to give integrals over the orthonormal orbitals.

The CI calculations using these basis functions were done with a CI program that does configuration interaction over spin eigenfunctions and that is described in Appendix II. All configurations of the form $\phi_a^2\phi_{Cn}$, $\phi_b^2\phi_{Cn}$, $\phi_a\phi_b\phi_{Cn}$, $\phi_{C1}^2\phi_a$, $\phi_{C1}^2\phi_b$, and $\phi_{C1}^2\phi_{Cn}$ as well as all single excitations to the χ_i's were included, giving ~ 210 spin eigenfunctions in most cases. The results of these calculations are given in the next section.

II. ENERGY RESULTS

Because of the formal ambiguity of calculating excited states with G1 or SOGI, the comparison of SOGI energies and wavefunctions with CI energies and wavefunctions is especially important since such a comparison will tell us if we have missed any states in the SOGI calculations. Table III contains G1, SOGI, and CI energies for geometries A, E, F, G, J, and K (see Table I). The most important result for this comparison is that, with one exception, the SOGI levels are correctly assigned. The evidence is twofold; first, the energy spacing of the two methods is nearly the same, the changes in spacing (on going from SOGI to CI) is small compared with the spacings themselves. The second point is that, in the CI wavefunction for the excited states, the dominant configurations are completely consistent with our SOGI description of the states. We will elaborate on this when the states are discussed individually. The one exception is for geometry F in which the second CI solution is missing from the SOGI spectrum. The nature of this state is clear from the CI coefficients. We have tried to obtain a corresponding SOGI solution, but in vain; the reason for this is not clear.

A second important point is that spin-coupling optimization is important only for the first two states of each geometry and then only when all the nucleii are close together. Indeed, for the highly symmetric cases, lowering of orbital symmetry is sometimes more important than a general spin coupling. For the third and higher states, G1 is within 1 kcal/mole of SOGI (except for the fourth state of geometry A, which is ~ 4 kcal/mole higher).

The geometries A, B, and C were chosen to bracket the minimum in the linear symmetric H_3^+ curve found by Conroy.[1] Table IV shows the SOGI and G1 energies of linear symmetric and linear asymmetric H_3 and H_3^+. The letters in parentheses following the molecular term symbol indicate the symmetry of the orbitals used. For H_3, the states described as (ℓru) or (ℓrg) have G1 coupling and those labeled (ggg) or (ggu) have a general (SOGI) spin coupling. For all the excited states, (ℓrg) or (ℓru) give the best description, as is the case with H_3^+. For H_3^+ in geometry D, I found two solutions, one by distorting the (ℓr) solution of geometry C and the other by distorting the (gg) solution.

Table V shows the predicted minimum (R_e), the energy at R_e, and the curvature at R_e for several states of linear, symmetric H_3^+ and H_3. The predicted R_e of the ground state, $1\ ^2\Sigma_u^+$ (gg'u) is too small because the points do not bracket the minimum for this state. It should be noted that R_e and the curvature at R_e for the excited states of H_3 are very much like those of H_3^+.

Figure 1 shows the SOGI energies of the states we have calculated at each geometry (Table I). The dotted lines represent states inferred from the CI calculations, their energies are uncertain by ~ 0.02 hartree.

The level at the top of each column marked "ion" is the SOGI energy of H_3^+ at that geometry.

Geometries A, B, C, G, and J all have a mirror plane, and I have denoted the symmetry of the state by G or U preceded by 1, 2, etc., indicating which G or U level. The column at the right labeled ∞ has three levels marked a, b, and c. $\underline{a}$ is the SOGI energy of

$$H_2 \; {}^1\Sigma_g^+ \; (R = 1.40) + H(1s) \; , \tag{6a}$$

level b is the SOGI energy of

$$H_2 \; {}^1\Sigma_g^+ \; (R = 1.40) + H(n = 2) \; , \tag{6b}$$

which is nearly degenerate with

$$H_2 \; {}^3\Sigma_u^+ \; (R = 1.40) + H(1s) \; , \tag{6c}$$

and level c is the SOGI energy of

$$H_2 \; {}^1\Sigma_g^+ \; (R = 1.40) + H^+ \; . \tag{6d}$$

We note that most of the excited levels are lower in energy than the limit (6b). For geometry F, however, the fourth and fifth states are higher than the energy (6b), while the corresponding levels for geometry E are lower, indicating a hump in those PES's. The existence of similar humps for the nonlinear approach is likely, but I have not done cases in which a hump appeared or would be expected. Such a hump would only be expected when one hydrogen is far from the other two, as in geometry F.

Table VI shows the SOGI ionization potentials of each state at several geometries in eV. These indicate that most states are more easily ionized than the corresponding state at infinity.

The energy of H_3^+ for geometry J is nearly the same as the limit (6b) or (6c), indicating that associative ionization is possible.

From Tables III, IV, V, and IX, we see that the excited states of H_3^+ are well described by G1 and have energy curves similar to H_3^+. If the excited states are well described as H_3^+ plus an electron, we can use the frozen H_3^+ bonding orbitals to form a Hamiltonian that, when diagonalized, will give the spectrum of excited states. In Table VIII we give a comparison of these so-called virtual energies with the self-consistent (SCF) G1 energies.

III. ORBITAL DESCRIPTION

A. Contour Plots

Figures 2 through 44 are contour plots for various orbitals of states of H_3 and H_3^+. The location of each atom is indicated by a cross (+). These plots differ significantly from the contour plots in Chapters I and II in that they are logarithmic plots; each contour level is a constant factor higher than the previous level. This is necessary since many of the orbitals have important diffuse components that would not show up on linear plots unless a very fine scale were used which would make the nondiffuse part become black blobs. The lowest contour (on all plots) is ± 0.01 a_0 and the ratio between contours is 2.0 (giving levels ± 0.02, ± 0.4, etc.). Dashed lines are nodes and dotted lines are negative contours. All the plots on any page are the same size (except as noted). The geometries refer to Table I. The figures are not in order of first reference in the text; rather, all the H_3^+ orbitals

are first in alphabetical geometry order followed by H_3 orbitals. The H_3 orbitals are grouped according to geometry first and then according to state. For each state the SOGI orbitals are first, the G1 orbitals next, and the G1 Natural Orbitals (vide infra) last.

B. H_3^+

In the following discussion, we will consider H_1 and H_2 as the two hydrogens originally close together; H_3 is the more distant hydrogen and will be closer to H_2 than to H_1. ϕ_a, ϕ_b, and ϕ_c will be the orbitals that began on H_1, H_2, and H_3, respectively.

For two electrons, there is only one singlet spin coupling that I will call G1.[9] Plots of the G1 orbitals of H_3^+ for geometries A, F, G, J, and K are shown in Figs. 2-6.

For those geometries in which there is a plane of reflection (A, B, C, G, and J), we can pick our orbitals as gg′ or $(g+u)(g-u) \equiv r\ell$.[10] For the linear cases (shown in Fig. 2), the latter choice is best for normal distances $(> \sim 1a_0)$ and gg′ is better for very short distances, since it allows the orbitals to split radially. For the equilateral triangle (geometry J, Fig. 5), the two descriptions are degenerate because one can write the gg′ orbitals as

$$g = a + y$$
$$g' = a - y \ , \tag{7}$$

where a is invariant under all the symmetry operations and y is the part of an E pair that is invariant under $\hat{m}$ (the mirror plane we are using). Thus we have

$$\tfrac{1}{2}(g'g + gg') = a^2 - y^2 \ . \tag{8}$$

The other choice, $r\ell$, can be written as

$$r = a + x$$
$$\ell = a - x \quad , \tag{9}$$

where x is that part of the E pair that changes sign under $\hat{m}$. Clearly, $r\ell$ $(= a^2 - x^2)$ is equivalent to gg' $(= a^2 - y^2)$; to get a pure A, many-electron state we <u>should</u> use $a^2 - (x^2 + y^2)$, but we can not do this with a G1 wavefunction. For isosceles triangles with base less than 2.5 a_0,[11] the right/left orbitals (one of which is shown in the lower part of Fig. 4) are better and correspond to the orbitals of H_2 delocalizing somewhat onto a distant proton. The other description, gg', corresponds to an H_2^+ plus a hydrogen atom, as can be seen in the upper part of Fig. 4. This description would be better for triangles with large bases.

In Fig. 3, for geometry F, we see that the H_2 orbitals have not delocalized much onto the incoming proton because it is too far away. In Fig. 5, geometry K, the incoming proton is much closer and the two orbitals correspond to two one-electron bonds, one between H_1 (see Table I) and H_2, and the other between H_2 and H_3.

C. H_3

1. The Ground State

The SOGI description of the ground state is given in detail in Chapter II and will not be repeated here except to note that the nonlinear cases (geometries G, J, and K) confirm the orbital phase changes already observed for linear cases. The orbitals are shown, as they will enter into the discussion of other states.

In the CI calculations the three configurations $\phi_a^2 \phi_c$, $\phi_b^2 \phi_c$, and $\phi_a \phi_b \phi_c$ always dominate the ground state. ϕ_a, ϕ_b, and ϕ_c are the orthogonalized SOGI orbitals of the SOGI ground state.

2.   Anti-Resonant State

Consider three ground state hydrogen atoms far apart. There are two linearly independent doublet wavefunctions, G1 and GF, which are degenerate at infinity. If we bring two of the H's together, the two wavefunctions split; the G1 wavefunction goes to H_2 $^1\Sigma_g^+$ + H (1s) and has lower energy than the GF wavefunction, which goes to H_2 $^3\Sigma_u^+$ + H(1s). If R_{H_2} = 1. 40 a_0, the $^3\Sigma_u^+$ is ~10 eV above the $^1\Sigma_g^+$ ground state, which is the same as the n = 1 to n = 2 excitation energy of the hydrogen atom. The $^3\Sigma_u^+$ is strongly repulsive for H_2. When we bring a third H up to this system, the energy goes down rapidly because of the favorable interaction of the incoming H 1s with both the other orbitals. In the valence bond view, we can form two linearly independent bonds from hydrogen 1s functions; one is between the two close hydrogens (H_1 and H_2)

$$\bullet H_3 \tag{10}$$

$$H_1 \quad H_2$$

and the other is the sum of bonds from H_3 to H_1 and H_3 to H_2

$$\tag{11}$$

In the ground state we take the favorable combination of these two structures, leaving the bad combination as the excited state. In the ground state, solving self-consistently for the orbitals led to the bonding orbitals (ϕ_a and ϕ_b) delocalizing onto center 3, while the nonbond-

ing orbital (ϕ_c) built in a node to keep small overlap between itself and the bonding orbitals. In the excited state the nonbonding orbital does not build in a node, thereby interfering with the bond and raising the energy very significantly (see Figs. 12, 13, 37, and 38).

I have been unable to find a SOGI state of this form for geometry F, but the state certainly exists as shown by the CI calculations. The second solution of the CI matrix for geometry F is dominated (coefficient = 0.746) by the second spin eigenfunction formed from $\phi_a \phi_b \phi_c$ (all taken from the ground state, Fig. 19). In this spin eigenfunction, ϕ_a and ϕ_b (which resemble the bonding orbitals on H_1 and H_2) are coupled into a triplet and then ϕ_c is coupled on to make a doublet. This state has exactly the form of the anti-resonant state we expect. There are completely analogous CI solutions for geometries E and K where we have orbital solutions and the picture is clear. The problem in finding the SOGI wavefunction for this state may be in finding the proper trial function or it may be that the iterative procedure is not stable for such a state. The proper spin coupling for such an anti-resonant state is the GF coupling. For GF coupling, all the orbitals of the same spin can be taken as orthogonal and indeed must be to obtain a unique set of orbitals. Since the SOGI program deals with general spin couplings, the simplifications arising from orthogonal orbitals have not and cannot be used. This has led to many problems when using GF or GF-like spin couplings and may be the cause of our problem here.

Such an anti-resonant state is stabilized only for intermediate distances, for as soon as we push all three protons into the same region of space, the exclusion effect pushes the energy of any wavefunction

constructed of only three H 1s's up very high. We cannot even build one Fermion wavefunction for the united atom, since $1s^3$ is not allowed. Thus the nonbonding orbital must start building in diffuse character. For geometries E and K we clearly see (Figs. 12, 13, 37, and 38) anti-resonant states in which the orbitals could be formed from 1s functions on each center. For geometries G and J, there are states for which the orbitals are basically made from 1s-functions but have significant diffuseness built in. Since the second state for geometries G or J has different symmetry from the ground state, the two valence-bond struc-tures do not mix and these states do not appear as the worst spin-coup-long for those orbitals, as is the case for the second state of geometries E and K. Note that, if we maintain C_{2v} symmetry (which becomes $D_{\infty h}$) by spreading H_1 and H_2 apart and bring H_3 in along the mirror plane, the second state of G or J goes into the $1\ ^2\Sigma_u^+$ ground state of linear H_3 while the ground state goes to the $^2\Pi_g$ state. If, on the other hand, we rotate H_1 and H_2 to obtain the linear system $(H_1 H_2 H_3)$, the ground state of geometry G or J becomes the ground state of the linear system and the second state becomes a Π state.

3.   Rydberg States

In the case of geometry A, there is no longer any question of building our second state wavefunction from hydrogen 1s functions, and so the second state of the system is $1\ ^2\Sigma_g^+$ with two orbitals forming the bond of H_3^+ and the third orbital forming a diffuse s orbital on the whole system (Fig. 9); this is a Rydberg state.

All the remaining states of H_3 are also best described as Rydberg states; two orbitals delocalize over the three protons forming a bonding

pair, while a third nonbonding orbital builds in nodal structure to give the various excited states of the system. The CI wavefunctions of these states confirm their Rydberg nature. The third, fourth, and fifth states at each geometry are dominated by the configurations $\phi_a \phi_b \phi_{Cn}$, $\phi_a^2 \phi_{Cn}$, and $\phi_b^2 \phi_{Cn}$, where ϕ_a and ϕ_b are the orthogonalized bonding orbitals of the SOGI ground state and ϕ_{Cn} stands for the orthogonalized third orbitals of the SOGI states up to the one under consideration (k). Because the orbitals have been orthogonalized, we must include all the lower orbitals to rebuild parts of ϕ_{Ck}^{SOGI} that have been orthogonalized away. Even so, the configurations directly involving the orthogonalized ϕ_{Ck} are the most important for the kth state, indicating that the parts of ϕ_{Ck}^{SOGI} which really determined the energy were orthogonal to the ϕ_c's of lower states.

Here we come to a significant problem in interpreting the orbitals. Look, for example, at the SOGI orbitals of the fourth state of geometry K (Fig. 41); all three orbitals look basically like H_3^+ bonding orbitals. True, ϕ_c does seem a bit mashed outward in the plus-y direction, but it is very hard to satisfactorily connect the states of geometry K to those of geometry E (linear) or geometry G (isosceles triangle). In particular, it is very difficult to see which of the K states becomes a pi state for linear geometry, although it is almost certain that one or more of them does because there are five K states and only four E $^2\Sigma^+$ states in the same energy range.

The solution to this problem is to note that most of the tight 1s character of ϕ_c gets projected away by the G^{dL} operator. Also note that because this state is like H_3^+ plus an electron in a diffuse orbital,

one could restrict the coupling to G1. The G1 orbitals for the fourth state of geometry K are in the upper part of Fig. 42; note that ϕ_a and ϕ_b have hardly changed, but ϕ_c has developed some slight negative amplitude on the minus y side of the node. ϕ_c still does not have any very striking structure, though. To obtain the really important structure, we do the following, which was originally suggested by Musher.[12] The spatial part of the G1 wavefunction is

$$(\phi_a \phi_b + \phi_b \phi_a)\phi_c = [(1 + S_{ab})\chi_1^2 + (1 - S_{ab})\chi_2^2]\phi_c \ , \qquad (12)$$

where $\chi_1 = (\phi_a + \phi_b)/\sqrt{2 + 2S_{ab}}$ and $\chi_2 = (\phi_a - \phi_b)/\sqrt{2 + 2S_{ab}}$ (and $\chi_2 = 0$ if $S_{ab} = 1$). Thus

$$G_1^d[\phi_a \phi_b \phi_c \,\alpha\beta\alpha] = (1 + S_{ab})/2 \ \mathcal{A}[\chi_1^2 \phi_c \,\alpha\beta\alpha] + (1 - S_{ab})/2$$
$$\times \ \mathcal{A}[\chi_2^2 \phi_c \,\alpha\beta\alpha] \ . \qquad (13)$$

If we set $S_{ab} = 1$, we obtain the Hartree-Fock wavefunction.

We can rewrite (13) as

$$G_1^d[\phi_a \phi_b \phi_c \,\alpha\beta\alpha] = (1 + S_{ab})/2 \ \sqrt{1 + S_{1c} - 2S_{1c}^2} \ \mathcal{A}[\chi_1^2 \chi_3 \,\alpha\beta\alpha]$$
$$+ (1 - S_{ab})/2 \ \sqrt{1 + S_{2c} - 2S_{2c}^2} \ \mathcal{A}[\chi_2^2 \chi_4 \,\alpha\beta\alpha] \ , \qquad (14)$$

where

$$\chi_3 = (\phi_c - S_{1c}\chi_1)/\sqrt{1 + S_{1c} - 2S_{1c}^2}$$

$$\chi_4 = (\phi_c - S_{2c}\chi_2)/\sqrt{1 + S_{2c} - 2S_{2c}^2}$$

$$S_{1c} = \langle \chi_1 | \phi_c \rangle$$

$$S_{2c} = \langle \chi_2 | \phi_c \rangle \ .$$

χ_3 is the part of ϕ_c orthogonal to χ_1, and χ_4 is the part of ϕ_c orthogonal

χ_2. We will refer to this set of orbitals as G1 Natural Orbitals. (In the figures they are labeled "ϕ_a" through "ϕ_d" instead of "χ_1" through "χ_4".)

The lower part of Fig. 42 shows the G1 Natural Orbitals for the fourth state of geometry K. We see that the small negative amplitude seen in the regular G1 ϕ_c has now become the dominant part of the non-bonding orbital. Clearly this is the state that becomes a pi state when we linearize the system. The G1 Natural Orbital (G1-NO) χ_4 (ϕ_d in Fig. 42) is almost identical to the regular G1 orbital (G1O) ϕ_c.

We find that the Rydberg states for geometries E, F, and K are best described in terms of the first and third G1-NO's. Neglecting the part of G1O ϕ_c, which is orthogonal to χ_1, requires some justification. To measure the effect of orthogonalizing ϕ_c to the first two natural orbitals, we have computed the energy of the following wavefunctions for geometry K, all five states,

$$\hat{\mathcal{U}}[\chi_1^2 \chi_3 \alpha\beta\alpha] = \psi_1$$

$$\hat{\mathcal{U}}[\chi_2^2 \chi_4 \alpha\beta\alpha] = \psi_2$$

$$G_1^d[\phi_a \phi_b \chi_3 \alpha\beta\alpha] = \psi_3$$

$$G_1^d[\phi_a \phi_b \chi_4 \alpha\beta\alpha] = \psi_4.$$

These energies are given in Table VIII.

For the ground state, the energies of ψ_2 and ψ_4 are very bad, which is understandable if one looks at the G1-NO's ϕ_b and ϕ_d. G1-NO ϕ_b is antibonding between H_1 and H_2, but G1O ϕ_c already has a node there, so G1-NO ϕ_d has to build in a node between H_2 and H_3 making it doubly non-bonding. $E(\psi_1)$ is fairly good and $E(\psi_3)$ is nearly as good as the G1 energy, indicating the error in $E(\psi_1)$ is due mostly to double occupation

of G1-NO ϕ_a rather than to our modification of G1O ϕ_c.

For the ground state, any modification of a variational wavefunction will cause the energy to go up. For excited states, however, taking away part of a variational wavefunction can cause the energy to go down. This is particularly true of valence excited states where the orbitals have a great deal of ground state character but arranged in the wrong way. This is true of the second state of K where $E(\psi_4)$ is below the G1 energy. Another symptom that state 2 is a valence state is that the difference between $E(\psi_1)$ and $E(\psi_2)$ is less than the difference between either of these and the G1 energy, indicating that both terms of (14) contribute strongly to the true wavefunction.

Altering a Rydberg orbital, on the other hand, should only raise the energy, particularly alterations that increase the number of nodes in the Rydberg orbital. For states three, four, and five of K, we observe that $E(\psi_1)$, $E(\psi_2)$, and $E(\psi_3)$ are all slightly higher than the G1 energy, while $E(\psi_4)$ is slightly lower. This is expected since in ψ_4 we have removed antibonding character from G1O ϕ_c. $E(\psi_3)$ is no more than 4 or 5 kcal/mole above the G1 energy, indicating that the energetically important parts of G1O ϕ_c are still present in G1-NO ϕ_c.

4.   Connection of States

I will now describe each state of the equilateral triangle (geometry J, Figs. 30 to 34) and then describe how the states change as we proceed to the isosceles triangle (geometry G, Figs. 27-29), and thence to the bent triangle (geometry K, Figs. 35-44), then to the linear geometry E (Figs. 11-18), then from E outward to F (Figs. 19-26), and inward to A (Figs. 7-10). Returning to J, we make the connection to A.

a) J to G

The equilateral triangle states can be viewed as states of a distorted lithium atom. The ground state is a degenerate E state composed of a core of A_1 symmetry and either of two molecular p orbitals. We can treat the two bonding orbitals as gg' or right/left as in H_3^+. As we saw in the discussion of H_3^+, the gg' orbitals are equivalent to $(a^2 - y^2)$ while left/right orbitals are equivalent to $(a^2 - x^2)$. Neither of these is of exactly A_1 symmetry so that $(a^2 - y^2)\bar{y}$ and $(a^2 - x^2)\bar{y}$ are not equivalent. The best combinations are $gg'p_x$ and $r\ell p_y$. On going to the isosceles triangle (geometry G), these two states split strongly. The E_y goes down toward H_2 $^1\Sigma_g^+ + H(1s)$, while the E_x goes up. The E_x could connect to H_2 $^1\Sigma_g^+ + H(2p_x)$ or H_2 $^3\Sigma_u^+ + H(1s)$, the orbitals in Fig. 27 suggest the latter since the u orbital remains on H_1 and H_2 while ϕ_a becomes a hydrogen 1s on H_3.

The next state of J (Fig. 32) is a beautiful molecular 2s that very clearly connects to the third state of G (Fig. 28). For this state, gg' (2s) and $r\ell$(2s) are equivalent. What happens to this state as we move H_3 to infinity is not definite, but the linear case (vide infra) suggests that the right/left/g description will become better and that ϕ_a and ϕ_b will localize on H_1 and H_2 while ϕ_c will become polarized away from H_1 and H_2. Eventually, this state will become a combination of 2s and 2p on H_3, polarized in the plus-x direction.

The third level (fourth and fifth states) of J is a second degenerate E state composed of a core of approximate A_1 symmetry and molecular 3p orbitals (Figs. 33 and 34). The y component of this set is connected to the fourth state of G (Fig. 29) while the x component connects to the

fifth state of G, for which I have not solved. This ordering is also given by the CI calculations.

b) G to K

When we rotate H_1 about the fixed H_2 and H_3 to obtain geometry K, the 2p's mix, the 2s remains rather pure, and the 3p's mix with each other.

The connection of the ground states of G and K (Figs. 27 and 35) is evident; the node that ran parallel to the H_1-H_2 axis in G cuts between H_1 and H_2 in K. The connection of the second states of G and K (Figs. 27, 37, and 38) is less obvious until one looks at the third G1-NO of Fig. 38; this orbital can readily be made into a u orbital since it has a node running through H_3 and bisecting the H_1-H_2 line. It is also clear from χ_3 (Natural Orbital ϕ_c in Fig. 38) that this state has some hydrogen 2p character since the node of ϕ_c runs through H_3, but the orbital has noticeable amplitude on either side of H_3. This 2p character is not very large because the plus-y side of H_3 ϕ_c never gets above 0.04 in amplitude while it reaches nearly 0.16 near H_1 and H_2.

The connection of the 2s states (Figs. 28, 39 and 40) is very clear. The diffuseness and general shape of the orbitals are very similar but in K the third orbital, ϕ_c, has gained some p character.

The fourth and fifth states of geometries G and K are close in energy and are both molecular 3p functions polarized in different directions. In geometry G, the 3p functions have g and u symmetry. By inspecting G1-NO ϕ_3 of Figs. 42 and 44, we see that these two functions have mixed to give 3p's of x+y and x-y polarization. In the fourth state of K (Fig. 42), the internal or radial nodes of a 3p are not fully formed

but the function is much more diffuse than the valence 2p functions of states 1 and 2 (Figs. 36 and 38).

Even though the two 3p states of G mix, one can see that the fourth state of K is more closely related to the x-polarized 3p of G, while the fifth state of K is related to the y-polarized 3p of G, because the fourth state of K has a node between H_1 and H_2 while the fifth state has them surrounded by a node. Figure 45 shows a sketch of how the nodal surfaces will move in going from K back to G.

c) K to E

As we continue the rotation of H_1-H_2 to give the linear geometry E, the connection of the ground state is again patent. The connection of the second state is also clear upon comparing Figs. 13 with 37 and 14 with 38. The important point is that the nonbonding SOGI orbital (ϕ_c) is in both cases nodeless in contrast to the ground state and that the SOGI spin-coupling is close to GF in both cases, as shown in Table IX.

ϕ_c of the third state of E (Fig. 15) has some 2s character but is not so diffuse as ϕ_c of the third state of K (Fig. 39). On inspection of the G1-NO's, we see that the important part of G1O ϕ_c is a diffuse s-p hybrid polarized in the plus-x direction, away from H_1 and H_2.

The fourth state of K goes into a pi state for linear geometries, for which we have not solved.

The fifth state of K (Figs. 43 and 44) is a molecular 3p that connects to the 3p of geometry E (Figs. 17 and 18). We infer this from the diffuseness and nodal structure of G1-NO's.

d) E to F

Once again, the ground state connection is obvious.

Not having a second solution for F, it is a bit difficult to discuss the connection of these states. The orbitals at F should look like a g and u orbital[13] on H_1 and H_2 coupled into a triplet with the third orbital looking very much like a 1s on H_3.

The third state of E (Figs. 15 and 16) connects to the third state of F (Figs. 21 and 22). At E, this state was called a molecular 2s with 2p character; at F it is a 2p with some 2s character and is definitely polarized away from the hydrogen molecule. As we noted for H_3^+, the bonding pair is delocalized over the three protons at E but not at F. At F, then, the outer electron sees a plus-one charge on H_3 and the repulsive closed-shell hydrogen-molecule electrons. In order to minimize this repulsive interaction, it must polarize away from the hydrogen molecule.

The fourth states of E (Figs. 17 and 18) and F (Figs. 23 and 24) also connect. At E, this state was mostly an H_3 2p since most of the H_3 2s had been used in the third state. At F, the third state, to avoid unfavorable overlaps with the hydrogen molecule orbitals, polarized away. Thus the fourth state at F polarizes toward the molecule giving rise to bad overlaps and the hump we noted in Sec. II.

The fifth state at F may not be well described in this basis. It has the appearance of an ionic state; a molecular 3p based on H_2^+---H which is higher than H_2---H^+.

e) E to A

Yet again, the ground states connect very smoothly.

The second state of A is 1 $^2\Sigma_g^+$ (Fig. 9), which is a molecular 2s that connects to the third state of E (Figs. 15 and 16). The second state of E (Figs. 13 and 14) was a valence excited state, and as we push the

protons close together it goes up in energy. The $2\ ^2\Sigma_g^+$ of A (Fig. 10) is the fourth state (counting the u states) and has a nodal structure resembling the second state of E (Fig. 14). The second state of E was a valence state in which G1-NO ϕ_c was composed of a hydrogen 1s on H_1 minus a hydrogen 1s on H_2 with a little 2p character on H_3. As we bring H_3 closer, the bonding orbitals delocalize more, the valence character of the nonbonding orbital becomes very favorable (from exclusion effects), and the new, more diffuse nonbonding orbital sees all three protons more or less equivalently. In the limit of equally spaced hydrogens, this state becomes a molecular 3d-sigma composed mostly of a hydrogen 2p on H_3 minus a hydrogen 2p on H_1 with some contribution from s functions on the hydrogens.

The nonbonding orbital (ϕ_c) of the $2\ \Sigma_u^+$ of A (Fig. 8) is the related molecular $3p_x$ composed of a hydrogen 2p on H_1 plus a hydrogen 2p on H_3 with contributions from s functions on H_1 and H_3 and the H 2p on H_2. This state could have some valence character, but the nonbonding orbital is diffuse and Rydberg-like. In addition, in the CI wavefunction for this state, the coefficients of valence configurations are very small ($< 10^{-2}$).

The orbitals of the $3\ ^2\Sigma_u^+$ are shown in Fig. 8. The third orbital has much the same structure as ϕ_c of the $2\ ^2\Sigma_u^+$ (shown above it). This state looks something like a 4p, and is probably badly described in this basis set; hydrogen 3p's would be required on each center.

f) J to A

The connections here are very simple and require only a glance at the orbitals for the lower states at least. The x component of the J

ground state (Fig. 30) goes to the sigma ground state of A. The y component (Fig. 31) goes to a Π_u state of A (not solved for); another example of a valence state becoming Rydberg-like. The nondegenerate second level of J (Fig. 32) becomes the $1\,^2\Sigma_g^+$ of A (Fig. 9). The x component of the second E state of J (Fig. 33) becomes the $2\,^2\Sigma_u^+$ of A (Fig. 8). The y component of this E state is most strongly related to the 3p pi state of A. There are two low-lying states of E, as shown in Table III, states 6 and 7 which should be 3d's. One of these, the (x^2-y^2), will connect to the 3d-sigma $2\,^2\Sigma_g^+$ of A and the other, (xy), to a 3d pi that should be fairly high in energy. The $3p_y$ and the $3d_{x^2-y^2}$ will mix somewhat.

IV. CONCLUSIONS

We have seen that the excited valence states of the reactants led at first to valence states in the interaction region and then to Rydberg states when all the atoms were close together, while the ground state remained a valence state for all distances considered. This was expected because of the exclusion principle and was easily seen in the orbitals. The Rydberg states of the reactants led to Rydberg states in the interaction region where they could be classified fairly well as S, P, or D.

The number of states at each geometry was easily rationalized and the hump in the fourth sigma state of linear cases explained. This hump for the fourth state and the absence of a hump in the third state is due to the degeneracy of the hydrogen 2s and 2p that allows the third state to polarize away from the hydrogen molecule until it has approached close enough for the bonding orbitals to delocalize over all the protons. This

should be a general feature of the interaction of excited hydrogen with closed-shell systems. For atoms such as K or Na or Li, the behavior should be different because the ns and np are no longer degenerate and there may be humps in all the excited-state PES's.

The CI calculations show that, even though there are significant absolute errors in the SOGI and G1 energies, the barrier of the ground state and humps and valleys of the excited states are reproduced by SOGI with semi-quantitative accuracy.

Thus the SOGI and G1 independent-particle methods give accurate and understandable pictures of the PES's of reaction for excited states as well as ground states and form a valuable basis for theories about the potential energy surfaces of chemical reactions.

ACKNOWLEDGEMENTS

REFERENCES

1. H. Conroy, J. Chem. Phys. $\underline{51}$, 3979 (1969).

2. W. A. Goddard III, Phys. Rev. $\underline{176}$, 106 (1968).

3. C. Melius and W. A. Goddard III, J. Chem. Phys. $\underline{54}$, 0000 (1971).

4. We count the nth excited state as the $n+1$ state of the system so that the ground state is the zeroth excited state.

5. If one used a rather bad trial function in forming $\underset{\sim}{B}$, nonzero, negative eigenvalues would appear. If the ground state is desired, we pretend that the negative eigenvalues are zeros and delete them. As the trial function approaches the ground state wavefunction, the negative eigenvalue smoothly goes to zero.

6. D. L. Huestis and W. A. Goddard III, "A New Aufbau Principle for Molecules and Their Excited States" and "The Projected GI Method and the Excited States of H_2," in preparation.

8. This is actually an assumption that the CI calculations support.

9. For this case, G1, GF, SOGI, and EHF are completely equivalent.

10. Functions denoted by g are unchanged under the reflection, $\hat{m}$, while those marked u change sign under $\hat{m}$. When there are other symmetry elements, there may be several g classes and several u classes, and degenerate representations may be resolved into g and u components. r and ℓ refer to functions localized on the right and left side of $\hat{m}$ such that $\hat{m}r = \ell$.

11. The $H_2 + H^+$ and $H_2^+ + H$ curves cross at 2.5 a_0; see Ref. 1.

12. S. Hameed, S. S. Hui, and J. I. Musher, J. Chem. Phys. $\underline{51}$, 502 (1969).

13. By g and u here I mean g and u with respect to the mirror plane between H_1 and H_2 ignoring the presence of H_3.

TABLE I. Geometries of Excited H_3 (all distances in bohr).

Name	Type	R_1	R_2		X	Y
A	linear symmetric $D_{\infty h}$	1.50	1.50	H_1	-1.50	0.0
				H_2	0.0	0.0
				H_3	1.50	0.0
B	linear symmetric $D_{\infty h}$	1.55	1.55	H_1	-1.55	0.0
				H_2	0.0	0.0
				H_3	1.55	0.0
C	linear symmetric $D_{\infty h}$	1.70	1.70	H_1	-1.70	0.0
				H_2	0.0	0.0
				H_3	1.70	0.0
D	linear asymmetric $C_{\infty v}$	1.50	1.70	H_1	-1.50	0.0
				H_2	0.0	0.0
				H_3	1.70	0.0
E	linear asymmetric $C_{\infty v}$	1.50	2.70	H_1	-1.50	0.0
				H_2	0.0	0.0
				H_3	2.70	0.0
F	linear asymmetric $C_{\infty v}$	1.50	4.25	H_1	-1.50	0.0
				H_2	0.0	0.0
				H_3	4.25	0.0

TABLE I. (continued)

Name	Type	R_1	R_2		X	Y
G	isosceles triangle C_{2v}	base = 1.50	height = 2.70	H_1	-0.75	0.0
				H_2	+0.75	0.0
				H_3	0.0	2.70
J	equilateral triangle C_{3v}	side = 1.68		H_1	-0.84	0.0
				H_2	+0.84	0.0
				H_3	0.0	1.45492268
K	bent 135° no symmetry	1.50	2.70	H_1	-1.50	0.0
				H_2	0.0	0.0
				H_3	1.9091883	1.9091883

TABLE IIa.   Basis Set for Linear H_3 Excited States.

A.   S Functions - Contracted 1s Gaussians

Exponent	First Contraction to 6 Functions	Second Contraction		
		1s	2s	tight S
82.4736	0.00234426			
12.3983	0.01772734	0.90078363	-0.34970777	1.0
2.83924	0.08624170			
0.814717	0.2617			
0.271838	1.0	0.48859394	-0.26999524	0.0
0.099482	1.0	0.30411215	-0.26192246	0.0
0.033161	1.0	0.02403873	0.76068717	0.0
0.011054	1.0	-0.00377805	0.51888897	0.0
0.0036847	1.0	0.00100811	-0.04977112	0.0
Energy (hartree)		-0.4999069	-0.12488	

B.   P Functions - Contracted 2p Gaussians

Exponent	First Contraction to 5 Functions	Second Contraction	
		2p	tight p
2.44001	0.00360092	0.00360092	1.0
0.567483	0.02859015		
0.18916	1.0	0.02859015	0.0
0.063053	1.0	0.13982444	0.0
0.0210176	1.0	0.51561382	0.0
0.00700589	1.0	0.47038677	0.0

TABLE IIb. Basis set for nonlinear H_3 excited states.

A. S functions - Contracted 1s Gaussians

Exponent	First contraction to 5 functions	Second Contraction		
		1s	2s	tight S
82.4736	0.00234426			
12.3983	0.01772734	0.90083785	-0.35088348	1.0
2.83924	0.0862417			
0.814717	0.2617			
0.271838	1.0	0.48844587	-0.26712944	0.0
0.099482	1.0	0.30457130	-0.27362876	0.0
0.033161	1.0	0.02307810	0.79343767	0.0
0.011054	1.0	-0.00237320	0.45889333	0.0
Energy (hartree)		-0.4999068	-0.12483	---

B. 2p function - Contracted 2p Gaussians[a]

Exponent	Coefficient
0.733825	0.02639
0.174211	0.18295
0.055713	0.53151
0.020185	0.41444
Energy	-0.124952

[a]From S. Huzinaga, J. Chem. Phys. 42, 1293 (1965).

TABLE III. G1, SOGI, and CI Energies for H_3. All quantities in Hartree atomic units.

State No.	G1-SCF[a]	SOGI-SCF[b]	G1[c] SOGI Orbitals	GF[d] SOGI Orbitals	E_1[e]	E_2[f]	SOGI[g] Lowering	CI[h]	CI Lowering[l]
A. Linear Symmetric H_3. $R_1 = R_2 = 1.50$ a_0. Basis Set 1.									
1(u)	-1.586200[j](ℓru)	-1.603350[k]	-1.586089	-0.422494	-1.603350	-0.405232	0.01726	-1.617007	0.01366
2(g)	-1.385159(ℓrg)	-1.364114	-1.363914	-0.362784	-1.364114	-0.362584	0.000200	-1.392627	0.00747
3(u)	-1.333510(ℓru)	-1.313706	-1.334597	-0.266701	-1.334633	-0.2666647	0.000036	-1.339930	0.00642
4(g)	-1.307876(ℓrg)	-1.286153	-1.313780	-0.225791	-1.313795	--	0.000015	-1.316279	0.00840
5(u)	-1.280810(ℓru)	-1.260600	-1.260594	-0.176936	-1.260600	--	0.000005	-1.285462	0.00465
6(g)	--	--	--	--	--	--	--	-1.276987	--
E. Linear H_3. $R_1 = 1.50$ a_0. $R_2 = 2.70$ a_0. Σ^+ states only. Basis Set 2.									
1	-1.632583	-1.633570	-1.633372	-1.154838	-1.633570	-1.154640	--	-1.638984	0.005414
2	-1.345363	*-1.351681	-1.591154	-1.352296	-1.591966	-1.351681	--	-1.360325	0.008644
3	-1.306336	*-1.306439	-1.507068	-1.306442	-1.507072	-1.306439	--	-1.319973	0.013534
4	-1.274718	*-1.274847	-1.329187	-1.300367	-1.354707	-1.274847	--	-1.286253	0.011406
5	--	--	--	--	--	--	--	-1.254784	--
F. Linear H_3. $R_1 = 1.50$ a_0. $R_2 = 4.25$ a_0. Σ^+ states only. Basis Set 2.									
1	-1.645522	-1.645531	-1.645530	-1.129304	-1.645531	-1.129303	0.0000008	-1.646231	0.000699
2	--	--	--	--	--	--	--	-1.321490	--
3	-1.274689	-1.274690	-1.274689	-0.773694	-1.274690	-0.773694	0.0000007	-1.277949	0.00326
4	-1.241683	-1.241921	-1.241904	-0.756225	-1.241921	--	0.000017	-1.244295	0.00237
5	-1.221310	-1.221320	-1.221293	-1.005272	-1.221320	--	0.000027	-1.234526	0.013205
6	--	--	--	--	--	--	--	-1.200301	--
G. Isosceles Triangle H_3. Base = 1.50 a_0. Height = 2.70 a_0. Basis Set 2.									
1(g)	-1.612088(ℓrg)	-1.594047(ggg)	-1.590933	-1.024716	-1.594047	-1.021602	0.003114	-1.620225	0.00782
2(u)	-1.379377(ggu)	-1.381364	-1.378149	-1.103285	-1.381364	-1.100070	0.003215	-1.402255	0.02089
3(g)	-1.333519(ggg)	-1.333520	-1.333475	-1.194826	-1.333520	-1.194781	0.000045	-1.348740	0.01522
4(g)	-1.292217(ggg)	-1.292234	-1.291866	-1.073881	-1.292234	-1.073514	0.000368	-1.309728	0.01749
5(u)	--	--	--	--	--	--	--	-1.281993	--
6(g)	--	--	--	--	--	--	--	-1.263256	--
7(u)	--	--	--	--	--	--	--	-1.162512	--

TABLE III. (continued)

J. Equilateral Triangle H_3[m]. Side = 1.68 a_0. Basis Set 2.

State No.	GI-SCF[a]	SOGI-SCF[b]	GI[c] SOGI Orbitals	GF[d] SOGI Orbitals	E_1[e]	E_2[f]	SOGI[g] Lowering	CI[h]	CI Lowering[i]
1(g)	-1.498952	-1.498333[n]	--	--	--	--	--	-1.524119	0.015786
2(u)	-1.494299	-1.488582[n]	--	--	--	--	--	-1.512846	0.02420
3(g)	-1.410527	-1.410528	--	--	--	--	--	-1.426590	0.01606
4(g)	-1.339990	-1.340810[p]	--	--	--	--	--	-1.355690	0.01487
5(u)	-1.338884	-1.340148[p]	--	--	--	--	--	-1.355741	0.01550
6(g)	--	--	--	--	--	--	--	-1.294871	--
7(u)	--	--	--	--	--	--	--	-1.294820	--

K. Bent 135°. No symmetry. R_1 = 1.50 a_0. R_2 = 2.70 a_0. Basis Set 2.

State No.	GI-SCF[a]	SOGI-SCF[b]	GI[c] SOGI Orbitals	GF[d] SOGI Orbitals	E_1[e]	E_2[f]	SOGI[g] Lowering	CI[h]	CI Lowering[i]
1	-1.630962	-1.630964	-1.630788	-1.144054	-1.630964	-1.143877	0.000176	-1.634432	0.00347
2	-1.343024	*-1.347964	-1.603224	-1.348096	-1.603356	-1.347964	0.000131	-1.361909	0.01394
3	-1.311719	-1.311725	-1.311722	-1.308793	-1.311725	-1.309790	0.0000031	-1.322345	0.01062
4	-1.299578	*-1.299593	-1.520240	-1.307118	-1.527766	-1.299593	0.007526	-1.316148	0.016558
5	-1.273648	*-1.274061	-1.37863	-1.32145	-1.426025	-1.274061	0.047393	-1.282536	0.008474
6	--	--	--	--	--	--	--	-1.240037	--
7	--	--	--	--	--	--	--	-1.231645	--

*Marks cases in which the SOGI energy is the second root of $\langle GI|H|GJ \rangle$.

TABLE III. (continued)

---

[a] Energy of G1 wavefunction with orbitals optimized for G1 coupling.

[b] SOGI energy, orbitals and spin coupling optimized together as explained in text.

[c] Energy obtained by applying G1 operator to SOGI orbitals.

[d] Energy obtained by applying GF operator to SOGI orbitals.

[e] Lowest root of $\langle GI|H|GJ \rangle$ matrix; see Appendix I.

[f] Highest root of $\langle GI|H|GJ \rangle$ matrix.

[g] Energy improvement from diagonalizing $\langle GI|H|GJ \rangle$.

[h] CI energy obtained with SOGI orbitals as basis functions.

[i] Improvement of CI over SOGI or G1.

[j] The symbols "(ℓru)" and "(ℓrg)" indicate the form of the orbitals. For consistency, we report the G1 energy of the first state with ℓru orbitals; the gg'u-G1 wavefunction has a lower energy for the first state.

[k] The SOGI wavefunctions for this geometry all have orbitals gg'x, where x can be g" or u.

[ℓ] Orbitals and states are classified g if symmetric with respect to the mirror plane and u if antisymmetric.

[m] We ignore the threefold axis and classify state only with respect to one of the mirror planes.

[n] The ground state should be a doubly-degenerate E state. The SOGI and G1 methods do not give the two orthogonal components as equivalent. The CI energies are much nearer; here the difference is due to slightly inequivalent lists of configurations.

[p] The SOGI excited E state is much more nearly degenerate than was the ground state; see Ref.

TABLE IV.

		Symmetric - Linear				Asymmetric - Linear			
Geometry		A	B	C		D	E (Basis Set 1)	E (Basis Set 2)	F
R_1 (bohr)		1.50	1.55	1.70		1.50	1.50	1.50	1.50
R_2 (bohr)		1.50	1.55	1.70		1.70	2.70	2.70	4.25
	State	Energy (hartree)			State	Energy (hartree)			
H_3^+	$1\ ^1\Sigma_u^+(\ell r)$	-1.2521888	-1.25272284	-1.2489326	$1\ ^1\Sigma^{+}{}''(\ell r)''$	-1.2503183	-1.2041410	-1.1933285	-1.1543788
	(gg)	-1.2312001	-1.23125384	-1.2261434	$''(gg')''$	-1.2285973	--	--	--
H_3	$1\ ^2\Sigma_u^+(\ell ru)$	-1.586202	-1.5912390	-1.5979082					
	(ggu)	-1.6033503	-1.6096592	-1.6204686	$1\ ^2\Sigma^+$	-1.6141348	-1.6369300	-1.6335702	-1.6455312
	$2\ ^2\Sigma_u^+(\ell ru)$	-1.3335100	-1.3341196	-1.3303393	$3\ ^2\Sigma^+$	-1.3319106	-1.3161827	-1.3064393	-1.2419214
	(ggu)	-1.3137065	--	--					
	$3\ ^2\Sigma_u^+(\ell ru)$	-1.2808095	-1.2814437	-1.2778260	$5\ ^2\Sigma^+$	-1.2792369	--	--	--
	(ggu)	-1.2605248	--	--					
	$1\ ^2\Sigma_g^+(\ell rg)$	-1.3851591	-1.3847354	-1.3783697	$2\ ^2\Sigma^+$	-1.3811695	--	-1.3516806	-1.2746901
	(ggg)	-1.3641139	-1.36325067	--					
	$2\ ^2\Sigma_g^+(\ell rg)$	-1.3078759	-1.3090145	--	$4\ ^2\Sigma^+$	-1.3072711	-1.2829847	-1.2748469	-1.2213203
	(ggg)	-1.2862530	-1.2864696	-1.2824343					

TABLE V.

State	Predicted Minimum (bohr)	Energy at Minimum (hartree)	Curvature at Minimum (hartree/bohr^2)
Linear Symmetric H_3^+			
$1\ ^1\Sigma_g^+$ (ℓr)	1.5547	-1.2527268	0.359487
$1\ ^1\Sigma_g^+$ (gg')	1.52806	-1.2313384	0.351445
Linear Symmetric H_3			
$1\ ^2\Sigma_u^+$ (ℓru)	1.7056	-1.597917	0.55114
$1\ ^2\Sigma_u^+$ ($gg'u$)	1.7582	-1.6213841	0.5414
$2\ ^2\Sigma_u^+$ (ℓru)	1.5576	-1.3341304	0.37394
$3\ ^2\Sigma_u^+$ (ℓru)	1.5595	-1.2814602	0.36803
$1\ ^2\Sigma_g^+$ (ℓrg)	1.50005	-1.3851591	0.339638

TABLE VI. Ionization Potentials of Various States and Geometries of H_3 (energies in eV).

State No.	Geometry					
	B	E	F	G	K	J
1	9.71	11.98	13.36	10.86	11.81	6.04
2	3.59	4.31	--	4.58	4.11	5.76
3	2.22	3.08	3.27	3.27	3.12	3.63
4	1.53	2.22	2.38	2.78	2.79	1.74
5	0.78	≤ 0	1.82	--	2.10	1.72

TABLE VII.   Linear H_3. G1 (ℓrg) and (ℓru) (energy in hartree).

State	$R_1 = R_2 = 1.50$ Geometry A	
	Energy from virtuals	SCF energy
$1\,^2\Sigma_u^+$	-1.5770980	-1.5862602
$1\,^2\Sigma_g^+$	-1.3851360	-1.3851591
$2\,^2\Sigma_u^+$	-1.3334797	-1.3335100
$2\,^2\Sigma_g^+$	-1.3079049	-1.3078759
$3\,^2\Sigma_u^+$	-1.280798	-1.2808095
	$R_1 = R_2 = 1.550$ Geometry B	
$1\,^2\Sigma_u^+$	-1.5821322	-1.5912390
$1\,^2\Sigma_g^+$	-1.3847105	-1.3847354
$2\,^2\Sigma_u^+$	-1.3340903	-1.3341196
$2\,^2\Sigma_g^+$	-1.3089194	-1.3090145
$3\,^2\Sigma_u^+$	-1.2814323	-1.2814437
	$R_1 = R_2 = 1.700$ Geometry C	
$1\,^2\Sigma_u^+$	-1.5890667	-1.5979082
$1\,^2\Sigma_g^+$	-1.3783366	-1.3983697
$2\,^2\Sigma_u^+$	-1.3303112	-1.3303393
$2\,^2\Sigma_g^+$	-1.3074950	
$3\,^2\Sigma_u^+$	-1.2798147	-1.2778260

TABLE VII. (continued)

	$R_1 = 1.50$	$R_2 = 1.70$ Geometry D
$1\ ^2\Sigma^+$	-1.5851244	
$2\ ^2\Sigma^+$	-1.3811264	-1.3811695
$3\ ^2\Sigma^+$	-1.3318770	-1.3319106
$4\ ^2\Sigma^+$	-1.3070794	-1.3072711
$5\ ^2\Sigma^+$	-1.2792240	-1.2792369

TABLE VIII. Energies of various states at geometry K with various wavefunctions (energy in hartree).

State	SOGI	CI	G1	$E(\psi_1)$	$E(\psi_2)$	$E(\psi_3)$	$E(\psi_4)$
1	-1.630964	-1.634432	-1.6300946	-1.6095668	-0.2232565	-1.6283960	-1.5471690
2	-1.3479642	-1.3619086	-1.3430238	-1.2705226	-1.24085718	-1.2940676	-1.3677528
3	-1.3117253	-1.322345	-1.3117193	-1.2821289	-0.7488616	-1.3091287	-1.3117320
4	-1.2995927	-1.3161485	-1.2995779	-1.2734156	-1.2097958	-1.2930756	-1.3013974
5	-1.2740615	-1.2825357	-1.2736476	-1.2476256	-1.0042478	-1.2697545	-1.2794010

119

TABLE IX. SOGI parameters for various states. $\Xi/2$ (degrees).

State No.	Geometry					
	A	E	F	G	J	K
1	18.84 (u)[a]	5.63	0.49	>15.0[b] (g)	1.14[b] (g)	5.25
2	0.81[b] (g)	17.8	--	9.85 (u)	10.25 (u)	19.49
3	0.52[b] (u)	3.32	0.13	0.24 (g)	0.14 (g)	0.58
4	0.22[b] (g)	3.04	2.73	0.90 (g)	0.03[b] (g)	1.95
5	0.29[b] (u)	--	0.782	--	2.03 (u)	6.31

[a] Symmetry of states indicated by letter in parentheses.

[b] G1 with $r\ell g$ or $r\ell u$ better.
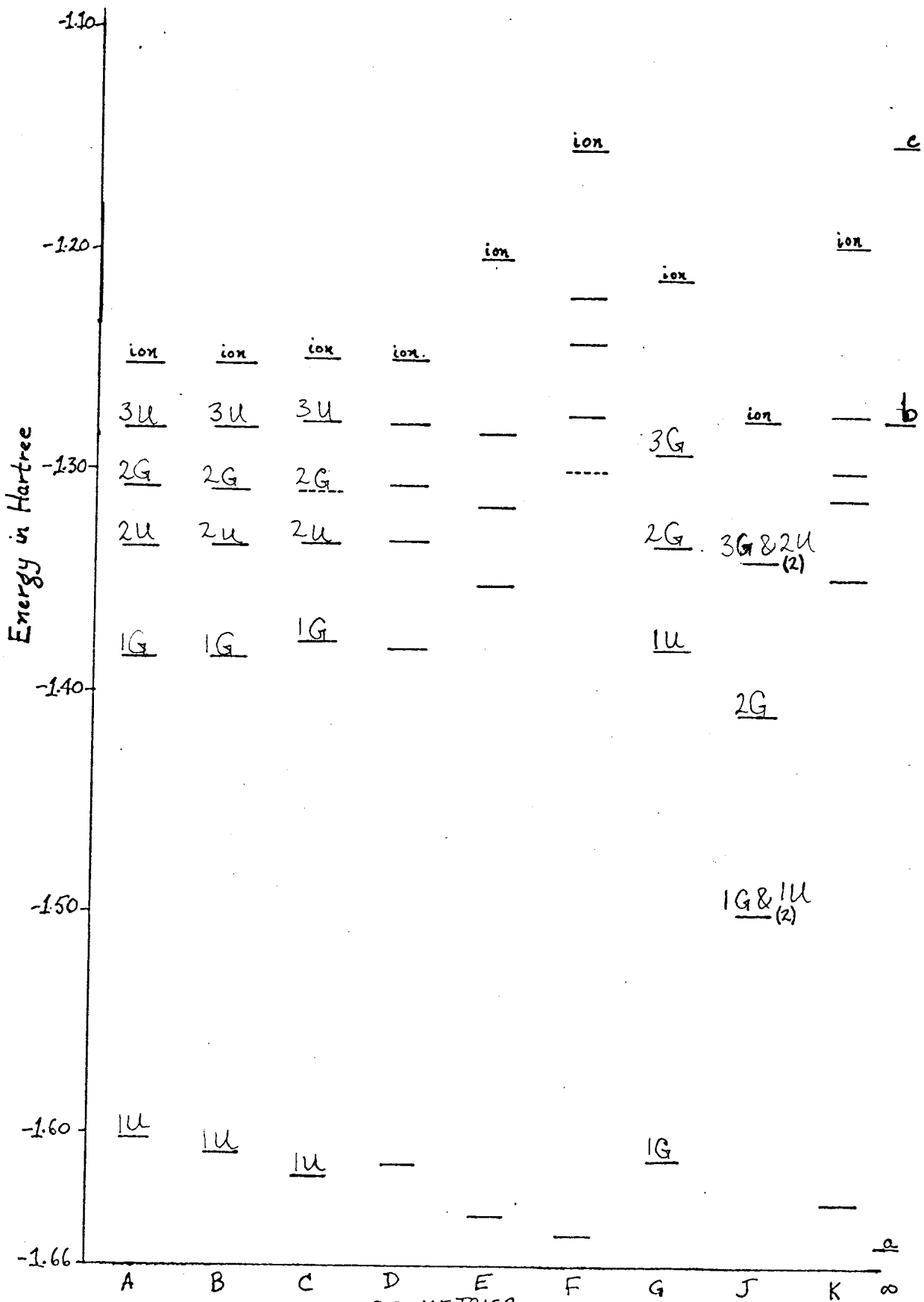
Figure 1.

Geometry A H_3^+

$\mathcal{G}1\ (gg')$

ϕ_a

ϕ_b

$\mathcal{G}1\ (\ell r)$

ϕ_a^ℓ
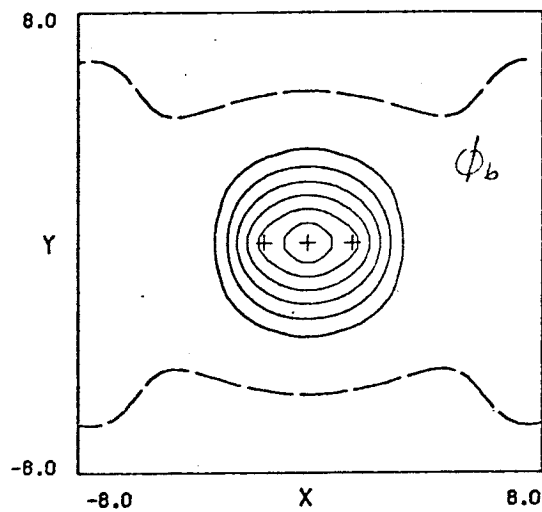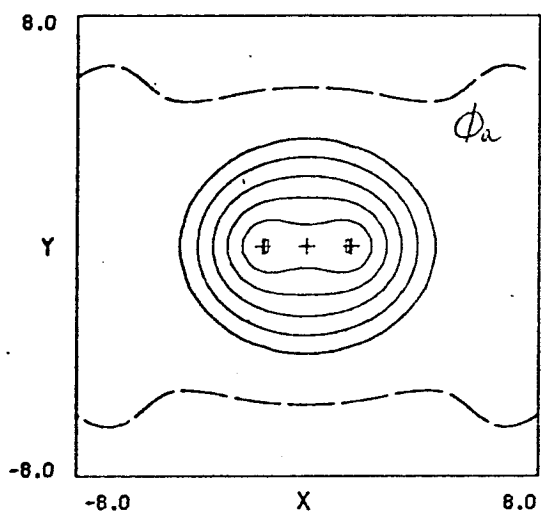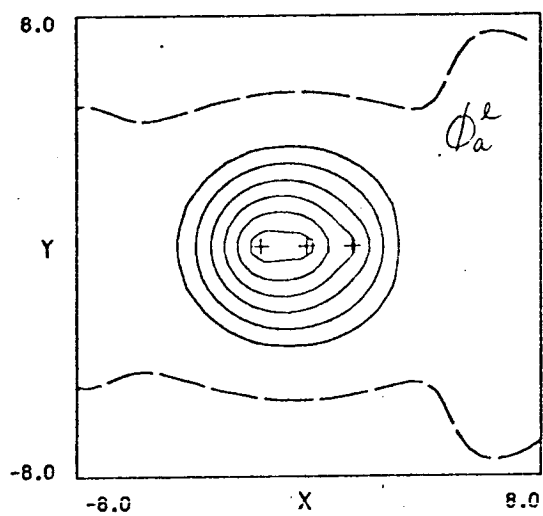
Figure 2.

Geometry f

H_3^+ g1
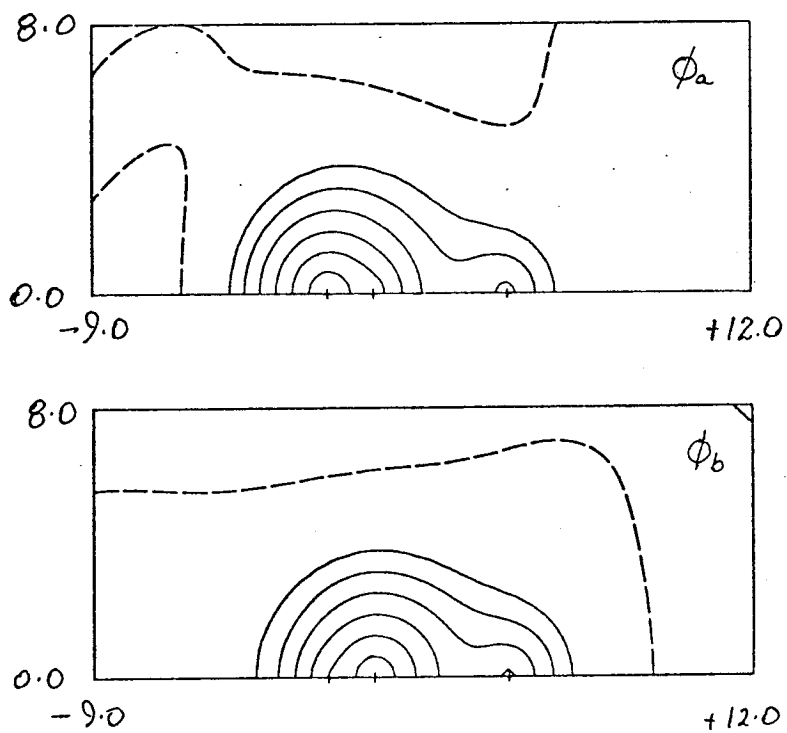
Figure 3.

GEOMETRY G

H_3^+ G1(gg')
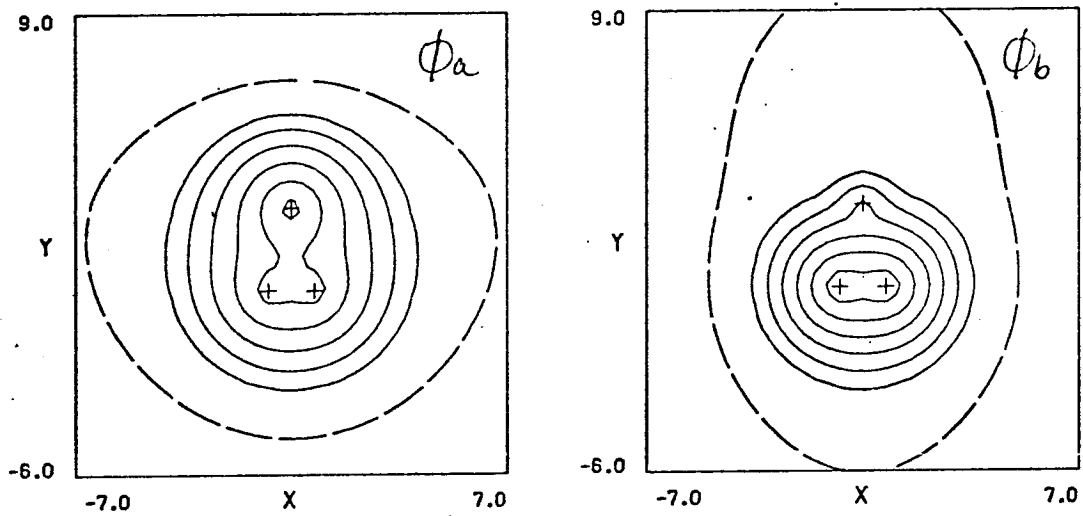
H_3^+ − G1(rl)
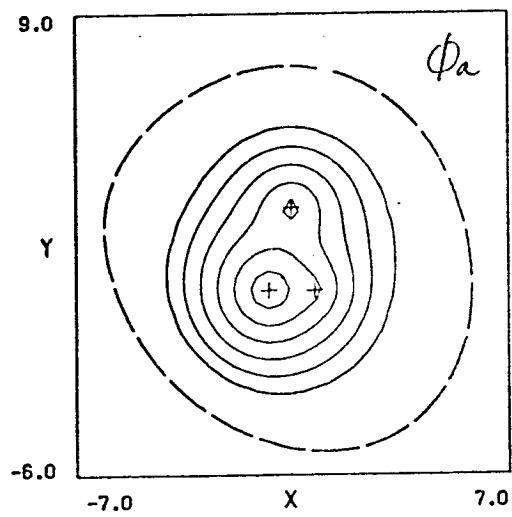
Figure 4.

Geometry J

H_3^+ $G1\,(gg')$
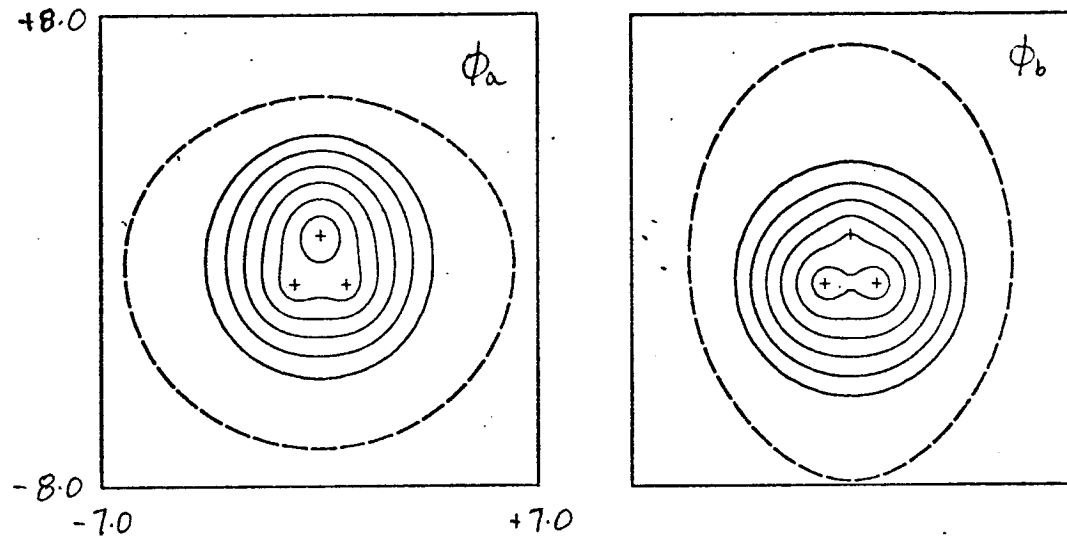
H_3^+ $G1\,(\ell r)$
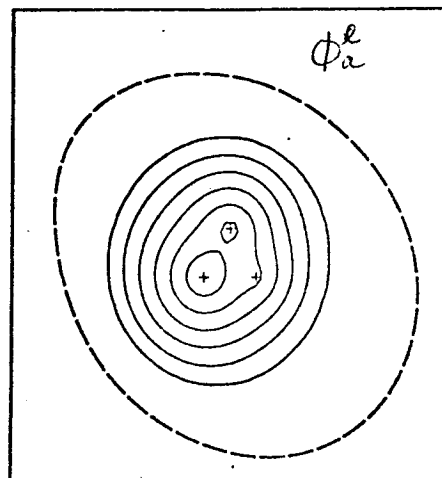
Figure 5.

Geometry K

$H_3^+ - G1$
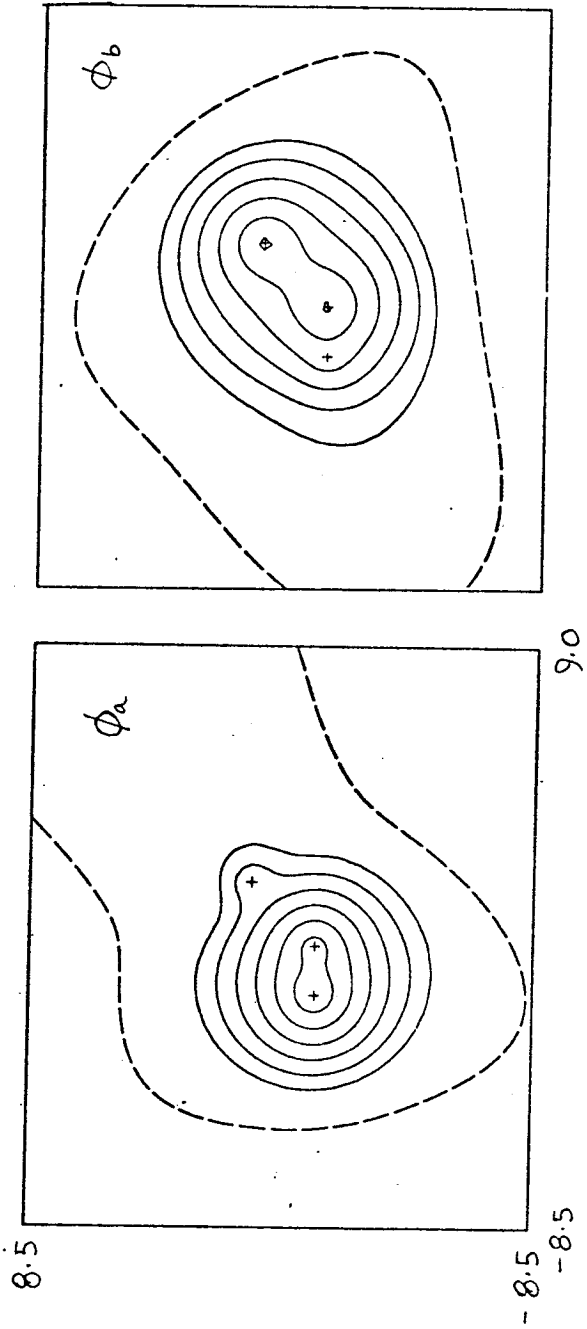
Figure 6.
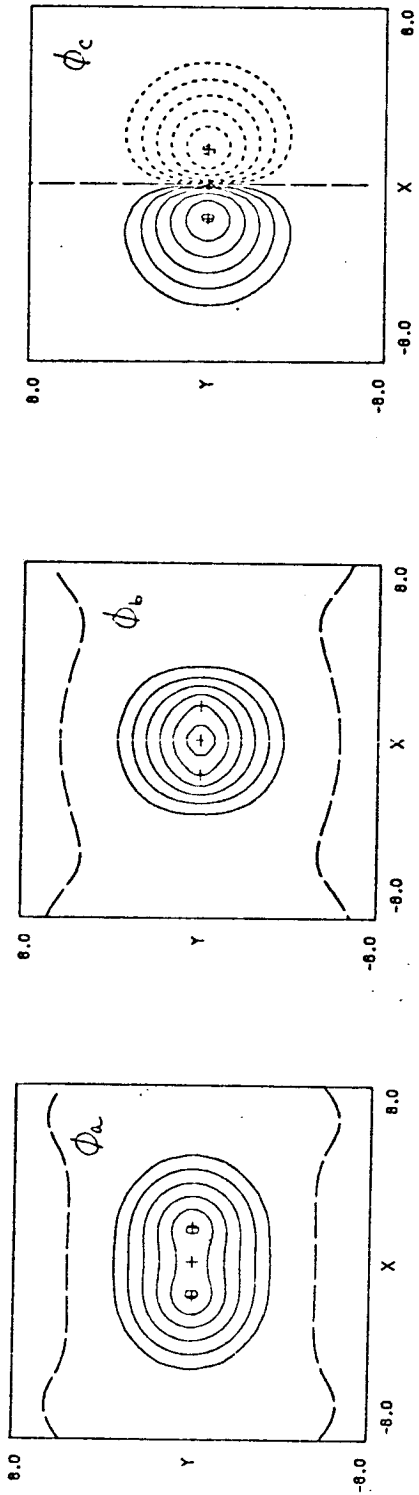
Figure 7.

Geometry A

$2\,^2\Sigma_u^+(\ell r u) - G1$
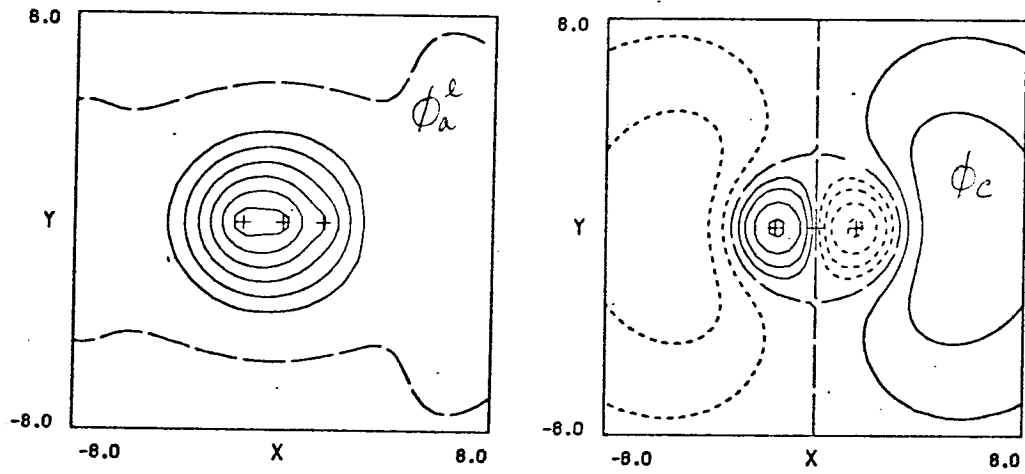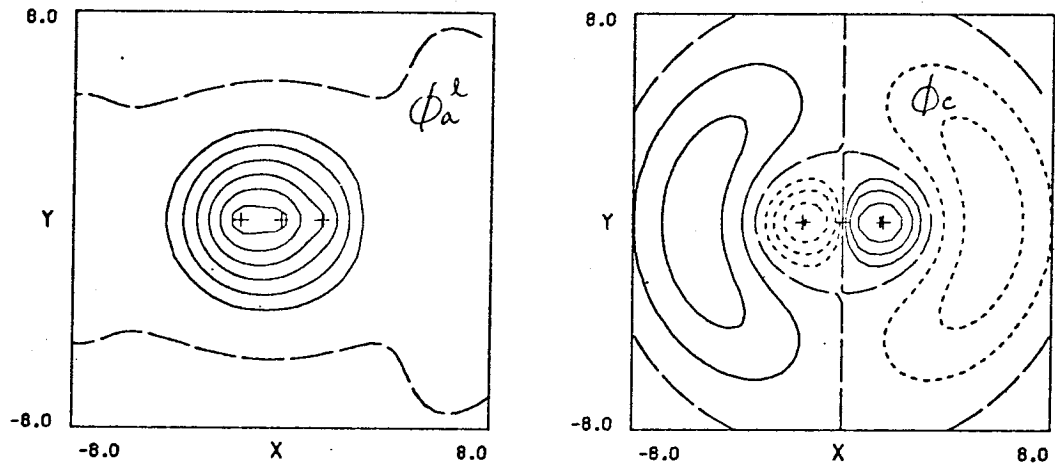
$3\,^2\Sigma_u^+(\ell r u) - G1$
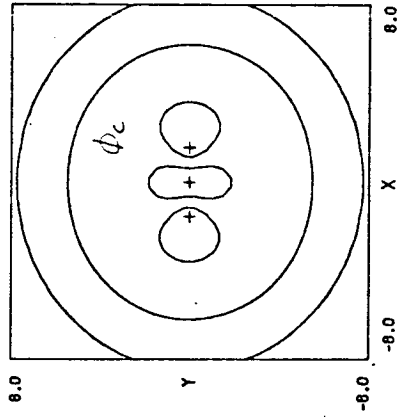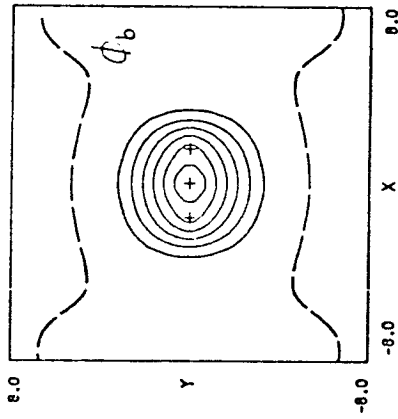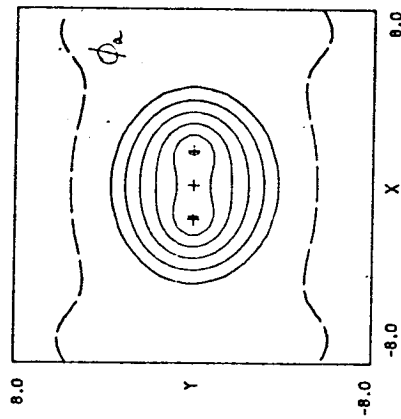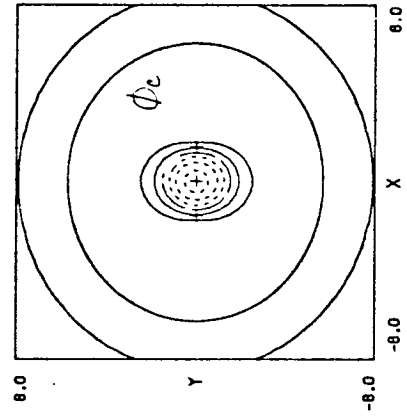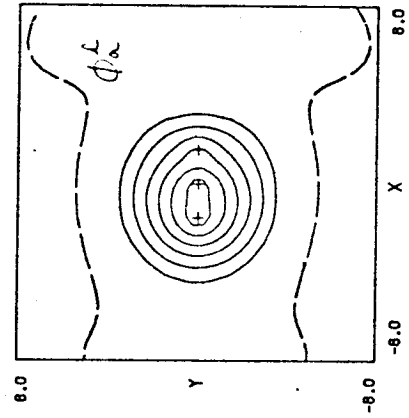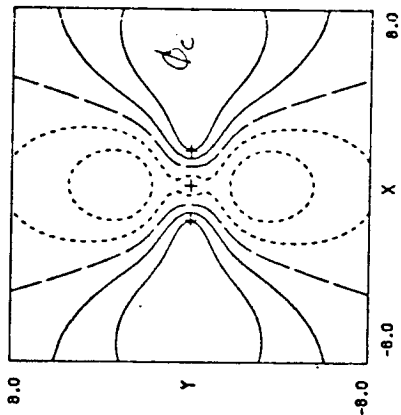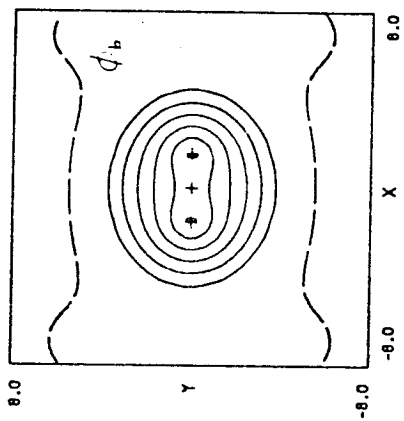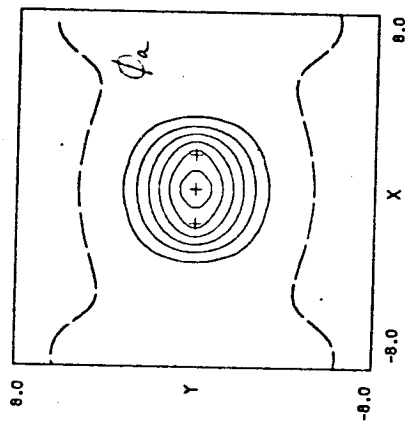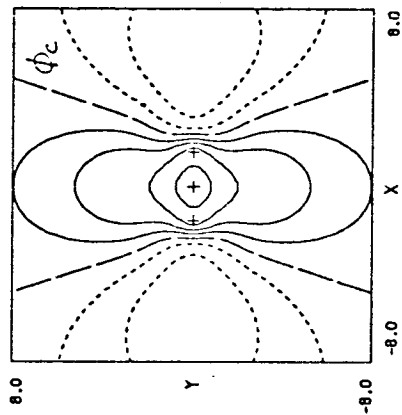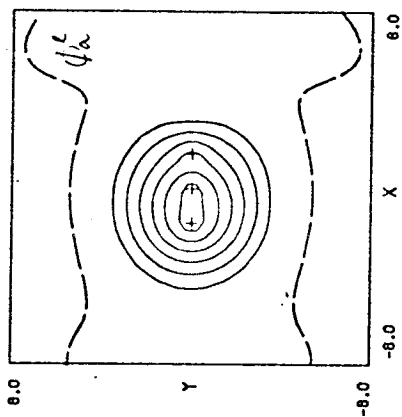
Figure 8.

Figure 9.

Figure 10.

GEOMETRY E $1\,^2\Sigma^+$ - SOGI
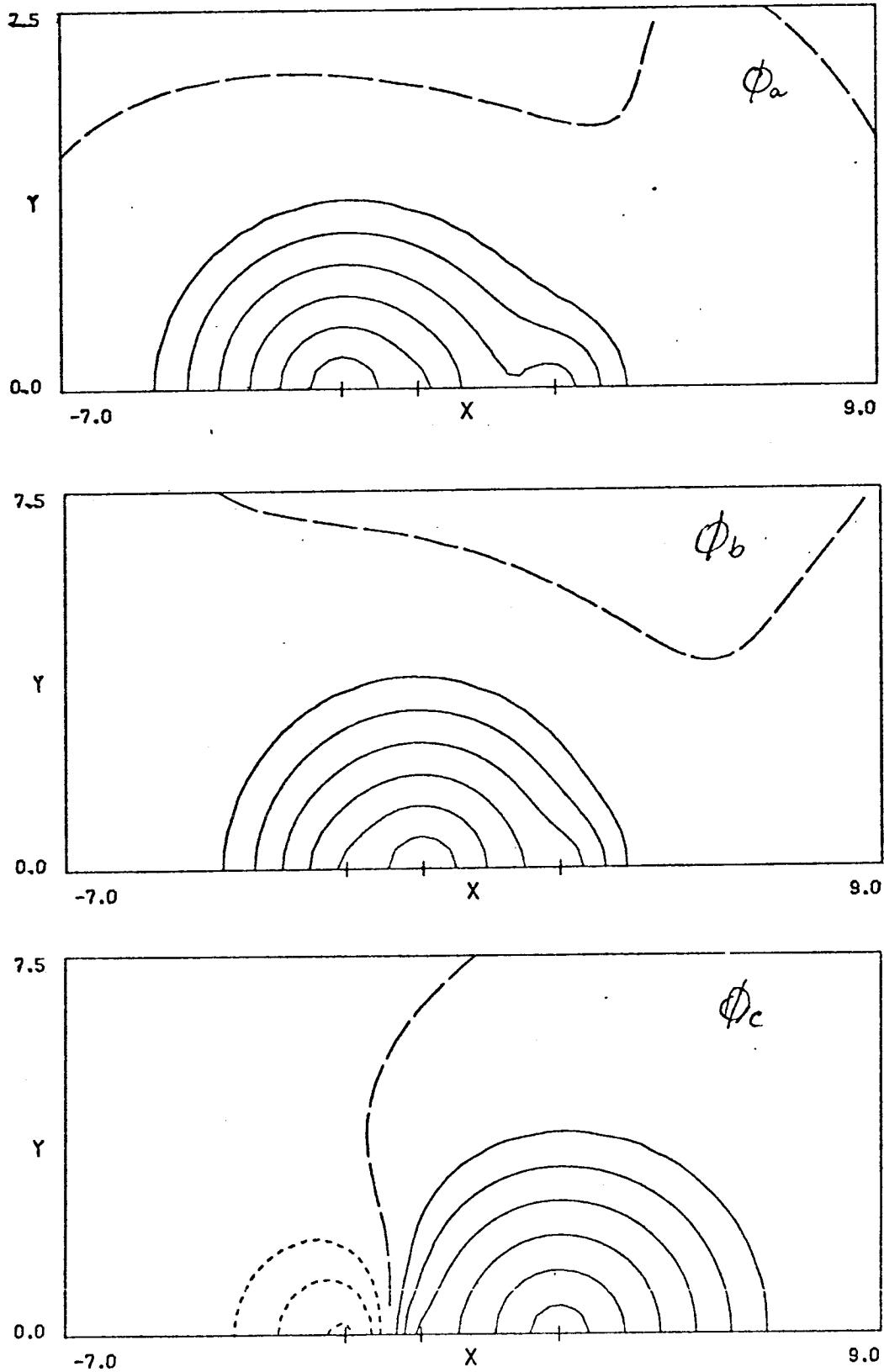
Figure 11.

GEOMETRY E

$1\,^2\Sigma^+ - G1$
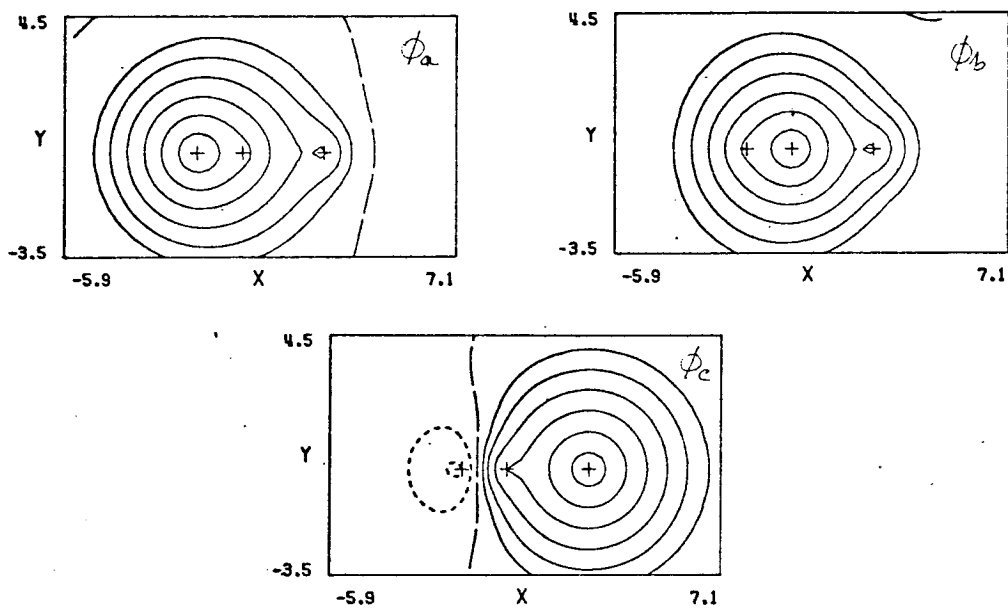
$1\,^2\Sigma_i'^+ - G1$ NATURAL ORBITALS
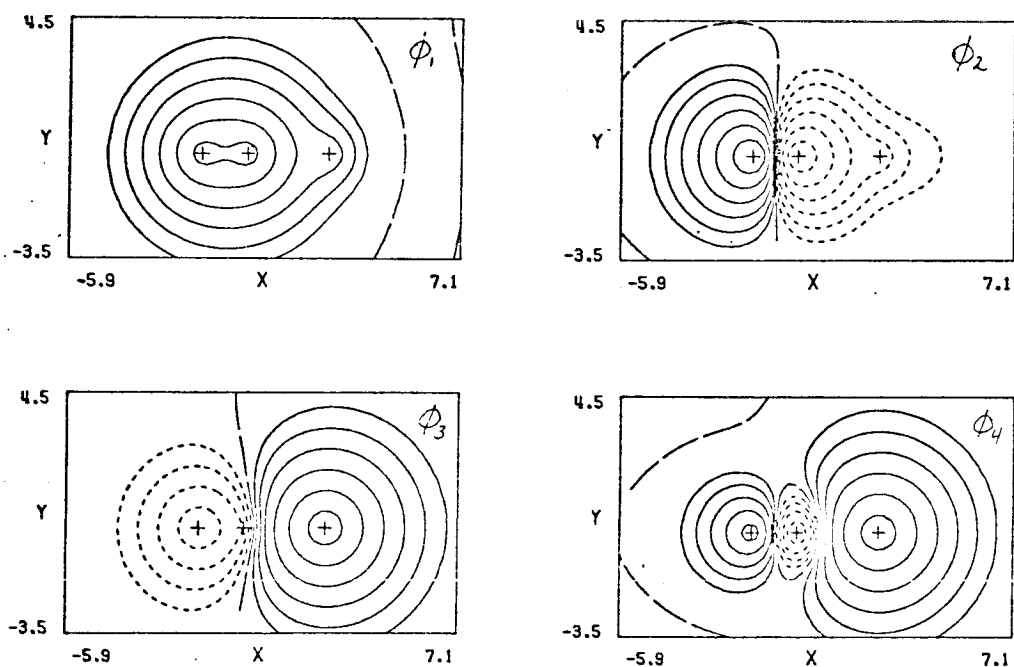
Figure 12.

GEOMETRY E

$2\,^2\Sigma_i^+ - SOGI$
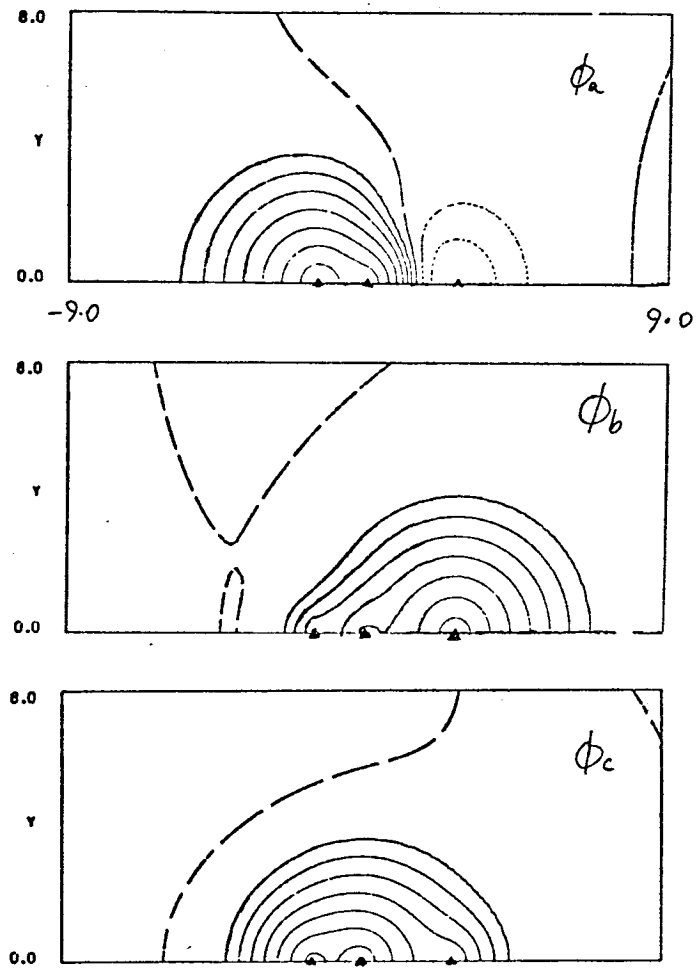
Figure 13.

GEOMETRY E

$2\ ^2\Sigma^+ - G1$
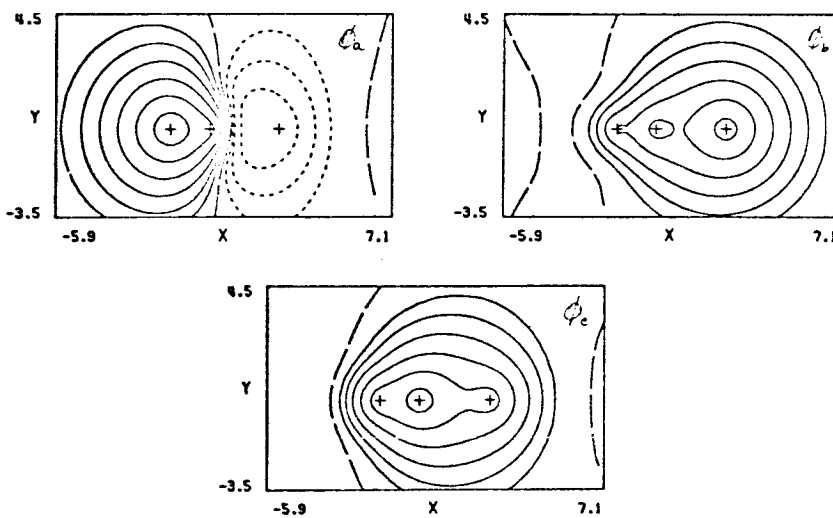
$2\ ^2\Sigma^+ - G1$ NATURAL ORBITALS
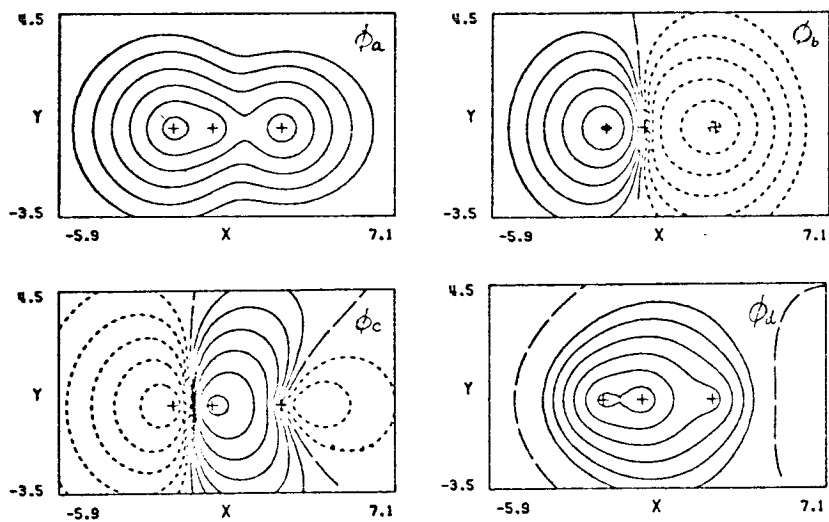
Figure 14.

GEOMETRY E

$3\,^2\Sigma_1^+ - SOGI$
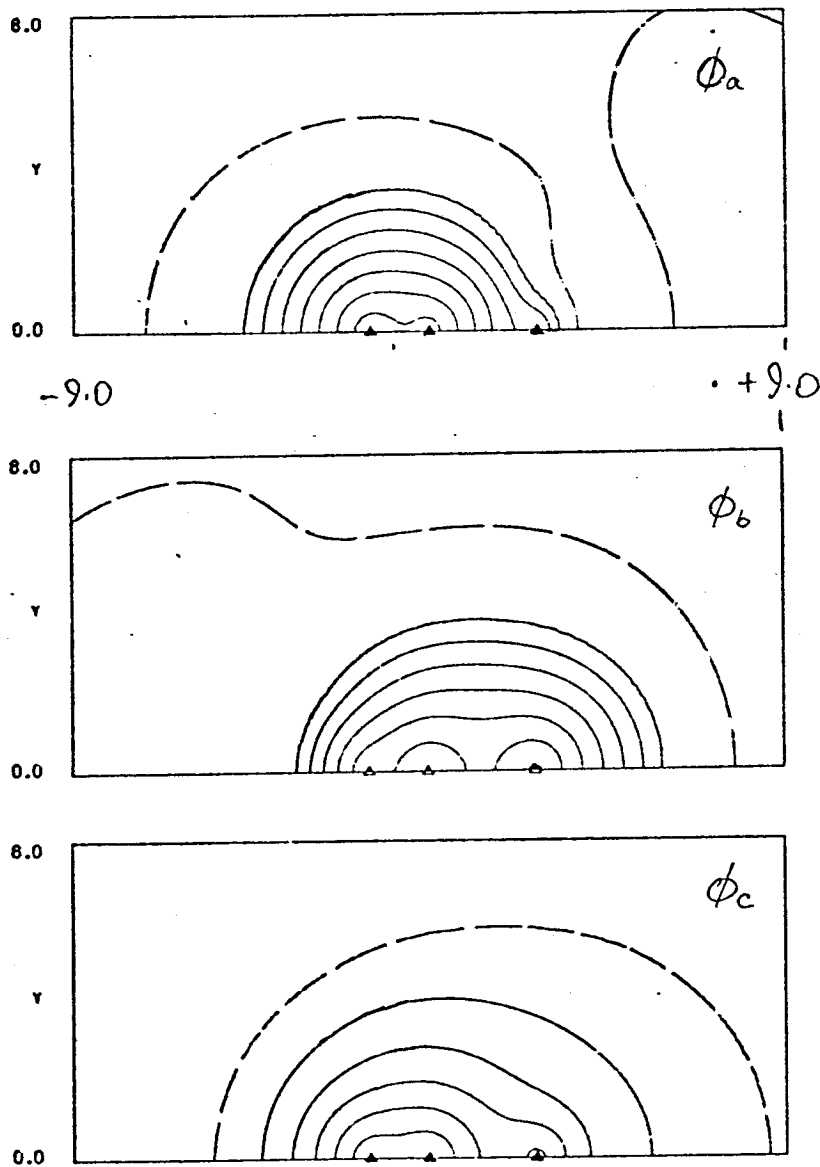
Figure 15.

GEOMETRY E

$3\,^2\Sigma^+ - G1$
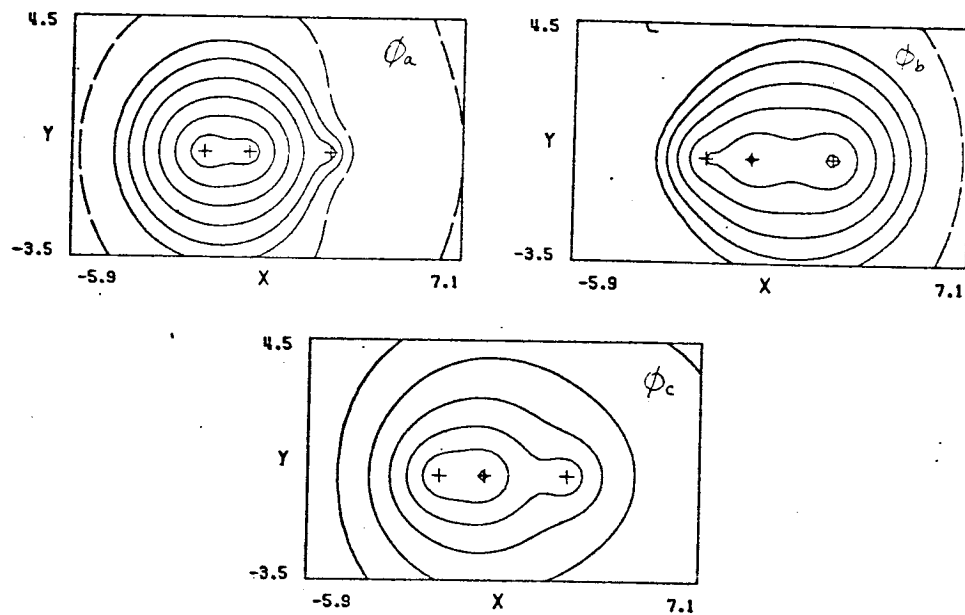
$3\,^2\Sigma^+ - G1$ NATURAL ORBITALS
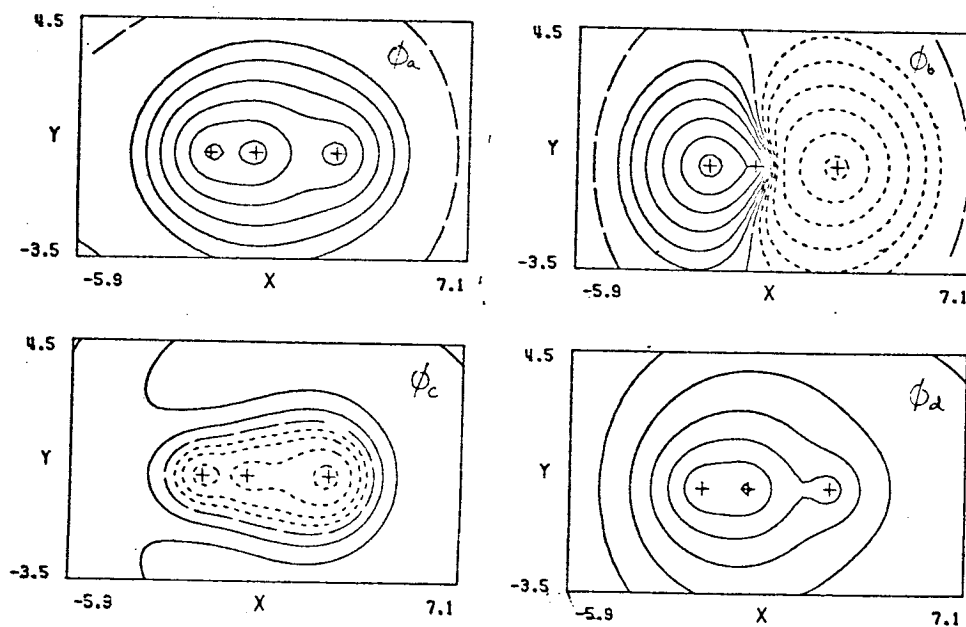
Figure 16.

GEOMETRY E

$4\,^2\Sigma^+ - SOGI$
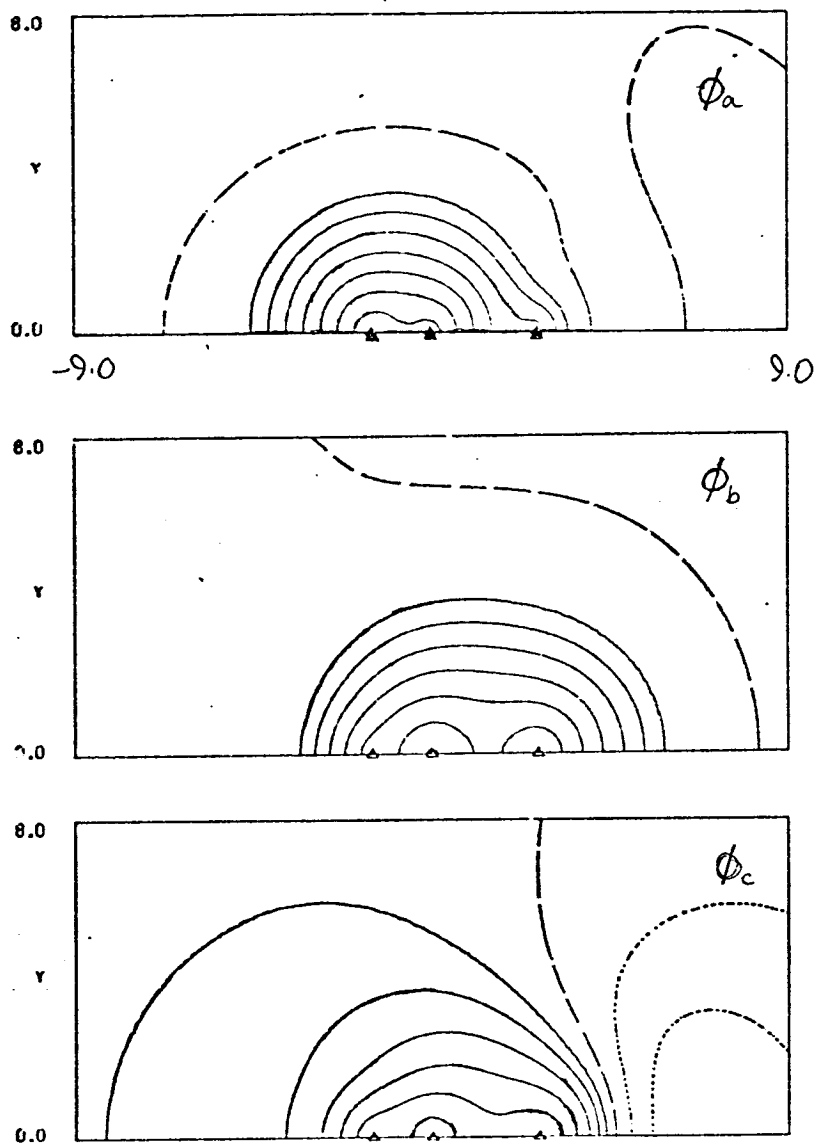
Figure 17.

GEOMETRY E

$4\,^2\Sigma_1^+ - G1$
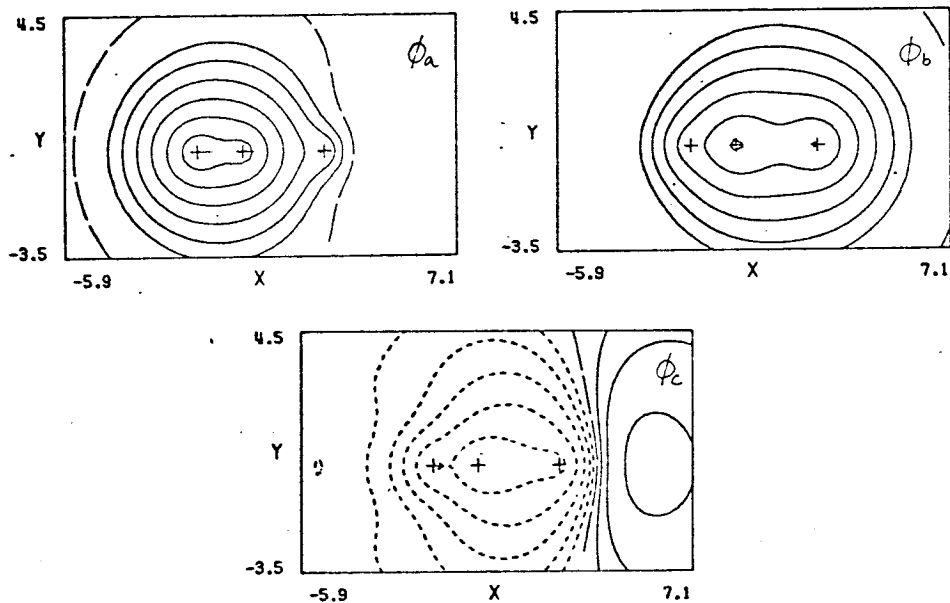
$4\,^2\Sigma_1^+ - G1$ Natural Orbitals
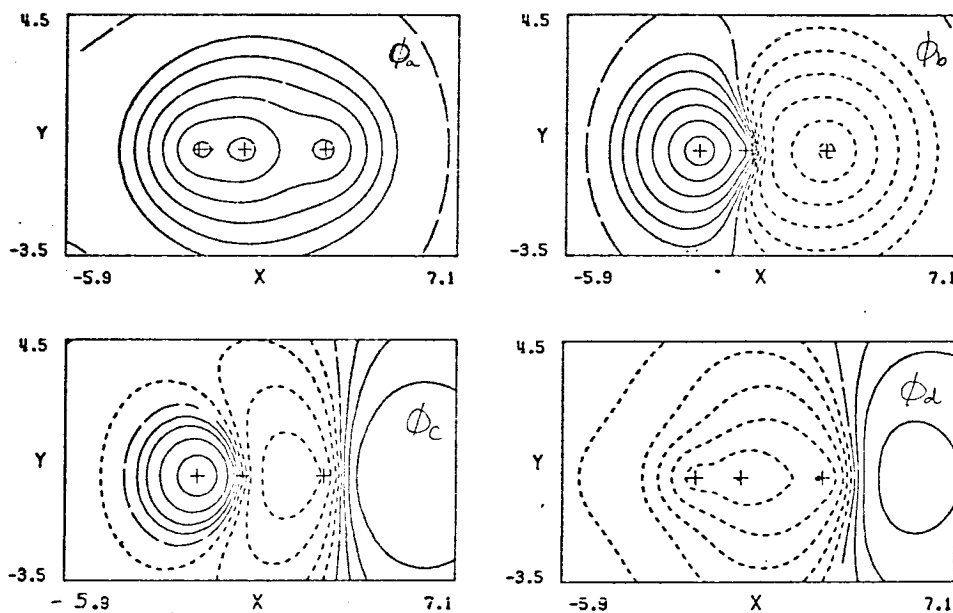
Figure 18.

Geometry f - Ground State

SOGI
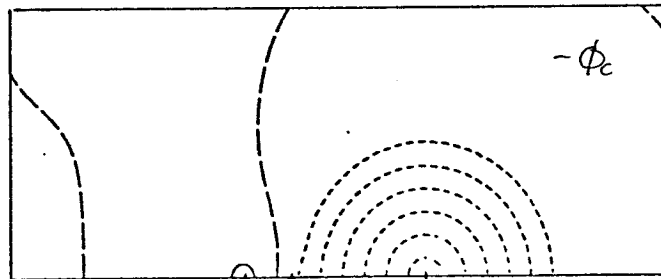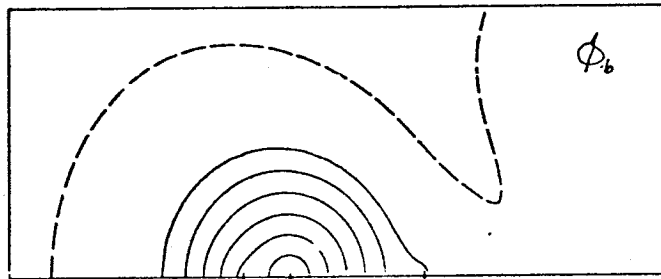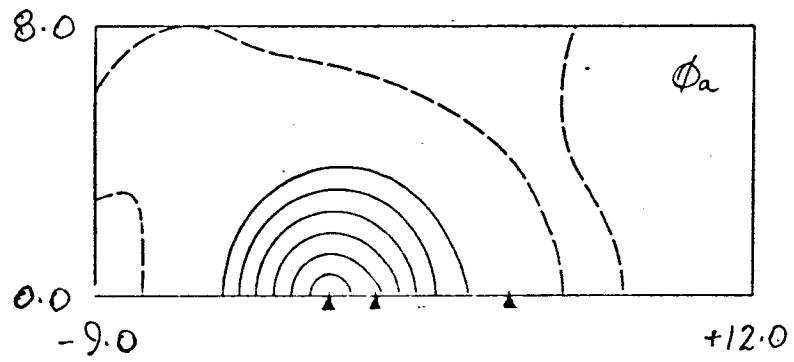
Figure 19.

Geometry f - Ground State

G 1
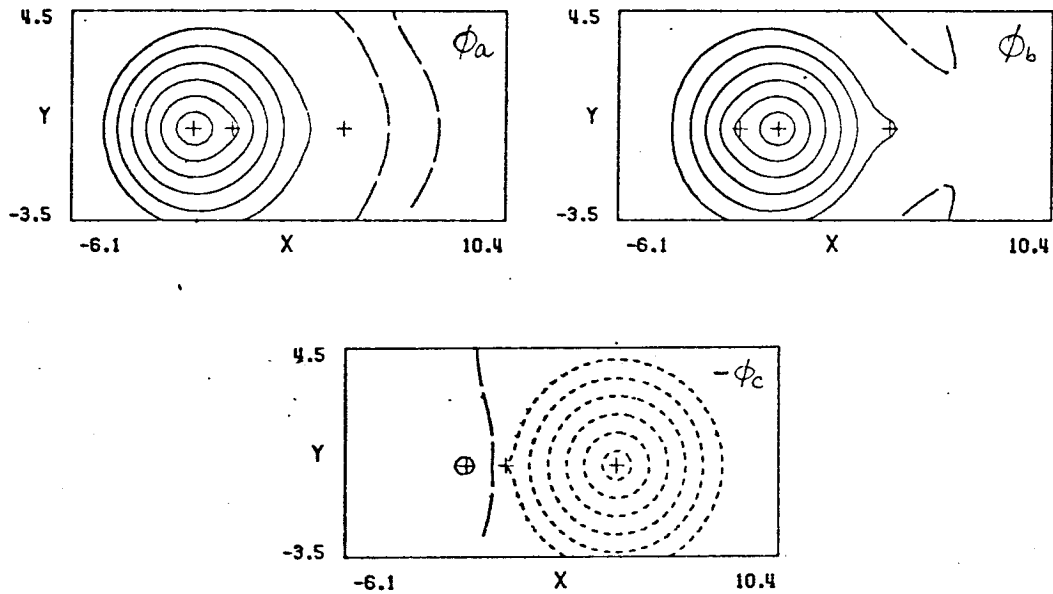
G 1 - Natural Orbitals
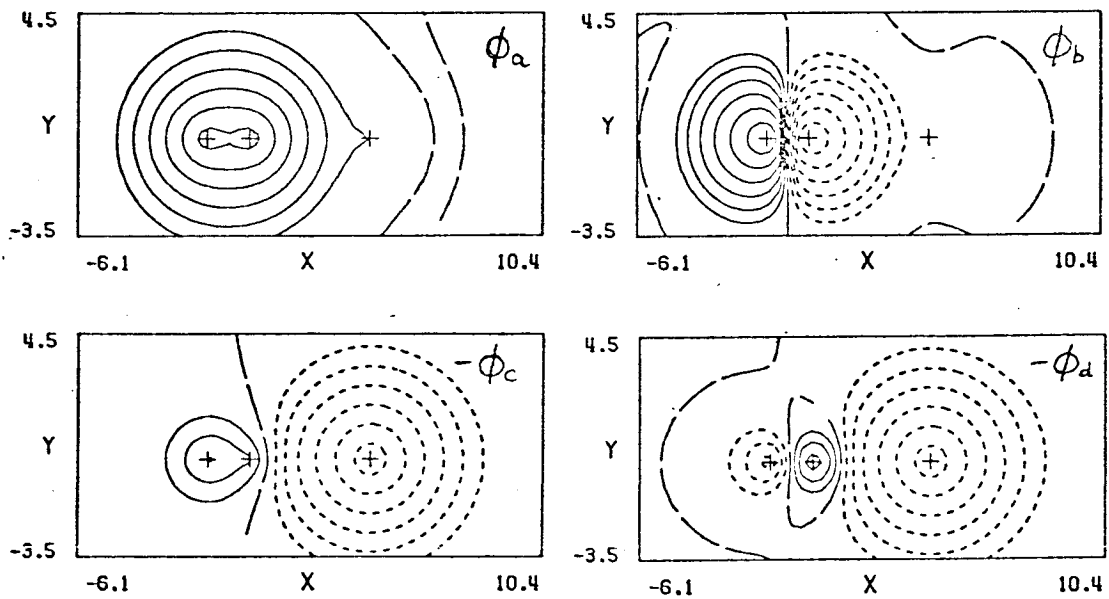
Figure 20.

Geometry f - Third State

SOGI
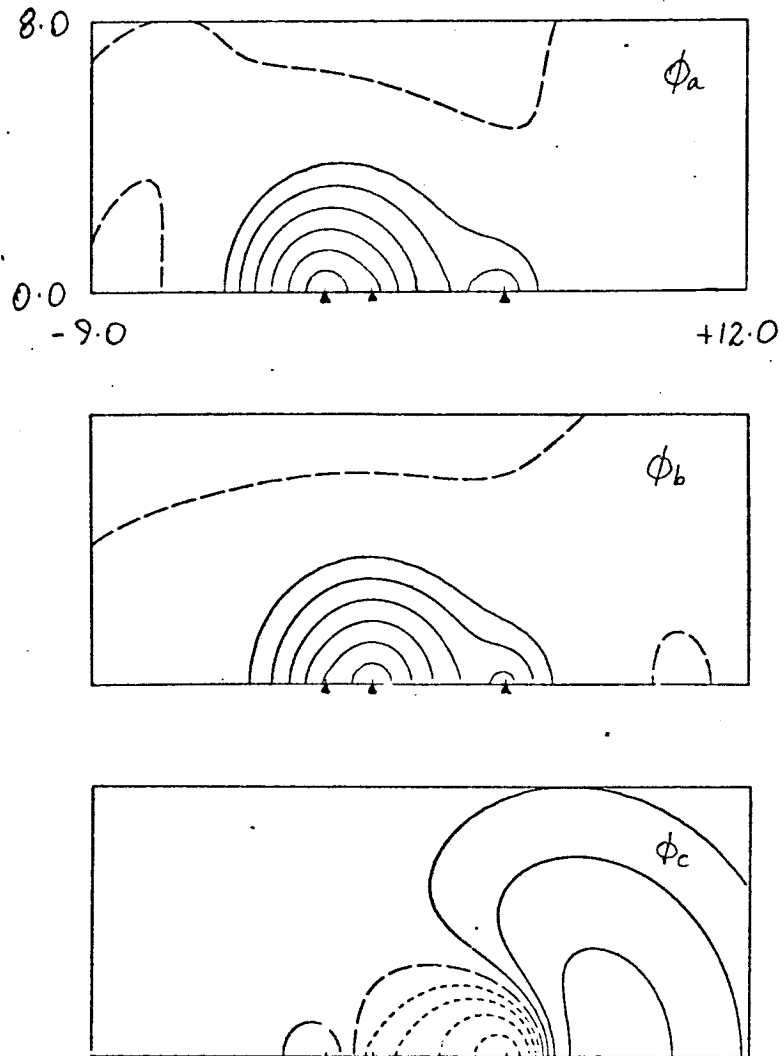
Figure 21.

Geometry f - Third State

G1
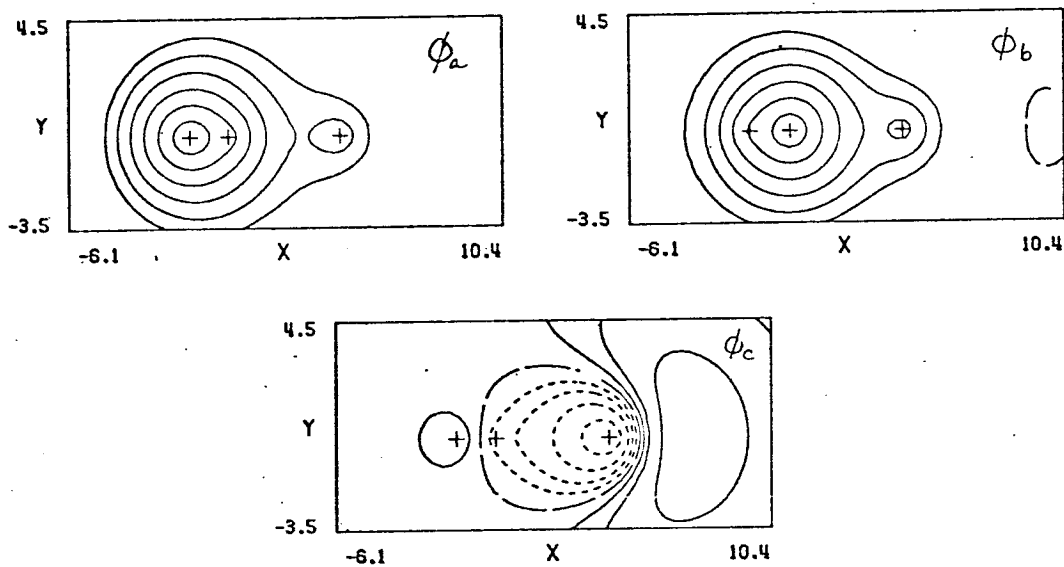
G1 - Natural Orbitals
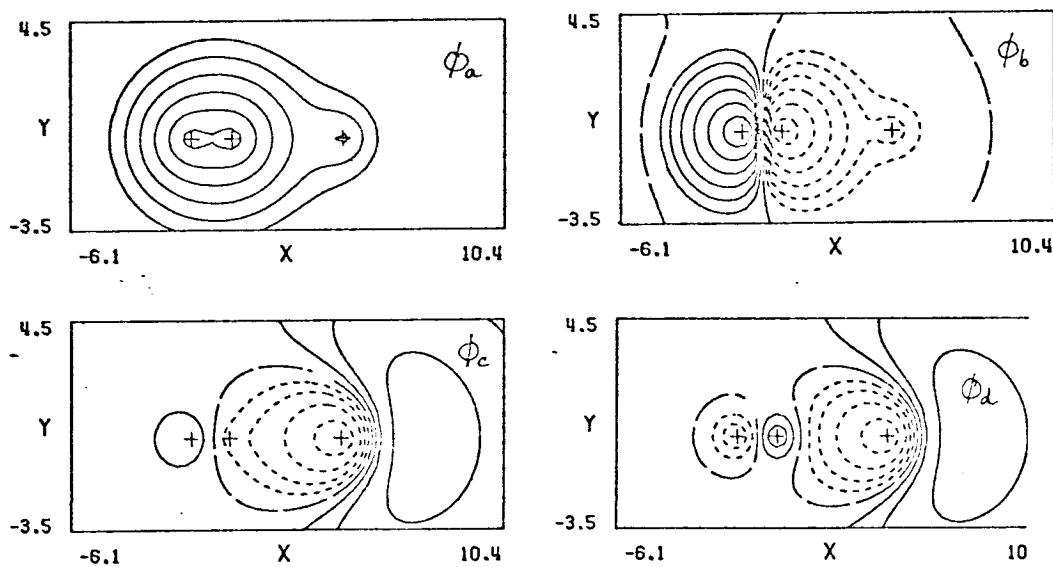
Figure 22.

Geometry f - Fourth State

SOGI
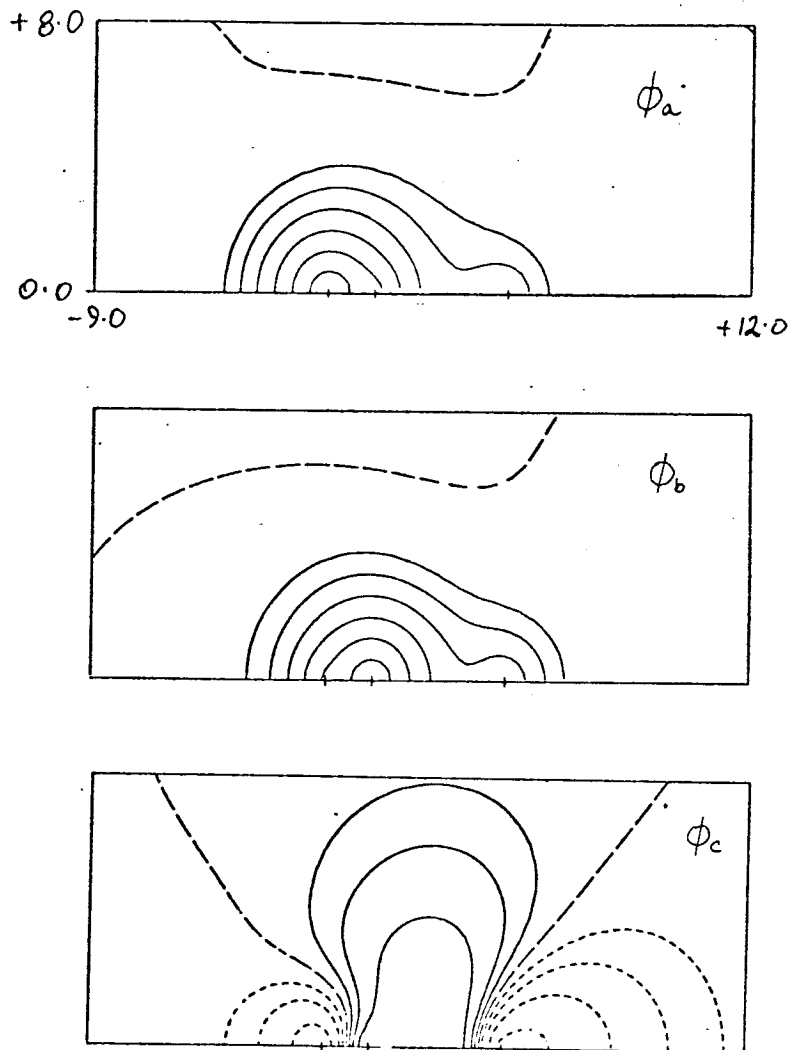
Figure 23.

Geometry f - Fourth State

G1
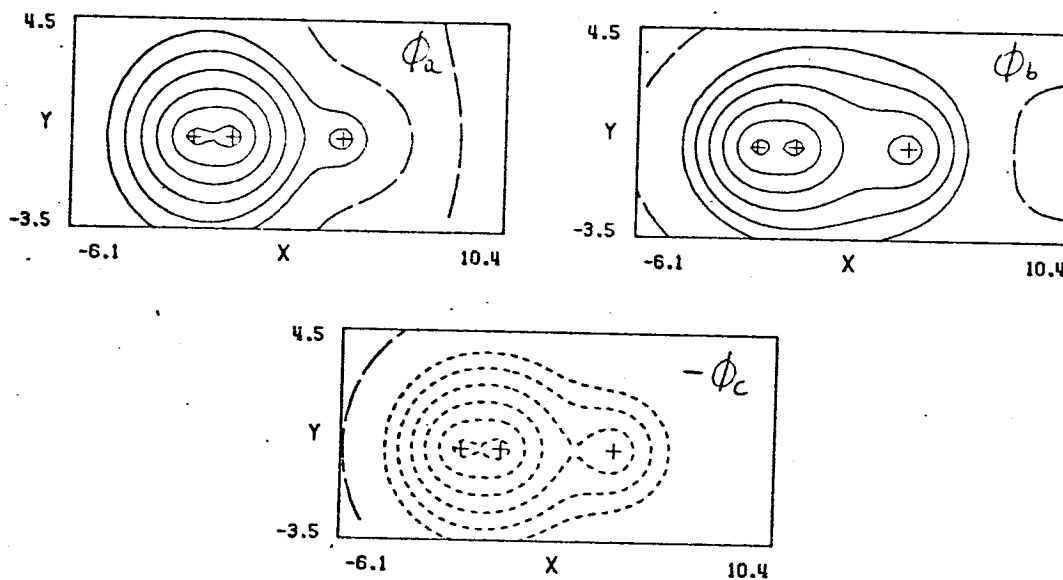
G1 - Natural Orbitals
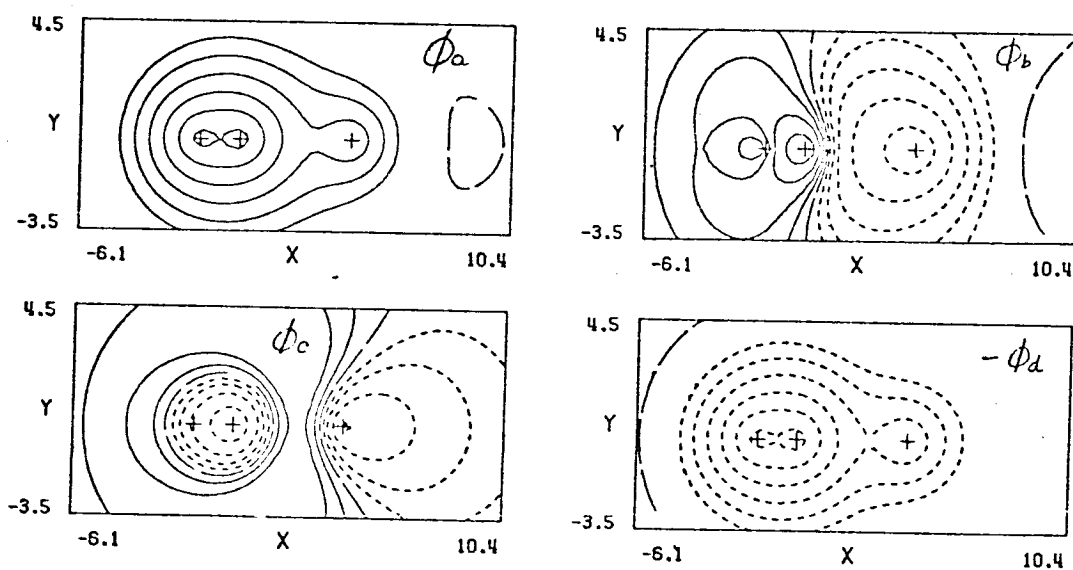
Figure 24.

Geometry f - Fifth State
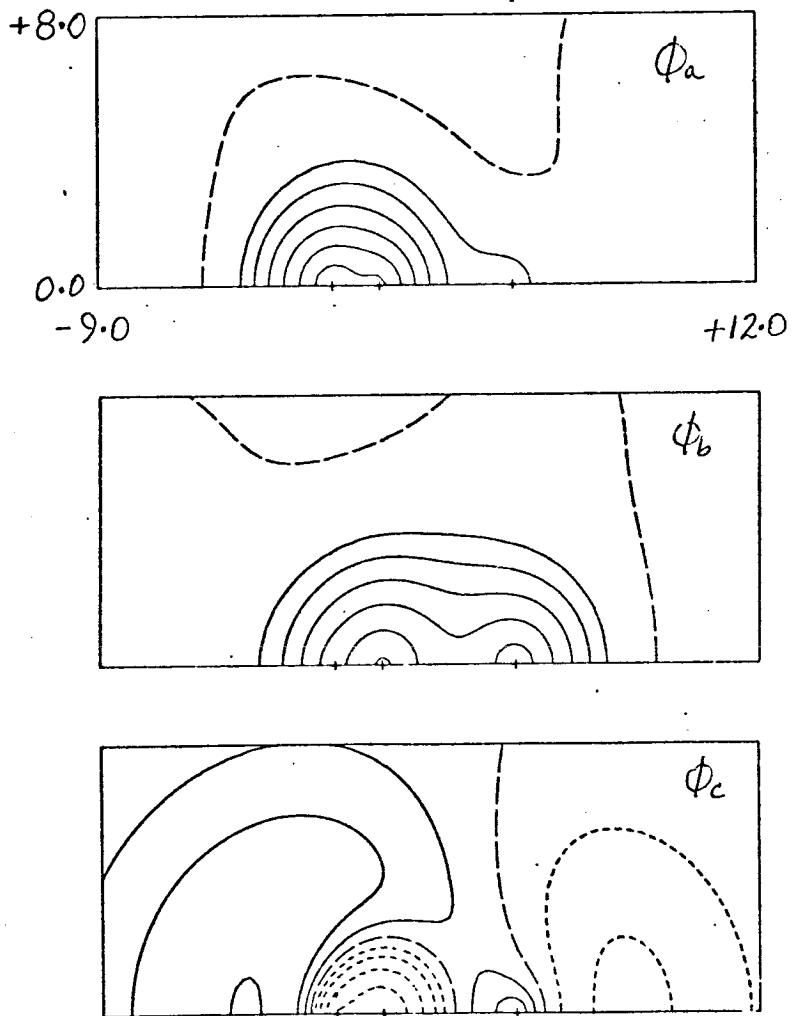
SOGI

Figure 25.

Geometry f - Fifth State

$\mathcal{G}1$
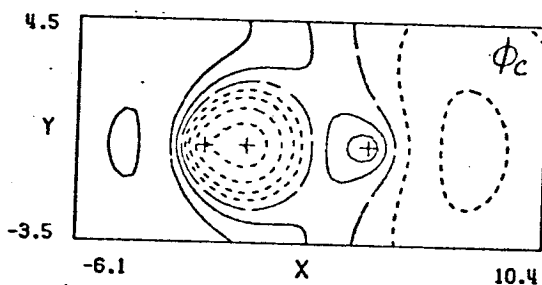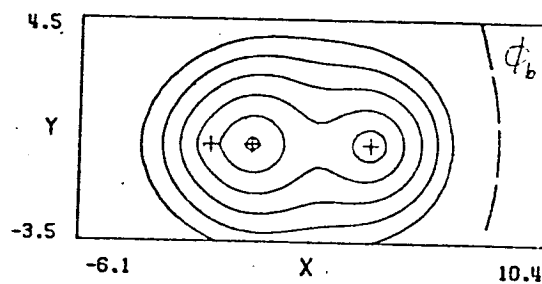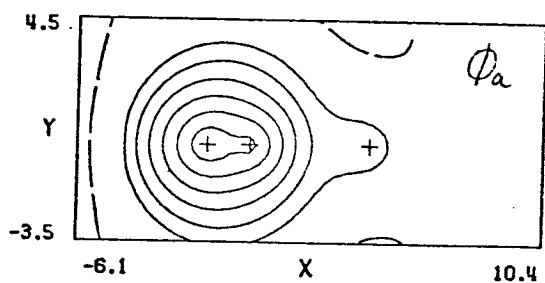
$\mathcal{G}1$ - Natural Orbitals
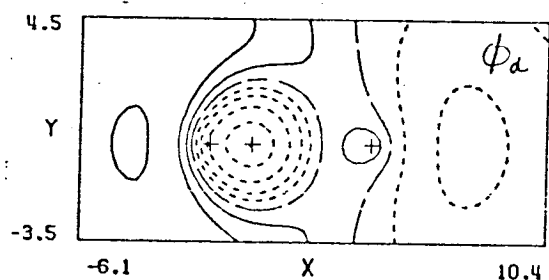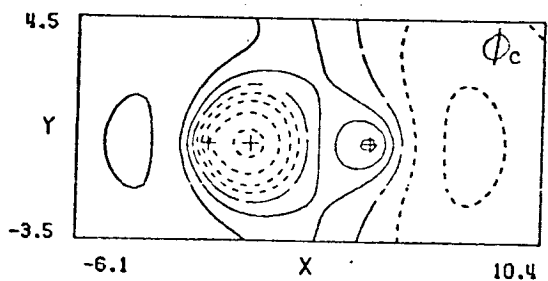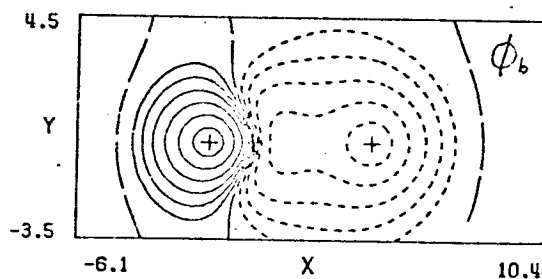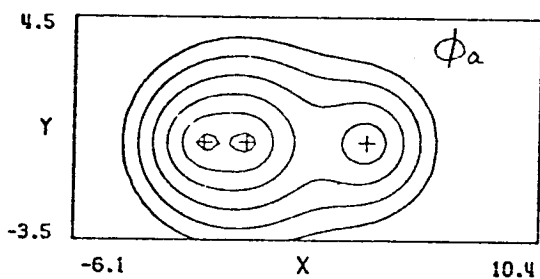
Figure 26.

Geometry G

Ground State - G 1
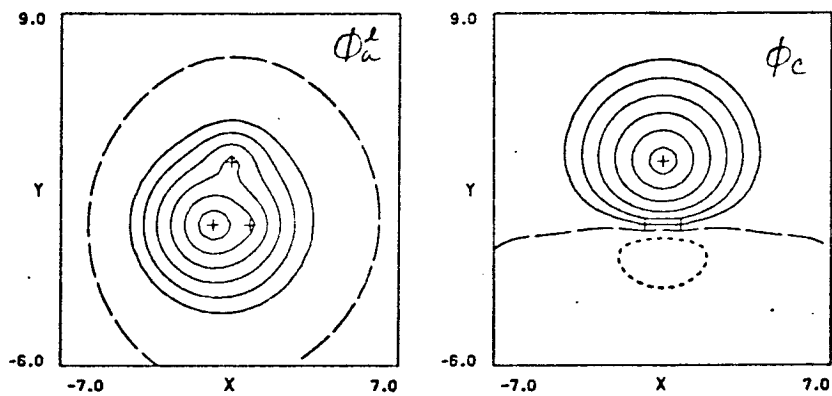
Second State

SOGI (gg'u)
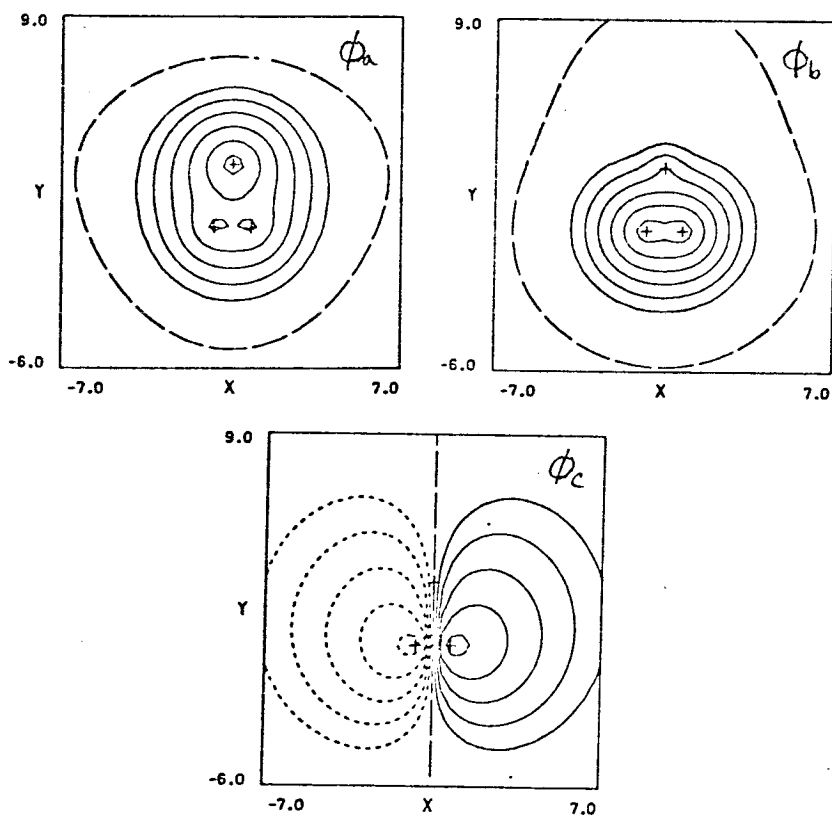
Figure 27.

Geometry G

Third State

SOGI (gg'g")
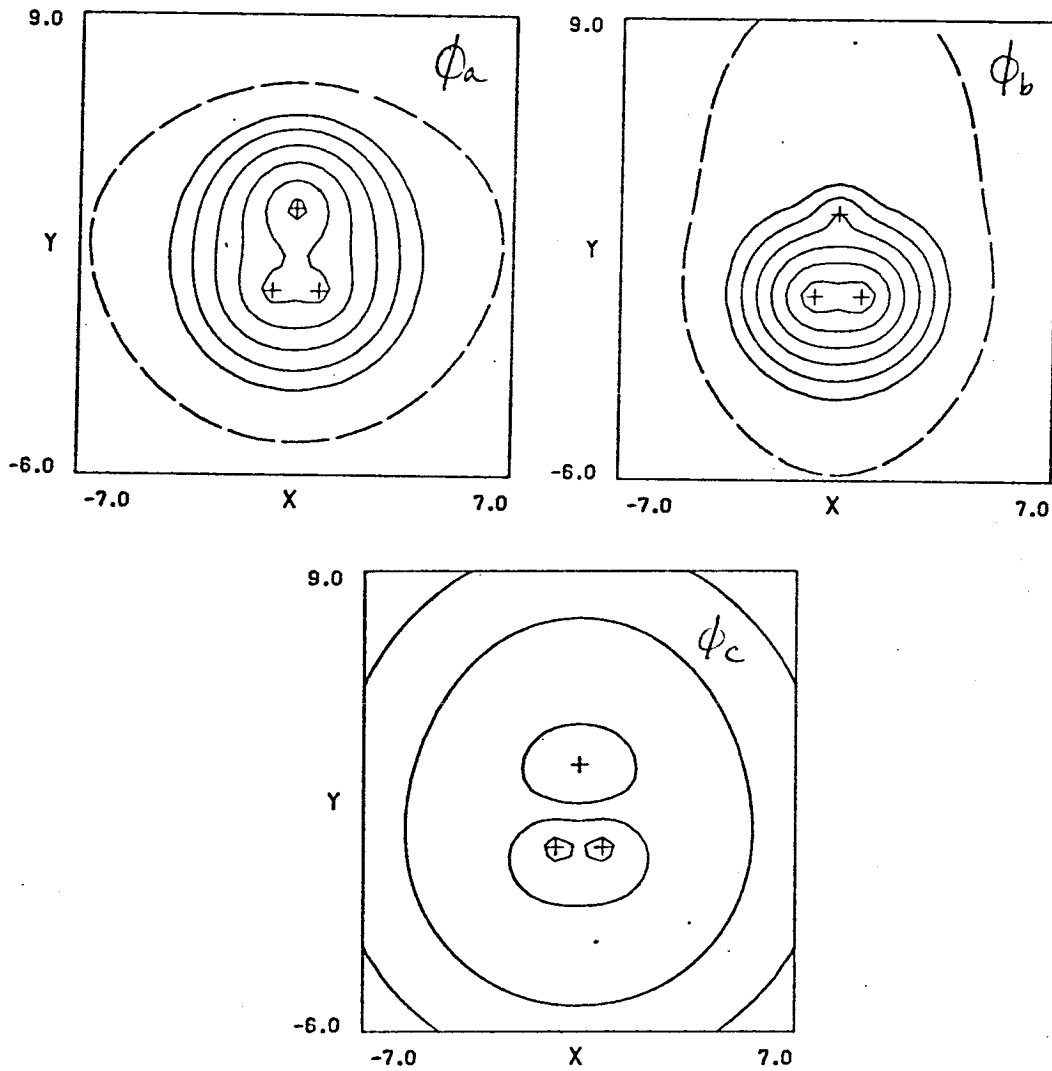
Figure 28.

Geometry G

Fourth State

$SOGI\ (gg'g'')$
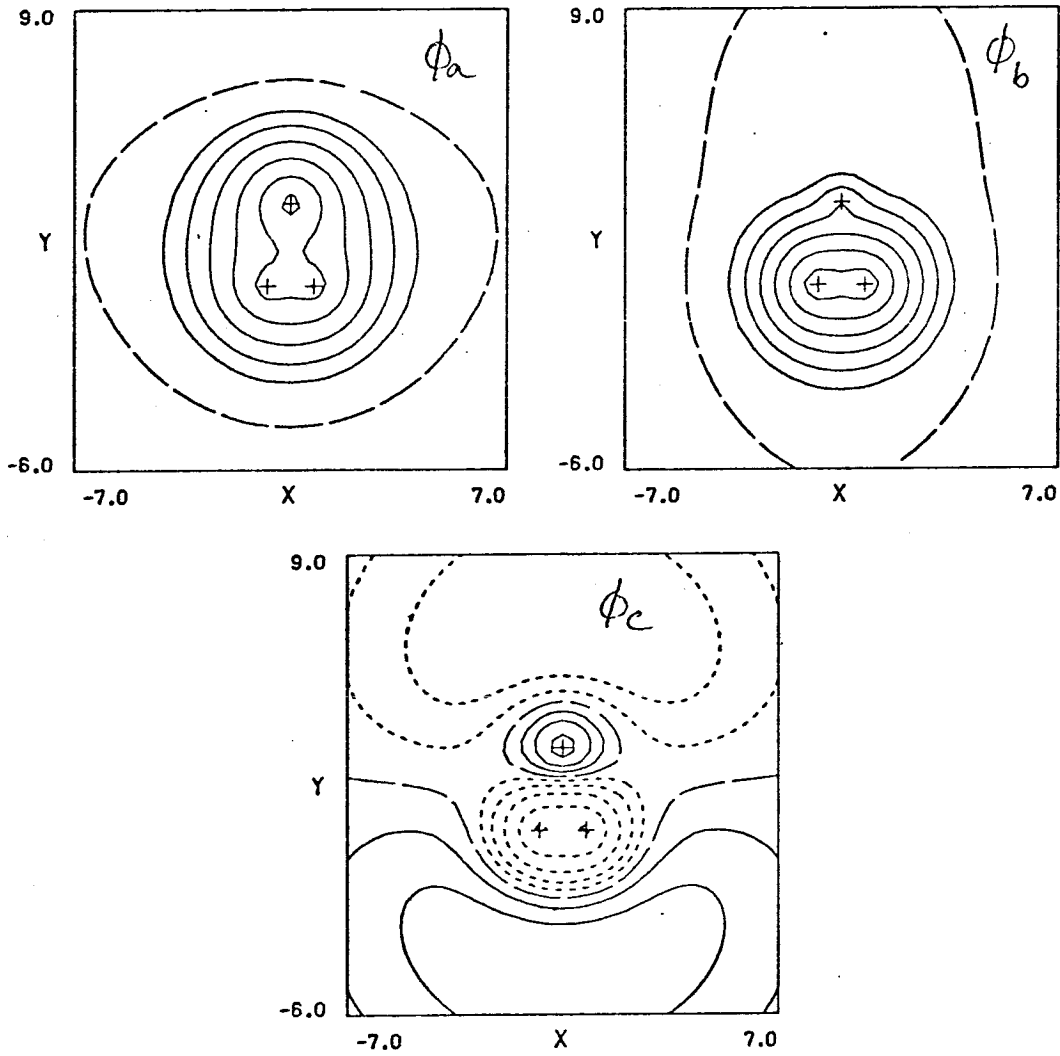
Figure 29.

Geometry J

X Component of Doubly-Degenerate Ground State

SOGI (gg'u)
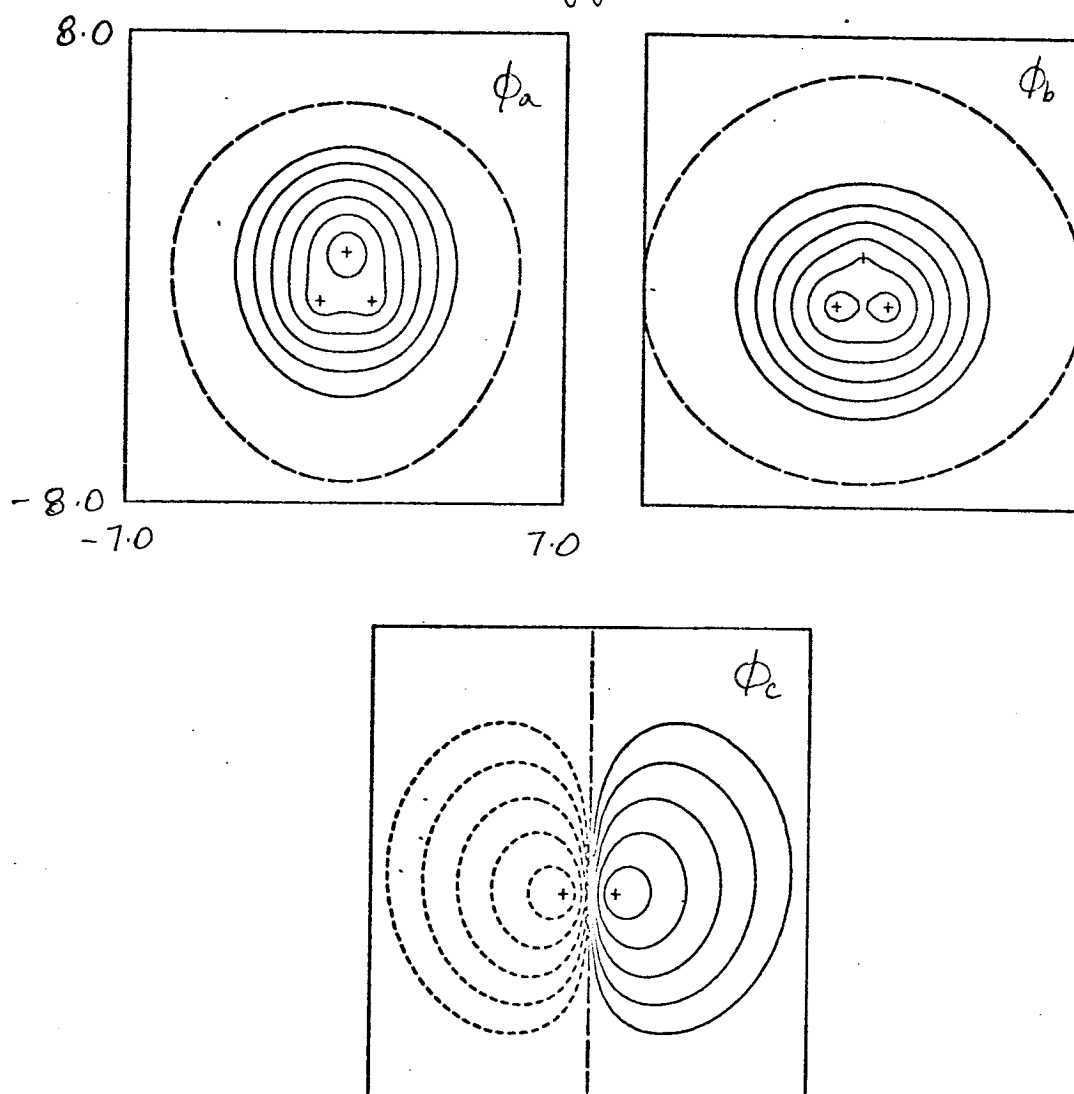
Figure 30.

Geometry J

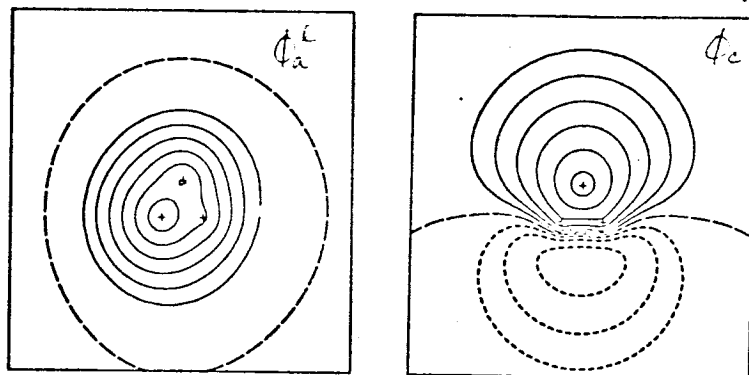*Y Component of Doubly-Degenerate Ground State*

SOGI (*gg'g"*)
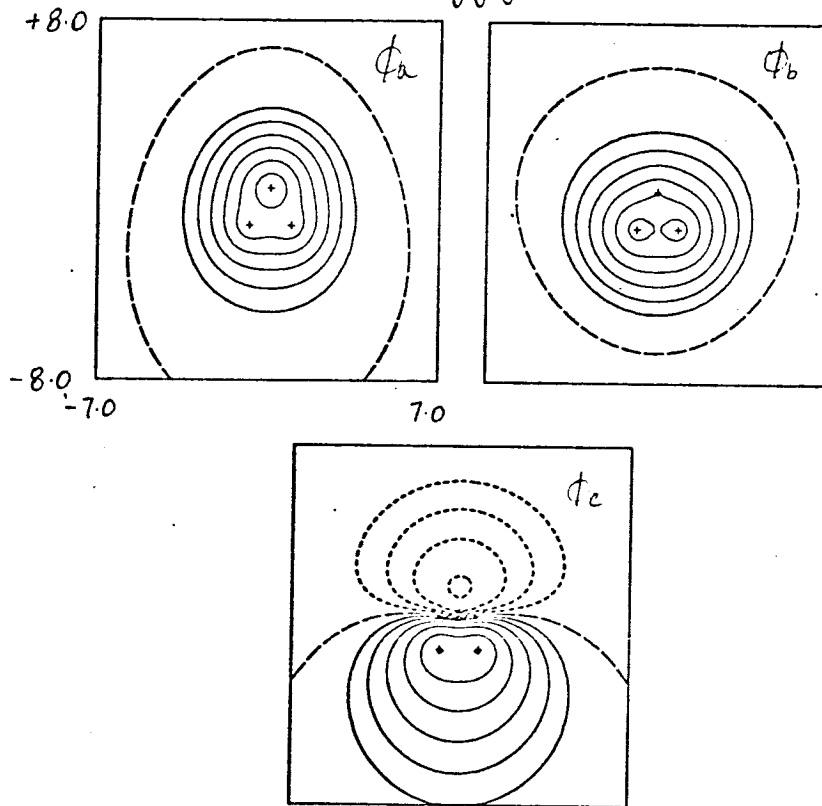
G1 (*lrg*)

Figure 31.

Geometry J
Non-Degenerate Second State
SOGI (gg'g')
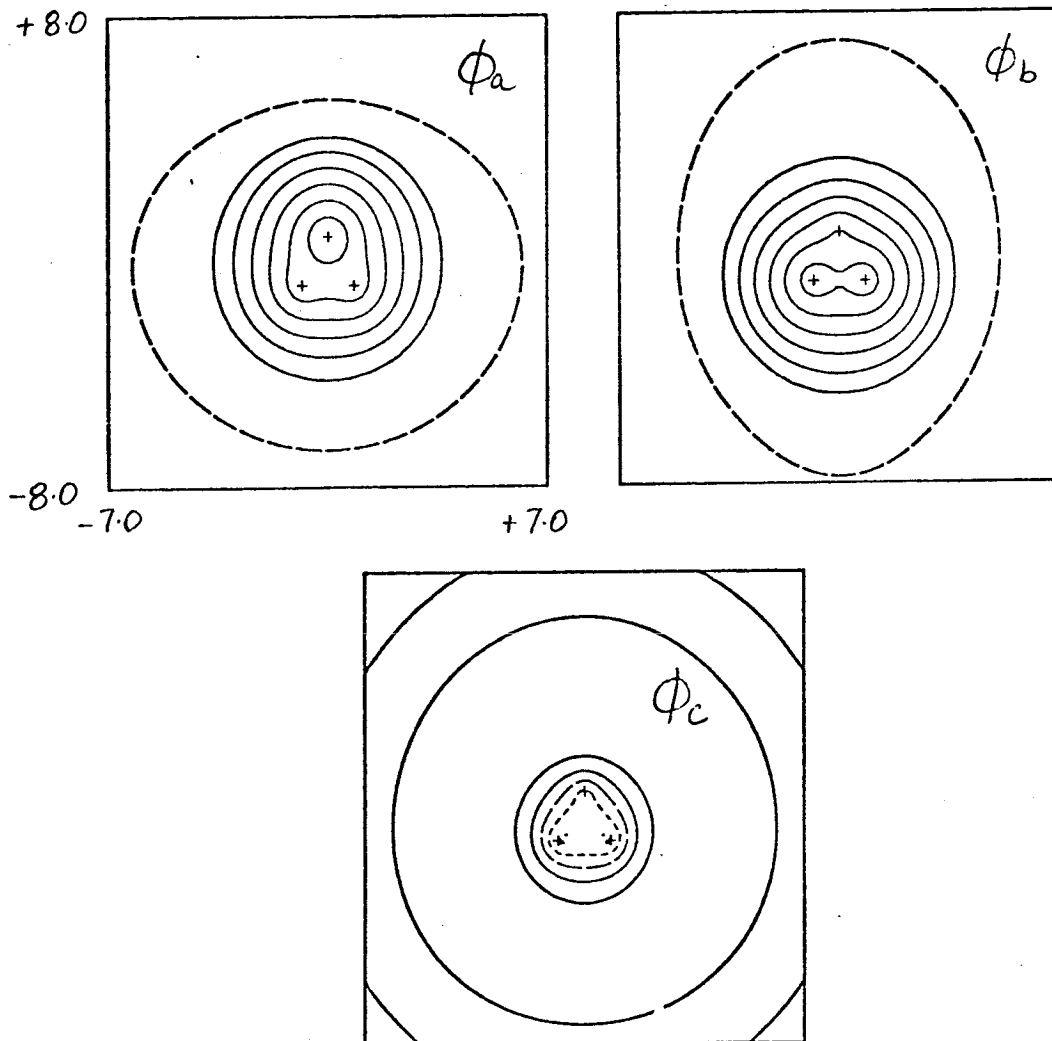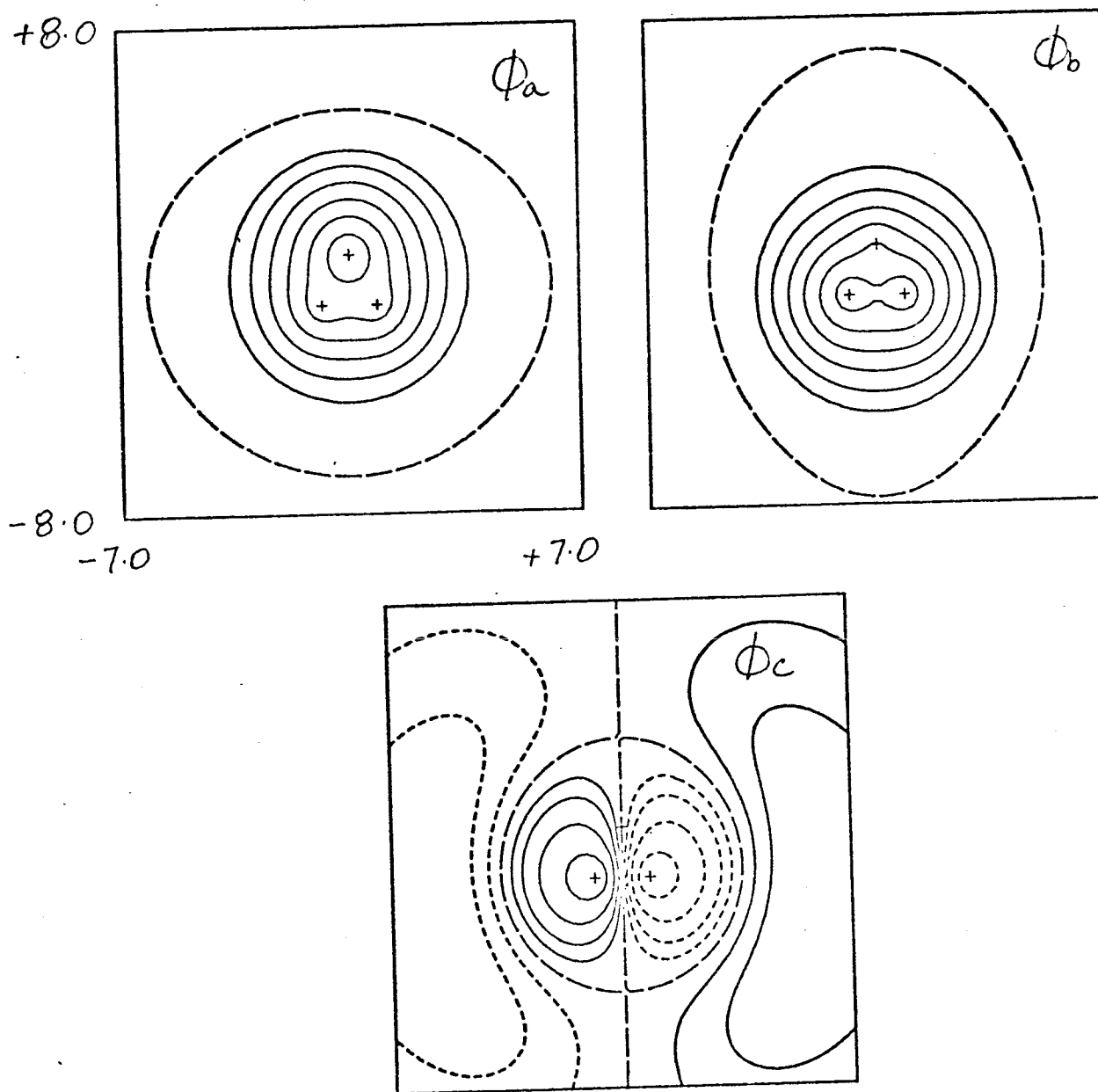

Figure 32.

Geometry J

X Component of Doubly Degenerate Third State

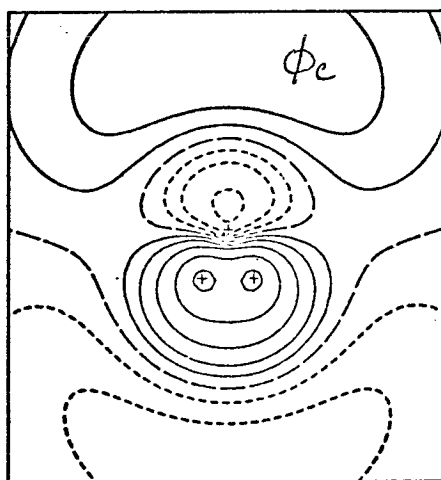Figure 33.

Geometry J

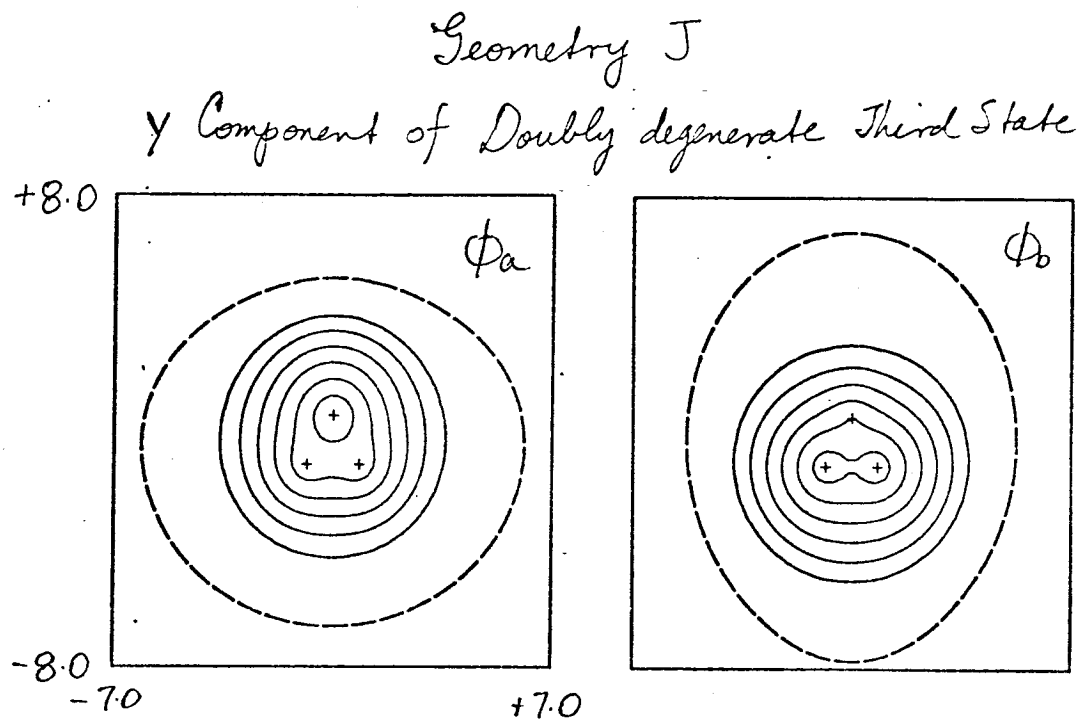y Component of Doubly degenerate Third State

Figure 34.

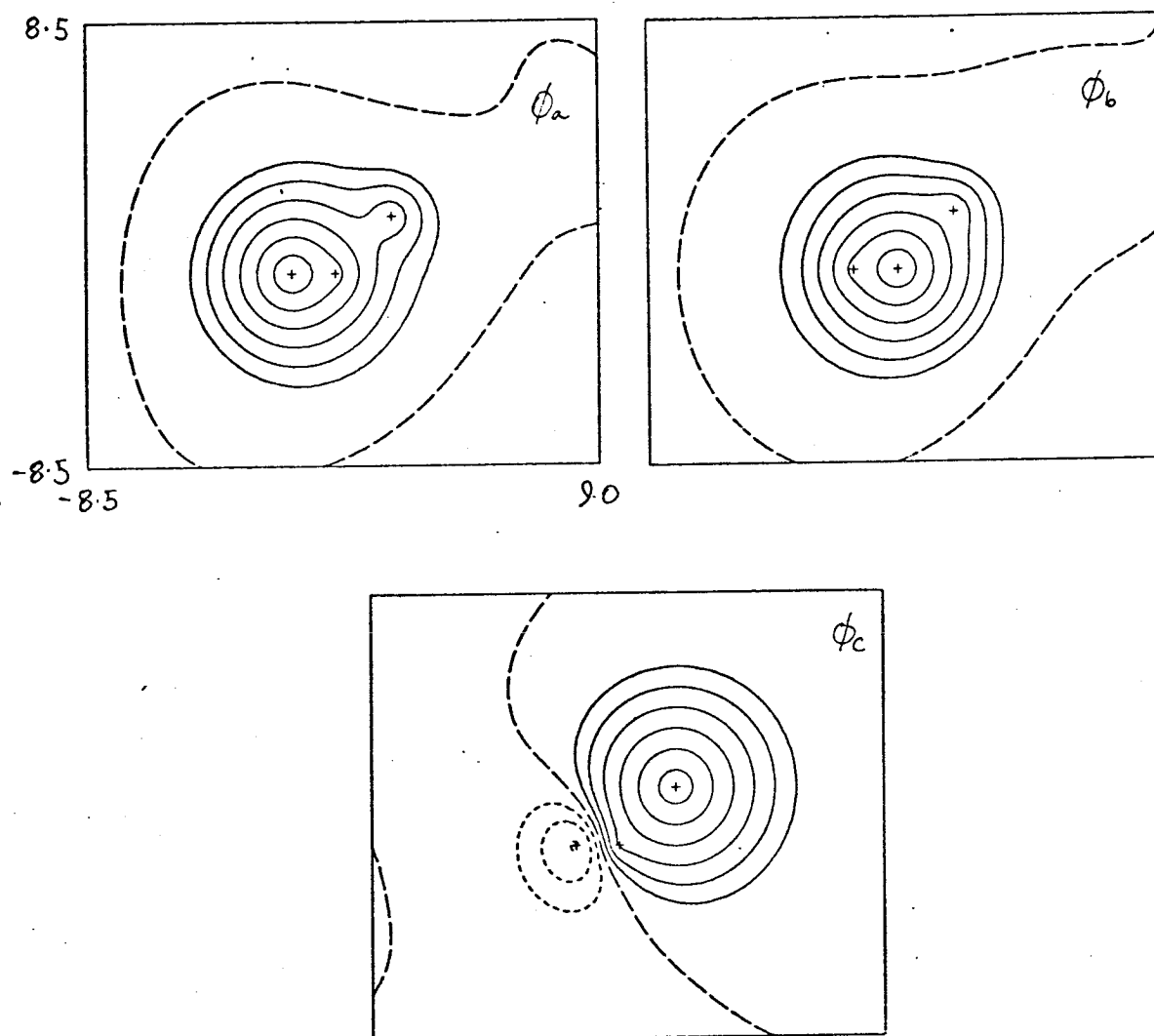*Geometry K*

Ground State — SOGI

Figure 35.

Geometry K - Ground State

G1

G1 - Natural Orbitals
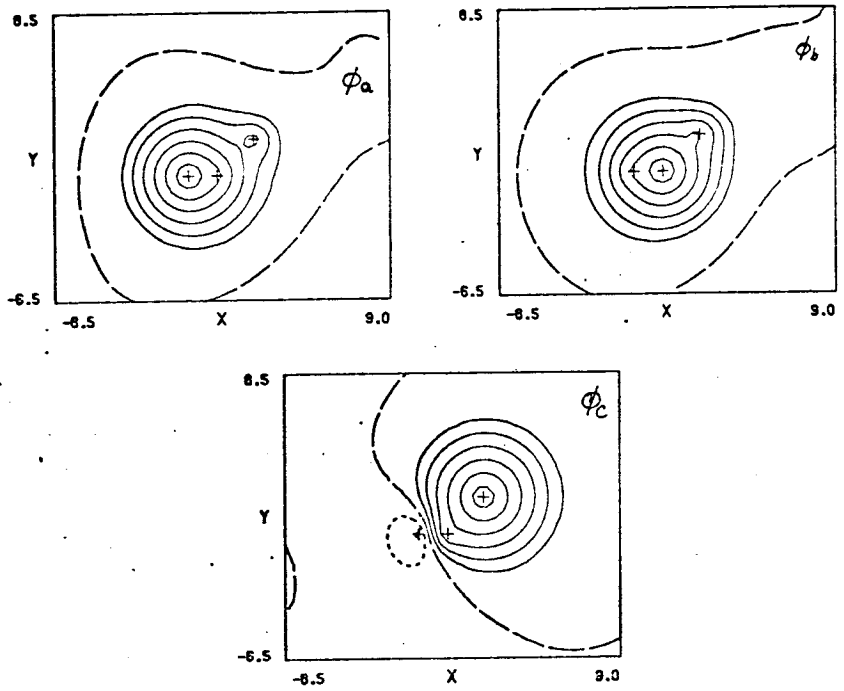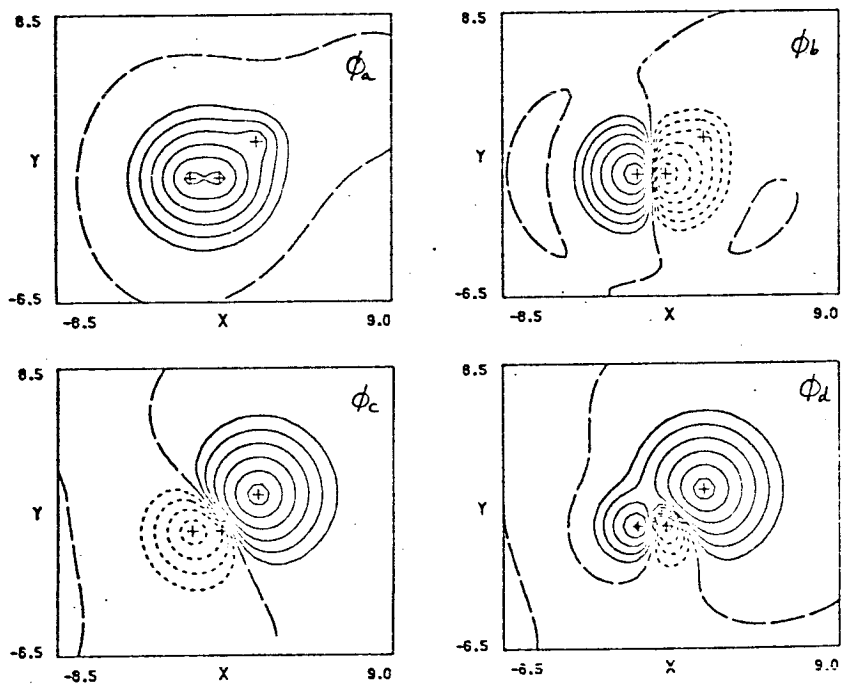

Figure 36.

Geometry K - Second State

SOGI

Figure 37.

Geometry K - Second State

G1

G1 - Natural Orbitals

Figure 38.

Geometry K   Third State

SOGI

Figure 39.

Geometry K — Third State

G1

G1- Natural Orbitals

Figure 40.

Geometry K

Fourth State - SOGI

Figure 41.

Geometry K - Fourth State

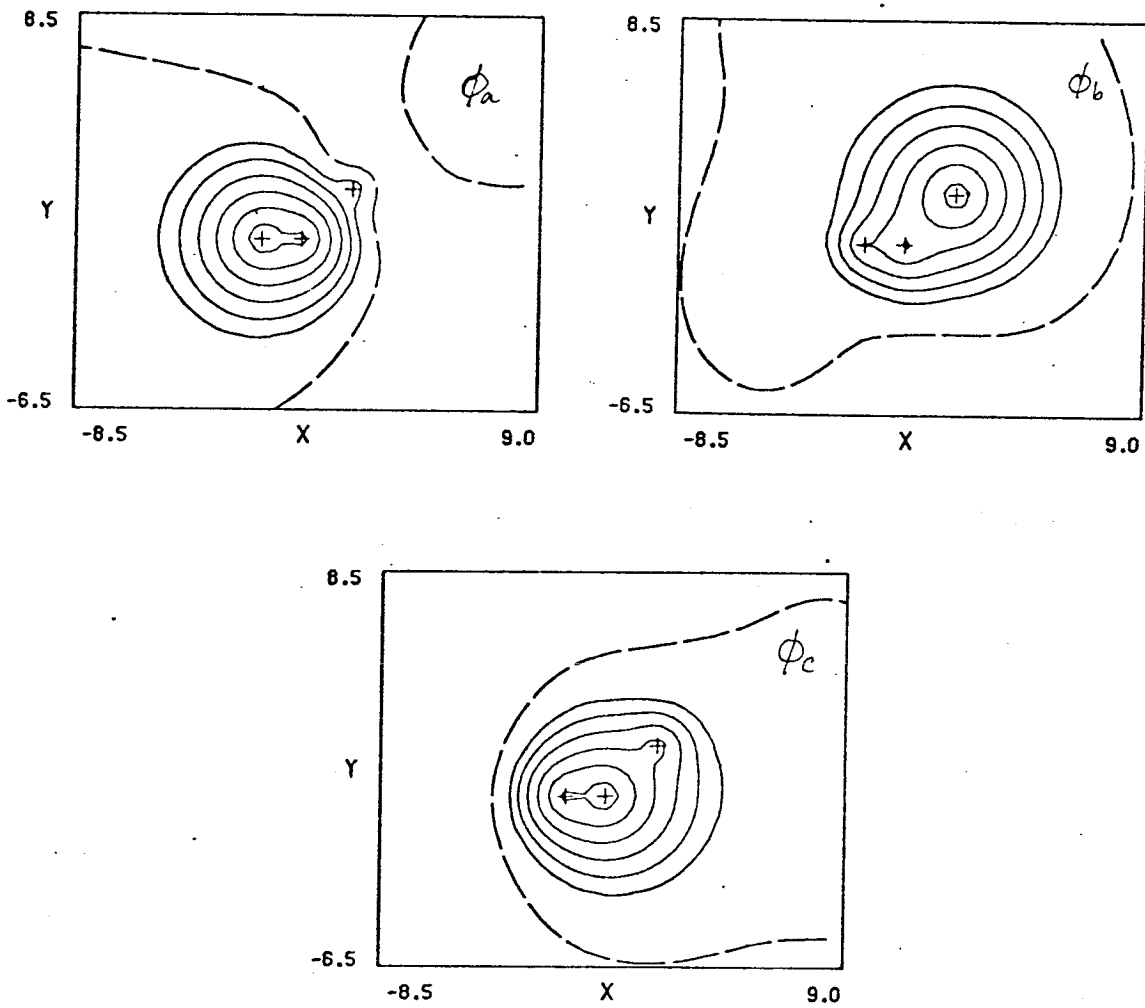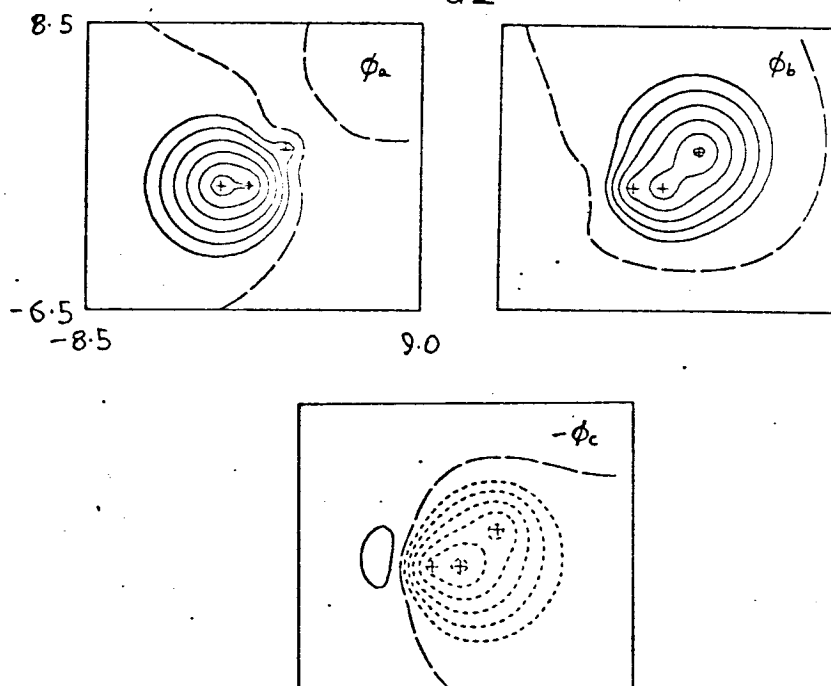$\mathcal{G}1$
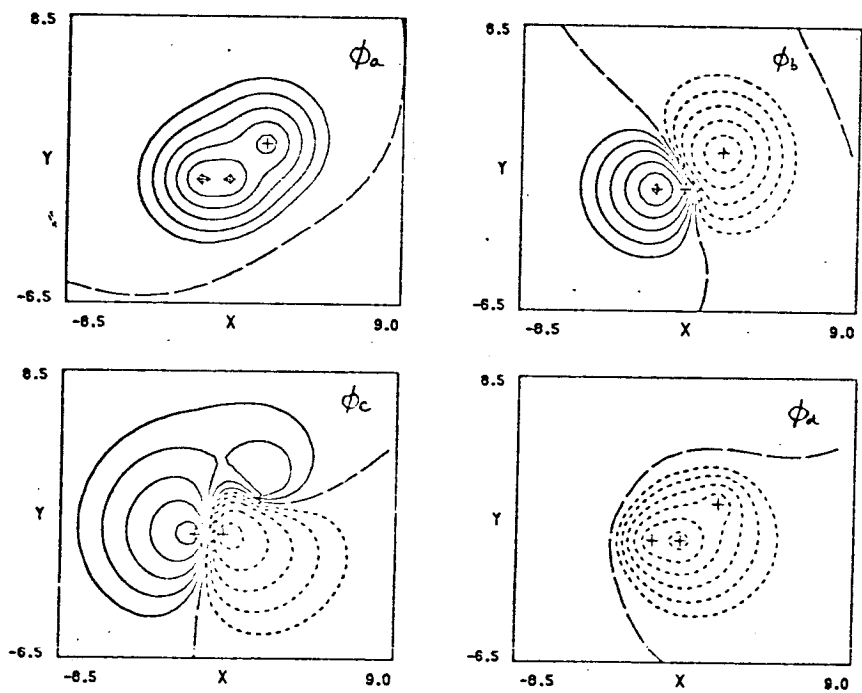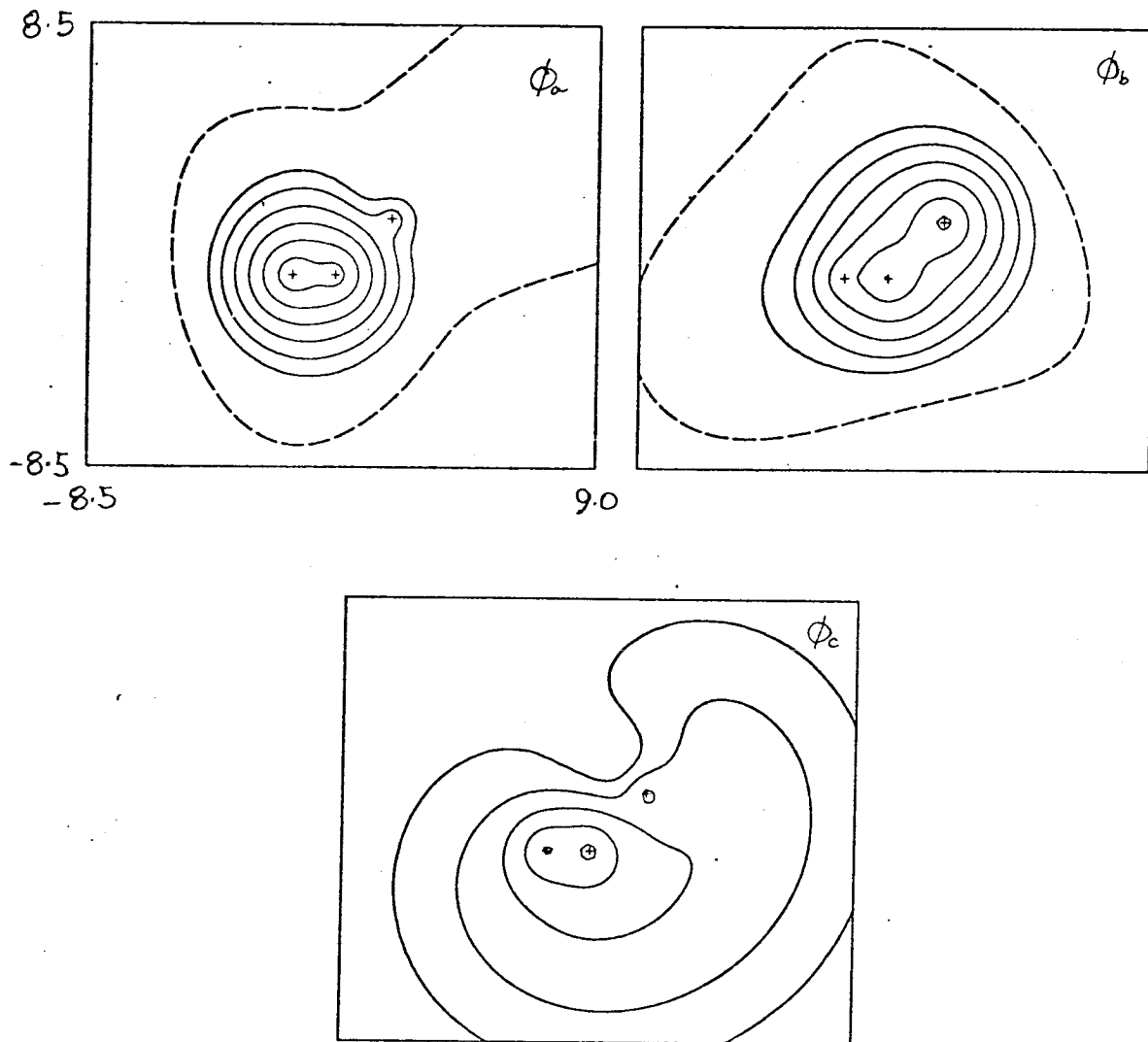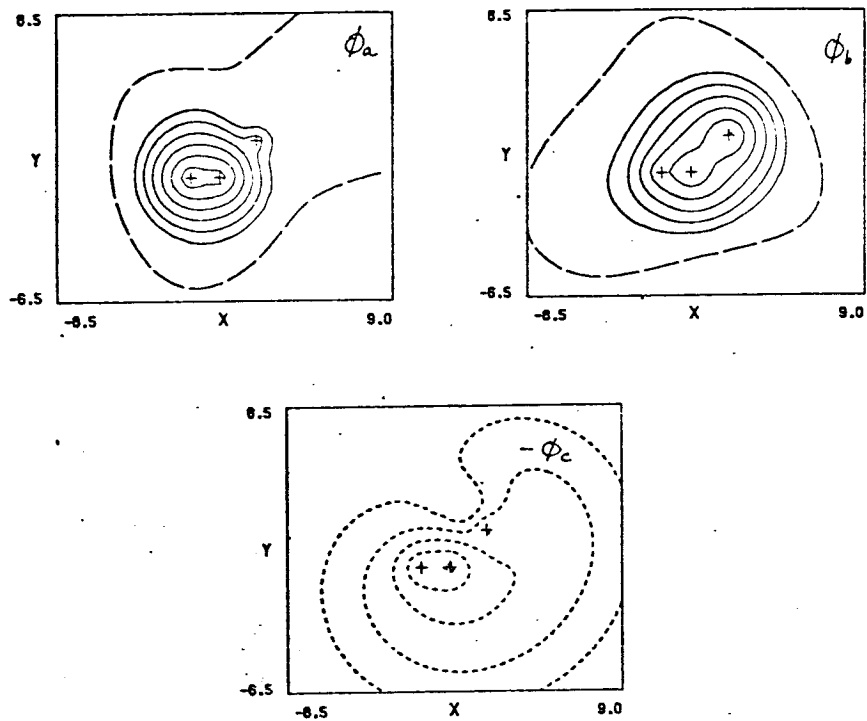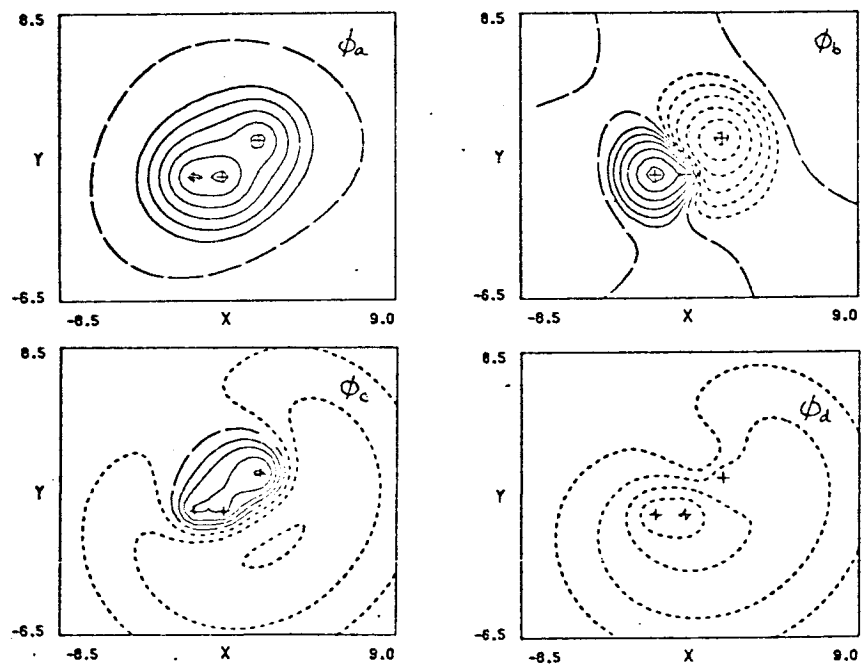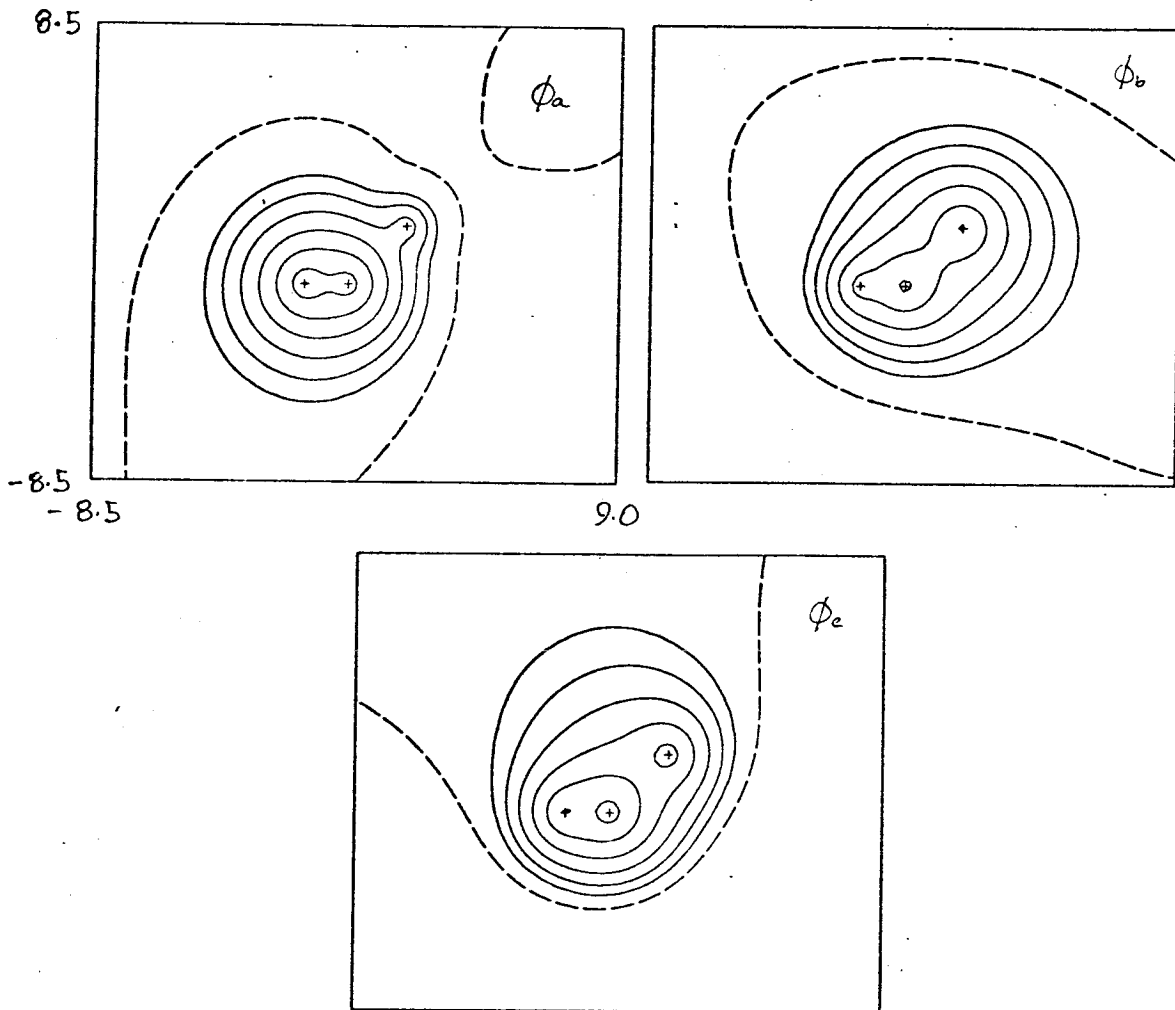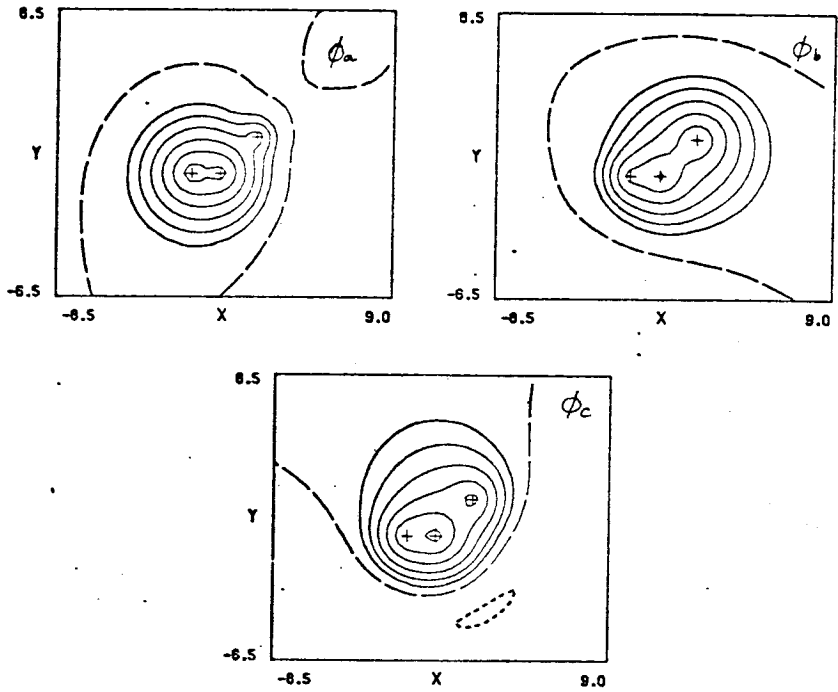

$\mathcal{G}1$ - Natural Orbitals
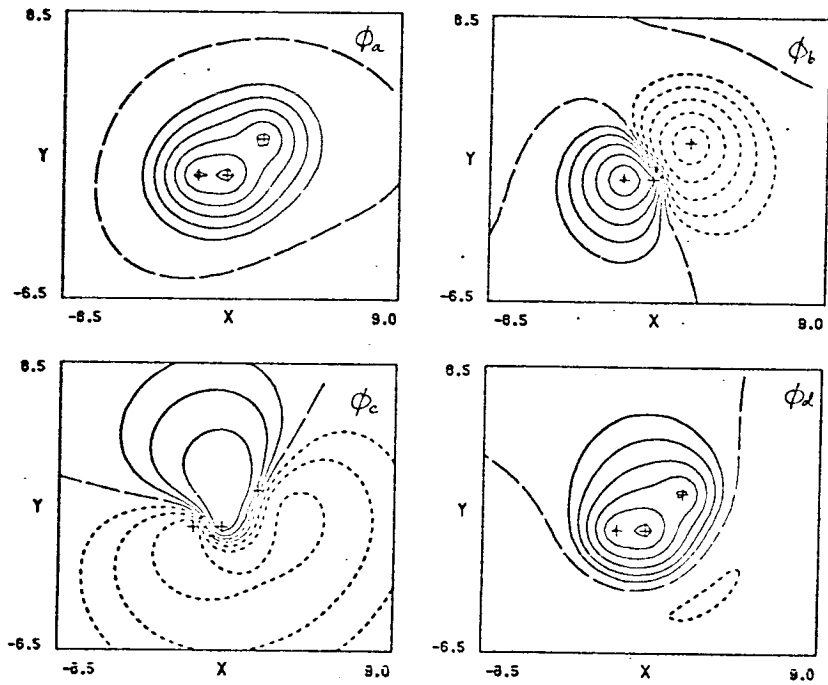
Figure 42.

Geometry K

Fifth State − SOGI
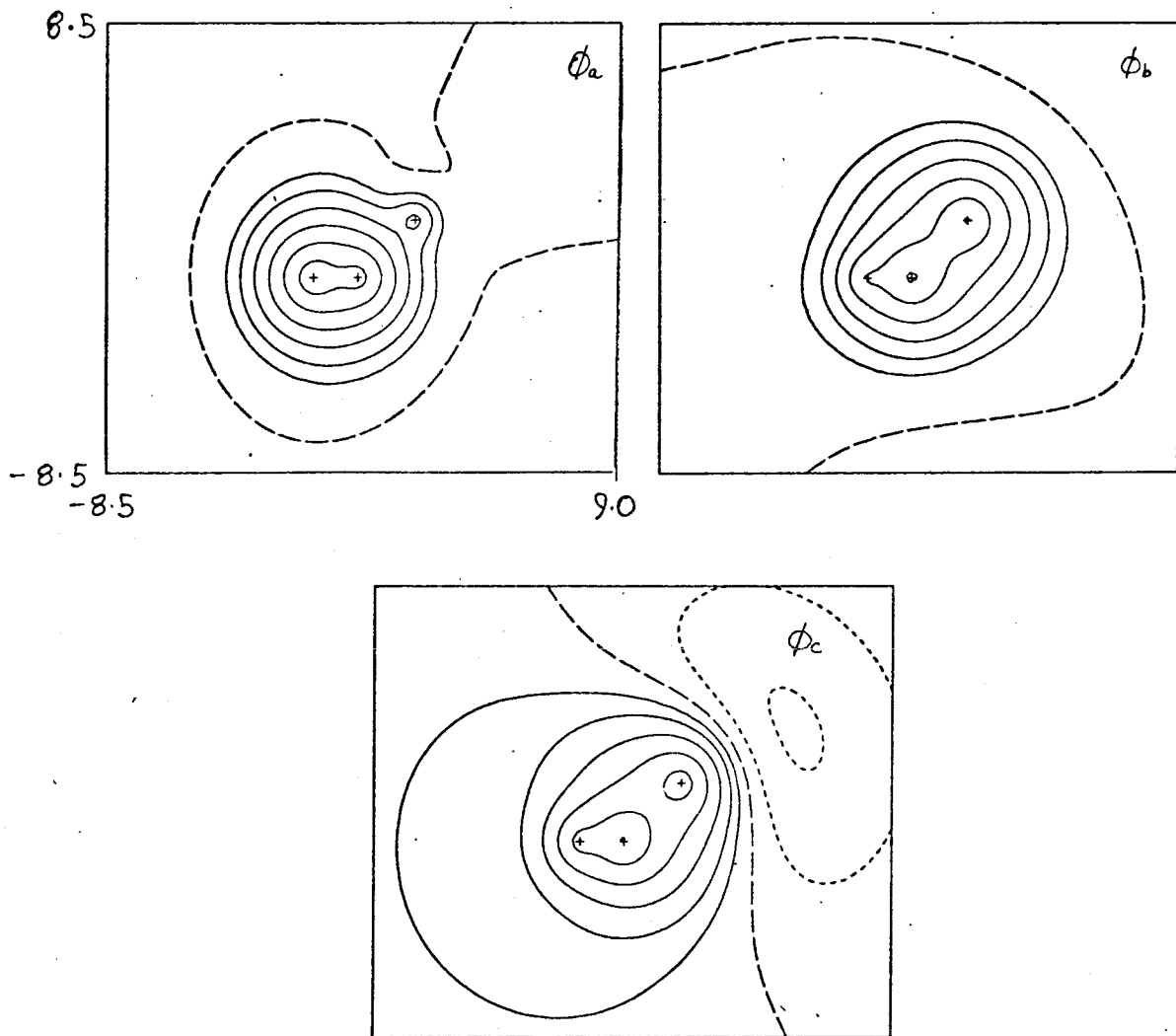
Figure 43.

Geometry K - Fifth State

G1
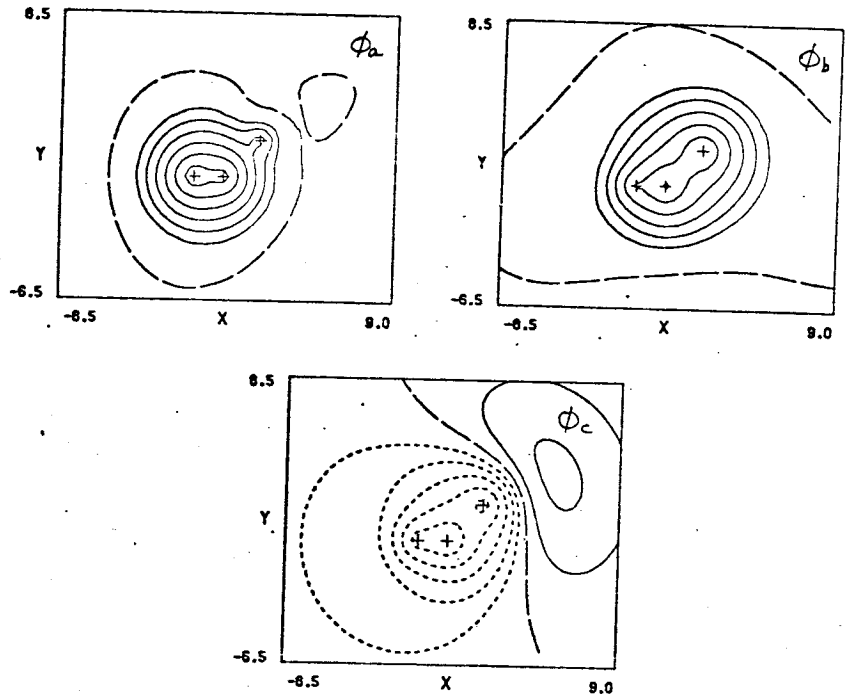
G1 - Natural Orbitals
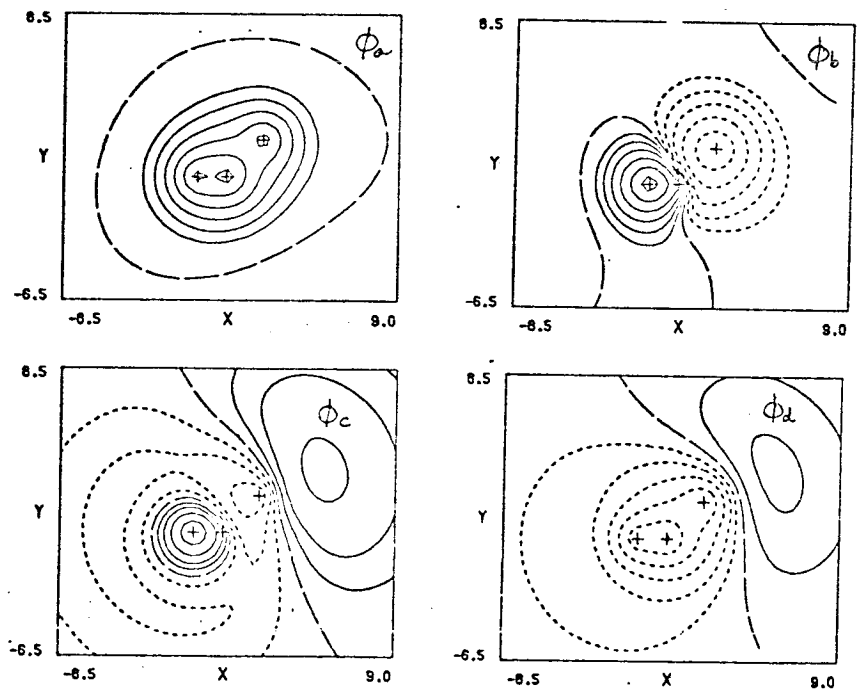
Figure 44.

G1 NATURAL ORBITAL $X_3 (\phi_c)$
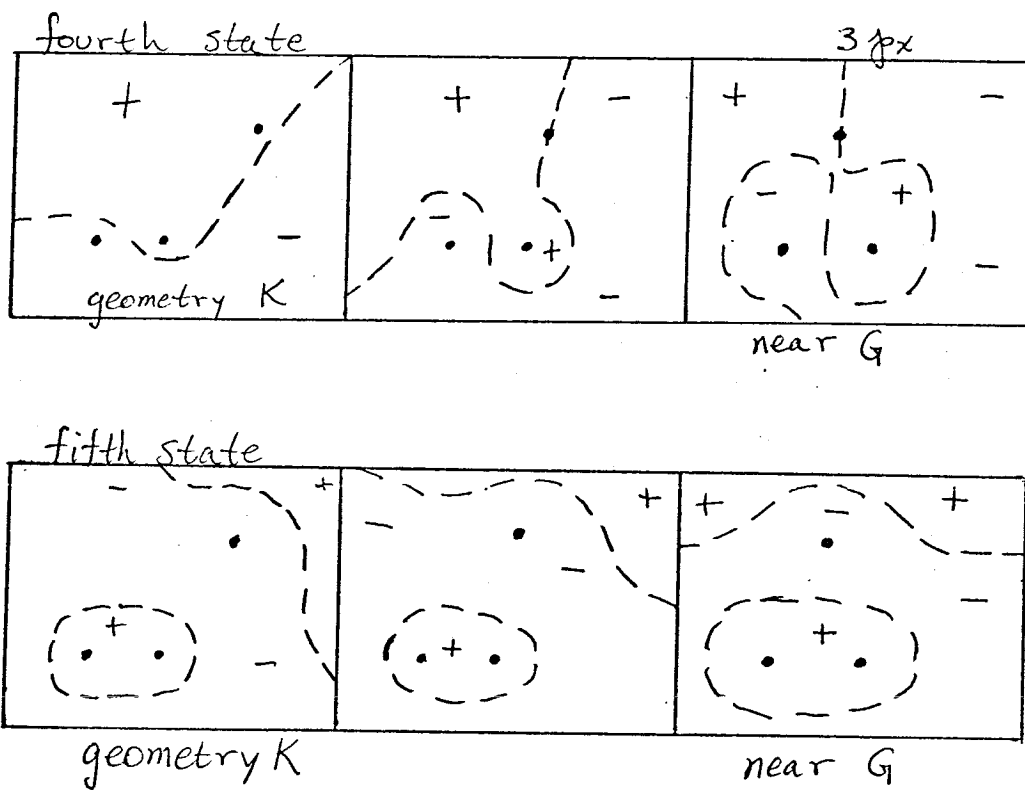
FIGURE 45

APPENDIX I: The SOGI Program

In the SOGI method we take our wavefunction as

$$\Psi = \sum_i C_i G_i^\gamma (\Phi\chi) , \qquad (1)$$

where the C_i's are numerical coefficients, the G_i^γ's are standard GI operators, Φ is a product of one-electron spatial functions, and χ is a product of one-electron spin functions (α or β). In the usual spin function one puts alternate α's and β's until he runs out of β's and then finishes with an unmitigated string of α's. The G_i^γ's are defined by

$$G_i^\gamma \equiv \sum_r \zeta_{\lambda_{ri}} O_{ri}^\gamma \omega_{\overline{r1}}^{\overline{\gamma}} . \qquad (2)$$

(Note that this definition differs from that in Chapter I in that $\omega_{\overline{r1}}^{\overline{\gamma}}$ is used rather than $\omega_{ri}^{\overline{\gamma}}$, which only changes the normalization.)

For a given set of orbitals, we want to find the optimum C_i's for (1). After finding the best C_i's, we find the best orbitals for those C_i's and alternate finding C_i's and orbitals until the process converges.

I. Orbital Variation

The approximate solution of the spatial GI equations has been approached in several ways. This Appendix will be concerned only with methods in which the unknown orbitals are expanded in terms of some known basis functions and the coefficients of the expansion are solved for iteratively. (As far as I know, no one has tried to solve the GI equations numerically.)

Historically, the first approach was to take the equation

$$H_k \phi_k = \epsilon_k \phi_k \qquad k = 1, NX$$

and to expand in terms of basis functions to give

$$H^k_{\nu\mu} C_{\mu k} = \epsilon_k S_{\nu\mu} C_{\nu k} \; .$$

The Hamiltonian matrices $(H^k_{\nu\mu})$ were evaluated with the trial function. After transforming to an orthogonal basis set, the Hamiltonians were diagonalized to give a new set of occupied and virtual orbitals and the orbital energies. This approach involved the formation and diagonalization of NX (number of electrons) different NBF by NBF matrices (NBF is the number of basis functions).

The problem with this method was that the new kth orbital was determined using the field due to the old NX - 1 other orbitals. Nothing was done to adjust ϕ_k for changes that were simultaneously being made in all the other ϕ's. This often led to oscillation that caused slow convergence or divergence.

A second approach was developed by Dick Blint and Bill Goddard in which the kinetic energy terms were evaluated using the new orbitals. Let $\bar{H}_k = H_k - T_k$, then

$$(T_k + \epsilon_k)\phi_k = \bar{H}_k \phi_k \; ,$$

which is valid for the self-consistent ϕ_k's. The iterative procedure here was to evaluate the right side with the trial function and then multiply by the inverse of $(T_k + \epsilon_k)$ to give a new ϕ_k. This approach was called the inhomogeneous method.

At first it was believed that this method had overcome the convergence problems of the homogeneous method, since SQCDIF's on the order of 10^{-8} were easily obtained even for systems that had diverged when treated by the homogeneous method. More careful investigation

on the part of Dick Blint revealed, however, that these wavefunctions had not actually converged but would continue to change slowly if the iterative procedure were continued. This problem is even more serious than divergence of the SCF scheme, since one would have to examine the wavefunction very closely after several different cycles of the SCF scheme to see if the wavefunction is changing in some systematic way pr oscillating or just bouncing about. This approach is not completely useless since it does generate fairly good approximations to the actual wavefunction beginning with even very crude guesses. As we shall see below, good initial guesses are necessary for the new approach that we have just developed.

A.   Derivation of the Supermatrix

For fixed C_i's in (1), it is advantageous to rewrite the energy as follows:

$$E = \frac{\langle \Psi | H | \Psi \rangle}{\langle \Psi | \Psi \rangle} \tag{3a}$$

$$= \frac{\langle \sum_i C_i G_i^{\gamma}(\Phi\chi) | H | \sum_j C_j G_j^{\gamma}(\Phi\chi) \rangle}{\langle \sum_r C_r G_r^{\gamma}(\Phi\chi) | \sum_s C_s G_s^{\gamma}(\Phi\chi) \rangle} \tag{3b}$$

$$= \frac{\langle \Phi\chi | H | \sum\limits_{irjs} C_i \zeta_{\lambda_{ri}} O^{\gamma}_{ir} \omega^{\overline{\gamma}}_{\overline{1r}} C_j \zeta_{\lambda_{sj}} O^{\gamma}_{sj} \omega^{\overline{\gamma}}_{\overline{s1}} (\Phi\chi) \rangle}{\text{(same stuff with } H = 1)} \qquad (3c)$$

$$= \frac{f^{\gamma} \langle \Phi\chi | H | (\sum\limits_{ij} \zeta_{\lambda_{ij}} C_i C_j O^{\gamma}_{ij}) \Phi \omega^{\gamma}_{\overline{11}} \chi \rangle}{\text{(same stuff with } H = 1)} \qquad \cdot \qquad (3d)$$

$$= \frac{\langle \Phi | H | (\sum\limits_{ij} \zeta_{\lambda_{ij}} C_i C_j O^{\gamma}_{ij}) \Phi \rangle}{\langle \Phi | \sum\limits_{ij} \zeta_{\lambda_{ij}} C_i C_j O^{\gamma}_{ij} \Phi \rangle} \qquad (3e)$$

$$\frac{\langle \Phi | H | O^C_{11} \Phi \rangle}{\langle \Phi | O^C_{11} \Phi \rangle} \quad , \qquad (3f)$$

where we define $O^C_{11} \equiv \sum\limits_{ij} \zeta_{\lambda_{ij}} C_i C_j O^{\gamma}_{ij}$.

Now to find a better set of orbitals we write each orbital ϕ_i in Φ as $\phi_i = \phi^0_i + \delta\phi_i$, where the ϕ^0_i's are the trial functions. By substituting the ϕ_i into the energy expression, we develop equations for the δ's. We can rewrite (3f) as

$$E = \frac{N_0 + N_1 + N_2 + O(\delta^3)}{F_0 + F_1 + F_2 + O(\delta^3)} \qquad (4)$$

where

$$N_0 = \langle \Phi^0 | H | O^C_{11} \Phi^0 \rangle \qquad (5)$$

$$N_1 = \sum\limits_j \{ \langle \Phi'_j \delta\phi_j | H | O^C_{11} \Phi^0 \rangle + \langle \Phi^0 | H | O^L_{11} \Phi'_j \delta\phi_j \rangle \} \qquad (6)$$

$$N_2 = \sum\limits_{i<j} \{ \langle \Phi''_{ij} \delta\phi_i \delta\phi_j | H | O^C_{11} \Phi^0 \rangle + \langle \Phi^0 | H | O^C_{11} \Phi''_{ij} \delta\phi_i \delta\phi_j \rangle \}$$

$$+ \sum\limits_{i,j} \langle \Phi'_i \delta\phi_i | H | O^C_{11} \Phi'_j \delta\phi_j \rangle \qquad (7)$$

and the F's are of the same form with $H = 1$, $\Phi^0 = \phi_1^0 \phi_2^0 \cdots \phi_N^0$ is the trial function, $\Phi_k' \delta \phi_k$ is Φ^0 with ϕ_k^0 replaced by $\delta \phi_k$, and $\Phi_{k\ell}'' \delta \phi_k \delta \phi_\ell$ is Φ^0 with ϕ_k^0 replaced by $\delta \phi_k$ and ϕ_ℓ^0 replaced by $\delta \phi_\ell$. Write

$$F_0 + F_1 + F_2 = F_0 (1 + \frac{F_1}{F_0} + \frac{F_2}{F_0}) \tag{8}$$

or

$$\frac{1}{F_0 + F_1 + F_2} = \frac{1}{F_0} [1 - \frac{F_1}{F_0} - \frac{F_2}{F_0} + (\frac{F_1}{F_0})^2 + O(\delta^3)] . \tag{9}$$

Now E in (4) becomes

$$E \cong \frac{N_0 + N_1 + N_2}{F_0} [1 - \frac{F_1}{F_0} - \frac{F_2}{F_0} + (\frac{F_1}{F_0})^2] . \tag{10}$$

Let $E^0 = N_0 / F_0$, then

$$E \approx [F_0 E^0 + N_1 + N_2 - E^0 F_1 - E^0 F_2 + \frac{E^0 F_1^2}{F_0} - \frac{N_1 F_1}{F_0} + O(\delta^3)]/F_0 \tag{11}$$

or dropping things of $O(\delta^3)$

$$F_0 (E - E^0) = (N_1 - E^0 F_1) + (N_2 - E^0 F_2) - \frac{(N_1 - E^0 F_1) F_1}{F_0} . \tag{12}$$

At convergence, $E = E^0$ so we set the left side of (12) to zero and solve for the δ's.

Let $\hat{O}_p = (H - E^0) O_{11}^C$, then

$$(1 - \frac{F_1}{F_0}) \sum_j \{ \langle \Phi_j' \delta \phi_j | \hat{O}_p | \Phi^0 \rangle + \langle \Phi^0 | \hat{O}_p | \Phi_j' \delta \phi_j \rangle \}$$

$$+ \sum_{i<j} \{ \langle \Phi_{ij}'' \delta \phi_i \delta \phi_j | \hat{O}_p | \Phi^0 \rangle + \langle \Phi^0 | \hat{O}_p | \Phi_{ij}'' \delta \phi_i \delta \phi_k \rangle \}$$

$$+ \sum_{i,j} \{ \langle \Phi_i' \delta \phi_i | \hat{O}_p | \Phi_j' \delta \phi_j \rangle \} = 0 \tag{13}$$

If we assume the orbitals are real, this becomes

$$2\sum_{j}\langle \Phi'_j \delta\phi_j | O_p | \Phi^0 \rangle + 2\sum_{j>i}\langle \Phi''_{ij} \delta\phi_i \delta\phi_j | O_p | \Phi^0 \rangle + \sum_{i,j}\langle \Phi'_i \delta\phi_i | O_p | \Phi'_j \delta\phi_j \rangle$$

$$-\frac{4}{F_0}\sum_{i,j}\{\langle \Phi'_i \delta\phi_i | O_{11}^C \Phi^0 \rangle \langle \Phi'_j \delta\phi_j | O_p | \Phi^0 \rangle\} = 0 \ . \tag{14}$$

Collecting factors of $\delta\phi_k$ we obtain

$$\sum_{k}\left\{2\langle \Phi'_k \delta\phi_k | O_p | \Phi^0 \rangle + 2\sum_{i\neq k}\langle \Phi''_{ki} \delta\phi_k \delta\phi_i | O_p | \Phi^0 \rangle \right.$$

$$+ 2\sum_{i}\langle \Phi'_i \delta\phi_k | O_p | \Phi'_i \delta\phi_i \rangle$$

$$-\frac{4}{F_0}\sum_{i}\{\langle \Phi'_k \delta\phi_k | O_{11}^C \Phi^0 \rangle \langle \Phi'_i \delta\phi_i | O_p | \Phi^0 \rangle$$

$$\left. + \langle \Phi'_i \delta\phi_i | O_{11}^C \Phi^0 \rangle \langle \Phi'_k \delta\phi_k | O_p | \Phi^0 \rangle\}\right\} = 0 \ . \tag{15}$$

Now expand ϕ_k^0 and $\delta\phi_k$ in a basis set,

$$\phi_k^0 = \sum_{\nu=1}^{NBF} \chi_\nu C_{\nu k} \tag{16a}$$

$$\delta\phi_k = \sum_{\nu=1}^{NBF} \chi_\nu \Delta_{\nu k} \tag{16b}$$

Let Φ_k^ν be Φ^0 with ϕ_k^0 replaced by χ_ν, and $\Phi_{k\ell}^{\mu\nu}$ be Φ^0 with ϕ_k^0 replaced by χ_μ and ϕ_ℓ^0 replaced by χ_ν.

Define

$$Q_{\mu k} = -\langle \Phi_k^\mu | O_p | \Phi^0 \rangle \tag{17a}$$

and

$$B_{\mu k, \nu\ell} = \langle \Phi_{k\ell}^{\mu\nu} | O_p | \Phi^0 \rangle (1 - \delta_{k\ell}) + \langle \Phi_k^\mu | O_p | \Phi_\ell^\nu \rangle$$

$$-\frac{2}{F_0}\langle \Phi_k^\mu | O_{11}^C \Phi^0 \rangle \langle \Phi_\ell^\nu | O_p | \Phi^0 \rangle - \frac{2}{F_0}\langle \Phi_k^\mu | O_p | \Phi^0 \rangle \langle \Phi_\ell^\nu | O_{11}^C \Phi^0 \rangle \ . \tag{17b}$$

The (15) becomes

$$\sum_{\mu k}\Delta_{\mu k}\{\sum_{\nu\ell}B_{\mu k, \nu\ell}\Delta_{\nu\ell}\} = \sum_{\mu k}\Delta_{\mu k}Q_{\mu k} \tag{18}$$

but the equality must be true for each $\Delta_{\mu k}$ independently, so we have

$$\sum_{\nu \ell} B_{\mu k, \nu \ell} \Delta_{\nu \ell} = Q_{\mu k} \quad \text{for all } \mu, k. \tag{19}$$

$\underset{\sim}{B}$ is called the supermatrix.

B. Application to Basis Set Expansion

Now to expand $Q_{\mu k}$ and $B_{\mu k, \nu \ell}$ in terms of molecular integrals. Latin letters will be used for orbitals and Greek letters for basis functions.

Define

$$V_{12} = \frac{1}{r_{12}} + \frac{h_1 + h_2}{(NX - 1)} \quad , \tag{20}$$

where $h_i = -\frac{1}{2} \nabla_i^2 + V_{nuclear(i)}$. We then need only the quantities

$$AMAM(\mu j \,|\, \nu k) = \int \chi_\mu(1) \chi_\nu(2) V_{12} \phi_j^0(1) \phi_k^{\mathbf{0}}(2) d\tau_1 d\tau_2 \tag{21}$$

$$AAMM(\mu \nu \,|\, jk) = \int \chi_\mu(1) \phi_j^0(2) V_{12} \chi_\nu(1) \phi_k^0(2) d\tau_1 d\tau_2 \tag{22}$$

$$AMMM(\mu n \,|\, jk) = \int \chi_\mu(1) \phi_j^0(2) V_{12} \phi_n^0(1) \phi_k^0(2) d\tau_1 d\tau_2 \tag{23}$$

$$XMMM(mn \,|\, jk) = \int \phi_m^0(1) \phi_j^0(2) V_{12} \phi_n^0(1) \phi_k^0(2) d\tau_1 d\tau_2 \quad . \tag{24}$$

The D matrices are defined in Chapter I and their indexing is discussed in Sec. D.

First we define

$$R_{\mu k} = \sum_{b \neq k} \sum_c \sum_{d \neq c} \{ AMMM(\mu c \,|\, bd) D_{cd}^{kb}$$

$$+ \sum_{a < b} \sum_{f \neq c} XMMM(af \,|\, bd) S_{\mu c} D_{cfd}^{kab} \} \quad . \tag{25}$$

where $S_{\eta k} = \int \chi_\eta(1) \phi_k(1) d\tau_1$. Now E^0 becomes

$$E^0 = (\sum_\mu R_{\mu 1} \varsigma_{\mu 1})/F_0 \tag{26}$$

and

$$Q_{\mu k} = -(R_{\mu k} - \sum_c E^0 S_{\mu c} D_c^k) . \tag{27}$$

$\underset{\sim}{B}$ was defined in (17b); we will expand each term separately.

1. $$\langle \Phi_k^\mu | O_p | \Phi_\ell^\nu \rangle = -E^0 S_{\mu\nu} D_\ell^k + \sum_{a \neq k} \sum_{s \neq \ell} \{ [AAMM(\mu\nu|as) D_{\ell s}^{ka}$$

$$+ (AMAM(\mu s|\nu a) - E^0 S_{\mu s} S_{\nu a}) D_{s\ell}^{ka}]$$

$$+ \sum_{\substack{b \neq a \ t \neq s \\ b \neq k \ t \neq \ell}} [(AMMM(\mu s|bt) S_{\nu a} + AMMM(\nu a|bt) S_{\mu s}) D_{s\ell t}^{kab}$$

$$+ \sum_{\substack{c < b \ u \neq t \\ c \neq a \ u \neq s \\ c \neq k \ u \neq \ell}} XMMM(bt|cu) S_{\nu a} S_{\mu s} D_{s\ell tu}^{kabc}] \} \tag{28}$$

where $S_{\eta\nu} = \int \chi_\eta(1) \chi_\nu(1) d\tau_1$.

2. (for $k \neq \ell$)

$$\langle \Phi_{k\ell}^{\mu\nu} | O_p | \Phi^0 \rangle = \sum_s \sum_{a \neq s} \{ AMAM(\mu s|\nu a) - E^0 S_{\mu s} S_{\nu a}) D_{sa}^{k\ell}$$

$$+ \sum_{\substack{b \neq k \ t \neq s \\ b \neq \ell \ t \neq a}} [(AMMM(\mu s|bt) S_{\nu a} + AMMM(\nu a|bt) S_{\mu s}) D_{sat}^{k\ell b}$$

$$+ \sum_{\substack{c > b \ u \neq s \\ c \neq k \ u \neq a \\ c \neq \ell \ u \neq t}} XMMM(bt|cu) S_{\mu s} S_{\nu a} D_{satu}^{k\ell bc}] \} . \tag{29}$$

3. $$\langle \Phi_k^\mu | O_{11}^C \Phi^0 \rangle \langle \Phi_\ell^\nu | O_p | \Phi^0 \rangle = (\sum_i S_{\mu k} D_k^i) R_{\nu\ell} . \tag{30}$$

C. Indexing of Molecular Integrals

There is symmetry in the indices of the quantities AAMM, AMAM, AMMM, and XMMM that is used to reduce the number of integrals to be calculated or stored. Here is how they are addressed.

1. AAMM's

$$AAMM(\mu\nu|k\ell) = AAMM(\nu\mu|k\ell)$$
$$= AAMM(\mu\nu|\ell k) = AAMM(\nu\mu|\ell k) .$$

Thus we can order both (ν, μ) and (k, ℓ). Let i be the larger of k and ℓ and j be the smaller, then the $k\ell$-pair number is $i(i-1)/2+j$; similarly for μ and ν. For convenience, define the function PN

$$PN(n_1, n_2) = \begin{cases} \dfrac{n_1(n_1-1)}{2} + n_2 & \text{if } n_1 \geqslant n_2 \\[3mm] \dfrac{n_2(n_2-1)}{2} + n_1 & \text{if } n_1 < n_2 \end{cases} \tag{32}$$

The AAMM's are stored in a linear array; the index of $AAMM(\mu\nu|k\ell)$ is I_{AAMM}

$$I_{AAMM} = [PN(\mu, \nu) - 1][\frac{NX(NX+1)}{2}] + PN(k, \ell),$$

where NX is the number of electrons.

2. AMAM's

$AMAM(\mu k|\nu\ell) = AMAM(\nu\ell|\mu k)$, thus we can order μ and ν but not k and ℓ. The index is I_{AMAM}

$$I_{AMAM} = [PN(\mu, \nu) - 1]NX^2 + (j-1)*NX + i ,$$

where $j = k$ and $i = \ell$ if $\mu \geqslant \nu$

but $j = \ell$ and $i = k$ if $\mu < \nu$.

3. AMMM's

$$\text{AMMM}(\mu m \mid np) = \text{AMMM}(\mu m \mid pn):$$

$$I_{\text{AMMM}} = (\mu - 1)(NX^3 + NX^2)/2 + (m - 1)(NX^2 + NX)/2 + PN(n, p).$$

4. XMMM's

$$\text{XMMM}(mn \mid pq) = \text{XMMM}(nm \mid pq) = \text{XMMM}(nm \mid qp)$$

$$I_{\text{XMMM}} = [PN(m, n) - 1](NX^2 + NX)/2 + PN(p, q).$$

All the quantities AAMM, AMAM, AMMM, and XMMM are produced by an efficient transformation program written by David Huestis.

D. Indexing of D-Matrices

The quantity

$$D_{\mu\nu}{}^{i_1, i_2, \cdots i_n}_{j_1, j_2, \cdots j_n} \tag{33}$$

is defined as the coefficient of

$$\phi_{i_1}^*(i_1)\phi_{i_2}^*(i_2)\cdots\phi_{i_n}^*(i_n)\phi_{j_1}(i_1)\phi_{j_2}(i_2)\cdots\phi_{j_n}(i_n) \tag{34}$$

in the integral

$$\int \Phi^* O_{\mu\nu}\Phi\, dx'_{i_1 \ i_2 \cdots \ i_n}\ , \tag{35}$$

where $\Phi = \phi_1(1)\phi_2(2)\cdots\phi_N(N)$, $\int \cdots dx'_{i_1 i_2 i_3 \cdots i_n}$ indicates that the integration extends over all coordinates except $i_1, i_2 \cdots i_n$, and N is the number of electrons. Efficient handling of these quantities is essential in doing SOGI calculations since the ——————————————————|

matrix-SOGI equations contain explicit reference to $D_{\mu\nu a}{}^i$ (called D-ones), $D_{\mu\nu ab}{}^{ij}$ (called D-twos), $D_{\mu\nu abc}{}^{ijk}$ (called D-threes), and $D_{\mu\nu abcd}{}^{ijk\ell}$ (called D-fours). These in turn depend implicitly on the higher D's through the relationship,

$$D_{\mu\nu}{}^{i_1, i_2, \cdots i_n}_{j_1, j_2, \cdots j_n} = \sum_{a \neq j_1, j_2 \cdots j_n} D_{\mu\nu}{}^{i_1, i_2, \cdots i_n, k}_{j_1, j_2, \cdots j_n, a} S_{ka}\ , \tag{36}$$

where k is any index ($k \leq N$, the number of electrons) not already used in the set ($i_1, i_2, \cdots i_n$) and S_{ka} is the overlap of orbitals k and a ($S_{ka} = \int \phi_k^*(1)\phi_a(1)\, dx_1$).

If n is the number of electrons, then we haven't integrated over any coordinate in (35) and the resulting D's (called D-N's) are just the coefficients of the different orbital products, $\phi_1^*(1)\phi_2^*(2)\cdots\phi_N^*(N)\phi_{j_1}(1)\phi_{j_2}(2)\cdots\phi_{j_N}(N)$ in the expression $\Phi^* O_{\mu\nu}\Phi$. Since $O_{\mu\nu} = \sum_\tau U_{\mu\nu}(\tau)\tau$, the D-N's

$(D_{\mu\nu}{}^{i_1,i_2\cdots i_N}_{j_1,j_2\cdots j_N})$ are just the $U_{\mu\nu}(\tau)$ matrices where τ is the permutation

which takes i_1 into j_1, i_2 into j_2, etc. Only the correspondence of i's and

j's matters, so we will rearrange the i's to be $1, 2, \cdots N$, which puts the

j's in the order where j_k is in the i_kth position. Since the i's (superscripts)

are always the set $(1, 2, \cdots N)$, we can ignore them and designate only the

subscripts (j's). The D-N's can be ordered by taking the set of j's as an

N digit number with radix N. Consider the case of four electrons. The

permutations of $1, 2, 3, 4$, in ascending order are

Index	Permuted Set	τ (in cycle notation) $\ni \tau[1234]$ = Permuted set
1	1234	ϵ
2	1243	(34)
3	1324	(23)
4	1342	(234)
5	1423	(243)
6	1432	(24)
7	2134	(12)
8	2143	(12)(34)
9	2314	(123)
10	2341	(1234)
11	2413	(1243)
12	2431	(124)
13	3124	(132)
14	3142	(1342)
15	3214	(13)
16	3241	(134)
17	3412	(13)(24)
18	3421	(1324)
19	4123	(1432)
20	4132	(142)
21	4213	(143)

22	4231	(14)
23	4312	(1423)
24	4321	(14)(23)

Suppose we want $D_{\mu\nu}{}^{1342}_{2143}$. First we put the superscripts in proper order $D_{\mu\nu}{}^{1342}_{2143} \equiv D_{\mu\nu}{}^{1234}_{2314}$. By inspecting the table, we see that 2314 is the ninth entry. The next problem is to find an algorithm for <u>calculating</u> the index rather than finding it by searching a table.

Using the subscripts as an N-digit number with radix N was adequate for ordering the permutations but this gives an index N^N which grows much more rapidly than N! This would leave us with a few numbers scattered through core and all the remaining space empty and wasted.

Notice that the entries in column two naturally break up into four blocks of six; the elements of each block all have the same first number. Further note that each block can be broken into three sub-blocks, each sub-block having a common second index. We can calculate the beginning of each block by the formula $I_1 = (j_1 \cdot 1) * 6 + 1$ (I_1 ranges from 1 to 19 by sixes). Calculating the position within a block, however, is complicated by the fact that the remaining three ——————————————— | indices are not generally adjacent; e.g., the last three indices in the 3-block are 1, 2, and 4 in some order, since 3 has already appeared. The permutations of the symbols 1, 2, and 4, however, are isomorphous with the permutations of 1, 2, and 3; all we need do is replace 4 everywhere by 3. Similarly, the last three indices of the 1-block can be converted to permutations of 1, 2, 3 by subtracting 1 from each index; in the 2-block we replace 3 by 2 and 4 by 3. The 4-block already has the desired form.

Now we can easily calculate the beginning of each sub-block by the formula $I_2 = 2 * (j_2' - 1)$ where $j_2' = j_2$ if $j_2 < j_1$ but $j_2' = (j_2 - 1)$ if $j_2 > j_1$ (I_2 ranges from 0 to 4 by twos). Similarly, we compute $I_3 = (j_3'' - 1)$ where $j_3' = j_3$ if $j_3 < j_1$ but $j_3' = (j_3 - 1)$ if $j_3 > j_1$; then $j_3'' = j_3'$ if $j_3' < j_2'$ but $j_3'' = (j_3' - 1)$ if $j_3' > j_2'$ (I_3 is either 0 or 1). Now the total index is $I_1 + I_2 + I_3$. Notice that j_4 never entered the calculation; this is as it should be, j_4 carries no information since its value can be inferred from the values of j_1, j_2, and j_3.

Thus we have the following algorithm (due to E. Kent Gordon) for N electrons.

1. Set $j_k' = j_k$ for $k = 1$ to $(N-1)$

2. Set $\ell = 1$

3. Set $j_k' = (j_k' - 1)$ if $j_k' > j_\ell'$ for $k = (\ell + 1)$ up to $(N-1)$

4. Set ℓ to $\ell + 1$

5. Go back to (3) if $\ell < (N-2)$

6. INDEX $= (j_1' - 1)(N-1)! + (j_2' - 1)(N-2)! + (j_3' - 1)(N-3)! + \cdots + j_{N-1}'$
    INDEX runs from 1 to N!

The index j_i' is the ordinal number of the subscript that does occur in the ith position, counting only the possible subscripts that can occur at that position, given the values of the preceding subscripts. For example, in the permutation 136524, $j_3' = 4$ because 6 is the fourth possible subscript in position 3, given that $j_1 = 1$ and $j_2 = 3$; $j_5' = 1$ because 2 is the first possible subscript in that location, given the previous subscripts. This finishes the case of the D-N's.

Now consider the case where $n < N$. We can no longer assume that the superscripts form the set $(1 2 3 \cdots N)$ since some of the numbers are missing. We can, however, take the superscripts as ordered. For each set of superscripts, we can pick the subscripts without any restrictions

except that no two can be equal. If we group all the D's with common superscript together, we obtain NB blocks of NE elements. NB is the number of ordered sets of n numbers that can be selected from the set $(1, 2, \cdots N)$.

$$NB = \overbrace{\frac{N*(N-1)*(N-2)\cdots(N-(n-1))}{n!}}^{n \text{ factors}} = \frac{N!}{(n!)(N-n)!} = C\binom{N}{n}.$$

NE is the number of ways we can select n numbers from $(1, 2, 3, \cdots N)$ without respect to order

$$NE = N*(N-1)*\cdots\cdots(N-(n-1)) = \frac{N!}{(N-n)!}$$

Thus the total number of D-n's is $\left(\frac{N!}{(N-n)!}\right)^2 \frac{1}{n!}$.

Since the possible set of subscripts does not depend on the superscripts, we will split the indexing into two parts and compute a block index from the superscripts and an index within the block from the subscripts. It seems convenient to have the block index formula depend only on n and not on N. This is done by grouping sets first by their largest index; each set with a common largest index is broken into subgroups based on second largest index, and so on. As an example, consider the D-3 super-scripts for six electrons. The order is

1	123	11	126
2	124	12	136
3	134	13	236
4	234	14	146
5	125	15	246
6	135	16	346
7	235	17	156
8	145	18	256
9	245	19	356
10	345	20	456

The superscript index function for D-3's is

$$I_{D_3}^{SUP} = (i_3 - 1)(i_3 - 2)(i_3 - 3)/6 + (i_2 - 1)(i_2 - 2)/2 + i_1 \ ,$$

and for D_4's the superscript index function is

$$I_{D_3}^{SUP} = I_{D_3}^{SUP} + (i_4 - 1)(i_4 - 2)(i_4 - 3)(i_4 - 4)/24.$$

For D_n's the superscript index function is

$$I_{D_n}^{SUP} = I_{D_{(n-1)}}^{SUP} + \frac{(i_n - 1)(i_n - 2) \cdots (i_n - n)}{n!} \ .$$

Note that the block <u>number</u> does not depend on the number of electrons but that the block <u>size</u> does.

The subscript index is calculated in a fashion similar to that used for the D-N's.

1. Set $j_k' = j_k$ for $k = 1$ to n

2. Set $\ell = 1$

3. Set $j_k' = (j_k' - 1)$ if $j_k' > j_\ell'$ for all k from $(\ell + 1)$ to n

4. Set $\ell = \ell + 1$

5. Go back to 3 if $\ell < (n - 1)$

6.
$$INDEX^{SUB} = \sum_{\mu=1}^{n-1} \left\{ (j_\mu' - 1) \prod_{\alpha=(N-n+1)}^{(N-n+\mu)} (\alpha) \right\} + j_n'$$

Therefore the total index of a D_n is

$$(I_{D_n}^{SUP} - 1) \frac{N!}{(N-n)!} + \sum_{\mu=1}^{n-1} \left\{ (j_\mu' - 1) \prod_{\alpha=(N-n+1)}^{(N-n+\mu)} (\alpha) \right\} + j_n' \ .$$

During solution of the spatial SOGI equations, $\mu = 1$ and $\nu = 1$ and the index given above is all that is needed. When doing spin-coupling variations, all μ and ν are needed. i and j are used as normal square-array indices and the index described above determines which square array.

E. Solution of Equations

The B matrix is constructed according to the formulae in (17b), (29), (30), and (31) in terms of the original basis functions. Since the original basis set is not orthonormal, we find a transformation that gives an orthonormal basis set

$$\widetilde{V} S V = 1 \ , \tag{37}$$

where V and S are NBF by NBF matrices. Now we transform B to this space by transforming each of the NBF by NBF subblocks that correspond to a given k and ℓ,

$$B^0_{\mu k, \nu \ell} = \sum_{\sigma=1}^{NBF} \sum_{\tau=1}^{NBF} B_{\sigma k, \tau \ell} V_{\mu \sigma} V_{\nu \tau} \ , \tag{38}$$

Q is transformed as a string of vectors; i.e.,

$$Q^0_{\mu k} = \sum_{\tau=1}^{NBF} Q_{\tau k} V_{\mu \tau} \qquad \text{for each k.} \tag{39}$$

Now we wish to solve Eq.(19) in this new basis set, i.e., invert B^0. Unfortunately B^0 is singular. The order of singularity is the number of ways in which the wavefunction can be changed without changing the energy. It is clear that each orbital can be renormalized without changing E, giving rise to N (the number of electrons) singularities. If there are n orbitals in an orthogonal set [W. A. Goddard III, Phys.

Rev., 157, 81 (1967)], there are n^2 transformations within the set that do not change the energy; these include the renormalization of those n orbitals. Thus the number of singularities (NS) of $\underset{\sim}{B}^0$ is $\sum_i n_i^2$, where n_i is the size of the ith orthogonal set. If an orbital cannot be taken orthogonal to any other orbitals, it constitutes an orthogonal set of its own of size 1.

If $\underset{\sim}{B}^0$ were not singular, we could invert it as follows: find an orthogonal matrix, $\underset{\sim}{U}$, such that

$$\underset{\sim}{U}\underset{\sim}{B}^0\underset{\sim}{U} = \underset{\sim}{b} \ , \tag{40}$$

where $\underset{\sim}{b}$ is diagonal. The inverse of $\underset{\sim}{b}$ is very simple

$$(\underset{\sim}{b}^{-1})_{ij} = 1/b_{ij} \ , \tag{41}$$

and the inverse of $\underset{\sim}{B}^0$ is

$$(\underset{\sim}{B}^0)^{-1} = \underset{\sim}{U}\underset{\sim}{b}^{-1}\underset{\sim}{U} \ . \tag{42}$$

Since $\underset{\sim}{B}^0$ is singular, NS of the elements of $\underset{\sim}{b}$ are near zero. The NS corresponding eigenvectors are linear combinations of the trial orbitals and do not contribute to first-order corrections in the energy. To prevent these functions from being added (in large arbitrary amount) to the corrects (δ's), we set the inverse of the nearly-zero eigenvalues to zero. Inverting the other elements of $\underset{\sim}{b}$ gives $\underset{\sim}{b}^{-1}$, which we treat just as if it were the true inverse of $\underset{\sim}{b}$.

After inverting $\underset{\sim}{B}^0$, we multiply $(\underset{\sim}{B}^0)^{-1}$ times $\underset{\sim}{Q}^0$ to give the δ^0's (δ in terms of orthonormal basis functions). To get $\underset{\sim}{\delta}$ in terms of the original basis set, we take the elements for each orbital separately and transform

$$\delta_{\mu k} = \sum_\eta V_{\mu\eta}\delta^0_{\eta k} \ . \tag{43}$$

The new ϕ's are now calculated by adding the $\hat{\delta}$'s and renormalizing; we had not required the orbitals to remain normalized during variation since that would have made the formulation even more complicated.

We deem the process converged when

$$\text{SQRDLT}(= \sum_{\mu=1}^{\text{NBF}} \sum_{k=1}^{\text{NX}} (\delta^0_{\mu k})^2) \text{ or } \text{SQCDIF}(= \sum_{\mu=1}^{\text{NBF}} \sum_{k=1}^{\text{NX}} (d^i_{\mu k} - d^{i-1}_{\mu k})^2)$$

become less than some preset criterion, e.g., 10^{-6}. The $\delta^0_{\mu k}$'s are in terms of orthonormal basis functions and the d^i's are the coefficients of the trial functions at the ith iteration, also in terms of orthonormal basis functions,

$$d^i_{\mu k} = \sum_{\sigma \eta} V_{\sigma \mu} S_{\sigma \eta} C^i_{\eta k} \,. \tag{44}$$

F.   Remarks on GI-SCF

This new approach is analogous to the generalized Newton-Raphson technique of solving for the zeros of a polynomial and thus we refer to the new method as the Newton-Raphson iterative approach to solving the GI-SCF equations (sometimes denoted as NRIAS-GI-SCF). In the region of convergence this method should converge quadrically (i.e., the norm of δ is squared with each iteration. In fact this does occur so that a typical sequence of SQCDIF (that is $\sum_i |\delta_i|^2$) might be 10^{-4}, 10^{-7}, 10^{-13}, and 10^{-24}. This type of approach had been previously suggested for MC-SCF and HF calculations by Hinze and Roothaan [Prog. Theor. Phys. (Kyoto) 40, 37 (1967)].

The problem with NRIAS-GI-SCF is that each iteration takes much longer than for the corresponding homogeneous calculation since we must now form a NBF*NX square array and then invert it every

iteration. However, the procedure seems to converge within three or four iteration for almost every system as opposed to the hundreds of iterations sometimes required by other approaches. Furthermore there are no doubts about whether a given wave function is self-consistent or not. If the norm of $\vec{\delta}$ is 10^{-12}, one can be certain that an additional iteration would give a $\vec{\delta}$ with a norm no large than 10^{-22} which means that no coefficient would change by as much as 10^{-11}.

II. VARIATION OF SPIN COUPLING

For spin-coupling variation, it is expedient to think of $G_i^{\gamma}(\Phi\chi)$ as a fixed function, called ψ_i, so that (1) becomes

$$\Psi = \sum_i C_i \psi_i .\tag{45}$$

i runs from one to N_t (the number of linearly independent spin functions also equal to the number of Young tableaux for this case).

Firse we take linear combinations of the ψ_i to obtain an orthonormal set ψ_i^0, then form the Hamiltonian between ψ_i^0's ($\mathcal{H}_{ij}^0 = \langle \psi_i^0 | H | \psi_j^0 \rangle$), and diagonalize to give the eigenfunctions. By transforming back to the original space of ψ_i's, we obtain the C_i's that are used to construct the O_{11}^C needed in (3f). One can fix certain parts of the spin-coupling by transforming H_{ij} to small dimension before diagonalization. If spin-coupling variation is not desired, O_{11}^C may be formed with a fixed set of C's.

If each of the ψ_i many-electron functions is orthonormalized and the C-vector is normalized, then all of the numerators of Eq.(3) are 1 and can be dropped.

Thus we first form

$$\mathcal{H}_{ij} = \langle \psi_i | H | \psi_j \rangle$$

$$= \langle \Phi | H | O_{ij}^{\gamma} \Phi \rangle \qquad (46)$$

$$= \sum_a \sum_b \sum_{c<a} \sum_{d\neq b} XMMM(ab|cd)D_{ijdb}^{ac}$$

in the nonorthogonal space. The overlap matrix is

$$_{ij} = \langle \psi_i | \psi_j \rangle$$

$$= \langle \Phi | O_{ij}^{\gamma} \Phi \rangle \qquad (47)$$

$$= \sum \sum S_{1a} S_{1b} D_{ijab}^{11} \quad .$$

We find an orthogonal matrix, $\underset{\sim}{Y}$, such that

$$\underset{\sim}{\tilde{Y}} \underset{\sim}{\mathscr{L}} \underset{\sim}{Y} = \underset{\sim}{\mathscr{D}} \quad . \qquad (48)$$

where $\underset{\sim}{\mathscr{D}}$ is diagonal. The columns of $\underset{\sim}{Y}$ are the linear combinations of ψ_i's which are orthogonal. To normalize the combinations, we divide each column of $\underset{\sim}{Y}$ by the square root of its eigenvalue to give $\underset{\sim}{Z}$,

$$Z_{ij} = Y_{ij} / \sqrt{\mathscr{D}_{ij}} \qquad \text{for all i and j.} \qquad (49)$$

Now we transform $\underset{\sim}{\mathcal{H}}$,

$$\underset{\sim}{\mathcal{H}}^{0} = \underset{\sim}{\tilde{Z}} \underset{\sim}{\mathcal{H}} \underset{\sim}{Z} \quad . \qquad (50)$$

Diagonalizing $\underset{\sim}{\mathcal{H}}^{0}$ gives the proper linear combinations of ψ_i^0's and the energies of these combinations. In most cases, the lowest energy and its eigenvector are all that are of interest, but some real excited states arise from the higher roots of $\underset{\sim}{\mathcal{H}}^{0}$. To obtain the C_i's, we must transform back to the ψ_i's. If e_{ik}^0 is the kth eigenvector of $\mathcal{H}^0$ that we want

to use, then the proper C's are given by

$$C_i = \sum_{\ell} Z_{i\ell} e^0_{\ell k} , \tag{51}$$

which are used to form the O^C_{11}'s of (3f).

In Eqs. (46) and (47) we have D matrices that have subscripts i and j in addition to the normal sub- and superscripts. As pointed out at the end of Section I. D, these D-matrices are handled as multidimensional arrays in which the i and j are handled as normal square-array indices while the other sub- and superscripts are used to compute which square array is involved.

III. FLOW CHART

The following two flow charts show how the current SOGI program handles the fomulae described in Sections I and II. In these flow charts the following abbreviations are used.

ITERNO: an integer indicating the number of the iterations now in progress.

CALC: calculate.

TRANSF: transform.

DN'S: transformed U_{11}'s; see Section I. D.

SCF: Self Consistent Field, refers to orbital variation.

ICONV, JCONV, KCONV: integers used as flags to indicate whether certain processes have converged. ICONV is for orbital variation, KCONV is for spin-coupling variation, and JCONV is for entire process. 0 means not converged but proceeding normally; 1 means abnormal condition, stop; 2 means normal convergence.

ITRMAX: maximum allowed number of iterations.

ONBS: Orthonormal Basis Set.

D'S: $D_0 (= \langle \Phi | O_{11}^C \Phi \rangle)$, D1's, D2's, D3's, and D4's.

E: Energy.

ABS: Atomic Basis Set, not necessarily the basis set for an atom. In this sense it refers to the original basis set for which we have the molecular integrals and in which the trial functions are given. The functions are only required to be linearly independent.

FLOW CHART 1

ENTRY

GET Ç's IN O.N.B.S. | 1

CALC D's FROM DN's | 2

CALC E & Q_{vi} | 3

E GOING UP | 4 — YES

NO

E OUT of BOUNDS | 5 — YES

NO

CALC E ONLY | 6 — YES

NO

FORM B | 7

SYMMETRIZE B & TRANSF. TO O.N.B.S. | 8

DIAGONALIZE B | 9

TRANSF. Q_{vi} TO O.N.B.S. | 10

GET δ_{vi} IN O.N.B.S. & CONVERT TO A.B.S. | 11

MODIFY ζ_{vi} | 12

NORMALIZE $\vec{\zeta}$'s | 13

TRANSF. INTEGRALS | 14

CALC. SQCDIF & SQDLTA | 15

SCF CONVERGED | 16 — NO

RETURN | 17

YES

SET FLAGS & RETURN | 18

CALC. ONE-ELECTRON PROPERTIES & VIRTUALS & RETURN | 19

WRITE MESSAGE, SET FLAG & RETURN | 20

FLOW CHART 2 — SCF CYCLE

APPENDIX II: The CI Program

The CI calculations reported in this thesis were carried out with a program written in FORTRAN IV for the Caltech IBM 370/155. All floating-point numbers were carried in double precision (8 bytes).

In this program, the wavefunction for the ith state of the system is taken as

$$\Psi_i = \sum_{n=1}^{NSPCF} \sum_{\ell=1}^{f_n} c_{n\ell}^i \hat{\mathscr{A}}[\Phi_n \chi_{n\ell}] \tag{1}$$

where NSPCF is the number of spatial configurations (SPCF's), f_n is the number of spin eigenfunctions for the nth spatial configuration, Φ_n is the nth spatial configuration, and χ_ℓ is a spin eigenfunction. The spatial configurations are products of orthonormal orbitals (also called basis functions), e.g.,

$$\Phi_8 = \phi_1^2 \phi_3 \phi_4^2 \phi_8 \phi_9 \tag{2}$$

assuming seven electrons; 8 is the number of this specific SPCF. The spin eigenfunctions (SEF's) $\chi_{n\ell}$ are those formed by using Young's orthogonal irreducible representation of $\mathscr{S}_n$ (the symmetric group on n objects) where n is the number of singly-occupied (also called open-shell) orbitals in Φ_n. One need worry about only the singly-occupied orbitals, since $\phi_a(1)\phi_a(2)\alpha(1)\beta(2)$ is a singlet without further ado. If NBF is the number of orbitals (or Number of Basis Functions), then an SPCF is determined by a string of NBF 0's, 1's, and 2's, indicating how often each available orbital was used; this string of numbers will be called an SPCF. In the case of Φ_8 in (2), the SPCF is

$$2\ 0\ 1\ 2\ 0\ 0\ 0\ 1\ 1\ 0 \tag{3}$$

assuming NBF = 10.

$\chi_{n\ell}$ depends on n only in that n determines <u>how many</u> open-shell orbitals there are in the nth SPCF. The χ's are sums of permuted products of α's and β's (Pauli spin functions). The number of α's (NA) and β's (NB) is input to the program. The difference, NSPIN = (NA - NB) determines the spin; the program always builds a wavefunction with $S=M_s=NSPIN/2$. Currently the program allows for singlets, doublets, and triplets. The maximum number of open-shell orbitals for each of these cases is singlets - six, doublets - five, and triplets - six. These could be increased by adding the appropriate code for forming determinants and SEF's.

The SEF's are constructed by taking linear combinations of Slater determinants that are specified by a list of NA orbitals with α spin and a list of NB orbitals with β spin. The determinants are generated by the following method. The SPCF is parsed to give a list of doubly-occupied orbitals and a list of singly-occupied orbitals. The numbers of the doubly-occupied orbitals are entered in both the alpha and beta lists for each of the determinants being built. Suppose there were KDBL doubly-occupied orbitals and NSNGL=(NA+NB)-2KDBL singly-occupied orbitals, of these, NAS=NA-KDBL must go into the alpha list of some determinant, and NBS=NB-KDBL must go to the beta list of that determinant. The program generates all distinct partitions of the NSNGL singly-occupied orbitals into two groups of size NAS and NBS and attaches them to the appropriate alpha and beta lists. When these determinants are combined with proper coefficients, we obtain the desired SEF's.

The program will read in SPCF's but also contains an option for generating SPCF's. Associated with each SPCF is an integer called an excitation number (EN). The generation of SPCF's begins by reading in one or more SPCF's with associated excitation number. New SPCF's are generated by moving an electron from an occupied orbital in the source SPCF to a different orbital in the object SPCF. KSOURCE is the number of the SPCF currently being used as source and KOUT is the number of the new object SPCF. the EN of an object SPCF is set to one less than its source SPCF. An SPCF with EN=0 is not used for source, thereby terminating SPCF production. Each SPCF is checked to see that it has the proper number of electrons and a suitable number of open-shell orbitals and for uniqueness.

The check for uniqueness of $SPCF_k$ uses a hash table technique to avoid a linear search of all previous SPCF's. Before checking any SPCF's, a table of 4200 four-byte integers (JTABLE) is set to zero. (4200 is picked to be larger than our hash number, 4007, which is prime.) $SPCF_k$ is treated as a ternary number, e.g., for $SPCF_8$ in (2), the ternary number is

$$I_8 = 2 \times 3^9 + 1 \times 3^7 + 2 \times 3^6 + 1 \times 3^2 + 1 \times 3 . \qquad (4)$$

I_k is taken modulo the hash number (vis. 4007) which gives a result between 0 and 4007. Call this result $INDEX_k$

$$INDEX_k = I_k \text{ MOD } 4007 . \qquad (5)$$

Now the $INDEX_k$ location of JTABLE is examined. If $JTABLE(INDEX_k)$ = 0, we know that $SPCF_k$ is unique so we store I_k in $JTABLE(INDEX_k)$ and go on. If $JTABLE(INDEX_k) \neq 0$, we check to see if the number

stored there is I_k or some other number. If JTABLE(INDEX$_k$) already equals I_k, we already have SPCF$_k$ in our list, so we discard the copy currently in hand and go on. If JTABLE(INDEX$_k$) is not equal to I_k, we increase INDEX$_k$ by one and check that location continuing until we either find an empty location meaning SPCF$_k$ is new or find I_k already in the table meaning SPCF$_k$ is old. For convenience, the end of the table is connected to the head; the table can never get full since we will never use 4200 SPCF's.

The algorithm for generating SPCF's is as follows:

1. Read basic SPCF's and EN's. NBASF is number of basic SPCF's.

2. Set KSOURCE=1, KOUT=1.

3. Check each basic SPCF for number of electrons, open-shell orbitals, and uniqueness. Each acceptable, unique SPCF is copied into a new list of SPCF's along with its EN. KOUT is incremented by 1 for each new SPCF. KOUT always points to first empty location in list of SPCF's (SPCFTBL).

4. If EN$_{KSOURCE}$ $\neq 0$, generate new SPCF's from SPCF$_{KSOURCE}$. EN of new SPCF is EN$_{KSOURCE}$ - 1. Each new SPCF is checked for uniqueness and number of open shells. KOUT is incremented by one for each new SPCF.

5. When SPCF$_{KSOURCE}$ is exhausted, set KSOURCE to KSOURCE + 1.

6. If KSOURCE < KOUT, go to 4.

After the SPCF's have been generated, they can be checked for symmetry if a multiplication table has been supplied. This is done as in the CIT Hartree-Fock program as implemented by Bill Hunt and is limited to Abelian groups.

After symmetry checking, the SPCF's can be checked for orbital occupations. All SPCF's in which the sum of the number of electrons in some specified set of orbitals is not within certain limits are discarded. As many as 10 orbitals are allowed in each set and up to ten sets are allowed. This is necessary since the SPCF generation algorithm can generate a very large number of SPCF's and this provides a way of weeding out ones that are probably unimportant.

The CI matrix is generated one block at a time and written on disk. During formation of the CI matrix, all the integrals over orbitals are kept in core. When the CI matrix has been formed, it is read back in and reconstructed, in lower triangular form in the space previously used for integral storage. After the desired number of eigenvectors and eigenvalues of the CI matrix have been found and printed, the program goes on to the next data set; there is currently no provision for finding natural orbitals or computing properties.

The blocks of the CI matrix are those corresponding to two SPCF's. Let ND_i and ND_j be the number of determinants derived from $SPCF_i$ and $SPCF_j$, while $NSEF_i$ and $NSEF_j$ are the number of spin eigenfunctions for those SPCF's. First we construct an ND_i by ND_j Hamiltonian matrix between the determinants of i and j. Then we take linear combinations of the rows to give a Hamiltonian matrix between SEF's of i and determinants of j. Then we add columns to give the Hamiltonian between SEF's of i and j.

The coefficients of the linear combinations of determinants are most easily obtained by building up from the spin functions of fewer electrons in the following way. Consider the Young tableau for the

spin function we are building, if it is of the form

(6)

then we take the spin function for N - 1 electrons obtained from this tableau with N deleted, and just multiply by α. If the tableau is of the form

(7)

we take the spin function for N - 1 electrons obtained from this tableau with N deleted, call the function f_{N-1}. Our spin function is, aside from normalization

$$f_N = C_1(f_{N-1}\beta) + C_2(\hat{S}^-_{N-1}f_{N-1}\,\alpha) \quad , \tag{8}$$

where $\hat{S}^-_{N-1}$ is the spin-lowering operator for N - 1 electrons. To fix the coefficients C_1 and C_2, we demand that our function give zero under the raising operator

$$\hat{S}^+_N f_N = \hat{S}^+_N(C_1 f_{N-1}\beta) + \hat{S}^+_N[C_2(\hat{S}^+_{N-1}f_{N-1})\alpha] \ . \tag{9}$$

Write

$$\hat{S}^+_N = \hat{S}^+_{N-1} + \hat{\jmath}^+(N) \ , \tag{10}$$

where $\hat{S}_N^+$ is the N-electron raising operator, $\hat{S}_{N-1}^+$ is the N - 1-electron operator, and $\hat{\mathcal{O}}^+(N)$ is the one-electron raising operator of the Nth electron.

Since

$$C_1\hat{S}_N^+ f_{N-1}\beta = C_1[\hat{S}_{N-1}^+ f_{N-1}\beta + f_{N-1}\hat{\mathcal{O}}^+(N)\beta] = C_1 f_{N-1}\alpha \qquad (11)$$

and

$$C_2\hat{S}_N^+[(\hat{S}_{N-1}^- f_{N-1})\alpha] = C_2(\hat{S}_{N-1}^+ \hat{S}_{N-1}^- f_{N-1})\alpha \qquad (12)$$

$$= C_2\{[S_{N-1}(S_{N-1} + 1)] - S_{N-1}^2 + S_{N-1})f_{N-1}\alpha,$$

we have

$$C_1 + 2C_2 S_{N-1} = 0 \qquad (13)$$

or

$$C_2 = -C_1/(2S_{N-1}).$$

Table I gives the spin functions for two, three, and four electrons, while Tables II, III and IV give the spin functions for five-electron doublets, six-electron singlets, and six-electron triplets. These functions are given for permuted products of α's and β's. The signs preceding the various terms have the following significance. The determinants are formed from the product of orbitals $\phi_a(1)\phi_b(2)\cdots\phi_x(n)$ with a spin function like $\alpha(1)\alpha(2)\beta(3)\beta(4)\alpha(5)\cdots\alpha(n)$. It is more convenient to have all the α's first and the β's last, so we tape the ϕ's to their α or β and reorder them so that the α's are first and the β's second. All the α orbitals are in ascending order and so are the β's. This reordering may change the sign of the determinant. The +'s and -'s before or above the spin products show whether the determinant does or does not change phase on reordering.

TABLE I.

A. Two-electron singlet

$$f = \frac{1}{\sqrt{2}} (\overset{(+)}{\alpha\beta} - \overset{(-)}{\beta\alpha})$$

B. Two-electron triplet

$$f = \alpha\alpha$$

C. Three-electron doublet

$$f_1 = \frac{1}{\sqrt{2}} (\overset{(-)}{\alpha\beta\alpha} - \overset{(+)}{\beta\alpha\alpha})$$

$$f_2 = \frac{1}{\sqrt{6}} (2\overset{(+)}{\alpha\alpha\beta} - \overset{(-)}{\alpha\beta\alpha} - \overset{(+)}{\beta\alpha\alpha})$$

D. Four-electron singlet

$$f_1 = \frac{1}{2}(\alpha\beta - \beta\alpha)(\alpha\beta - \beta\alpha) = \frac{1}{2}(\overset{(-)}{\alpha\beta\alpha\beta} + \overset{(-)}{\beta\alpha\beta\alpha} - \overset{(+)}{\alpha\beta\beta\alpha} - \overset{(+)}{\beta\alpha\alpha\beta})$$

$$f_2 = \frac{\sqrt{3}}{6}[2(\alpha\alpha\beta\beta + \beta\beta\alpha\alpha) - (\alpha\beta + \beta\alpha)(\alpha\beta + \beta\alpha)]$$

$$= \frac{\sqrt{3}}{6}(2\overset{(+)}{\alpha\alpha\beta\beta} + 2\overset{(+)}{\beta\beta\alpha\alpha} - \overset{(-)}{\alpha\beta\alpha\beta} - \overset{(+)}{\alpha\beta\beta\alpha} - \overset{(-)}{\beta\alpha\beta\alpha} - \overset{(+)}{\beta\alpha\alpha\beta})$$

E. Four-electron triplet

$$f_1 = \frac{1}{\sqrt{2}}(\alpha\beta - \beta\alpha)\alpha\alpha = \frac{\sqrt{2}}{2}(\overset{(+)}{\alpha\beta\alpha\alpha} - \overset{(-)}{\beta\alpha\alpha\alpha})$$

$$f_2 = \frac{\sqrt{6}}{6}(2\overset{(-)}{\alpha\alpha\beta\alpha} - \overset{(+)}{\alpha\beta\alpha\alpha} - \overset{(-)}{\beta\alpha\alpha\alpha})$$

$$f_3 = \frac{\sqrt{3}}{6}(3\overset{(+)}{\alpha\alpha\alpha\beta} - \overset{(-)}{\alpha\alpha\beta\alpha} - \overset{(+)}{\alpha\beta\alpha\alpha} - \overset{(-)}{\beta\alpha\alpha\alpha})$$

TABLE II.

Orthonormal Spin Functions for Five-Electron Doublets

		$-f_1$	f_2	f_3	$-f_4$	f_5
$+\alpha\alpha\alpha\beta\beta$	(123)	0	0	0	0	$\sqrt{2}/2$
$-\alpha\alpha\beta\alpha\beta$	(124)	0	0	0	2/3	$+\sqrt{2}/6$
$+\alpha\beta\alpha\alpha\beta$	(134)	0	0	$\sqrt{3}/3$	+1/3	$-\sqrt{2}/6$
$-\beta\alpha\alpha\alpha\beta$	(234)	0	0	$+\sqrt{3}/3$	-1/3	$+\sqrt{2}/6$
$+\alpha\alpha\beta\beta\alpha$	(125)	0	$\sqrt{3}/3$	0	+1/3	$-\sqrt{2}/6$
$-\alpha\beta\alpha\beta\alpha$	(135)	1/2	$+\sqrt{3}/6$	$+\sqrt{3}/6$	1/6	$+\sqrt{2}/6$
$+\beta\alpha\alpha\beta\alpha$	(235)	+1/2	$-\sqrt{3}/6$	$\sqrt{3}/6$	-1/6	$-\sqrt{2}/6$
$+\alpha\beta\beta\alpha\alpha$	(145)	+1/2	$-\sqrt{3}/6$	$-\sqrt{3}/6$	+1/6	$\sqrt{2}/6$
$-\beta\alpha\beta\alpha\alpha$	(245)	1/2	$+\sqrt{3}/6$	$-\sqrt{3}/6$	-1/6	$-\sqrt{2}/6$
$+\beta\beta\alpha\alpha\alpha$	(345)	0	$\sqrt{3}/3$	0	-1/3	$\sqrt{2}/6$

TABLE III. Orthonormal Spin Functions for Six-Electron Singlets

		$-f_1$	f_2	f_3	$-f_4$	f_5
$+\alpha\alpha\alpha\beta\beta\beta$	(123)	0	0	0	0	1/2
$-\alpha\alpha\beta\alpha\beta\beta$	(124)	0	0	0	$\sqrt{2}/3$	-1/6
$+\alpha\beta\alpha\alpha\beta\beta$	(134)	0	0	$\sqrt{6}/6$	$+\sqrt{2}/6$	-1/6
$-\beta\alpha\alpha\alpha\beta\beta$	(234)	0	0	$+\sqrt{6}/6$	$-\sqrt{2}/6$	-1/6
$+\alpha\alpha\beta\beta\alpha\beta$	(125)	0	$\sqrt{6}/6$	0	$+\sqrt{2}/6$	-1/6
$-\alpha\beta\alpha\beta\alpha\beta$	(135)	$\sqrt{2}/4$	$+\sqrt{6}/12$	$+\sqrt{6}/12$	$\sqrt{2}/12$	-1/6
$+\beta\alpha\alpha\beta\alpha\beta$	(235)	$+\sqrt{2}/4$	$-\sqrt{6}/12$	$\sqrt{6}/12$	$-\sqrt{2}/12$	-1/6
$+\alpha\beta\beta\alpha\alpha\beta$	(145)	$+\sqrt{2}/4$	$-\sqrt{6}/12$	$-\sqrt{6}/12$	$+\sqrt{2}/12$	1/6
$-\beta\alpha\beta\alpha\alpha\beta$	(245)	$\sqrt{2}/4$	$+\sqrt{6}/12$	$-\sqrt{6}/12$	$-\sqrt{2}/12$	1/6
$+\beta\beta\alpha\alpha\alpha\beta$	(345)	0	$\sqrt{6}/6$	0	$-\sqrt{2}/6$	1/6
$-\alpha\alpha\beta\beta\beta\alpha$	(126)	0	$+\sqrt{6}/6$	0	$-\sqrt{2}/6$	-1/6
$+\alpha\beta\alpha\beta\beta\alpha$	(136)	$+\sqrt{2}/4$	$\sqrt{6}/12$	$-\sqrt{6}/12$	$-\sqrt{2}/12$	-1/6
$-\beta\alpha\alpha\beta\beta\alpha$	(236)	$\sqrt{2}/4$	$-\sqrt{6}/12$	$-\sqrt{6}/12$	$\sqrt{2}/12$	-1/6
$-\alpha\beta\beta\alpha\beta\alpha$	(146)	$\sqrt{2}/4$	$-\sqrt{6}/12$	$+\sqrt{6}/12$	$-\sqrt{2}/12$	1/6
$+\beta\alpha\beta\alpha\beta\alpha$	(246)	$+\sqrt{2}/4$	$\sqrt{6}/12$	$\sqrt{6}/12$	$+\sqrt{2}/12$	1/6
$-\beta\beta\alpha\alpha\beta\alpha$	(346)	0	$+\sqrt{6}/6$	0	$\sqrt{2}/6$	1/6
$+\alpha\beta\beta\beta\alpha\alpha$	(156)	0	0	$\sqrt{6}/6$	$-\sqrt{2}/6$	1/6
$-\beta\alpha\beta\beta\alpha\alpha$	(256)	0	0	$+\sqrt{6}/6$	$\sqrt{2}/6$	1/6
$+\beta\beta\alpha\beta\alpha\alpha$	(356)	0	0	0	$+\sqrt{2}/3$	1/6
$-\beta\beta\beta\alpha\alpha\alpha$	(456)	0	0	0	0	-1/2

TABLE IV. Orthonormal Spin Functions for Six-Electron Triplets

		$-f_1$	f_2	f_3	$-f_4$	f_5	f_6	f_7	$-f_8$	f_9
$+\alpha\alpha\alpha\alpha\beta\beta$	(1234)	0	0	0	0	0	0	0	0	$\sqrt{15}/5$
$-\alpha\alpha\beta\alpha\beta\beta$	(1235)	0	0	0	0	0	0	0	3/4	$+\sqrt{15}/20$
$+\alpha\alpha\beta\alpha\alpha\beta$	(1245)	0	0	0	0	0	0	$\sqrt{2}/2$	$+1/4$	$-\sqrt{15}/20$
$-\alpha\beta\alpha\alpha\alpha\beta$	(1345)	0	0	0	0	0	$\sqrt{6}/4$	$+\sqrt{2}/4$	$-1/4$	$+\sqrt{15}/20$
$+\beta\alpha\alpha\alpha\alpha\beta$	(2345)	0	0	0	0	0	$+\sqrt{6}/4$	$-\sqrt{2}/4$	$+1/4$	$-\sqrt{15}/20$
$+\alpha\alpha\alpha\beta\beta\alpha$	(1236)	0	0	0	0	$\sqrt{2}/2$	0	0	$+1/4$	$-\sqrt{15}/20$
$-\alpha\alpha\beta\alpha\beta\alpha$	(1246)	0	0	$\sqrt{3}/3$	2/3	$+\sqrt{2}/6$	0	$+\sqrt{2}/6$	1/12	$+\sqrt{15}/20$
$+\alpha\beta\alpha\alpha\beta\alpha$	(1346)	0	0	$+\sqrt{3}/3$	$+1/3$	$\sqrt{2}/6$	$+\sqrt{6}/12$	$\sqrt{2}/12$	$-1/12$	$-\sqrt{15}/20$
$-\beta\alpha\alpha\alpha\beta\alpha$	(2346)	0	0	$+\sqrt{3}/3$	$-1/3$	$+\sqrt{2}/6$	$\sqrt{6}/12$	$-\sqrt{2}/12$	1/12	$+\sqrt{15}/20$
$+\alpha\alpha\beta\beta\alpha\alpha$	(1256)	0	0	0	$+1/3$	$-\sqrt{2}/6$	0	$-\sqrt{2}/6$	$+1/6$	$\sqrt{15}/30$
$-\alpha\beta\alpha\beta\alpha\alpha$	(1356)	1/2	$+\sqrt{3}/6$	$+\sqrt{3}/6$	$+1/6$	$+\sqrt{2}/6$	$-\sqrt{6}/12$	$-\sqrt{2}/12$	$-1/6$	$-\sqrt{15}/30$
$+\beta\alpha\alpha\beta\alpha\alpha$	(2356)	-1/2	$-\sqrt{3}/6$	$\sqrt{3}/6$	$-1/6$	$-\sqrt{2}/6$	$-\sqrt{6}/12$	$\sqrt{2}/12$	$+1/6$	$\sqrt{15}/30$
$+\alpha\beta\beta\alpha\alpha\alpha$	(1456)	-1/2	$-\sqrt{3}/6$	$-\sqrt{3}/6$	$+1/6$	$\sqrt{2}/6$	$+\sqrt{6}/12$	$-\sqrt{2}/12$	$-1/6$	$\sqrt{15}/30$
$-\beta\alpha\beta\alpha\alpha\alpha$	(2456)	1/2	$+\sqrt{3}/6$	$-\sqrt{3}/6$	$-1/6$	$-\sqrt{2}/6$	$\sqrt{6}/12$	$+\sqrt{2}/12$	1/6	$-\sqrt{15}/30$
$+\beta\beta\alpha\alpha\alpha\alpha$	(3456)	0	$\sqrt{3}/3$	0	$-1/3$	$\sqrt{2}/6$	0	$\sqrt{2}/6$	$-1/6$	$\sqrt{15}/30$